



HAL
open science

Initiation des efflorescences phytoplanctoniques en zone côtière: le rôle de la température et des interactions biologiques

Thomas Trombetta

► **To cite this version:**

Thomas Trombetta. Initiation des efflorescences phytoplanctoniques en zone côtière: le rôle de la température et des interactions biologiques. Sciences agricoles. Université Montpellier, 2019. Français. NNT: 2019MONTG088 . tel-02868643

HAL Id: tel-02868643

<https://theses.hal.science/tel-02868643>

Submitted on 15 Jun 2020

HAL is a multi-disciplinary open access archive for the deposit and dissemination of scientific research documents, whether they are published or not. The documents may come from teaching and research institutions in France or abroad, or from public or private research centers.

L'archive ouverte pluridisciplinaire **HAL**, est destinée au dépôt et à la diffusion de documents scientifiques de niveau recherche, publiés ou non, émanant des établissements d'enseignement et de recherche français ou étrangers, des laboratoires publics ou privés.

THÈSE POUR OBTENIR LE GRADE DE DOCTEUR DE L'UNIVERSITÉ DE MONTPELLIER

En Écologie Fonctionnelle

École doctorale GAIA

Unité de recherche MARBEC (MARine Biodiversity, Exploitation and Conservation)

Initiation des efflorescences phytoplanctoniques en zone côtière : le rôle de la température et des interactions biologiques

Présentée par Thomas TROMBETTA

Le 13 décembre 2019

Sous la direction de Behzad MOSTAJIR et Francesca VIDUSSI

Devant le jury composé de

Paul NIVAL, Professeur émérite Sorbonne Université, LOV, Villefranche-sur-Mer

Pascal CLAQUIN, Professeur Université Caen Normandie, BOREA, Caen

Rutger De WIT, Directeur de recherche CNRS, MARBEC, Montpellier

Antoine SCIANDRA, Directeur de recherche CNRS, LOV, Villefranche-sur-Mer

François-Yves BOUGET, Directeur de recherche CNRS, LOMIC, Banyuls-sur-Mer

Francesca VIDUSSI, Chargée de recherche CNRS, MARBEC, Montpellier

Behzad MOSTAJIR, Directeur de recherche CNRS, MARBEC, Montpellier

Rapporteur

Rapporteur

Président du Jury

Examineur

Examineur

Co-encadrante

Directeur de thèse



UNIVERSITÉ
DE MONTPELLIER

Résumé

Dans les écosystèmes marins des zones tempérées, la majeure partie de la production primaire annuelle est générée au printemps lors de phénomènes d'accumulation rapide de biomasse phytoplanctonique, appelés « efflorescences », supportant la diversité et le fonctionnement de ces systèmes. Plusieurs mécanismes physico-chimiques et biologiques expliquant l'initiation des efflorescences phytoplanctoniques sont évoqués pour ces écosystèmes. En revanche pour les zones côtières peu profondes sous influence de forçages complexes, les mécanismes à la base de ce phénomène restent encore mal connus. L'objectif de cette thèse était donc d'identifier et hiérarchiser les facteurs contribuant à l'initiation des efflorescences phytoplanctoniques dans ces zones, notamment le rôle des forçages physico-chimiques et des interactions biologiques au sein du réseau microbien, mais également de tenter de comprendre les conséquences de l'élévation de la température sur ce fonctionnement dans le contexte du réchauffement climatique.

Dans cette optique, un suivi à deux approches a été réalisé dans la lagune de Thau (lagune côtière du Nord-Ouest de la Méditerranée) : un suivi *in situ* à haute fréquence (15 min) des paramètres hydrologiques (salinité, turbidité, température de l'eau, etc.), météorologiques (vents, lumière incidente, température de l'air, etc.) et biologiques (fluorescence de la chlorophylle *a*) ; et un suivi hebdomadaire de l'abondance de la communauté microbienne (virus, bactéries, phytoplancton, flagellés hétérotrophes et ciliés) et de sa diversité avec une attention particulière pour le phytoplancton. Ces suivis ont été réalisés de l'hiver au printemps sur deux années consécutives, 2015 et 2016. En plus de ces suivis, une expérimentation en mésocosmes *in situ* a été réalisée au printemps 2018, simulant l'élévation de la température selon le scénario du réchauffement climatique attendu dans le futur, et en présence et absence du mésozooplancton. L'objectif de cette expérience était d'identifier les effets directs du réchauffement et ceux indirects dus au zooplancton sur la dynamique, la composition pigmentaire et la succession du phytoplancton, avant, pendant et après une efflorescence phytoplanctonique.

Une analyse basée sur les réseaux de corrélations entre 110 différents groupes/taxon/espèces observés (« *correlation network analysis* » en anglais) a permis de mettre en évidence les interactions majeures au sein du réseau planctonique microbien qui caractérisaient les périodes phénologiques et leurs différences entre les deux années étudiées. Pendant les périodes d'efflorescences les interactions de compétition intraguilde au sein du phytoplancton dominaient, tout comme les interactions mutualistes entre le phytoplancton et les bactéries hétérotrophes, suggérant un transfert d'énergie basée à la fois sur la biomasse phytoplanctonique et bactérienne effectué par la prédation du microzooplancton. Pendant les épisodes sans efflorescence, les interactions entre les ciliés et les bactéries (bactériorie) dominaient, suggérant un transfert d'énergie basée essentiellement sur la biomasse bactérienne. Dans le même temps,

les résultats obtenus par le suivi à haute fréquence ont permis de mettre en évidence le rôle prépondérant de l'augmentation de la température de l'eau, notamment à la sortie de l'hiver, dans l'initiation des efflorescences phytoplanctoniques. La combinaison du métabolisme du phytoplancton stimulé par l'augmentation de la température et la faible pression de broutage permettrait l'accumulation de la biomasse phytoplanctonique à l'origine des efflorescences phytoplanctoniques. De plus, l'année 2016, avec l'hiver le plus chaud jamais enregistré par Météo France, était caractérisée par une plus faible accumulation de la biomasse phytoplanctonique à la sortie de l'hiver, une dominance du phytoplancton de plus petite taille au détriment des diatomées, et une dominance des interactions entre microorganismes de petite taille. Les résultats de l'expérimentation en mésocosmes *in situ* ont confirmé l'effet de l'élévation de la température dans la réduction de l'amplitude des efflorescences phytoplanctoniques (diminution de près de 50% de la concentration en chlorophylle *a*) et de la favorisation du petit phytoplancton comme les petites algues vertes (caractérisés par la chlorophylle *b*) ainsi que des dinoflagellés (caractérisés par la péridinine) au détriment des diatomées (caractérisés par la fucoxanthine). De plus, ils ont permis de mettre en évidence que cette modification de l'amplitude et de la composition des efflorescences était principalement liée à un effet indirect sur le phytoplancton due à l'augmentation de la pression de broutage exercée par le zooplancton. De plus, il est apparu que c'était principalement le microzooplancton qui contrôlait la dynamique et la biomasse phytoplanctonique et que le mésozooplancton jouait essentiellement le rôle de consommateur secondaire.

Les résultats obtenus lors de cette thèse suggèrent que dans un avenir plus chaud, les efflorescences phytoplanctoniques seront potentiellement fortement réduites et dominées par des espèces de plus petites tailles. Le transfert de ces petites espèces phytoplanctoniques et du bactérioplancton vers les niveaux trophiques supérieurs s'effectuerait davantage au travers du microzooplancton. Ainsi, le réchauffement climatique futur dans la zone côtière peu profonde avantagerait l'établissement du réseau microbien avec potentiellement une efficacité de production et de transfert moins importante que celle du réseau classique.

Mots clefs : Phytoplancton, efflorescences, zone côtière, forçages physico-chimiques, réseau d'interactions microbien, microzooplancton, prédation, compétition, réchauffement climatique, mésocosme.

Abstract

In temperate marine ecosystems, the major part of the annual primary production is generated in spring during rapid phytoplankton biomass accumulation periods, called ‘blooms’, supporting the diversity and the functioning of these ecosystems. Several physical, chemical and biological mechanisms triggering the bloom initiation were evocated for these ecosystems. However, for shallow coastal zones, under the influence of complex environmental forcing factors, mechanisms triggering blooms are not well known. The objective of the present thesis was to identify and classify the forcing factors contributing to the bloom initiation in these zones, especially the role of physical and chemical forcing factors and biological interactions in the microbial network, but also to understand the consequences of the temperature elevation on this functioning in the global warming context.

In this frame, a monitoring with a dual approach was carried out in Thau lagoon (coastal lagoon of the North-Western Mediterranean Sea): a high frequency (15 min) *in situ* monitoring of hydrological (salinity, turbidity, water temperature, etc.), meteorological (wind, incident light, air temperature, etc.) and biological (chlorophyll *a* fluorescence) parameters; and a weekly monitoring of the abundance of the microbial community (virus, bacteria, phytoplankton, heterotrophic flagellates and ciliates), and its diversity, with a particular look at phytoplankton. These monitoring were carried out from winter to spring in two consecutive years, 2015 and 2016. Besides these monitoring, an *in situ* mesocosm experiment was carried out during the 2018 spring to simulate the temperature elevation according to the global warming scenario, in the presence and the absence of mesozooplankton. The objective of this experiment was to identify the direct effect of warming and the indirect effect of the zooplankton on the phytoplankton dynamic, the pigment composition and succession, during the pre-bloom, bloom and post-bloom periods.

A correlation network analysis between 110 various groups/taxa/species highlighted the major interactions characterizing the microbial interaction network during the bloom and the non-bloom periods and the differences between these two years. During the bloom periods, intraguild phytoplankton competition and mutualism between phytoplankton and heterotrophic bacteria dominated the microbial food web. This suggested an energy transfer based on both bacterial and phytoplanktonic biomass, through the microzooplankton predation. During the non-bloom periods, interaction between ciliates and heterotrophic bacteria (bacterivory) dominated, suggesting an energy transfer mainly based on bacterial biomass. Besides, the high frequency monitoring highlighted the predominant role of the water temperature increase, especially during the early spring, in the initiation of the phytoplankton blooms.

The combination between the phytoplankton metabolism stimulated by the temperature increase and the low grazing pressure triggered the phytoplankton biomass accumulation starting the blooms. Furthermore, 2016 year, with the warmer winter recorded in France (Meteofrance), was characterized by a weaker phytoplankton biomass accumulation during the early spring, a dominance of the small phytoplankton at the expense of diatoms, and a dominance of interactions between small size microorganisms. The mesocosm experiment confirmed the role of the temperature elevation on the bloom amplitude reduction (diminution of 50% of the chlorophyll *a* concentration) and the promotion of small phytoplankton such as small green algae (characterized by chlorophyll *b*) and dinoflagellates (characterized by peridinin), at the expense of diatoms (characterized by fucoxanthin). This amplitude and composition modification of phytoplankton blooms was mainly due to the indirect effect of the zooplankton grazing increase under warming. Furthermore, the results underlined that it was microzooplankton which mainly controlled the phytoplankton dynamic and biomass and the mesozooplankton was mainly accomplished the role of the secondary consumer in this system.

The results of the present thesis suggest that in the future warmer conditions context, phytoplankton blooms could strongly be reduced and dominated by small phytoplankton. The energy transfer of these small phytoplankton species and heterotrophic bacteria to the higher trophic levels through the microzooplankton grazing could be strengthened. Therefore, under the future warming of the shallow coastal zones, the microbial food web could be promoted with a potential lower production and transfer efficiency than the classical food web.

Keywords: Phytoplankton, blooms, coastal zones, physical and chemical forcing factors, microbial interaction network, microzooplankton, predation, competition, global warming, mesocosm

Remerciements

Avant toutes choses, je voudrais remercier l'ensemble des membres du jury de thèse, Pr. Paul Nival, Pr. Pascal Claquin, Dr. Rutger De Wit, Dr. Antoine Sciandra et Dr. François-Yves Bouget, d'avoir accepté de participer à l'évaluation de ce travail de thèse. J'en suis profondément honoré.

Behzad, Francesca, je ne vous remercierai jamais assez de m'avoir donné l'opportunité de réaliser cette thèse au sein de votre écosystème. La chaleur de votre accueil a toujours été le moteur de notre réseau d'interaction. A vos côtés j'ai appris le pouvoir de la remise en question. J'ai appris, grandi, mûri et me suis épanoui grâce à vous. Merci de m'avoir sans relâche poussé sur les sentiers sinueux de la recherche, et de m'avoir guidé vers le bon chemin quand d'aventure je m'égarais. Votre bienveillance a été pour moi la clé vers l'aboutissement de ces travaux.

Merci à mon comité de suivi de thèse, Benoît Jaillard, Jean-Marc Fromentin et Antoine Sciandra, pour leurs conseils avisés lors de ces réunions de suivi de thèse qui m'ont permis de prendre du recul et mettre en perspective mes résultats.

Merci à tous les membres de la MEDIMEER et de la SMEL, en particulier Sébastien, Solenn et Rémy. Votre joie, votre bonne humeur mais surtout votre humour à toute épreuve a fait de cette éreintante expérimentation en mésocosme un moment de bonheur suspendu dans le temps. Et ça donne même envie de recommencer encore et encore. Merci de m'avoir sorti de l'eau (littéralement), pourtant assez bonne pour un jour d'octobre sous la tempête.

Merci à tous les membres de la plateforme Microbex, Patrice, Cécile et Claire pour votre aide précieuse, vos conseils bienveillants et votre soutien pendant ses longues et interminables heures cloîtrées dans le noir, les yeux vissés sur un microscope ou sur un cytogramme.

Cette thèse a été réalisée au sein de cette grande UMR Marbec. Ainsi je voudrais remercier tous ses membres pour leur accueil chaleureux. Merci à Monique pour ses précieux conseils et son aide concernant les statistiques. Merci à Delphine et Frédérique pour m'avoir accordé l'opportunité

d'enseigné avec vous. Merci à Béatrice pour son indéfectible bonne humeur. Merci à Fabien de m'avoir permis de prendre la relève dans la représentation des doctorants au CU, tu étais toujours là pour aider les autres et j'espère avoir continué dans cette voie.

Si j'ai pu faire mes premiers pas dans la recherche, si je me suis familiarisé avec cet univers, si j'ai eu l'envie d'en découvrir encore plus, c'est grâce à vous Philippe, Jory et Gesche. Maitres de stages dans la fonction, vecteurs de vocation avant tout.

Quand on est dans le grand navire de la thèse, on a quelque fois la chance de naviguer avec des collègues, qui deviennent rapidement des amis. C'était mon cas. Tanguy et Justine, mes petits frères et sœurs de thèse, je débarque enfin à bon port, puisses les vents vous êtres favorables pour le reste de votre voyage.

Dans notre bureau nous étions trois à avoir commencé notre thèse ensemble. Nous finissons à trois également, après trois années les coudes serrés. Merci à Raquel et Mariam pour la bonne humeur, la bonne ambiance, les franches rigolades et le soutien permanent.

Comment ne pas vous oublier vous, mes amis du bureau du haut. Le plus bruyant, celui que l'on rejoint aisément les yeux fermés, en suivant les apostrophes et les rires. Ce bureau fait l'effet d'un aimant. Laura et Thibaut, merci pour tout, et même plus encore.

A Montpellier, j'y suis resté longtemps. Et depuis tout ce temps, il y a Antoine, Fanny et Raphaël. Amis, colloqs, confidents, camarades de soirées, il y a 7 ans plus ou moins jour pour jour, nous asseyions côte à côte sur les bancs des amphis de l'Université de Montpellier. Beaucoup de choses ont changés depuis, mais j'ai une montagne de souvenirs à vos côtés. Alors merci pour ça. Bien sûr, je n'oublie pas Yacine, Rudy, Marine et Yann.

Viennent enfin mes amis les plus précieux. Thibault et Mathieu. J'ai toujours pu compter sur vous, en tout instant et toutes circonstances. Depuis les premiers jours, jusqu'aux derniers. Slapsgiving c'est pour toujours. Et Manon, je ne t'oublie pas, voilà bien longtemps que tu nous supportes tous les trois !

Il paraît que chez les italiens, la famille est sacrée. Je ne sais pas si c'est une vérité générale, mais en tout cas chez moi c'est le cas. J'ai une famille exceptionnelle. Papy, Mamie, Nathalie, Patrick, Olivier, Karine, Hugo, Léo, Baptist. Et puis Anaïs aussi, Bibi, Solange, Mariel, Julien, Charlie, Alida. Merci d'être là, tout simplement.

Elsa, tu es mon soutien, ma force, mon énergie, la source de mes convictions. Tu es ma certitude.

Papa, Maman, Nina et Robin, vous êtes mes piliers, sans vous je m'effondre.

À Papy Marcel, c'est un peu grâce à toi que je fais ça, j'espère que tu es fier.

Table des matières

Résumé	I
Abstract	III
Remerciements	V
Liste des figures	XII
Liste des tableaux	XIV
Introduction générale	2
1 Phytoplancton dans l'océan mondial	2
1.1 Généralités sur le phytoplancton	2
1.2 Phytoplancton au sein du réseau microbien	5
1.2.1 Généralités sur le réseau microbien	5
1.2.2 Composantes du réseau microbien	7
1.2.3 Interactions entre micro-organismes au centre du fonctionnement des réseaux	9
2 Efflorescences phytoplanctoniques	15
2.1 Initiation des efflorescences phytoplanctoniques : concepts et paradigmes	15
2.2 Efflorescences phytoplanctoniques : cas des zones côtières peu profondes	18
3 Phytoplancton et réseau microbien face au réchauffement climatique	20
3.1 Changement global et le réchauffement climatique	20
3.2 Effets du réchauffement climatique sur la production primaire océanique	22
3.3 Effets de l'augmentation de la température sur les interactions entre micro-organismes au sein du réseau microbien	23
4 Objectifs et articulation de la thèse	25
Chapitre 1 : Facteurs physico-chimiques d'initiation des efflorescences phytoplanctoniques en zone côtière peu profonde : le rôle de la température	28
Avant-propos	28
Abstract	31
1 Introduction	31
2 Materials and methods	34
2.1 Study site	34
2.2 High-frequency monitoring of the meteorological data, Chl <i>a</i> fluorescence and physical and chemical properties of the water	36
2.3 Weekly monitoring of nutrients, Chl <i>a</i> concentrations, phytoplankton abundance and diversity	37

2.4	Chl <i>a</i> fluorescence correction and bloom identification.....	39
2.5	Data analysis.....	39
3	Results	41
3.1	Bloom identification based on Chl <i>a</i> fluorescence data	41
3.2	High-frequency meteorological and hydrological data	43
3.3	Relationships between Chl <i>a</i> fluorescence, meteorological and hydrological data.....	45
3.4	Time-lag correlations between high-frequency Chl <i>a</i> fluorescence, meteorological and hydrological data.....	47
3.5	Nutrient dynamics	48
3.6	Dynamics of phytoplankton abundances.....	50
4	Discussion.....	54
4.1	Role of water temperature and winter cooling in phytoplankton blooms	54
4.2	Role of other environmental forcing factors in phytoplankton blooms.....	57
4.3	Small phytoplankton species benefit and diatoms lose out in warmer conditions	60
4.4	Toward a general explanation of bloom initiation in shallow coastal waters and general considerations	63
	Acknowledgments.....	66
	Chapitre 2 : Fonctionnement du réseau d'interaction microbien en zone côtière peu profonde : différence entre périodes d'efflorescences et épisodes sans efflorescences.....	68
	Avant-propos.....	68
	Abstract	71
1	Introduction	71
2	Materials and methods.....	74
2.1	Study site.....	74
2.2	Sampling design and planktonic diversity and abundance.....	75
2.3	Microbial network construction and analysis.....	76
2.4	Statistical analysis	78
2.5	Novel approach to detect the statistical differences between empirical networks	79
3	Results	80
3.1	Microbial community phenology	80
3.2	Correlation networks of the microbial communities	82
3.2.1	Comparison between 2015 and 2016 networks.....	82
3.2.2	Comparison between bloom and non-bloom networks	82
3.3	Network degree comparison.....	85
3.4	Interactions between microbial groups.....	86
3.4.1	Comparison based on years 2015 and 2016	86

3.5	Interactions between size classes of microbial groups	89
4	Discussion.....	92
4.1	Network complexity increases during phytoplankton bloom.....	93
4.2	Phytoplankton intraguild competition and interactions with bacteria dominate during bloom 96	
4.3	Bacterivory of ciliates dominate during non-bloom.....	99
4.4	Warming favors interactions among smaller organisms	100
4.5	Warming intensifies trophic cascade.....	101
5	Conclusions	103
6	Acknowledgments	104
7	Supplementary material	105
	Encadré.....	111
	Chapitre 3 : Effet de l'élévation de la température et du zooplancton sur la dynamique des efflorescences phytoplanktoniques : une expérimentation <i>in situ</i>	112
	Avant-propos.....	112
	Abstract	116
1	Introduction	117
2	Material and Methods.....	119
2.1	Experimental design.....	119
2.2	Exclusion of mesozooplankton and increased water temperature treatments	120
2.3	Physico-chemical sampling and analysis	120
2.4	Phytoplankton pigment analysis and bloom identification.....	121
2.5	Statistical analysis	123
3	Results	123
3.1	Physico-chemical dynamic.....	123
3.2	Bloom identification and Chl <i>a</i> dynamic and Bloom identification.....	126
3.3	Taxonomic pigments dynamic	129
3.4	Treatments effects on nutrient, Chl <i>a</i> and taxonomic pigment concentrations during pre- bloom, bloom and post-bloom periods	131
3.4.1	Treatments effects on nutrient concentrations.....	131
3.4.2	Treatments effects on Chl <i>a</i> and taxonomic pigments concentrations	133
4	Discussion.....	136
4.1	Warming reduces the amplitude and the duration of the phytoplankton bloom.....	136
4.2	Warming modifies the phytoplankton succession inducing an early bloom of small green flagellates and a late bloom of diatoms.....	139
4.3	Small green algae and dinoflagellates benefit from warming	140

4.4	The influence of mesozooplankton on the phytoplankton dynamic and composition and its modification under warming.....	142
4.5	Warming disrupts the balance between bottom-up and top-down control of phytoplankton dynamic.....	144
5	Acknowledgments	146
	Encadré.....	147
Discussion générale.....		148
1	Approche de la thèse et apport des différentes méthodes développées.....	148
1.1	Apport des données hautes fréquences dans la compréhension des processus écologiques. 150	
1.2	Apport et perspectives de l'approche réseau.....	152
1.3	Apport et perspectives de l'approche mésocosme.....	154
2	Apport de la thèse à la connaissance des processus écologiques.....	155
2.1	Mécanisme d'initiation des efflorescences phytoplanctoniques en zone côtière	155
2.2	Importance des interactions microbiennes dans la dynamique du phytoplancton et dans le fonctionnement du réseau microbien	158
2.2.1	Fonctionnement des réseaux d'interactions microbiens.....	158
2.2.2	Circulation de l'énergie pendant les périodes d'efflorescences phytoplanctoniques et comparaison avec les périodes de non efflorescence.....	161
2.2.3	Étude des réseaux d'interactions, vers une meilleure compréhension des processus modulant les communautés.....	163
2.3	Avenir des efflorescences phytoplanctoniques et du transfert de l'énergie en zone côtière peu profonde face au réchauffement climatique.....	164
2.3.1	Modification de la phénologie des efflorescences phytoplanctoniques	164
2.3.2	Réduction de l'ampleur des efflorescences phytoplanctoniques	165
2.3.3	Vers une dominance du phytoplancton de plus petite taille au détriment des diatomées 167	
2.3.4	Fonctionnement du réseau trophique microbien et avenir du transfert de l'énergie face au réchauffement climatique	169
3	Conclusion.....	171
Bibliographie.....		173
Annexe 1 : Article du Chapitre 1 version Plos One		205
Annexe 2 : Formations, contribution à la vie du laboratoire, enseignements et congrès scientifiques		234
Annexe 3 : Description de l'ANR PHOTO-PHYTO		235

Liste des figures

Introduction générale

Figure 1: Typologie des traits fonctionnels du phytoplancton lié aux fonctions écologiques.....	4
Figure 2 : Représentation du réseau trophique microbien et de la circulation de la matière et de l'énergie entre ses différentes composantes	6
Figure 3 : Résumé des interactions écologiques entre différentes espèces	10
Figure 4 : Comparaison des trois théories majeures d'initiation des efflorescences phytoplanctoniques	17
Figure 5 : Changements observés et projetés de la température de surface atmosphérique et océanique	21
Figure 6 : Tendances du stock de chlorophylle (Chl) et de la production primaire nette (NPP) dans l'océan global.....	23

Chapitre 1

Figure 1 : Location of the sampling station.....	35
Figure 2 : Chlorophyll <i>a</i> fluorescence and daily net growth rates.....	42
Figure 3 : Environmental variables	45
Figure 4 : Principal component analysis (PCA) of environmental variables	46
Figure 5 : Nutrient concentrations.....	50
Figure 6 : Phytoplankton abundances and diversity.....	52

Chapitre 2

Figure 1 : Weekly abundances of the main microbial plankton groups during 2015 (left panels) and 2016 (right panels).	81
Figure 2 : Correlation networks of the microbial communities in 2015 (left) and 2016 (right).....	84
Figure 3 : Network degree distributions during 2015 and 2016.....	86
Figure 4 : Interactions between microbial food web groups	88

Figure 5 : Interactions between size classes of microbial food web groups.....	91
Supplementary Figure 1	105
Supplementary Figure 2	108
Supplementary Figure 3	110

Chapitre 3

Figure 1 : Daily water temperature means (\pm range of the observations) for the different treatments	124
Figure 2 : The daily mean (\pm range of the observations) of nutrient concentrations in the mesocosms for the different treatments of the experiment.....	126
Figure 4 : Chl <i>a</i> concentrations in the different treatments	127
Figure 3 : Mean (\pm range of the observations) of daily net growth rates (<i>r</i>) of the different treatments	128
Figure 5 : Means of pigment concentrations (\pm range of the observations) in the different treatments.	130
Figure 6 : Median of nutrient concentrations (NO ₂ , NO ₃ , NH ₄ , Si(OH) ₄ and PO ₄) in the mesocosms between the different treatments for pre-bloom, bloom and post-bloom periods.	132
Figure 7 : Median of Chl <i>a</i> concentrations in the different treatments during pre-bloom, bloom and post-bloom periods.....	133
Figure 8 : Median concentrations of taxonomic pigments in the different treatments during pre-bloom, bloom and post-bloom periods.....	135

Discussion générale

Figure 1 : Représentation du réseau trophique microbien et de la circulation de la matière et de l'énergie entre ses différentes composantes	162
Figure 2 : Représentation du réseau trophique microbien et de la circulation de la matière et de l'énergie entre ses différentes composantes pendant les efflorescences en conditions de fortes températures..	170

Liste des tableaux

Chapitre 1

Table 1 : Type and acquisition characteristics of the studied variables	38
Table 2 : Time-lag correlations between meteorological and hydrological data.....	48
Table 3 : Relative contributions of the dominant phytoplankton groups to the carbon biomass and abundance.....	53

Chapitre 2

Table 1 : Network descriptors	84
Supplementary Table 1 : Groups/taxa/species used for the construction of the correlation networks. The following details are provided: group/taxa/species IDs, mean body size, taxonomic classification and size class	105
Supplementary Table 2	109

Chapitre 3

Table 1 : Taxonomic pigments, their abbreviations, taxonomic meaning and theoretical size class.	122
--	-----

Homme libre, toujours tu chériras la mer !

Charles Baudelaire – Les Fleurs du mal

Introduction générale

1 Phytoplancton dans l'océan mondial

1.1 Généralités sur le phytoplancton

Le plancton du grec « planktos » signifiant « errant » a été pour la première fois utilisé par le zoologiste allemand Victor Hensen en 1887. Il désigne l'ensemble des organismes aquatiques vivant librement dans la colonne d'eau, et dont les mouvements propres ne leur permettent pas de lutter contre ceux des masses d'eau les portants. De ce fait, l'ensemble de la vie planctonique (croissance, reproduction, mortalité, etc.) et des interactions entre les organismes (compétition, prédation, mutualisme, etc.) est régi par les paramètres physico-chimiques tels que le mouvement et le mélange des masses d'eau, la température, la pénétration de la lumière, la salinité, la concentration en sels nutritifs ou en matière organique. Le plancton peut être autotrophe, hétérotrophe ou mixotrophe, viral, procaryote ou eucaryote, animal ou végétal, unicellulaire (*e.g.* protozoaire) ou pluricellulaire (*e.g.* métazoaire) et de taille très variable (Sieburth et al. 1978).

Le plancton autotrophe, plus communément appelé phytoplancton (du grec « phytón », « végétal »), est producteur primaire, et se sert donc de la lumière, du CO₂, des sels nutritifs et de l'eau pour fabriquer de la matière organique. De par son ubiquité, le phytoplancton participe à près de la moitié de la production primaire mondiale (Field et al. 1998) malgré le fait qu'il ne représente seulement que 1% de la biomasse des organismes photosynthétique du globe. Il joue donc un rôle crucial dans l'assimilation du CO₂ et sa séquestration sous forme de matière carbonée dans les océans, permettant ainsi de réduire activement la concentration atmosphérique de ce gaz à effet de serre, régulant le climat à l'échelle mondiale (Raven and Falkowski 1999). De ce fait le phytoplancton est considéré comme un

des puits de carbone les plus importants de la planète (Walsh et al., 1981; Raven and Falkowski, 1999). De plus, une part de l'O₂ produit lors de la production primaire est libérée dans l'atmosphère, assurant le renouvellement de l'O₂ respiré par les organismes terrestres. Le phytoplancton procaryote (cyanobactéries) est d'ailleurs considéré comme l'un des premiers producteurs primaires apparu dans l'histoire de l'évolution et est à l'origine de la Grande Oxygénation et la désacidification des océans il y a 2,45 Ga (*giga annum*, milliards d'années) au cours du Paléozoïque (Kopp et al. 2005; Rasmussen et al. 2008).

Le phytoplancton est le support principal d'une large majorité des écosystèmes marins à travers le globe puisque la matière produite par la photosynthèse est la source principale d'énergie alimentant l'ensemble du réseau trophique. Le transfert de l'énergie à l'ensemble de l'écosystème peut se faire de deux façons. La première, majoritairement issue d'une production par le micro-phytoplancton assure le transfert de l'énergie via le broutage direct du phytoplancton par le métazooplancton, venant alimenter les niveaux trophiques supérieurs par prédation. C'est ce que l'on appelle communément le réseau trophique classique, ou herbivore (Cushing 1989). La deuxième, majoritairement issue d'une production pico et nano-phytoplanctonique, assure le transfert de l'énergie aux niveaux trophiques supérieurs des protistes brouteurs. C'est ce que l'on appelle communément le réseau trophique microbien, qui inclut également la production bactérienne (Azam et al. 1983). De ce fait à travers l'océan mondial, le phytoplancton joue un rôle fonctionnel primordial dans le support de la biodiversité des écosystèmes, qu'ils soient côtiers ou océaniques, polaires ou tropicaux.

Au-delà de son rôle de producteur primaire fournissant l'énergie principale nécessaire aux niveaux trophiques supérieurs, le phytoplancton présente une diversité taxonomique et fonctionnelle importante (Falkowski et al. 2004; Litchman and Klausmeier 2008). La diversité taxonomique, basée sur des critères génétiques, est représentée par plusieurs milliers d'espèces phytoplanctoniques qu'elles soient procaryotes (cyanobactéries) ou eucaryotes, réparties en au moins huit groupes phylogénétiques (Falkowski et al. 2004). Par exemple, le groupe des diatomées est considéré comme le groupe assurant

de la plus grosse part de la production primaire à travers le globe jouant donc un rôle majeur dans le transfert de l'énergie aux niveaux trophiques supérieurs (Carstensen et al. 2015).

La très grande diversité taxonomique implique une tout aussi large diversité de traits physiologiques, métaboliques, écologiques et comportementaux, assurant diverses fonctions écologiques (Figure 1). Cette diversité est appelée diversité fonctionnelle (Litchman and Klausmeier 2008). La diversité phytoplanctonique, et notamment fonctionnelle, module fortement les interactions entre organismes, et donc le flux d'énergie au sein des écosystèmes. A titre d'exemple, nous pouvons citer la taille des cellules phytoplanctoniques qui influence l'ensemble des fonctions écologiques et conditionne de ce fait les autres traits écologiques. Des cellules plus petites vont augmenter le rapport surface/volume et donc favoriser l'assimilation et l'utilisation des nutriments (Chisholm 1992), mais seront plus facilement ingérables par les prédateurs (Legrand et al. 1998).

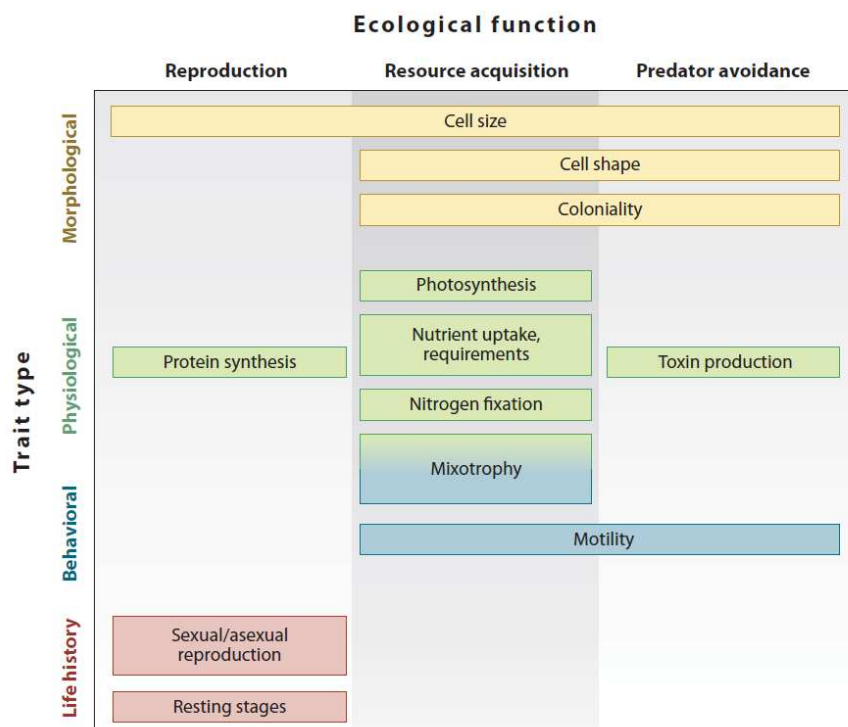


Figure 1: Typologie des traits fonctionnels du phytoplancton liés aux fonctions écologiques. D'après Litchman and Klausmeier (2008).

1.2 Phytoplancton au sein du réseau microbien

1.2.1 Généralités sur le réseau microbien

Le réseau microbien est le réseau d'interactions trophiques entre micro-organismes. Depuis les années 1920, les micro-organismes sont reconnus comme une composante non négligeable dans le fonctionnement des écosystèmes marins (Vernadsky 2012). Cependant, il faudra attendre près de 60 ans pour que le concept de réseau microbien soit établi (Pomeroy 1974). Pomeroy dans ce papier met en évidence le rôle clé de la fraction du phytoplancton de petite taille dans la production primaire, et celui des micro-organismes dans la respiration et dans le transfert de l'énergie vers les niveaux trophiques supérieurs. Jusqu'à ce jour, c'était la chaîne trophique classique ou herbivore (micro)phytoplancton → (méta)zooplancton → poissons qui dominait la notion du fonctionnement des réseaux trophiques. Cette vision était parfaitement adaptée aux organismes planctoniques de grandes tailles, facilement observables et de ce fait, le rôle des micro-organismes a largement été négligé. Plus tard, avec le développement de nouveaux outils d'observation des micro-organismes, tels que le microscope à épifluorescence ou le microscope électronique à balayage (Hobbie et al. 1977), ce modèle simpliste a progressivement été modifié, et le réseau trophique microbien a pris une place fondamentale dans la compréhension du fonctionnement des réseaux trophiques marins.

Ces avancées ont permis de mettre en évidence une autre voie dans le transfert de l'énergie accordée aux métazoaires que la voie autotrophe (Figure 2). Ainsi, une grande partie de la production primaire, celle essentiellement produite par le pico- et le nano-phytoplancton, est consommée (broutée) par des protistes hétérotrophes tels que des flagellés et ciliés. Cependant une partie de cette production primaire peut être également transférée, par exsudation notamment, dans le pool de matière organique dissoute (MOD) assimilable par les bactéries hétérotrophes, qui seront prédatées par le protozooplancton, c'est la boucle microbienne (Azam et al. 1983; Mostajir et al. 2015). A leur tour, ces protistes seront consommés par le métazooplancton, les bivalves et les poissons (Figure 2). C'est ce que l'on appelle la voie de transfert hétérotrophe. Il est estimé qu'une part allant de 10% à 50% de la

production primaire phytoplanctonique n'est pas broutée par les métazoaires mais est exsudée sous forme de MOD, transitant ainsi par la boucle microbienne. Dans un système, quand le transfert de l'énergie se fait de façon significative à la fois par la voie hétérotrophe et par la voie autotrophe, on parle alors de réseau, ou de voie multivore.

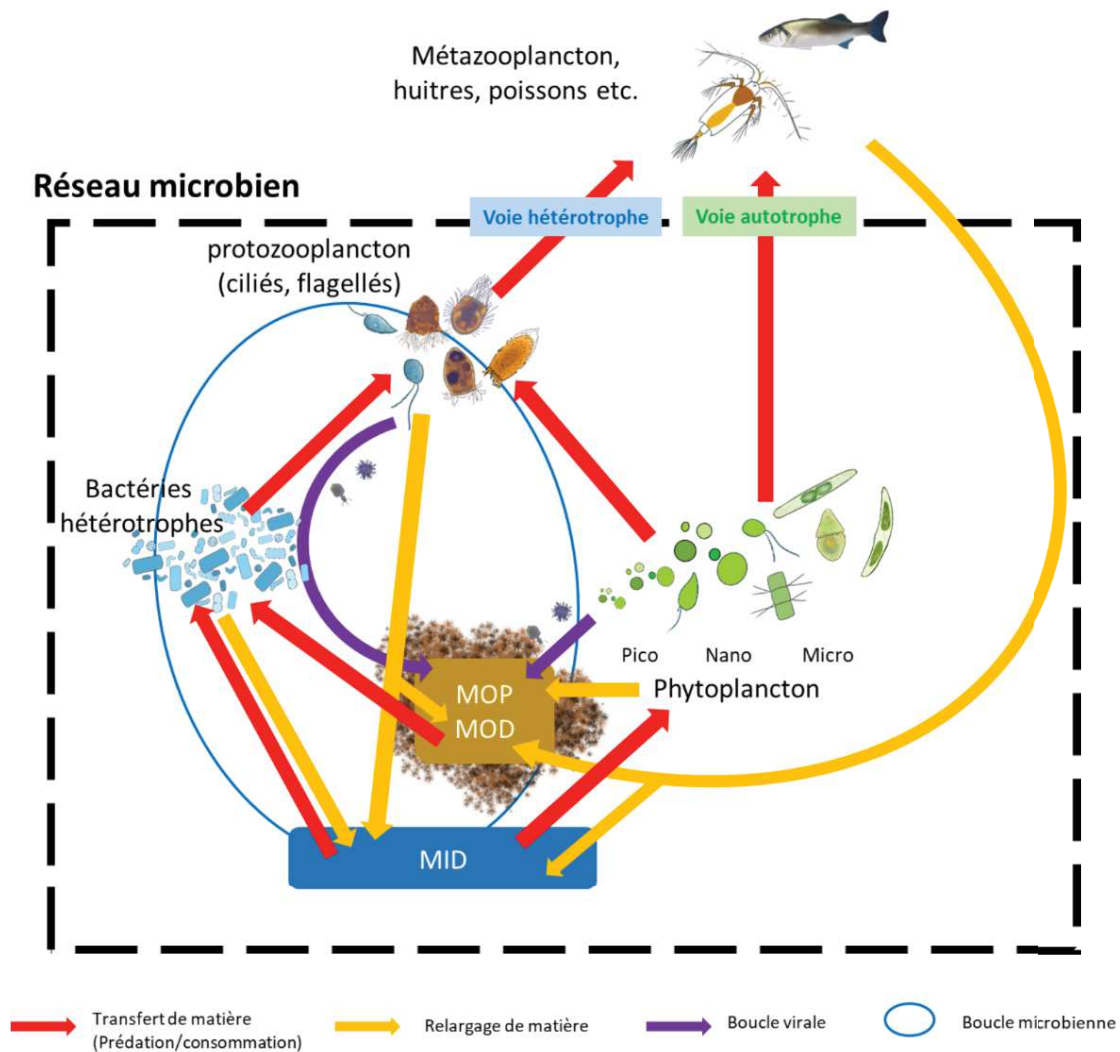


Figure 2 : Représentation du réseau trophique microbien et de la circulation de la matière et de l'énergie entre ses différentes composantes. MOP : Matière organique particulaire ; MOD : Matière organique dissoute ; MID : Matière inorganique dissoute. Le sens des flèches représente le sens du transfert de l'énergie ou de la matière organique. Les flèches violettes indiquent une recharge de MOP/MOD par lyse virale. La taille des organismes ne sont pas proportionnelles à leur taille réelle. L'épaisseur des flèches n'est pas proportionnelle à la quantité de matière circulant. Schéma inspiré de (Mostajir et al. 2015).

1.2.2 Composantes du réseau microbien

Divers types d'organismes interagissant entre eux composent le réseau microbien planctonique. Pour appréhender le fonctionnement de ce réseau, on distingue ces organismes selon différents critères comme leur type cellulaire (acaryote, eucaryote ou procaryote) ou leur mode trophique (autotrophe ou hétérotrophe).

La découverte du rôle des virus dans les écosystèmes marins est relativement récente (Proctor and Fuhrman 1990). L'abondance virale est estimée autour de 10^7 virus mL^{-1} dans les systèmes marins et peut atteindre 10^8 virus mL^{-1} dans les milieux côtiers productifs (Guixa-Boixereu et al. 1999; Suttle 2005). Elle est étroitement liée à l'abondance de leurs hôtes potentiels, les organismes procaryotes (Proctor and Fuhrman 1990; Suttle 2005). Ainsi, les virus représentent le deuxième réservoir de carbone dans les écosystèmes marins après les procaryotes (Suttle 2005). La lyse virale des micro-organismes marins est l'une des causes majeures de mortalité. Elle est même considérée comme ayant une contribution égale à celle de la mortalité due au broutage zooplanctonique (Suttle, 1994; Fuhrman and Noble, 1995). De ce fait, les virus participent activement à la régulation des communautés microbiennes. De plus, ils contribuent significativement aux cycles biogéochimiques via les produits de lyse, notamment par l'apport de MOD (Suttle 2005), et supportent donc paradoxalement la production bactérienne. C'est ce que l'on appelle la « boucle virale ». Il a notamment été montré que cette boucle virale pouvait être responsable de 6 à 26 % de la remise en circulation de la matière organique produite par photosynthèse (Wilhelm and Suttle 1999).

Dans l'étude du fonctionnement des réseaux microbiens, on regroupe souvent les bactéries hétérotrophes et les archées au sein d'un même groupe. Ceci est notamment dû au fait qu'ils partagent des fonctions écologiques communes et qu'ils ne peuvent pas être différenciés par les méthodes de comptage généralement utilisées : la microscopie et la cytométrie. Ainsi, dans ce manuscrit, les bactéries hétérotrophes et les archées seront référencées tout simplement comme « bactéries hétérotrophes ». Ces

bactéries hétérotrophes sont un maillon essentiel du réseau microbien. Après les virus, c'est l'entité biologique la plus abondante dans les milieux marins, allant de 10^5 cellules mL^{-1} dans les milieux oligotrophes, à 10^7 cellules mL^{-1} dans les milieux les plus riches (Mostajir et al. 2015). En plus d'être la source d'une voie trophique à part entière, comme vu précédemment, ces bactéries hétérotrophes jouent un rôle clé dans les cycles biogéochimiques. Elles sont responsables de l'assimilation de la majeure partie de la MOD des océans, et sont donc à l'origine de la plus grande part de la respiration océanique (Azam et al. 1983). Dans ce processus de respiration, sont produits, en plus du CO_2 , des éléments nutritifs tels que le NH_4 et le PO_4 (Kirchman 1994). Ainsi les bactéries hétérotrophes sont à l'origine de la reminéralisation de la MOD, en éléments nutritifs supportant la production primaire.

Le protozooplancton, ou protistes hétérotrophes, comprend l'ensemble des micro-organismes unicellulaires eucaryotes hétérotrophes. De ce fait la plupart de ces organismes sont des brouteurs phagotrophes de phytoplancton, de bactéries ou d'autres protistes hétérotrophes (Kivi and Setälä 1995; Johansson et al. 2004; del Campo et al. 2013). Cependant, de plus en plus d'études montrent qu'une fraction non-négligeable de ces micro-organismes est en réalité mixotrophe, et peut donc moduler leur mode trophique en fonction du type de ressources disponible dans le milieu (Mitra et al. 2014). Dans le réseau microbien, le protozooplancton fait le lien trophique entre la production (bactérienne et pico et nanophytoplanctonique) et le métazooplancton. Le protozooplancton est un terme générique qui englobe une grande diversité taxonomique et fonctionnelle. Nous pouvons notamment distinguer le groupe des flagellés, des ciliés nus (sans lorica) ou des tintinnides (ciliés avec lorica), qui ont des fonctions trophiques différentes au sein du réseau microbien (Sherr and Sherr 2002). Les flagellés hétérotrophes forment un groupe hétérogène d'un point de vue morphologique et physiologique (Sherr and Sherr 2002). Mesurant entre 1 et 30 μm , ils font partie des plus petites classes de taille du protozooplancton, mais la plupart des espèces avoisinent les 5 μm . Ils sont considérés comme les plus petits prédateurs marins (del Campo et al. 2013), et prédatent principalement du picoplancton, plus particulièrement du bactériplancton (Sherr and Sherr 2002). De ce fait, ils sont considérés comme les principaux

contributeurs du transfert d'énergie de la production bactérienne vers les niveaux trophiques supérieurs. Les ciliés nus (sans lorica) sont en moyenne plus gros, avec des tailles allant de 5 à 100 μm , la plupart mesurant autour de 30 μm (Johansson et al. 2004; Foissner et al. 2009). Certains ciliés peuvent présenter une structure minérale extracellulaire protectrice appelée « lorica », ce sont des tintinnes. Ils sont généralement plus gros que les ciliés nus, pouvant mesurer jusqu'à plus de 300 μm (Dolan et al. 2013). Ils sont considérés comme les prédateurs principaux du picophytoplankton et du nanophytoplankton (Sherr and Sherr 2002; Weisse 2002). Ils sont également responsables d'une part importante du broutage des bactéries dans les systèmes côtiers (Sherr et al. 1988; Sherr and Sherr 1994; Weisse 2002). Cependant, les ciliés peuvent aussi être mixotrophes, détritivores, omnivores ou carnivores, participant de ce fait à une partie de la production primaire ainsi qu'à la mortalité due à la prédation du protozooplancton, des flagellés et des ciliés. Bien souvent, ils peuvent adapter ces modes trophiques en fonction des ressources disponibles dans l'environnement (Mitra et al. 2016).

1.2.3 Interactions entre micro-organismes au centre du fonctionnement des réseaux

Les micro-organismes au sein du réseau microbien sont de taxonomie, taille et fonction diverses, et sont soumis à des forçages physico-chimiques variables en fonction du temps et de l'espace. Pour cette raison, les interactions écologiques entre ces organismes sont multiples et diverses. Ces interactions peuvent avoir des effets différents sur les organismes impliqués, des effets positifs (interaction gagnante), négatifs (interaction perdante), ou nuls (Faust and Raes 2012). Les interactions entre deux organismes peuvent donc être classées en fonction des combinaisons de leur résultante : gagnante, perdante ou neutre (Figure 3). Ainsi, on identifie plusieurs types d'interactions entre micro-organismes : la prédation, la compétition, le parasitisme, le mutualisme, le commensalisme et l'amensalisme. L'ensemble de ces interactions affectent la valeur sélective des organismes impliqués, et de ce fait contrôlent la dynamique et la diversité des communautés, et *in fine* le fonctionnement des réseaux microbiens.

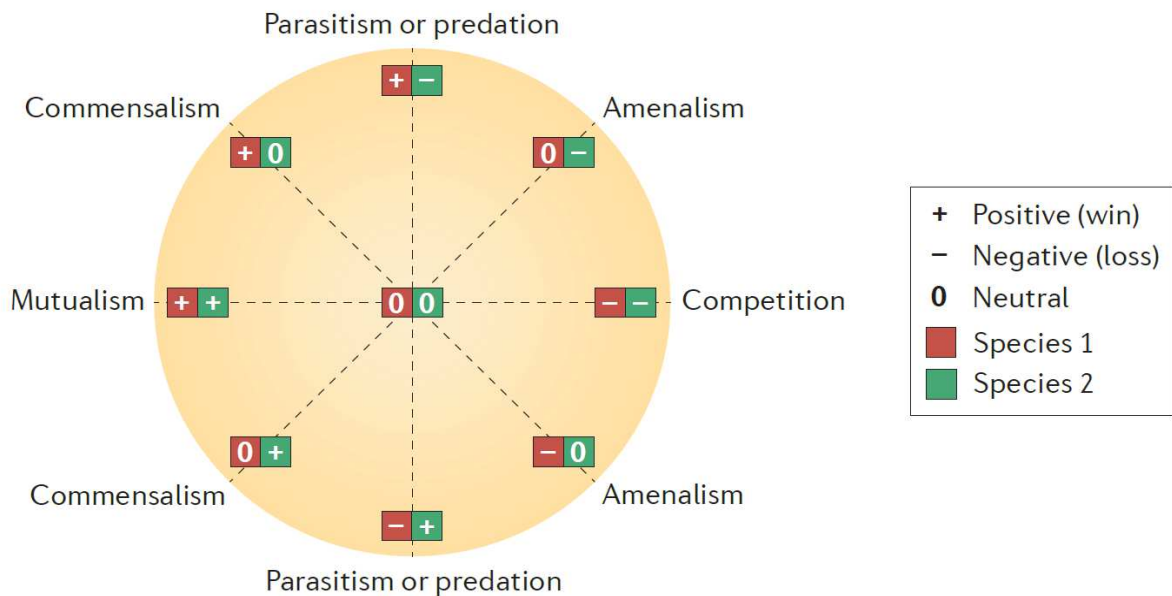


Figure 3 : Résumé des interactions écologiques entre différentes espèces. Cette roue adaptée de Lidicker (1979) représente toutes les paires d'interactions possibles entre organismes. Pour chaque espèce (Species) impliquée dans une interaction, il y a trois résultantes possibles : positive (+), négative (-) ou neutre (0). Figure tirée de (Faust and Raes 2012).

La **prédation** est le type d'interaction le plus décrit dans la littérature et souvent considéré comme l'interaction principale modulant la biodiversité d'un écosystème (Menge and Sutherland 1976). La prédation est l'interaction de consommation d'un organisme par un autre. Ce type d'interaction est essentiellement déterminé par la taille de la proie et celle du prédateur (Hansen et al. 1994). Un organisme sera généralement consommé par les organismes plus gros que lui. On peut distinguer également différents types de prédateurs par le type de proie qu'ils consomment. Ainsi, un consommateur primaire va consommer des producteurs primaires (phytoplancton), un consommateur secondaire prédatra ces consommateurs primaires, et ainsi de suite. De ce fait, ce type d'interaction permet le transfert d'énergie aux niveaux trophiques supérieurs par prédatons consécutives, tout en contrôlant la production des niveaux trophiques inférieurs, supportant ainsi la biodiversité et régulant la dynamique des écosystèmes (Frederiksen et al. 2006). Dans le réseau microbien, les flagellés

hétérotrophes sont considérés comme les premiers consommateurs primaires prédatant essentiellement le picoplancton (del Campo et al. 2013). Les ciliés nus ou tinitinnides, de plus grande taille, sont aussi consommateurs primaires de l'ensemble du phytoplancton en fonction de leur taille, mais peuvent être également consommateurs secondaires de flagellés hétérotrophes ou même d'autres ciliés (Johansson et al. 2004). Ces organismes sont généralement prédatés eux-mêmes par du métazooplancton tel que les copépodes (Calbet and Saiz 2005), assurant le transfert de l'énergie aux niveaux trophiques supérieurs. A noter que certaines espèces prédatrices ciblent des espèces de façon précise, c'est la prédation sélective, tout comme d'autres espèces se nourrissent d'une large diversité de proies, c'est de la prédation généraliste. Au sein du réseau microbien les micro-organismes sont unicellulaires, la prédation se fait par phagocytose ou myzocytose.

La **compétition** est l'interaction de rivalité entre deux organismes (ou deux espèces) pour l'accès à une même ressource limitante (lumière, nutriments, matière organique, etc.), et peut être intra- ou interspécifique (Begon et al. 2006). Ainsi, cette compétition a un effet négatif sur les deux organismes impliqués puisque la ressource en question est partagée. Néanmoins, sur le long terme, l'organisme le plus adapté à l'acquisition de la ressource en question sort vainqueur de cette compétition, au détriment de l'autre. La compétition peut se manifester au travers de plusieurs mécanismes, qu'ils soient directs (interférence ; Case and Gilpin (1974)) ou indirects (exploitation ; Tilman (1982)). La compétition indirecte est basée sur la performance des organismes impliqués dans l'exploitation de la ressource. Cette performance est liée au métabolisme et à la physiologie intrinsèque des deux compétiteurs. L'organisme qui aura le métabolisme ou la physiologie le plus adapté à l'acquisition et à l'utilisation de la ressource convoitée, aura la meilleure croissance et sera donc le gagnant de la compétition, entraînant dans certains cas l'exclusion de l'espèce perdante (Sommer 2002). Par exemple, ce type de compétition peut exister entre deux espèces phytoplanctoniques pour l'accès à la lumière ou aux nutriments, l'espèce la plus compétitive pour l'exploitation de ces ressources ressortant gagnante. Au sein du réseau microbien, ce type de compétition peut également avoir lieu entre le phytoplancton et les bactéries pour

l'accès au phosphore (Vadstein 2000). La compétition directe, ou compétition par interférence, résulte d'une altération de la performance d'acquisition de la ressource d'un organisme envers son compétiteur. Cette compétition peut se traduire par une modification comportementale, par empêchement, agression, ou bien chimique, par la production d'inhibiteurs (Case and Gilpin 1974). Par exemple, de nombreuses espèces phytoplanctoniques sont connues pour libérer des substances allélochimiques affectant la valeur sélective de leurs compétiteurs, et donc leur performance dans l'acquisition des ressources (Rice 2012).

Le **parasitisme** est une interaction par laquelle un des deux organismes impliqués (le parasite) tire profit de l'autre (l'hôte) pour se nourrir, s'abriter ou se développer à ses dépens (Crofton 1971). De ce fait, le parasite en tire un bénéfice au détriment de son hôte. Dans les cas des parasitoïdes, l'infection est létale pour l'hôte (Skovgaard 2014), mais ce n'est pas toujours le cas puisque souvent, ils entraînent seulement une diminution de la valeur sélective de l'hôte (Albaina and Irigoien 2006). Le parasitisme est considéré comme une stratégie relativement commune au sein des écosystèmes marins. Il se révèle être une voie de circulation de l'énergie sous-estimée au sein des réseaux planctoniques, en particulier microbiens (Skovgaard and Saiz 2006; Skovgaard 2014) du fait qu'il soit probable qu'une minorité seulement des organismes parasites planctoniques aient été identifiés (Skovgaard 2014). Le parasitisme est très répandu au sein des micro-organismes marins et n'est pas exclusif de taxons en particulier. La plupart des parasites protistes sont des parasitoïdes, c'est-à-dire létaux pour leurs hôtes. De ce fait, en plus d'être une voie de circulation alternative de l'énergie, les interactions de parasitisme exercent une importante régulation de la population des hôtes (Skovgaard 2014). C'est le cas par exemple des flagellés *Pirsonia* spp. responsables d'infections à large échelle de plusieurs espèces de diatomées en milieu côtier (Schnepf et al. 1990; Kühn et al. 1996; Tillmann et al. 1999). Mais le parasitisme est également une stratégie commune chez les bactéries (Park et al. 2004) et obligatoire chez les virus (Suttle 2005) dans les écosystèmes marins. De plus, quand il entraîne la mort des hôtes le parasitisme devient un important acteur dans les cycles biogéochimiques notamment par l'apport de MOD supportant la production bactérienne.

Le **mutualisme**, est une interaction dans laquelle les deux organismes impliqués en tirent un bénéfice, augmentant leur valeur sélective. Contrairement à la symbiose, cette interaction n'est pas obligatoire pour la survie de ces organismes. Au sein du réseau microbien marin, le mutualisme s'opère essentiellement via échange de ressources organiques ou inorganiques (Kazamia et al. 2016). Les interactions mutualistes entre les bactéries et le phytoplancton sont les plus décrites dans la littérature et semblent être d'une importance fondamentale dans le fonctionnement des écosystèmes marins. De récentes études démontrent que les interactions bactéries-phytoplancton sont essentiellement dominées par du mutualisme, contrairement aux anciennes visions qui suggéraient que ces interactions étaient majoritairement antagonistes, de type parasitisme ou compétition (Amin et al. 2015; Seymour et al. 2017). Ces interactions peuvent impliquer l'échange de différents composés en fonction des espèces. Par exemple, certaines bactéries sont capables de synthétiser des vitamines nécessaires à un certain nombre d'espèces phytoplanctonique. En échange de carbone organique ou d'acides aminés issus d'exsudats, les bactéries fournissent ces vitamines nécessaires à la croissance phytoplanctonique (Croft et al. 2005; Grant et al. 2014; Paerl et al. 2017). D'autres bactéries, fixatrices d'azote, fournissent au phytoplancton l'azote nécessaire à leur croissance en échange de carbone organique (Foster et al. 2011). De récentes découvertes montrent que ces échanges peuvent être bien plus complexes qu'un simple recyclage du phytoplancton détritique par les bactéries. Par exemple, en échange d'ammonium produit par la Rhodobacteraceae *Sulfitobacter* sp. SA11, la diatomée *Pseudo-Nitzschia multiseriis* fournit à ces dernières des composés organosulfurés tels que la taurine ou la DMSP (Amin et al. 2015).

Le **commensalisme** au sein des réseaux microbiens marins peut être souvent confondu avec le mutualisme. Dans le cas du commensalisme, c'est seulement l'un des deux organismes impliqués qui tire un bénéfice de cette interaction en termes de valeur sélective. L'autre organisme impliqué n'est ni positivement, ni négativement affecté par cette interaction. Par exemple, dans les cas des interactions phytoplancton-bactéries décrites plus haut, si l'organisme bactérien en question n'est pas capable de synthétiser des vitamines ou d'azote supportant la croissance phytoplanctonique, celui-ci sera le seul à

tirer bénéfice de cette interaction par l'utilisation des exsudats phytoplanctonique pour sa propre croissance, sans contrepartie (Bratbak and Thingstad 1985). Certains foraminifères tels que *Globigerina bulloides*, *G. falconensis*, *Turborotalita quinqueloba* ou *Hastigerina pelagica* offrent un microhabitat pour des dinoflagellés, favorisant leur maintien dans la zone euphotique lors de leur phase végétative non-mobile en leur fournissant des nutriments via leurs déchets métaboliques et une protection efficace contre les brouteurs (Alldredge and Jones 1973; Spero and Angel 1991).

L'**amensalisme** est un type d'interaction nuisible pour l'un des deux organismes impliqués, sans affecter l'autre. Ce type d'interaction est très peu décrit dans la littérature mais se révèle être commun au sein du réseau microbien. Ce type d'interaction apparait majoritairement lors de l'excrétion par les micro-organismes de produits dérivés de processus métaboliques dans l'environnement. C'est le cas par exemple des bactéries productrices d'antibiotiques affectant la valeur sélective des organismes dans leur environnement proche (Lemos et al. 1991).

La structure du réseau d'interactions microbien, et notamment son rôle dans la circulation de l'énergie et de la matière est très peu connu au sein des écosystèmes marins, et plus particulièrement les zones côtières peu profondes et productives. Il est donc crucial de mieux étudier ces réseaux, leur dynamique et leur restructuration en fonction des différentes périodes de production, comme par exemples les périodes avec efflorescences et sans efflorescence. Une des motivations principales dans la compréhension du fonctionnement des réseaux d'interactions microbiens est notamment de mieux saisir les enjeux liés aux changements globaux, notamment le réchauffement climatique, et ainsi de mieux prévoir le fonctionnement des écosystèmes dans un futur proche plus chaud.

2 Efflorescences phytoplanctoniques

2.1 Initiation des efflorescences phytoplanctoniques : concepts et paradigmes

Dans les écosystèmes marins tempérés, on observe de la fin de l'hiver au printemps une accumulation rapide de biomasse phytoplanctonique que l'on appelle « efflorescence » ou « bloom » en anglais (Cloern 1991; Platt et al. 1991; Alpine and Cloern 1992), pouvant aller de quelques jours à quelques semaines (Behrenfeld 2010). Ces grandes quantités de phytoplancton dans le système entraînent une augmentation de la biomasse des organismes s'en nourrissant, supportant ainsi tout le réseau trophique.

La première théorie sur les facteurs d'initiation des efflorescences fut émise par Sverdrup en 1953 lors des observations d'efflorescences dans les zones hauturières de l'Atlantique Nord (Sverdrup 1953). Selon cette théorie appelée "*Critical depth hypothesis*" (Figure 4A), Sverdrup énonce que l'initiation d'une efflorescence peut se faire seulement quand la croissance phytoplanctonique brute (production par photosynthèse) excède les pertes due à la respiration et la mortalité (broutage, etc.). La capacité de photosynthèse des autotrophes étant corrélée à la pénétration de la lumière dans la colonne d'eau, celle-ci décroît avec la profondeur. En contrepartie, Sverdrup suppose que le taux de mortalité est constant dans toute la colonne d'eau ce qui induit donc l'existence d'une "profondeur critique", au-dessus de laquelle la croissance photosynthétique excède les pertes (croissance nette positive) et permet donc l'initiation des efflorescences. Ainsi, à la fin de l'hiver, quand la limite inférieure de la couche de mélange de surface remonte au-dessus de cette "profondeur critique", la production totale intégrée sur cette couche est supérieure à la mortalité, déclenchant ainsi une efflorescence phytoplanctonique.

Ce paradigme est encore largement répandu de nos jours malgré qu'il ait été remis en question à de nombreuses reprises, du fait des observations ne corroborant pas toujours le modèle proposé par Sverdrup (Townsend et al. 1992, 1994; Behrenfeld 2010). En réalité, le phénomène d'initiation des efflorescences semble beaucoup plus complexe et englobe de nombreux autres facteurs. En effet, il a été observé que les efflorescences phytoplanctoniques pouvaient avoir lieux avant la remontée de la couche

de mélange au printemps, et ce notamment, quand la turbulence de la colonne d'eau s'atténuant au printemps et permet le maintien des organismes phytoplanctoniques en surface suffisamment longtemps pour déclencher une efflorescence (Huisman et al. 1999; Taylor and Ferrari 2011). C'est l'hypothèse de turbulence critique (*Critical Turbulence Depth*) émise par Huisman et al. (1999) (Figure 4B). D'autres études montrent qu'en fonction des systèmes étudiés, ce sont d'autres facteurs physico-chimiques qui régissent l'initiation des efflorescences, comme la teneur en nutriments (contrôle bottom-up) (Alpine and Cloern 1992), les phénomènes de marées (Blauw et al. 2012), les structures hydrodynamiques (Mahadevan et al. 2012), la photopériode (Mignot et al. 2016) ou encore les interactions trophiques (Alpine and Cloern 1992).

Banse (1994), puis plus tard Behrenfeld (2010) et Behrenfeld et al. (2013) remettent en cause la théorie de Sverdrup en émettant l'hypothèse que l'efflorescence phytoplanctonique est due à une perturbation venant rompre temporairement la relation étroite existant entre le phytoplancton et leurs prédateurs (zooplancton herbivore). Ce facteur de perturbation, en altérant la balance entre la croissance phytoplanctonique et la mortalité due au broutage, devient favorable à la croissance et donc à l'accumulation de biomasse phytoplanctonique, initiant ainsi l'efflorescence. C'est l'hypothèse de perturbation-rétablissement (*Disturbance-recovery hypothesis* ; Figure 4C). En Atlantique Nord, ce serait l'abaissement de la limite inférieure de la couche de mélange pendant l'hiver qui serait le facteur de perturbation. En hiver, lorsque la limite inférieure de la couche de mélange est plus profonde, les proies et leurs prédateurs sont dilués dans la colonne d'eau, limitant ainsi la probabilité de rencontre, et entraînant donc la diminution de la pression de broutage et par conséquent la mortalité du phytoplancton. Ainsi, le taux de croissance phytoplanctonique est très faible, mais malgré tout supérieur au taux de mortalité, ce qui entraîne un bilan positif en termes d'accumulation de biomasse laquelle reste relativement faible. Au printemps, quand la limite inférieure de la couche de mélange de surface remonte, elle engendre une concentration des organismes planctoniques et des nutriments dans la couche euphotique entraînant une forte activité photosynthétique et donc de croissance phytoplanctonique.

Cependant cela engendre aussi une plus forte abondance des brouteurs en même temps que leurs proies, augmentant, avec une période de latence, la mortalité phytoplanctonique due au broutage. La pression de prédation est alors supérieure à la croissance phytoplanctonique, mettant fin à l'efflorescence. Behrenfeld et al. (2013) précisent que dans d'autres systèmes, les facteurs de perturbation venant rompre les interactions prédateurs-proies peuvent être différents. Par exemple, pour des efflorescences d'upwellings, ce sont les nutriments qui sont le facteur de perturbation (Wilkerson et al. 2006). La remontée de masses d'eaux chargées en nutriments dans la zone euphotique, due aux vents en zone d'upwelling côtiers par exemple, fournit au phytoplancton les ressources nutritives nécessaires à sa croissance, excédant ainsi les pertes dues au broutage.

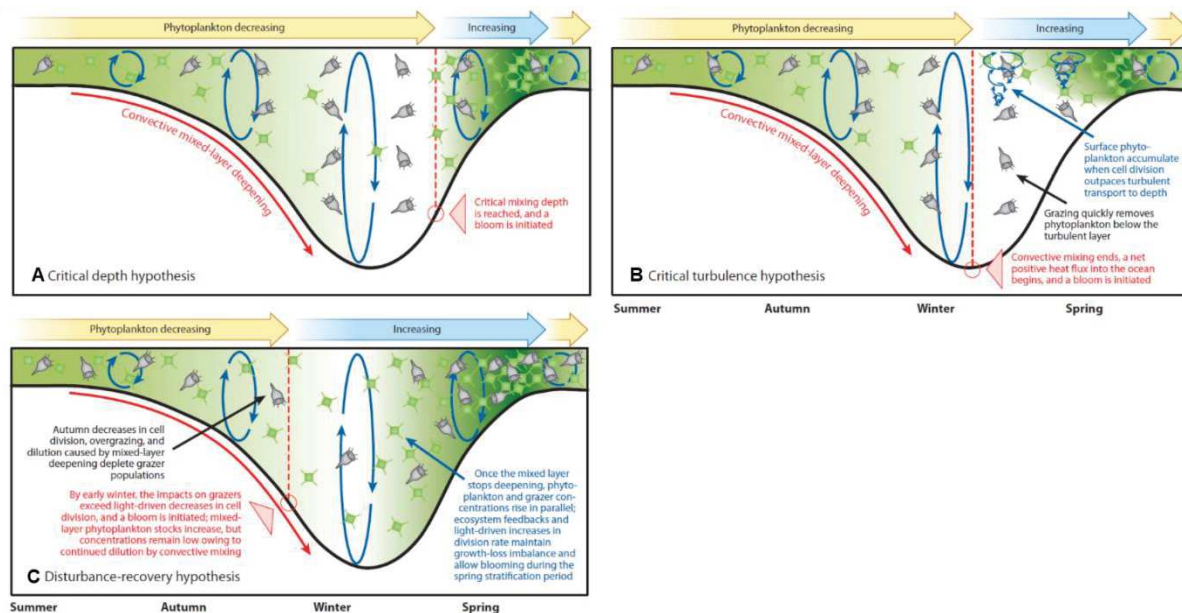


Figure 4 : Comparaison des trois théories majeures d'initiation des efflorescences phytoplanctoniques. (A) The *Critical depth hypothesis*, (B) the *Critical turbulence hypothesis* and (C) the *Disturbance-recovery hypothesis*. Dans ces schémas, le cycle saisonnier commence avec l'été sur la gauche et se termine avec le printemps sur la droite. La densité des cellules phytoplanctoniques vertes et l'intensité du fond vert est proportionnel à la concentration en phytoplancton. Les ciliés en gris représentent les brouteurs du phytoplancton. Les flèches au-dessus de chaque cadre représentent les changements d'abondances phytoplanctoniques. Dans le cadre C, la flèche bleue correspond d'abord à la biomasse phytoplanctonique intégrée sur la colonne d'eau, et ensuite, quand la couche de mélange commence à remonter, elle correspond à la concentration en phytoplancton. La *Critical depth hypothesis* et la *Critical turbulence hypothesis* supposent que le taux de pertes phytoplanctoniques (par unité de temps) est constant. De ce fait, les cadres A et B représentent des concentrations constantes en zooplancton dans le temps. En revanche, les concentrations en phytoplancton et en zooplancton pour la

Disturbance-recovery hypothesis sont corrélées dans le temps. Pour la *Critical depth hypothesis*, les concentrations phytoplanctoniques commencent à augmenter seulement à partir du moment où un seuil de profondeur est atteint. Avant ce point, les concentrations phytoplanctoniques diminuent. Pour la *Critical turbulence hypothesis*, les changements en concentration phytoplanctoniques sont les mêmes que pour la *Critical depth hypothesis* durant la période de plongement de la couche de mélange. Une fois que le flux net de chaleur devient positif, les concentrations phytoplanctoniques proches de la surface commencent à augmenter, tant que les taux de division à la surface surpassent le taux auquel la turbulence distribue ce phytoplancton en profondeur (où ils sont consommés). Pour la *Disturbance-recovery hypothesis*, les changements à l'automne ont un impact plus important sur les brouteurs que sur le taux de division phytoplanctonique (μ), si bien qu'en début d'hiver μ dépasse les pertes (l) et l'abondance du phytoplancton intégré sur la couche de mélange augmente (mais pas la concentration). Cet excès de μ sur l est soutenu durant la stratification printanière car l'augmentation de la pression de prédation se fait en parallèle de l'augmentation de la division phytoplanctonique. Figure modifiée d'après Behrenfeld and Boss, (2014).

2.2 Efflorescences phytoplanctoniques : cas des zones côtières peu profondes

Les zones marines côtières, incluant les estuaires, les herbiers, les récifs coraliens et les plateaux continentaux couvrent seulement 6% de la surface du globe mais sont responsables d'entre 22% et 43% de la valeur mondiale estimée des services écosystémiques (Costanza et al. 1997, 2014). Ils sont d'une importance capitale pour les populations locales puisqu'ils sont sources de matière première, d'alimentation et d'activité récréatives (Costanza et al. 1997). Les zones côtières participent également de façon importante aux cycles biogéochimiques, tel que le cycle des nutriments. De plus, ils jouent un rôle écologique crucial puisqu'ils fournissent des habitats et refuges pour les espèces, participent au contrôle de la biodiversité et jouent un rôle primordial dans la régulation de perturbations environnementales (Costanza et al. 1997).

Les zones côtières peu profondes, particulièrement les lagunes, sont des systèmes très dynamiques sous influences multiples, du fait de leur position à l'interface entre la terre et la mer (Kjerfve 1994). Les forçages tels que les apports des rivières ou marins, les vents, les marées, la balance précipitation/évaporation ou les flux de chaleur en surface affectent de façon importante la dynamique de ces zones (Kjerfve 1994). Ces forçages influencent fortement la teneur en nutriments, la salinité, la

température et la pénétration de la lumière, et conditionnent donc la production primaire dans ces systèmes. De plus, ces milieux sont peu profonds, moins de 5m en moyenne, et donc peu stratifiés sauf en cas de coup de chaleur. Ces zones présentent de façon générale une forte production primaire et secondaire, mais sont très sensibles aux forçages anthropogéniques du fait de leur proximité avec la côte, souvent fortement anthropisée (Kjerfve 1994).

Les efflorescences phytoplanctoniques sont des événements également caractéristiques des zones côtières telles que les estuaires et les lagunes, et surviennent de façon récurrente ou épisodique (Carstensen et al. 2015). Ils sont d'une grande importance dans ces zones puisqu'ils sont à la base du transfert de l'énergie alimentant les réseaux trophiques, supportant les pêcheries (Houde and Rutherford 1993), les cultures aquacoles (Bacher et al. 1998), la respiration des organismes (Hopkinson and Smith 2005) et les processus microbiens, faisant de ces zones des *hotspots* biogéochimiques (Carstensen et al. 2015). Les espèces dominantes composant ces efflorescences côtières sont très diverses en fonction des systèmes (Carstensen et al. 2015). La plupart des efflorescences dans ces systèmes sont dominées par une seule espèce, généralement des diatomées (58%) ou des dinoflagellés (19%), et plus rarement des cyanobactéries, chlorophytes, cryptophytes ou d'autres groupes (Carstensen et al. 2015). La date d'initiation de ces efflorescences peut être également très variable en fonction de la latitude et suit de ce fait le cycle annuel de radiation solaire, avec des efflorescences de plus en plus tardives avec la latitude.

Les facteurs d'initiation des efflorescences phytoplanctoniques en zone côtières sont encore mal connus. Cela provient du fait qu'il existe une grande diversité de systèmes, avec des caractéristiques géologiques, topologiques et environnementales diverses, et qu'elles sont, comme évoqué plus haut, très sensibles aux forçages environnementaux. De plus, dans ces zones, les efflorescences sont initiées en un temps très court, les rendant difficile à appréhender. De ce fait, les nombreux processus venant contrôler la croissance, la mortalité et la dispersion horizontale du phytoplancton, sont responsables du développement des efflorescences. Par exemple, dans la baie de San Francisco, c'est l'intensification

des phénomènes de marées au printemps qui déclenche l'efflorescence phytoplanctonique, par l'apport de nutriments dû à un intense mélange (Cloern 1996). Dans de nombreux systèmes, les apports de nutriments par les rivières sont également déclencheurs d'efflorescences, mais un débit trop important, crée l'effet inverse par dispersion horizontale (Peierls et al. 2012). Dans certains systèmes non-limités par les nutriments, les efflorescences phytoplanctoniques peuvent être déclenchées par l'augmentation de l'irradiance à la fin de l'hiver (Glé et al. 2007). En revanche, il existe à notre connaissance aucune étude qui discute clairement du lien entre les paradigmes généraux d'initiation des efflorescences et les observations *in situ* dans les milieux côtiers peu profonds.

3 Phytoplancton et réseau microbien face au réchauffement climatique

3.1 Changement global et le réchauffement climatique

Depuis l'époque industrielle, l'amélioration de la productivité, de la santé, l'augmentation de la démographie et les constants progrès techniques ont dramatiquement augmenté la pression anthropique sur l'environnement. Cette pression croissante est aujourd'hui reconnue comme étant à l'origine de nombreux changements environnementaux tels que la modification du climat, l'érosion de la biodiversité, la dégradation des sols, l'acidification des océans, la raréfaction des sources d'énergie fossiles, la pollution chimique etc. Tous ces changements sont étroitement liés les uns aux autres par la connectivité des enveloppes superficielles terrestres telles que l'atmosphère, l'hydrosphère, la biosphère ou la géosphère, et par l'évolution globale des pressions anthropiques. De ce fait, ces changements environnementaux sont désormais visibles à l'échelle du globe et sont désignés sous le terme de « changement global ».

Parmi ces changements globaux, le réchauffement climatique est l'un des plus médiatisés et des plus étudiés. Il est dû à l'augmentation de la concentration de gaz à effets de serre dans l'atmosphère, notamment le CO₂, se répercutant sur les températures de surface de l'ensemble des océans. La température atmosphérique a notamment augmenté de 0,78°C en moyenne entre 1901 et 2012 (Figure 5), entraînant une augmentation moyenne de la température de surface des océans de 0,11°C. Les

scénarios du GIEC prédisent une augmentation de la température atmosphérique moyenne à l'échelle du globe de 0,9°C et 5,4°C à l'horizon 2080 en fonction des différents scénarios, entraînant une augmentation de 0,6 à 2°C de la température moyenne de surface des océans (IPCC 2013). La Méditerranée figure parmi les zones susceptibles de connaître les plus importantes augmentations de la température de surface.

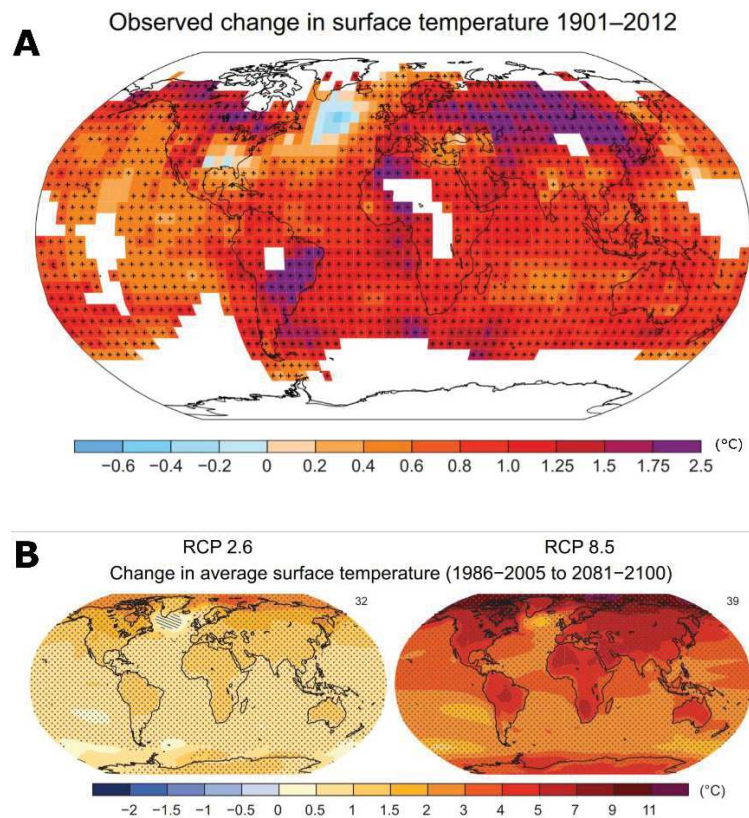


Figure 5 : Changements observés et projetés de la température de surface atmosphérique et océanique. (A) Changements moyens de température observés entre 1901 et 2012, déterminés à partir de régressions linéaires calculées grâce aux observations des anomalies de températures. (B) Projection des changements de la température moyenne de surface entre 2005 et 2100 selon le scénario le plus optimiste (RCP 2.6) et le moins optimiste (RCP 8.5). Ces projections sont basées sur le multi-modèle CMIP5. Les nombres en haut à droite des cartes indiquent le nombre de modèles utilisés pour calculer la projection. Figure modifiée du rapport du GIEC de 2013 (IPCC 2013).

3.2 Effets du réchauffement climatique sur la production primaire océanique

Un des effets majeurs attribués au réchauffement des océans est la diminution de la production primaire nette et de la biomasse phytoplanctonique à l'échelle du globe durant le dernier siècle et plus particulièrement la dernière décennie (Figure 6; Behrenfeld et al. 2009; Boyce et al. 2010). Cette diminution à l'échelle globale est due à l'augmentation de la stratification des océans résultant de l'augmentation de la température, particulièrement aux basses latitudes, qui empêche le mélange vertical et donc l'apport en nutriments supportant la production phytoplanctonique (Polovina et al. 2008; Behrenfeld et al. 2009). Ce déclin de la biomasse phytoplanctonique planétaire est estimé à environ 1% de la médiane globale par année (Boyce et al. 2010). La production phytoplanctonique à l'échelle du globe est en déclin due aux tendances des océans, comptant pour 75% de la production primaire aquatique (Pauly and Christensen 1995). En revanche, la tendance au niveau des zones côtières et des plateaux continentaux s'avère, être à l'augmentation depuis les années 1980 (Boyce et al. 2010). Ce phénomène peut être attribué à l'augmentation de l'eutrophisation côtière et du ruissellement des bassins versants, enrichissant le milieu en éléments nutritifs (Gregg et al. 2005), mais également au réchauffement climatique. Par exemple, dans les eaux de la péninsule Antarctique, le retrait saisonnier précoce de la banquise a augmenté la durée d'exposition de la colonne d'eau aux rayonnements solaires, qui a de ce fait augmenté la production primaire annuelle (Moreau et al. 2015). Dans les systèmes côtiers dont la production est régie par les upwellings, la production primaire annuelle a également augmenté grâce au réchauffement climatique. Dans ces zones, les upwellings induits par des vents côtiers entraînent un déplacement des masses d'eaux et une remontée d'eaux profondes chargées en nutriments, déclenchant d'importantes phases de production phytoplanctoniques. L'augmentation de la température atmosphérique réchauffant davantage les terres que la surface de l'océan, intensifie les vents favorables aux upwellings (Bakun 1990; García-Reyes and Largier 2010), augmentant ainsi la production primaire et l'amplitude des efflorescences dans ces systèmes (Kahru et al. 2009).

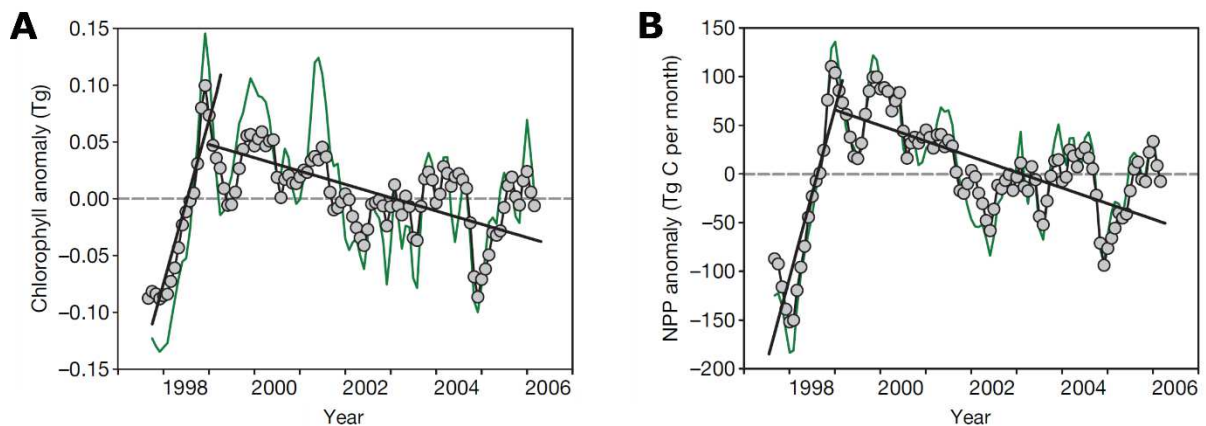


Figure 6 : Tendances du stock de chlorophylle (Chl) et de la production primaire nette (NPP) dans l'océan global. (A) Anomalies globales (ligne verte) et dans les régions de stratification permanente (cercles gris et ligne noire) de la concentration en Chl intégrée dans la colonne d'eau. (B) Anomalies globales (ligne verte) et dans les régions de stratification permanente (cercles gris et ligne noire) de la NPP. Il est à noter que les tendances de la concentration de Chl et de la NPP à l'échelle globale sont essentiellement dues aux changements se produisant dans les régions de l'océan qui sont en permanence stratifiées. D'après Behrenfeld et al. (2009).

3.3 Effets de l'augmentation de la température sur les interactions entre micro-organismes au sein du réseau microbien

Les effets du réchauffement climatique sur les réseaux microbiens à l'échelle globale sont très peu connus. Cela vient notamment de l'absence de suivi de la communauté microbienne à longue échelle et du fait que les micro-organismes sont considérés comme moins sensibles aux changements environnementaux que les organismes pluricellulaires des niveaux trophiques supérieurs (Voigt et al. 2003). Mais il n'est pas à exclure que des effets mineurs à la base des réseaux trophiques peuvent être potentiellement amplifiés le long de la chaîne trophique. Comme précédemment expliqué, les micro-organismes jouent un rôle majeur dans les cycles biogéochimiques ainsi que dans le cycle du carbone, et un changement, même mineur de leur biomasse ou de leur activité peut avoir un impact majeur sur ces processus (Sarmiento et al. 2010). L'augmentation expérimentale de la température est déjà reconnue comme favorisant l'activité hétérotrophique par rapport à l'activité autotrophique des protistes (Rose

and Caron 2007), et également comme augmentant significativement la production et la respiration bactérienne (López-Urrutia and Morán 2007; Vázquez-Domínguez et al. 2007).

De nombreuses études démontrent également l'effet expérimental de l'augmentation de la température sur les interactions au sein du réseau microbien. Notamment, les plus hautes températures favorisent le métabolisme hétérotrophe chez les protistes (Rose and Caron 2007), une augmentation de la température aurait ainsi pour effet d'augmenter le taux de prédation du protozooplancton sur le phytoplancton (Caron et al. 2000; Rose et al. 2009; Peter and Sommer 2012). Les interactions de mutualisme et de commensalisme entre le phytoplancton et les bactéries hétérotrophes sont également reportées comme s'intensifiant avec la température. Il a été récemment montré qu'une augmentation de 4°C de la température augmente significativement le transfert d'azote des bactéries vers le phytoplancton et le transfert de carbone du phytoplancton vers les bactéries (Arandia-Gorostidi et al. 2017). L'augmentation de la température semble également affecter la compétition entre les organismes. C'est le cas par exemple de la compétition pour l'acquisition des ressources chez les protistes bactériovores, où l'augmentation de la température renforce la compétition interspécifique et induit des changements d'espèces exclues et gagnantes par compétition (Jiang and Morin 2004). Ce phénomène est peut-être notamment dû à l'augmentation du taux de consommation pour satisfaire leurs besoins énergétiques avec l'augmentation de la température, qui peut être variable selon les espèces. L'effet de la température sur les interactions entre les virus et leurs hôtes est encore très peu décrit, mais il semblerait que son augmentation favoriserait le taux d'infection virale et la susceptibilité des hôtes (Cottrell and Suttle 1995; Nagasaki and Yamaguchi 1998; Danovaro et al. 2011).

Cependant, à notre connaissance, aucune étude ne s'attarde sur le rôle de la température *in situ* ou en condition expérimentale sur la modification des réseaux microbiens dans leur ensemble afin de mieux comprendre les enjeux du réchauffement climatique sur leur fonctionnement. La potentielle modification de ce fonctionnement peut entraîner des répercussions sur la production des écosystèmes,

et plus particulièrement celles des zones côtières, qui sont considérées comme les plus vulnérables dans le contexte du réchauffement climatique.

4 Objectifs et articulation de la thèse

De par leur rôle majeur dans la productivité des systèmes, dans le maintien de la biodiversité et des services écosystémiques associés, il est crucial de mieux apprécier les mécanismes d'initiation des efflorescences phytoplanctoniques des zones côtières peu profondes et productives. Cependant, nous avons vu que le phytoplancton fait partie d'une mosaïque d'organismes très diversifiés, ayant des rôles, fonctions et caractéristiques propres. Ces organismes sont tous liés différents types d'interactions formant un réseau complexe d'actions et de rétroactions, dans lequel chaque composante est un rouage indispensable au fonctionnement de la machine trophique. Ainsi, pour mieux appréhender les effets des changements globaux et notamment l'augmentation de la température, il est nécessaire de comprendre le fonctionnement des efflorescences phytoplanctoniques en les étudiant au sein du réseau microbien en interaction avec les autres composantes de ce réseau.

L'objectif de cette thèse est d'identifier les forçages responsables de l'initiation des efflorescences phytoplanctoniques et notamment le rôle de la température et des interactions biologiques au sein du réseau microbien. Cet objectif général peut être subdivisé en plusieurs sous-objectifs correspondants aux trois Chapitres de cette thèse :

Chapitre 1 : Facteurs physico-chimiques d'initiation des efflorescences phytoplanctoniques en zone côtière peu profonde : le rôle de la température

Sous-objectif 1 : Déterminer l'influence des facteurs physico-chimiques, notamment la température, dans l'initiation des efflorescences phytoplanctoniques en zone côtière peu profonde et caractériser la dynamique phytoplanctonique durant deux années climatiques contrastées.

**Chapitre 2 : Fonctionnement du réseau d'interaction microbien en zone côtière peu profonde :
différences entre périodes d'efflorescences et épisodes sans efflorescences**

Sous-objectif 2 : Eclaircir le fonctionnement du réseau d'interaction microbien durant les périodes d'efflorescences et les épisodes sans efflorescences, ainsi que sa réponse à des années climatiques contrastées, afin d'identifier le rôle potentiel des interactions dans l'initiation des efflorescences phytoplanctoniques en zone côtière peu profonde.

**Chapitre 3 : Effets de l'élévation de la température et du zooplancton sur la dynamique des
efflorescences phytoplanctoniques : une expérience en mésocosmes *in situ***

Sous-objectif 3 : Dans une expérimentation en mésocosmes *in situ*, déterminer l'influence de l'augmentation de la température ainsi que des différentes fractions de taille du zooplancton (micro- et mésozooplancton) sur la dynamique et la composition de la communauté phytoplanctonique.

J'ai fait le choix de rédiger les chapitres de cette thèse sous forme d'articles scientifiques en anglais (publié, soumis ou en préparation) pour une meilleure valorisation et diffusion des travaux de thèse. Chaque chapitre sera introduit par un avant-propos en français, remplaçant l'article suivant au sein du contexte de la thèse et expliquant l'approche méthodologique utilisée. Une discussion générale en français à la fin du manuscrit de thèse viendra apporter des éléments supplémentaires de discussion sur les apports méthodologiques et écologiques de ces travaux de thèse en faisant le lien entre les différents Chapitres.

Le premier chapitre fait l'objet d'un article publié dans la revue Plos One le 5 avril 2019. La version publiée de cet article est disponible en Annexe 1. Le Chapitre 2 fait l'objet d'un article soumis

Objectifs et articulation de la thèse

tel quel dans la revue *Frontiers in Microbiology* le 2 octobre 2019 et le chapitre 3 est la version la plus aboutie d'un article en vue d'une soumission.

Au cours de cette thèse, j'ai également eu l'opportunité de participer à des formations scientifiques et éthiques, des UE d'enseignement en tant qu'intervenant, des congrès nationaux et internationaux ainsi que de contribuer activement à l'animation scientifique et à l'amélioration de la vie de l'UMR Marbec. Toutes ces expériences venues enrichir mon parcours professionnel sont détaillées en Annexe 2.

Cette thèse est financée par l'ANR PHOTO-PHYTO et ce travail s'inscrit dans ses objectifs. Les objectifs et le détail de cet ANR sont fournis en Annexe 3.

Chapitre 1

Facteurs physico-chimiques d'initiation des efflorescences phytoplanctoniques en zone côtière peu profonde : le rôle de la température

Avant-propos

Ce chapitre a pour objectif de présenter les travaux effectués visant à déterminer l'influence des facteurs physico-chimiques, notamment la température, dans l'initiation des efflorescences phytoplanctoniques en zone côtière peu profonde et caractériser la dynamique phytoplanctonique durant deux années climatiques contrastées.

Les zones côtières peu profondes sont des systèmes très dynamiques répondant très rapidement aux forçages physico-chimiques. Ainsi un moindre forçage peut entraîner une réponse très rapide de la communauté phytoplanctonique. De ce fait, pour identifier les mécanismes responsables de l'initiation des efflorescences, une méthodologie adaptée est nécessaire. En conséquence, pour répondre au présent objectif, un innovant couplage entre un suivi à haute fréquence (toutes les 15 min) multiparamétrique de la fluorescence de la Chlorophylle *a* (Chl *a*) et des paramètres hydrologiques et météorologiques ainsi qu'un suivi hebdomadaire de la concentration en nutriments et de l'abondance et la diversité de la communauté phytoplanctonique, a été réalisé. Ces suivis ont été réalisés de l'hiver à la fin du printemps dans la lagune de Thau sur deux années consécutives, 2015 et 2016. L'année 2015 était une année climatique de référence (Pernet et al. 2012a) tandis que l'année 2016 était exceptionnelle, avec l'hiver le plus chaud jamais enregistré en France (Météofrance).

Les résultats de ce chapitre mettent pour la première fois en évidence le rôle de l'augmentation de la température dans l'initiation des efflorescences phytoplanctoniques en zone côtière peu profonde, ainsi que l'effet d'une année climatique particulièrement chaude sur la composition de la communauté phytoplanctonique *in situ*.

Ce suivi a bénéficié de l'infrastructure MEDIMEER (*Mediterranean platform for Marine Ecosystems Experimental Research*) de l'OSU OREME (Observatoire de Recherche Méditerranéenne de l'Environnement) à Sète. Ayant commencé ma thèse en novembre 2016, j'ai réalisé une partie de l'analyse des échantillons de phytoplancton < 6 µm au cytomètre, et entièrement procédé à l'analyse au microscope inversé de la diversité et l'abondance du phytoplancton 6 – 200 µm. Le suivi sur le terrain, ainsi que les analyses en laboratoire des autres paramètres, ont été conçus et réalisés par les co-auteurs de l'article qui suit, avec l'aide de nombreux stagiaires, techniciens, ingénieurs et chercheurs (Benjamin Sembeil M2 en 2015, Océane Schenkels M2 en 2016, Judith Duhaméeuw M1 en 2015 et M2 en 2016, Ludovic Pancin L3 en 2016 et Cécile Roques AI MARBEC).

Ce chapitre a fait l'objet d'un article publié dans la revue *Plos One* en avril 2019, intitulé : **Water temperature drives phytoplankton blooms in coastal waters**. La version publiée de cet article est disponible en Annexe 1. Seule la bibliographie de l'article publié n'est pas présentée dans ce chapitre. Les références citées dans ce chapitre sont disponibles dans la bibliographie générale, à la fin du manuscrit de thèse.

Water temperature drives phytoplankton blooms in coastal waters

**Trombetta Thomas^{1*}, Francesca Vidussi¹, Sébastien Mas², David Parin², Monique Simier³,
Behzad Mostajir¹**

¹MARBEC (Marine Biodiversity, Exploitation and Conservation), Centre National de la Recherche Scientifique, Université de Montpellier, Institut Français de Recherche pour l'Exploitation de la Mer, Institut de Recherche pour le Développement, Montpellier, France.

²MEDIMEER (Mediterranean platform for Marine Ecosystems Experimental Research), Observatoire de Recherche Méditerranéen de l'Environnement, Centre National de la Recherche Scientifique, Université de Montpellier, Institut de Recherche pour le Développement, Institut National de Recherche en Sciences et Technologies pour l'Environnement et l'Agriculture, Sète, France.

¹MARBEC (Marine Biodiversity, Exploitation and Conservation), Centre National de la Recherche Scientifique, Université de Montpellier, Institut Français de Recherche pour l'Exploitation de la Mer, Institut de Recherche pour le Développement, Sète, France.

*** Correspondence:**

Corresponding Author: Thomas Trombetta; email: thomas.trombetta@cnrs.fr

Keywords: Mesocosm, phytoplankton pigments, phytoplankton composition, global warming.

Abstract

Phytoplankton blooms are an important, widespread phenomenon in open oceans, coastal waters and freshwaters, supporting food webs and essential ecosystem services. Blooms are even more important in exploited coastal waters for maintaining high resource production. However, the environmental factors driving blooms in shallow productive coastal waters are still unclear, making it difficult to assess how environmental fluctuations influence bloom phenology and productivity. To gain insights into bloom phenology, Chl *a* fluorescence and meteorological and hydrological parameters were monitored at high-frequency (15 min) and nutrient concentrations and phytoplankton abundance and diversity, were monitored weekly in a typical Mediterranean shallow coastal system (Thau Lagoon). This study was carried out from winter to late spring in two successive years with different climatic conditions: 2014/2015 was typical, but the winter of 2015/2016 was the warmest on record. Rising water temperature was the main driver of phytoplankton blooms. However, blooms were sometimes correlated with winds and sometimes correlated with salinity, suggesting nutrients were supplied by water transport via winds, saltier seawater intake, rain and water flow events. This finding indicates the joint role of these factors in determining the success of phytoplankton blooms. Furthermore, interannual variability showed that winter water temperature was higher in 2016 than in 2015, resulting in lower phytoplankton biomass accumulation in the following spring. Moreover, the phytoplankton abundances and diversity also changed: cyanobacteria (< 1 µm), picoeukaryotes (< 1 µm) and nanoeukaryotes (3-6 µm) increased to the detriment of larger phytoplankton such as diatoms. Water temperature is a key factor affecting phytoplankton bloom dynamics in shallow productive coastal waters and could become crucial with future global warming by modifying bloom phenology and changing phytoplankton community structure, in turn affecting the entire food web and ecosystem services.

1 Introduction

Ocean phytoplankton generate almost half of global primary production (Field et al. 1998), making it one of the supporting pillars of marine ecosystems, controlling both diversity and functioning.

Phytoplankton in temperate and subpolar regions are characterized by spring blooms, a seasonal phenomenon with rapid phytoplankton biomass accumulation due to a high net phytoplankton growth rate (Cloern 1991). This peak biomass of primary producers in the spring supports the marine food web through carbon transfer to higher trophic levels from zooplankton to fishes. Spring phytoplankton blooms are a common phenomenon in all aquatic systems, from open oceans to coastal waters and from transient waters to inland freshwaters. The magnitude, timing and duration of blooms are as diverse as the ecosystems in which they occur.

For more than half a century, several paradigms and theories have been developed to explain the general mechanism of bloom initiation; however from the earliest critical depth hypothesis of Sverdrup in 1953 (Sverdrup 1953) they have been, and still are, subject to scientific debate. The critical depth hypothesis is a bottom-up model based on abiotic drivers and proposes that a bloom starts when there is sufficient solar radiation and the surface mixing layer becomes shallower. This change induces stratification (Townsend et al. 1992; Behrenfeld 2010; Taylor and Ferrari 2011; Ferrari et al. 2015), allowing phytoplankton to remain in the surface layer, such that their growth rates overcome their losses (i.e., mostly by zooplankton grazing). This hypothesis has been questioned several times, as observations have shown that blooms can occur in the absence of stratification. The mixing layer is defined by density, and since the critical depth hypothesis was put forth, other bottom-up mixing models have been proposed to explain bloom onset. These models are based on actively mixed layers that may occur in turbulence windows (the critical turbulence hypothesis; Huisman et al. (1999)) or under deep convection shutdown (the convection shutdown hypothesis; Ferrari et al. (2015)), allowing the phytoplankton to remain in the surface layer long enough to benefit from favorable light conditions and start a bloom.

Recently, the disturbance recovery hypothesis of Behrenfeld et al. (Behrenfeld et al. 2013b; Behrenfeld and Boss 2014) formalized a new theory based on biotic drivers (top-down control) that had already been suggested several years before (Cushing 1959; Banse 1994). This biotic driver theory

Introduction

proposes that a disturbance factor, such as environmental forcing, disrupts zooplankton-phytoplankton predator-prey interactions, allowing the prey (phytoplankton) to grow rapidly, creating a bloom. Later, when the predator-prey interactions recover, the bloom ends as the losses by predation overwhelm the gains in prey biomass. This general ecological theory was proposed for the North Atlantic, where the establishment of deep-water mixing provides the ecosystem disturbance that disrupts predator-prey interactions. In other systems, different sources of disturbance can play this role, such as monsoon forcing in the Arabian Sea (Marra and Barber 2005) or upwelling in coastal systems (Cushing 1959). However, the role played by bottom-up and top-down drivers in phytoplankton spring blooms is still a source of debate (Chiswell 2013; Behrenfeld et al. 2013c).

Coastal waters and lakes are highly dynamic and productive ecosystems where phytoplankton blooms are common (Sommer 2012; Carstensen et al. 2015). Coastal phytoplankton blooms are a major ecological event providing a substantial part of the annual primary production and energy transfer supporting the entire marine food web. These highly productive periods in coastal systems occur mainly in spring and autumn and are believed to be influenced by several factors such as increasing irradiance, anticyclones and nutrient inputs (Colijn and Cadée 2003; Glé et al. 2007; Tian et al. 2011). However, clear links between general theories and field observations in coastal waters have not yet been established. In particular, the factors that might disturb predator-prey relationships in these shallow systems have been neglected. Coastal waters, including estuaries, sea grass beds, coral reefs and continental shelves, cover only 6% of the world's surface but provide between 22% and 43% of the estimated value of the world's ecosystem services (Costanza et al. 2014). In addition to hosting major biochemical and ecological processes, such as nutrient cycling and biological control, and providing habitats and refugia, coastal waters are of great economic importance for local populations because they provide food, raw materials and recreational activities (Costanza et al. 1997). Coastal waters can be strongly affected by climatic events due to their higher reactivity and lower inertia compared to open-ocean waters, making them highly sensitive to environmental forcing fluctuations (Rabalais et al. 2009).

Nevertheless, in open oceans, increasing water temperature due to global warming changes the start and end timing of the blooms, and reduces their amplitude, affecting the survival and hatching time of commercially important species (Platt et al. 2003; Koeller et al. 2009). Furthermore, experimental studies have shown that warmer conditions change the composition and trophic interactions of plankton communities, propagating the effects to higher trophic levels (Sommer and Lengfellner 2008; Vidussi et al. 2011; Calbet et al. 2014). However, the impact of environmental forcing factors on spring bloom phenology in shallow waters is not well studied, making it difficult to assess the future of coastal water ecosystems in a global climate change context.

The objective of the present study was to investigate spring bloom dynamics and the associated phytoplankton diversity in a typical shallow coastal system to identify the environmental factors triggering the blooms. The study combined high-frequency monitoring of chlorophyll *a* (Chl *a*) fluorescence as a proxy of phytoplankton biomass, high-frequency monitoring of environmental parameters in the air and water and weekly water sampling of the phytoplankton community and nutrients in the water. The study was undertaken during winter and spring of 2015 and 2016 in Thau Lagoon, a typical productive coastal site on the edge of the Mediterranean Sea.

2 Materials and methods

2.1 Study site

The study site, Thau Lagoon (Figure 1), was chosen as it is a productive coastal site of economic interest (principally oyster farms representing 10% of French production) characterized by large seasonal temperature variation (from approximately 4 to 30°C throughout the year; Pernet et al. (2012)). Thau Lagoon is located on the French coast of the northwestern Mediterranean Sea (43°24'00" N, 3°36'00" E). It is a shallow lagoon with a mean depth of 4 m, a maximum depth of 10 m (excluding deep depressions) and an area of 75 km² and is connected to the Mediterranean Sea by three channels. Thau Lagoon is a mesotrophic lagoon with a turnover rate of 2% (50 days), mostly through the Sète channel (Fiandrino et al. 2012). Recent studies have suggested that the lagoon is a phosphorus- and

Materials and methods

nitrogen-limited system (Souchu et al. 2010). The water column was monitored at a high frequency (at mid-depth, approximately 1.5 m below the surface) using several sensors at a fixed station (Coastal Mediterranean Thau Lagoon Observatory 43°24'53" N, 3°41'16" E) (Mostajir et al. 2018a) near the Mediterranean platform for Marine Ecosystem Experimental Research (MEDIMEER), in the city of Sète. This fixed station was also used for weekly water sampling. The depth of the station is 2.5-3 m, and the station is situated less than 50 m from the entrance of the major channel where the water residence time is the lowest (20 days) (Fiandrino et al. 2012); therefore, the station is mostly influenced by seawater intake rather than inland freshwater. Meteorological data were also collected at a high frequency on the MEDIMEER pontoon less than 5 m from the location of high-frequency water monitoring. The study was carried out from January 7 to May 19, 2015, and from December 1, 2015, to July 6, 2016, as part of the French Agence Nationale de la Recherche (ANR) Photo-Phyto project. Hereafter, these two periods are referred to as 2015 and 2016 for simplicity. No specific permissions were required for the sampling site for the present research activities as the study site is not protected. No endangered or protected species were involved in this work.

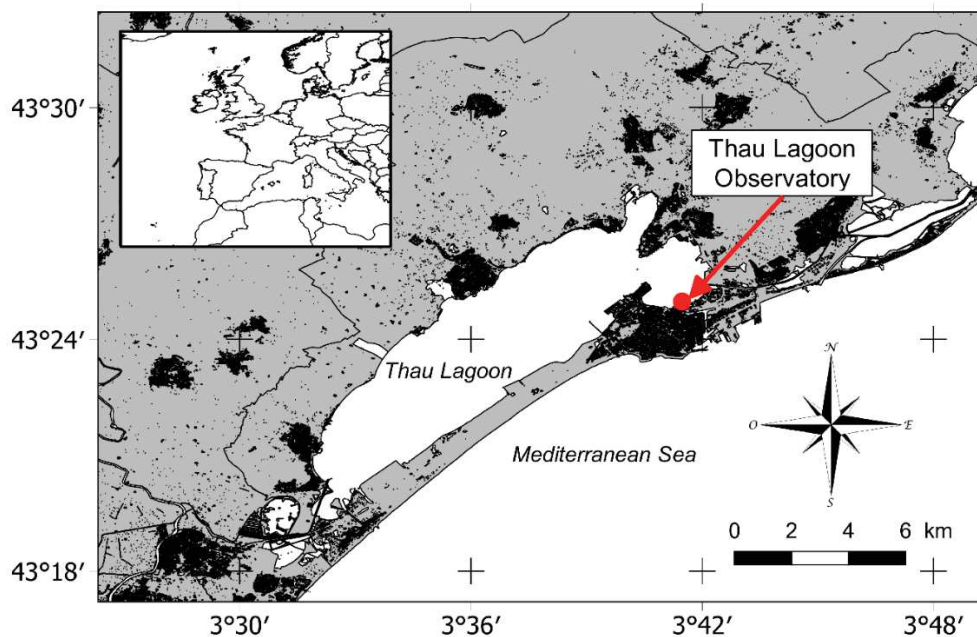


Figure 1 : Location of the sampling station.

2.2 High-frequency monitoring of the meteorological data, Chl *a* fluorescence and physical and chemical properties of the water

For the meteorological parameters (Table 1), air temperature, wind speed and direction, photosynthetically active radiation (PAR, 400-700 nm) and ultraviolet radiation A and B (UVA, 320-400 nm, and UVB, 280-320 nm) were recorded at a high frequency (every 15 min) using a Professional Weather Station (METPAK PRO, Gill instruments) with PAR, UVA and UVB sensors (Skye Instruments).

For the water properties at mid-depth (Table 1), the water temperature and salinity were recorded with an NKE STPS sensor (Table 1). The dissolved O₂ concentration and saturation were recorded using an optical sensor (AADI Oxygen Optode, Aanderaa). The turbidity and the *in situ* Chl *a* fluorescence were recorded with an ECO FLNTU fluorometer (Wetlabs). Water properties were recorded at the same frequency and over the same periods as the meteorological parameters, except for water temperature and conductivity in 2016, where the monitoring started ten days later (from December 11, 2015, to July 6, 2016). All sensors were calibrated before deployment. The temperature sensor was calibrated from 5 to 25°C in 5°C steps using a reference thermometer and thermostatic bath. The salinity sensor was calibrated at 25°C using seawater standards of 10, 30, 35 and 38 (Linearity Pack, OSIL, UK). The 0 standard was made with ultrapure water (MilliQ®). The oxygen sensor was calibrated at 0% and 100% O₂ saturation using the Winkler method (Carritt and Carpenter 1966) for measuring the O₂ concentration. The Chl *a* fluorescence sensor was calibrated using several types of phytoplankton cultures at various concentrations, with the concentrations measured by spectrofluorometry. All sensors were cleaned weekly to prevent biofouling, and measurement drift was checked after each measurement campaign using the same methods as those used to calibrate each sensor.

2.3 Weekly monitoring of nutrients, Chl *a* concentrations, phytoplankton abundance and diversity

In addition to high-frequency monitoring, water samples were collected weekly to determine nutrient and Chl *a* concentrations and phytoplankton abundances and diversity (Table 1). Samples were collected using a Niskin bottle 1 m below the surface from January 15 to May 12, 2015, and from January 12 to July 6, 2016, between 09:00 and 10:00 am.

To determine the nutrient concentrations, 50 mL seawater subsamples were taken using acid-precleaned polycarbonate bottles and then filtered through Gelman 0.45 μm filters that had been prewashed three times. Then, 13 mL of the filtrate was stored at -20°C until analysis. Nitrate (NO_3), nitrite (NO_2), phosphate (PO_4) and silicate ($\text{Si}(\text{OH})_4$) concentrations were measured using an automated colorimeter (Seal Analytical) following standard nutrient analysis methods (Tréguer and Le Corre 1975).

To determine Chl *a* concentrations, 1 L subsamples were taken, filtered through glass fiber filters (GF/F Whatman: 0.25 mm, nominal pore size: 0.7 μm), and stored at -80°C until analysis. Pigment concentrations, including Chl *a* concentrations, were measured by high performance liquid chromatography (HPLC, Waters) following the extraction protocol described in Vidussi et al. (2011) and the HPLC method described by Zapata et al. (2000).

Phytoplankton ($< 6 \mu\text{m}$) abundances were estimated by flow cytometry (FACSCalibur, Becton Dickinson), and phytoplankton (6-200 μm) abundances and diversity, by optical microscopy (Olympus IX-70). For the phytoplankton ($< 6 \mu\text{m}$) abundances, duplicate 1.8 mL subsamples were taken, fixed with glutaraldehyde following the protocol described in Marie et al. (2001) and then stored at -80°C until analysis. Cyanobacteria ($< 1 \mu\text{m}$), picoeukaryotes ($< 3 \mu\text{m}$) and nanoeukaryotes (in this study, 3-6 μm cell diameter; see Results) abundances were estimated using the flow cytometry method described by Pecqueur et al. (2011). Phytoplankton (6-200 μm) abundance and diversity were estimated by microscopy. Duplicate 125 mL subsamples were taken, fixed in 8% formaldehyde and then settled for

24 h in an Utermöhl chamber. Cells of each identified phytoplankton taxon were counted under an inverted microscope. Phytoplankton were identified to the lowest possible taxonomic level (species or genus) using standard keys for phytoplankton taxonomy (Sournia et al. 1986). Carbon biomasses of phytoplankton analyzed by flow cytometry were estimated using the conversion factors of 0.21 pgC cell⁻¹ for cyanobacteria and 0.22 pgC μm^{-3} for picoeukaryotes and nanoeukaryotes (Kemp et al. 1993). For microscopic observations, phytoplankton biovolumes were estimated for the most common taxa using the best shape (Wetzel and Likens 2000), and carbon biomasses were then calculated using the conversion factors (Moal et al., 1987; Menden-Deuer and Lessard, 2000).

Table 1 : Type and acquisition characteristics of the studied variables. PAR: photosynthetically active radiation; UVA and UVB: ultraviolet A and B, respectively; O₂: dioxygen, Chl *a*: chlorophyll *a*; NO₃: nitrate; NO₂: nitrite; PO₄: phosphate and Si(OH)₄: silicate.

Type of data	Acquisition frequency	Variable	Type of instrument
Meteorological	High frequency: every 15 min	Air temperature	Sensor: Professional Weather Station (METPAK PRO, Gill instruments)
		Wind speed	
		Wind direction	
		PAR (400-700 nm)	Light sensors: Skye Instruments
		UVA (320-400 nm)	
		UVB (280-320 nm)	
Hydrological	High frequency: every 15 min	Water temperature	Sensors: NKE STPS
		Salinity	
		O ₂ concentration	Sensors: AADI Oxygen Optode (Anderaa)
		O ₂ saturation	
		Turbidity	Sensor: ECO FLNTU fluorometer (Wetlabs)
Biological	High frequency: every 15 min	Chl <i>a</i> fluorescence	Sensor: ECO FLNTU fluorometer (Wetlabs)
Biological	Weekly	Chl <i>a</i> concentrations	Water sample collected by a Niskin bottle and analyzed using high performance liquid chromatography (Waters)
		Phytoplankton abundances (cell diameter: < 6 μm)	Water sample collected by a Niskin bottle and analyzed using flow cytometry (FACSCalibur, Becton Dickinson)
		Phytoplankton abundances (cell diameter: 6-200 μm)	Water sample collected by a Niskin bottle and analyzed using optical microscopy (Olympus IX-70)
Chemical	Weekly	Nutrient concentrations (NO ₃ , NO ₂ , PO ₄ and Si(OH) ₄)	Water sample collected by a Niskin bottle and analyzed using an automated colorimeter (Seal Analytical)

2.4 Chl *a* fluorescence correction and bloom identification

Chl *a* fluorescence is commonly used as a proxy for phytoplankton biomass. Chl *a* fluorescence data from the fluorometer were corrected using the weekly measurements of Chl *a* concentrations by HPLC to provide coherent high-frequency Chl *a* fluorescence data (Roesler et al. 2017).

Bloom periods were identified by estimating the net phytoplankton growth rate (Eq 1) using the biomass gain or loss (Behrenfeld 2010; Behrenfeld et al. 2013b). The high-frequency Chl *a* fluorescence data over 24 h were used to calculate the daily mean phytoplankton biomass (C_t). The daily net growth rate (here daily net production; r_t) was the difference in phytoplankton biomass between two consecutive days. A negative value indicates a biomass loss, whereas a positive r value indicates a biomass gain.

$$r_{t+1} = C_{t+1} - C_t \quad (1)$$

A bloom was identified as a period 1) that started with at least 2 consecutive days of positive growth rates and 2) where the sum of net growth rates over at least 5 consecutive days was positive. The end of the bloom was the day before 5 consecutive days with negative growth. A 1-day peak of net growth was considered a “sporadic event” and not a bloom. When close successions of 5-day blooms were identified, they were coalesced into “bloom periods” followed by “post-bloom periods” to identify key events. The means of the daily net growth rates were calculated for bloom periods to compare the mean growth rates among the different periods.

2.5 Data analysis

Some of the operations required to maintain the quality of the high-frequency sampling, such as sensor recalibration and cleaning or drift correction, occasionally induced single or multiple missing measurements or outliers, which were removed from the data set. In our study, the fraction of missing values for each variable was generally low, i.e., between 0.06% (water temperature, 2015) and 23.48% (O_2 saturation, 2016). Only the UVA data in 2016 had a higher rejection rate (61.96%), due to a technical problem. Consequently, UVA data were not included in the data analysis for 2016 but were included in

the 2015 analysis. All the other missing high-frequency data were estimated using a moving average in a 480 data point window (5 days) (Rousseeuw 2014).

The daily mean of the high-frequency data except for PAR, UVA and UVB was calculated to remove daily variation patterns; for the three exceptions, the daily cumulative value was calculated. The whole data set (i.e., daily values of biological, meteorological and hydrological data) was kept as a separate set for each study period. The two resulting data sets were divided into separate data sets for each period as bloom periods (winter, early spring and spring), post-bloom periods (post-winter bloom and post-early spring bloom) and a winter latency period. The winter latency period was defined as a period where the daily net growth rate was low, with a mean daily net growth rate close to zero. A post-spring bloom in 2015 and a pre-winter bloom in 2016 were identified. However, these blooms were too short to perform a strong statistical test; therefore, we did not keep them in the analysis of identified periods. These separations between different periods therefore provided 5 data sets for 2015 and 4 data sets for 2016. Then, autoregressive and moving average (ARMA) models were used for each time series in each data set to identify ARMA processes (Aragon 2011) before first-differencing the fitted series to remove stationarity (Pyper and Peterman 1998). Principal component analysis (PCA) was used on the fitted and first-differenced time series in the 2015 and 2016 data sets to identify the relationships between environmental variables graphically. Then, Spearman's rank correlation tests were applied pairwise to highlight significant correlations in the 2015 and 2016 data sets. As Chl *a* may exhibit a delayed response to environmental forcing factors, time-lag correlation tests were performed on the 11 different data sets. Time-lag correlations are based on simple Spearman's rank correlation tests between two variables repeated with time-shifted data to identify the delayed influence of a variable on the Chl *a* dynamics.

The weekly data (nutrient concentrations and phytoplankton abundances and diversity) were kept as a separate data set for each study period but were not divided into identified periods because the quantity of data would have been insufficient (19 data points for 2015 and 23 data points for 2016). For

Results

the high-frequency data, ARMA models were used for each time series in each data set when needed. Paired Wilcoxon signed-rank tests were used to compare the mean values of the phytoplankton abundances and diversity and the nutrient concentrations between the 2015 and 2016 data sets. Sample dates were paired by week number (ISO 8601). For example, the sampling dates of January 8, 2015, and January 12, 2016, both corresponding to the 2nd week of the year, were paired. To identify correlations between weekly data and high-frequency environmental data, daily means of the environmental data for the sampling days were added to the weekly data sets before using ARMA models and first-differencing each time series. Spearman's rank correlation tests were then performed pairwise on the 2015 and 2016 data sets.

3 Results

3.1 Bloom identification based on Chl *a* fluorescence data

Three blooms were identified in 2015, while only two blooms were identified in 2016 (Figure 2A and B). Blooms were defined as consecutive days of biomass gain (positive values of daily net growth rates), while post-bloom periods were consecutive days of biomass loss (negative values; Figure 2C and D, respectively). There were winter blooms in January for 2015 and one month earlier, in December 2015, for 2016 (Figure 2A and B). The 2016 winter bloom was stronger, with Chl *a* concentrations reaching 3.64 $\mu\text{g L}^{-1}$ in 2016 and 2.77 $\mu\text{g L}^{-1}$ in 2015 (Figure 2A and B) and maximum daily net growth rates of 0.54 $\mu\text{g d}^{-1}$ in 2016 and 0.49 $\mu\text{g d}^{-1}$ in 2015 (Figure 2C and D). The mean daily net growth rate was 0.055 $\mu\text{g L}^{-1} \text{d}^{-1}$ in 2016, almost double the 0.031 $\mu\text{g L}^{-1} \text{d}^{-1}$ in 2015. However, it should be noted that the 2015 winter bloom had already started at the beginning of the monitoring. The winter blooms in 2015 and 2016 were followed by post-bloom periods, with the Chl *a* concentration falling to 0.54 $\mu\text{g L}^{-1}$ in 2015 and 0.62 $\mu\text{g L}^{-1}$ in 2016. In 2015, there was an early spring bloom between February 11 and March 11 that was weaker than the preceding winter bloom (maximum Chl *a*: 2.01 $\mu\text{g L}^{-1}$ and mean daily net growth rate: 0.023 $\mu\text{g L}^{-1} \text{d}^{-1}$). This early spring bloom was followed by a post-bloom period, with the Chl *a* concentration falling to 0.54 $\mu\text{g L}^{-1}$. In 2016, however, instead of an early spring bloom,

there was a winter latency period from January 6 to March 11. During this period, the daily net growth rates were low (Figure 2D), with a mean daily net growth rate close to zero. Then, the main spring blooms occurred from April 9 to May 14 (36 days) in 2015 and from March 24 to July 05 (104 days) in 2016. Notably, the monitoring periods had been planned to end on May 19, 2015, and July 6, 2016; therefore the spring blooms might have continued after these dates. In 2016, the spring bloom showed a maximum Chl *a* concentration of $3.16 \mu\text{g L}^{-1}$, which was higher than the value of $2.93 \mu\text{g L}^{-1}$ recorded in 2015, but with a mean daily net growth rate ($0.010 \mu\text{g L}^{-1} \text{d}^{-1}$) lower than that ($0.022 \mu\text{g L}^{-1} \text{d}^{-1}$) recorded in 2015.

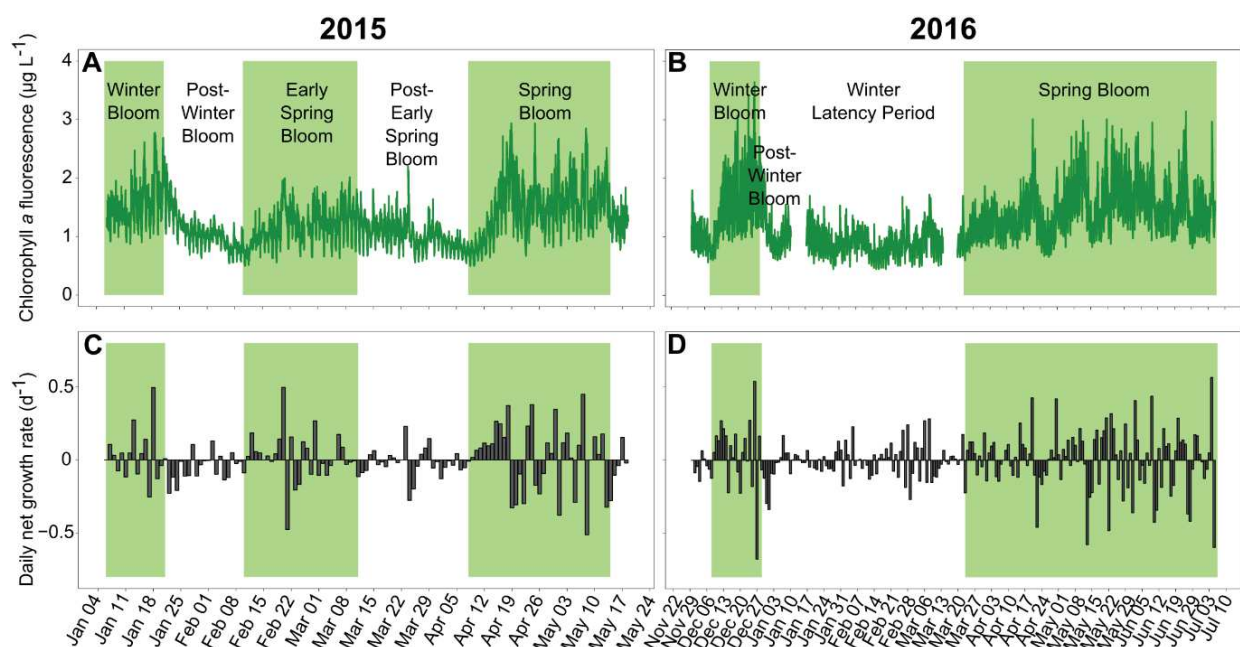


Figure 2 : Chlorophyll *a* fluorescence and daily net growth rates. *In situ* Chl *a* fluorescence in 2015 (A) and 2016 (B) and daily net growth rates in 2015 (C) and 2016 (D), indicating daily biomass gains (positive values) and losses (negative values). The bloom periods have a green background, and the post-bloom periods and winter latency period have a white background.

3.2 High-frequency meteorological and hydrological data

The PAR was lowest when the winter blooms occurred in both 2015 and 2016 (Figure 3A and B). Then, the PAR slowly increased to reach its maximum of 2688 $\mu\text{mol m}^2 \text{s}^{-1}$ on April 19, 2015, and 2865 $\mu\text{mol m}^2 \text{s}^{-1}$ on June 18, 2016.

Two dominant winds were identified. Dominance of wind was based on the frequency of occurrence of wind directions over the two studied periods (Figure 3C and D). The first wind was from the northwest (49.5% of the data between 270° and 359°), and the second was from the southeast (21% of the data between 90° and 180°). There were three windy periods with northwesterly winds (median of 302°) in 2015 (Figure 3E) during the post-winter bloom period (max = 16.6 m s^{-1}), the early spring bloom period (max = 17.4 m s^{-1}) and the post-early spring bloom period (max = 16.5 m s^{-1}). The wind speed was lower during the winter bloom, the onset of the early spring bloom and the spring bloom (means of 3.3, 1.9 and 3.1 m s^{-1} , respectively). In 2016 (Figure 3F), the wind speeds were low during the winter bloom (mean = 1.8 m s^{-1}); otherwise, the wind was erratic, with numerous short windy events exhibiting mean wind speed values higher than those observed during the winter bloom.

During the 2015 study period, the mean air temperature dropped from 19.9°C in early January to 1.1°C in early February (Figure 3G). It then increased until the end of the study period, with a maximum of 25.7°C on May 14. During the 2016 study period, the air temperature was stable from early December to mid-March (mean: 10.9±2.7°C, minimum: 2.9°C and maximum: 18.5°C) with a quick chill in early January (Figure 3H). Then the air temperature increased from mid-March until the end of the study period, with a maximum of 30.8°C on July 7.

The water temperature was less variable than the air temperature (Figure 3I and J). In 2015, the water temperature was stable during January (8.5±0.6°C), decreased to a minimum of 4.0°C on February 6 and then increased to 21.7°C on May 14. In 2016, the water temperature was 11.8±0.5°C from December 12 to January 11, followed by a quick chill to a minimum of 7.0°C on January 17. Then, the

water temperature was stable until March 10 ($9.9\pm 0.8^{\circ}\text{C}$), followed by an increase until the end of the study period, reaching a maximum of 25.1°C on July 6.

The salinity was also different between 2015 and 2016 (Figure 3K and Figure 3L). In 2015, the salinity was 34.95 ± 0.56 , while in 2016, it was higher (37.34 ± 0.95) and more variable and exhibited a large decrease during April, reaching a minimum value of 33.85 on April 18.

The turbidity (Figure 3M and N) was 1.69 ± 0.87 NTU in 2015, which was lower than the 2.25 ± 1.06 NTU observed in 2016, with sporadic peaks reaching 13.15 NTU in 2015 and 14.19 NTU in 2016.

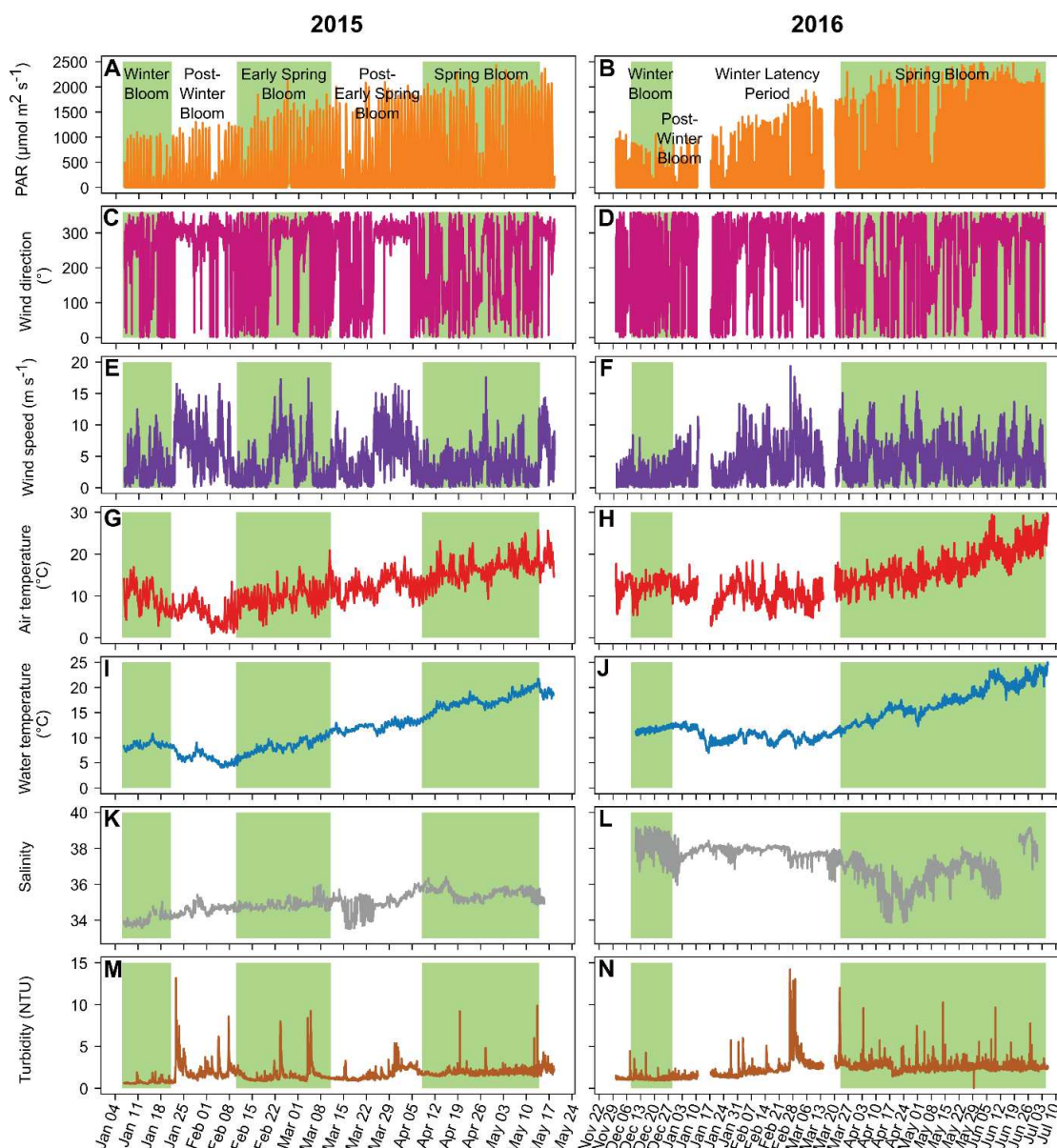


Figure 3 : Environmental variables. Main environmental variables for 2015 (left) and 2016 (right). A to H are the meteorological data: PAR (A and B), wind direction (C and D), wind speed (E and F) and air temperature (G and H); and I to N are the hydrological variables: water temperature (I and J), salinity (K and L) and turbidity (M and N). The background colors for the various periods are the same as in Figure 2.

3.3 Relationships between Chl *a* fluorescence, meteorological and hydrological data

The general relationships between Chl *a*, meteorological and hydrological data in 2015 and 2016 based on PCA are shown in Figure 4A and B. For both data sets, there was a group on the second

axis, comprising the wind conditions (speed and direction) and turbidity. Spearman's rank correlations were strong between wind speed and wind direction for both data sets (2015: $\rho = 0.38$, p -value < 0.001 ; 2016: $\rho = 0.48$, p -value < 0.001). However, the turbidity was correlated with the wind conditions in 2015 (speed: $\rho = 0.41$, p -value < 0.001 ; direction: $\rho = 0.19$, p -value < 0.05) but not in 2016. Another group, on the first PCA axis of both data sets, comprised the light parameters, i.e., PAR, UVA (only in 2015) and UVB, and oxygen concentration and saturation. Spearman's rank correlations were significant between light conditions and oxygen (2015: all p -values < 0.01 ; 2016: all p -values < 0.001). Chl *a* fluorescence was opposed to both these groups in both 2015 and 2016, with significant negative correlations with the wind conditions (all p -values < 0.05) and the light conditions (all p -values < 0.05). The PCA for both data sets also showed a positive correlation between water temperature and air temperature (2015: $\rho = 0.36$, p -value < 0.001 ; 2016: $\rho = 0.29$, p -value < 0.001). The water temperature was positively correlated with Chl *a* fluorescence in 2015 ($\rho = 0.25$, p -value < 0.01) but not in 2016.

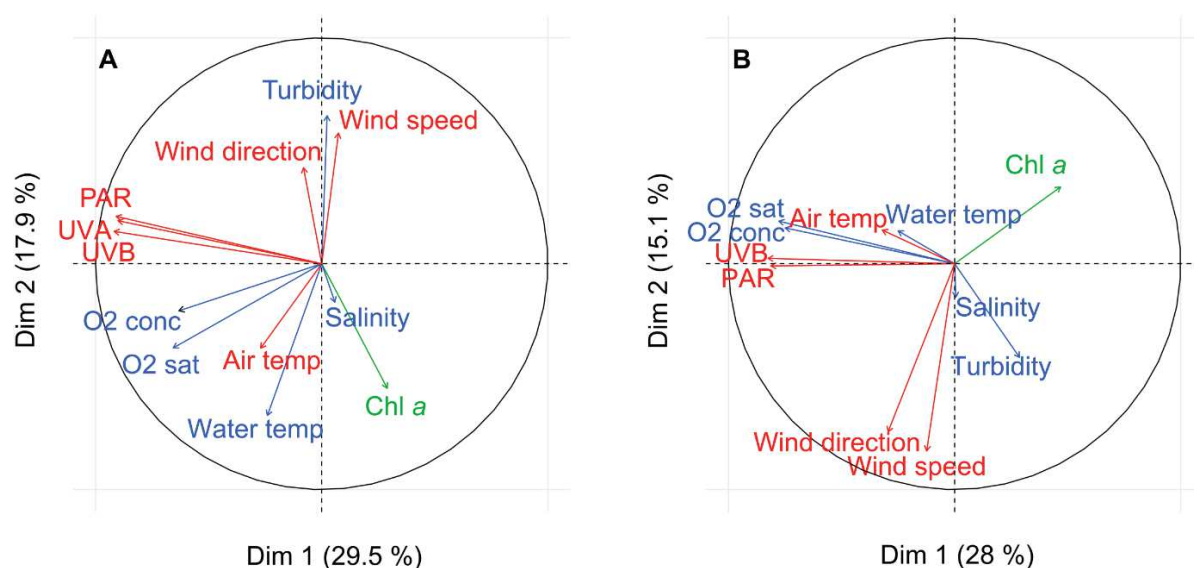


Figure 4 : Principal component analysis (PCA) of environmental variables. PCA of Chl *a*, meteorological and hydrological data for the 2015 data set (A) and 2016 data set (B). PCA allows the variables to be projected in multidimensional space to highlight the relationships between them. Here, only two dimensions are represented as they explain the environmental dynamic well. The arrows represent the variables. When arrows are far from the center and close to each other, they are positively correlated, whereas when they are symmetrically opposed, they are negatively correlated. If the arrows are orthogonal, they are not correlated. Finally, when the variables are close to the center, they are not

well projected in the dimensions represented; consequently, it is hard to conclude that a relationship occurs between these variables. In this last case, to highlight masked links, we coupled the PCA with pairwise Spearman's rank correlations as described in the Material and methods.

3.4 Time-lag correlations between high-frequency Chl *a* fluorescence, meteorological and hydrological data

As Chl *a* fluorescence may have exhibited a delayed response to environmental forcing factors, the time series were tested for time-lag correlations (Table 2). Chl *a* fluorescence was positively correlated with the water temperature (0- and 5-day lags, strong p -values < 0.01) as well as salinity (1- and 3-day lags, p -values < 0.05) in both the 2015 and 2016 data sets. As found using PCA, Chl *a* fluorescence was negatively correlated with the light conditions (PAR, UVA and UVB), with a 0-day lags in both 2015 and 2016. However, there was a positive correlation between Chl *a* fluorescence and light conditions with a 1-day lag, but only in 2015. There were negative correlations between Chl *a* fluorescence and wind conditions (speed and direction) with a lag of 0 to 2 days in both 2015 and 2016 (p -values < 0.05).

For the separate periods (bloom, post-bloom and winter latency periods), Chl *a* fluorescence was positively correlated with water temperature, with a lag of from 0 to 5 days during four of the five bloom periods (p -values from < 0.05 to < 0.001). Chl *a* fluorescence was negatively correlated with the wind conditions (speed and/or direction), with a range of lags between 0 and 4 days for four blooms (p -values from < 0.05 to < 0.001). Salinity was positively correlated with Chl *a* fluorescence during the early spring bloom in 2015 (p -value < 0.001) and negatively correlated with Chl *a* fluorescence during the winter bloom in 2016 (p -value < 0.001). Chl *a* fluorescence was negatively correlated with light conditions for 3 blooms with 0-day lags (p -values from < 0.05 to < 0.001), while for the spring bloom in 2015, they were positively correlated with a 1-day lag (p -value < 0.05). There was little correlation during the post-bloom periods. Chl *a* fluorescence was negatively correlated with PAR and UVA during the post-winter bloom in 2015 (5-day lags, p -value < 0.05) as well as with the wind speed in for 2016

(0-day lag, p -value < 0.05) and was positively correlated with the wind direction (5-day lags, p -value < 0.05) during the post-early spring bloom period in 2015.

Table 2 : Time-lag correlations between meteorological and hydrological data. Spearman's rank time-lag correlations between Chl *a* fluorescence and environmental variables in 2015 and 2016. Whole: tests performed on the whole data set for a study period. Only significant results are shown. The signs + and - represent significant positive and negative correlations, respectively; a single sign represents p -value < 0.05; ++ or -- represents p -value < 0.01; and +++ or --- represents p -value < 0.001. The time lag (in days) and coefficient of the correlations are in parentheses. For example, +(2;0.40) represents a positive correlation with a p -value < 0.05, 2-day lag and coefficient of 0.40. The bloom periods have a green background.

Year	Period	PAR	UVA	UVB	Wind speed	Wind direction	Air temperature	Water temperature	Salinity	Turbidity
2015	Whole	-- (0;0.27) +++ (1;0.31)	-- (0;0.24) +++ (1;0.32)	- (0;0.22) +++ (1;0.31)	- (0;0.17) -- (1;0.28)	-- (0;0.24)		++ (0;0.25)	+ (3;0.18)	
	Winter Bloom					++ (0;0.71) -- (4;0.79)				
	Post-Winter Bloom	- (5;0.56)	- (5;0.55)							+ (3;0.54)
	Early Spring Bloom	- (0;0.40)	- (0;0.39)		+ (5;0.43)			+++ (0;0.60)	+++ (0;0.56) - (4;0.43)	- (0;0.38)
	Post-Early Spring Bloom					+ (5;0.54)				
	Spring Bloom	- (0;0.41) + (1;0.39)	-- (0;0.43) + (1;0.41)	- (0;0.41) + (1;0.39)	+ (2;0.40)	-- (0;0.53)		+ (2;0.35)		
2016	Whole	--- (0;0.38)		--- (0;0.36)	- (0;0.17) - (2;0.30)	-- (0;0.30) - (2;0.15)		++ (5;0.17)	+ (1;0.15) ++ (3;0.21)	+ (0;0.16)
	Winter Bloom					-- (0;0.57)		+ (0;0.54)	--- (0;0.72)	
	Post-Winter Bloom				- (0;0.86)					
	Winter Latency Period	- (0;0.25) ++ (3;0.32)		-- (0;0.31) ++ (3;0.34)		- (0;0.24) ++ (4;0.32)			++ (3;0.32)	++ (0;0.35) -- (1;0.32)
	Spring Bloom	--- (0;0.44)		--- (0;0.44)	--- (0;0.35) + (5;0.21)	-- (0;0.27) - (1;0.22) + (5;0.23)		- (0;0.25) - (2;0.20) + (5;0.21)		

3.5 Nutrient dynamics

During the winter bloom and the post-winter bloom periods, the PO₄, NO₂ and NO₃ concentrations were on average 3 to 9 times lower in 2015 (0.01±0.00, 0.07±0.03 and 0.72±0.24 μmol L⁻¹, respectively) (Figure 5A, E and G) than in 2016 (0.09±0.05, 0.20±0.05 and 2.26±0.63 μmol L⁻¹, respectively) (Figure 5B, F and H). The Si(OH)₄ concentration (Figure 5C and D) in 2015 (8.67±2.05 μmol L⁻¹) was, however, twice that in 2016 (3.86±0.57 μmol L⁻¹) over the same period. In 2015, the

Results

Si(OH)₄ concentrations then gradually decreased until the end of the early spring bloom, reaching a mean of $2.14 \pm 0.29 \mu\text{mol L}^{-1}$ in March.

In 2015, from the early spring bloom to the end of the spring bloom, the PO₄, NO₂ and NO₃ concentrations remained at the same levels as in the winter, even though there were peaks in the PO₄ ($0.08 \mu\text{mol L}^{-1}$) and NO₃ ($6.01 \mu\text{mol L}^{-1}$) concentrations on March 12. In 2016, over the same period, the PO₄, NO₂ and NO₃ concentrations fluctuated more than in 2015, but the mean values were similar (0.04 ± 0.06 , 0.04 ± 0.02 and $1.24 \pm 0.83 \mu\text{mol L}^{-1}$, respectively). The mean Si(OH)₄ concentration during the spring bloom in 2015 ($1.62 \pm 1.00 \mu\text{mol L}^{-1}$) was approximately half that in 2016 ($2.74 \pm 0.80 \mu\text{mol L}^{-1}$).

Wilcoxon signed-rank tests showed that the PO₄ and NO₃ concentrations were significantly higher in 2016 than in 2015 (p -values < 0.05). The N:P ratios (Redfield ratios) were between 11 and 94 (mean: 45 ± 25) in 2015 and between 6 and 124 (mean: 46 ± 35) in 2016. Spearman's rank correlations showed significant correlations between Chl *a* and nutrient concentrations in neither 2015 nor 2016.

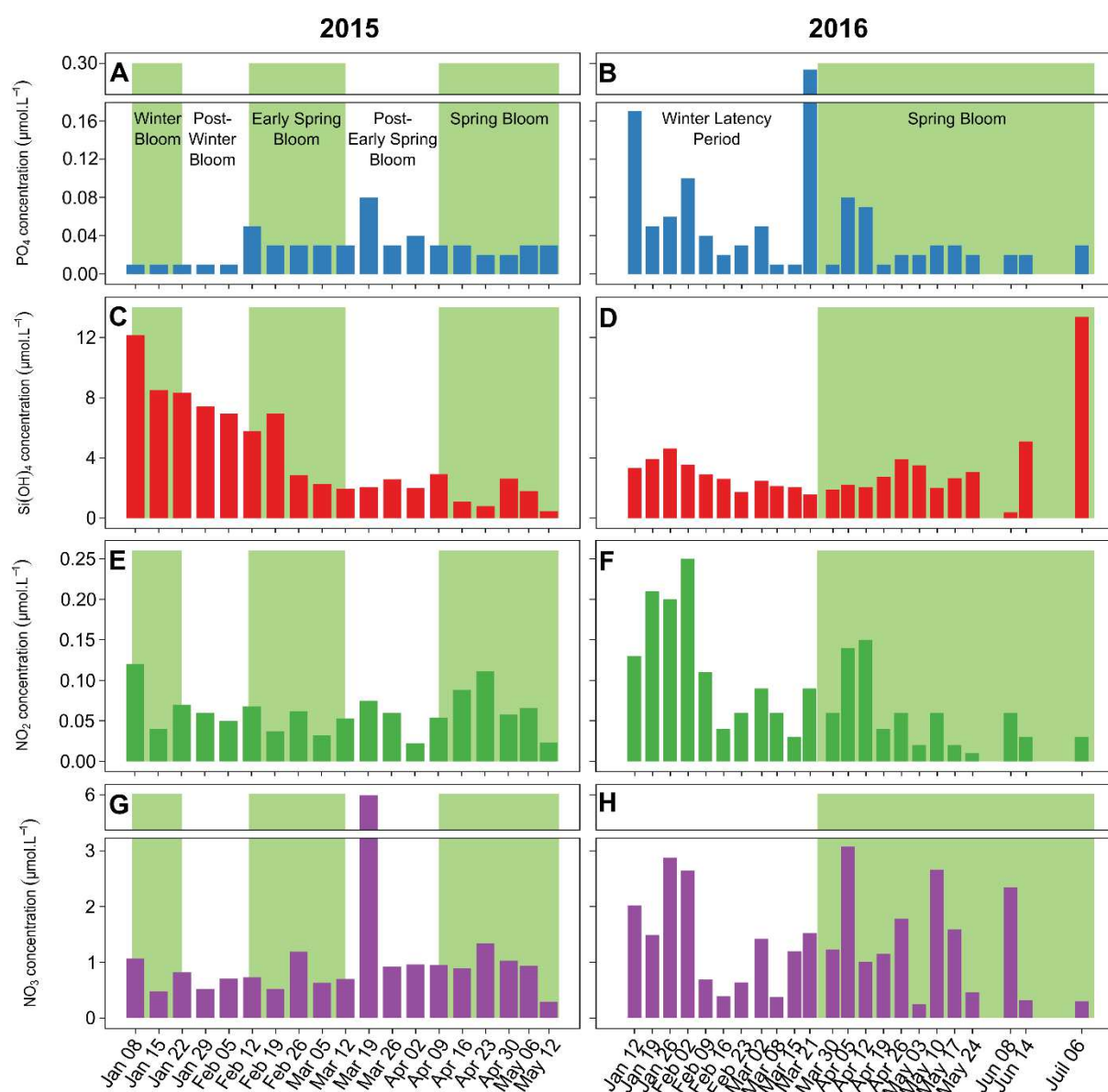


Figure 5 : Nutrient concentrations. Nutrient concentrations in 2015 (left) and 2016 (right) for PO_4 (A and B), Si(OH)_4 (C and D), NO_2 (E and F), and NO_3 (G and H). The background colors for the various periods are the same as in Figure 2.

3.6 Dynamics of phytoplankton abundances

Three groups of picophytoplankton, namely, cyanobacteria ($< 1 \mu\text{m}$ diameter), picoeukaryotes ($< 1 \mu\text{m}$ diameter) and picoeukaryotes (1-3 μm diameter), and one group of nanoeukaryotes (3-6 μm diameter) were enumerated by flow cytometry (Figure 6A to D). The abundances of picoeukaryotes ($< 1 \mu\text{m}$ and 1-3 μm) and nanoeukaryotes were similar between 2015 and 2016: the total abundance of

Results

these three groups was $2.14 \pm 1.30 \times 10^4$ cells mL⁻¹ in 2015 and $2.84 \pm 1.41 \times 10^4$ cells mL⁻¹ in 2016. However, the mean abundance of picoeukaryotes and nanoeukaryotes during the spring bloom in 2016 ($6.53 \pm 1.38 \times 10^4$ cells mL⁻¹) was more than twice that in 2015 ($2.84 \pm 1.73 \times 10^4$ cells mL⁻¹). One of the main differences between 2015 and 2016 was that during winter and early spring, the cyanobacteria (< 1 µm) abundance in 2016 ($2.19 \pm 2.19 \times 10^3$ cells mL⁻¹) was almost 10 times higher than that in 2015 ($3.02 \pm 2.55 \times 10^2$ cells mL⁻¹). Then, during the spring bloom, cyanobacteria abundances increased to a maximum on May 06, 2015 (6.01×10^4 cells mL⁻¹), and a lower maximum on May 10, 2016 (2.70×10^4 cells mL⁻¹). The Wilcoxon signed-rank test showed that the mean abundances of cyanobacteria (p -value < 0.01), picoeukaryotes (< 1 µm) (p -value < 0.01) and nanoeukaryotes (p -value < 0.05) were significantly higher in 2016 than in 2015, but there was no significant difference for picoeukaryotes (1-3 µm). Tests for correlations between the biological variables (picophytoplankton and nanophytoplankton abundances and Chl *a* fluorescence) and the environmental variables (wind conditions, light conditions, salinity, air and water temperature, oxygen, turbidity and nutrients) showed a negative correlation of picoeukaryotes (1-3 µm) with PO₄ concentrations in 2015 ($\rho = -0.54$, p -value < 0.05) and with NO₃ in 2016 ($\rho = -0.50$, p -value < 0.05). Picoeukaryotes (< 1 µm) were negatively correlated with wind conditions in 2015 (wind speed: $\rho = -0.57$, p -value < 0.05; wind direction: $\rho = -0.50$, p -value < 0.05).

The patterns of community composition and total abundances of phytoplankton (6-200 µm) were different between 2015 and 2016 (Figure 6E to J). The total abundances of phytoplankton (6-200 µm) were quite similar during winter and early spring in 2015 (266 ± 81 cells mL⁻¹) and 2016 (212 ± 91 cells mL⁻¹). During the spring bloom, however, the total phytoplankton (6-200 µm) abundances in 2015 were almost three times those in 2016 (982 ± 433 cells mL⁻¹ and 378 ± 123 cells mL⁻¹, respectively). This result was confirmed by the Wilcoxon signed-rank test showing that total phytoplankton abundances (6-200 µm) were significantly higher in 2015 than in 2016 (p -value < 0.01). The maximum abundances of phytoplankton (6-200 µm) were reached on May 6, 2015, and June 8, 2016 (1470 cells mL⁻¹ and 923 cells mL⁻¹, respectively). In 2015, during the winter and early spring blooms and their post-bloom

periods, the phytoplankton community was dominated numerically by *Plagioselmis prolonga*, a cryptophyte with a diameter of 8-12 μm ($41\pm 13\%$), and chlorophytes ($\sim 6 \mu\text{m}$) ($38.0\pm 8.5\%$). In addition, chrysophyceae ($\sim 6 \mu\text{m}$) were also abundant during the early spring bloom ($18\pm 2\%$). In 2016, *P. prolonga* dominated the phytoplankton (6-200 μm) community during the winter latency period and the first 11 weeks of the spring bloom ($48\pm 11\%$), and chlorophytes ($\sim 6 \mu\text{m}$) were also abundant but less abundant than in 2015 ($29\pm 9\%$). *Pseudo-nitzschia* sp. (25-50 μm) and *Chaetoceros* spp. (10-50 μm), which are large, colonial diatoms, successively dominated the phytoplankton (6-200 μm) community during the spring bloom in early April 2015 ($72\pm 13\%$) and the second part of the spring bloom from mid-May 2016 ($65\pm 23\%$) until the end of the study periods. *Chaetoceros* spp. abundances were significantly lower in 2015 than in 2016 (Wilcoxon signed-rank test, p -value < 0.05), but *Pseudo-nitzschia* sp. abundances were not.

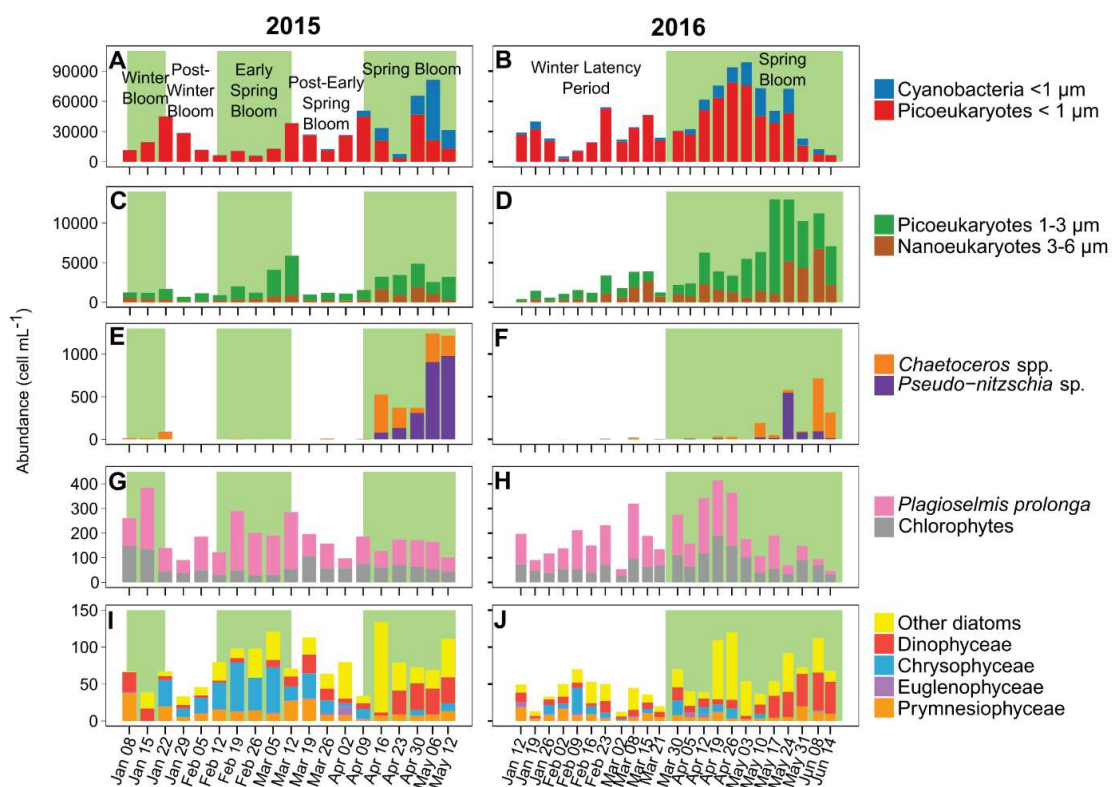


Figure 6 : Phytoplankton abundances and diversity. Analyzed by flow cytometry for 2015 (A and C) and 2016 (B and D). Dominant taxa observed by microscopy for 2015 (E, G and I) and 2016 (F, H and J). The background colors for the various periods are the same as in Figure 2.

Results

The phytoplankton community was dominated numerically by picoeukaryotes (< 1 µm), accounting for 51 to 95%, depending on the period (Table 3). However, in terms of carbon biomass, picoeukaryotes were never dominant. In 2015, the carbon biomass was dominated by *P. prolonga* in the winter and early spring blooms and by *Chaetoceros* spp. in the spring bloom. Nanoeukaryotes contributed most of the carbon biomass throughout 2016.

Correlations between weekly measurements of phytoplankton abundances (6–200 µm), Chl *a* fluorescence and environmental variables were calculated separately for 2015 and 2016. In 2015, *P. prolonga* abundance ($\rho = -0.60$, p -value < 0.05) was negatively correlated with PO₄ concentration, and *Chaetoceros* spp. abundance was positively correlated with Chl *a* fluorescence ($\rho = 0.67$, p -value < 0.01). In 2016, *Pseudo-nitzschia* sp. abundance was positively correlated with Chl *a* fluorescence ($\rho = 0.55$, p -value < 0.05), and *Chaetoceros* sp. abundance was positively correlated with NO₃ concentration ($\rho = 0.58$, p -value < 0.01).

Table 3 : Relative contributions of the dominant phytoplankton groups to the carbon biomass and abundance. Mean relative contribution (in percent) to the carbon biomass (C) and numerical abundance (Ab) of the dominant phytoplankton groups during each period. Species and period abbreviations and background colors are the same as in Table 2. The highest contribution for each period is in bold.

	2015								2016							
	Winter Bloom		Post-Winter Bloom		Early Spring Bloom		Post-Early Spring Bloom		Spring Bloom		Winter Latency Period		Spring Bloom			
	C	Ab	C	Ab	C	Ab	C	Ab	C	Ab	C	Ab	C	Ab		
Cyanobacteria (< 1 µm)	0.17	0.62	0.54	0.89	0.38	1.54	1.10	1.92	7.81	40.60	3.48	6.83	5.67	19.82		
Picoeukaryotes (< 1 µm)	6.86	90.50	16.03	94.74	5.49	79.06	14.43	89.49	2.78	51.43	12.38	86.50	5.45	67.86		
Picoeukaryotes (1-3 µm)	4.81	4.07	8.60	3.25	15.05	13.88	16.49	6.54	3.62	4.29	7.96	3.56	9.73	7.75		
Nanoeukaryotes (3-6 µm)	28.52	3.01	13.44	0.64	35.26	4.06	28.87	1.43	14.26	2.11	46.23	2.59	39.87	3.97		
<i>Plagioselmis prolonga</i>	31.99	0.92	19.02	0.24	37.41	1.17	27.93	0.38	4.50	0.18	22.43	0.34	6.77	0.18		
<i>Chlorophytes</i>	14.68	0.81	5.61	0.14	4.63	0.28	9.11	0.23	1.58	0.12	5.91	0.17	2.69	0.14		
<i>Chaetoceros</i> spp.	12.97	0.08	36.76	0.10	1.78	0.01	1.92	0.01	52.96	0.45	1.43	0.00	27.31	0.17		
<i>Pseudo-nitzschia</i> sp.	0.00	0.00	0.00	0.00	0.00	0.00	0.14	0.00	12.48	0.82	0.17	0.00	2.50	0.11		

4 Discussion

4.1 Role of water temperature and winter cooling in phytoplankton blooms

Based on the time-lag correlations, water temperature played a significant role in determining Chl *a* dynamics, especially the onset of blooms (Table 2). This is the first time that rising water temperature has been identified as the main factor triggering phytoplankton blooms in an aquatic ecosystem (ocean, coastal zone or lake). This relationship was true for all the main blooms observed in 2015 and 2016, and the strength, number of occurrences and consistent positive sign of the correlations between water temperature and Chl *a* fluorescence suggested that water temperature was the main driver. Other parameters such as wind conditions and salinity were correlated with blooms (see below) but the number of occurrence and non-consistent sign of the correlations suggested that they were not the main drivers. The water temperature was positively correlated with Chl *a* fluorescence with 0 to 5 days of lag suggesting that the biomass accumulation represented by increasing Chl *a* fluorescence was driven by the increase in water temperature over the 5 previous days. Furthermore, every bloom onset corresponded to a period of increase in water temperature, while such correspondence was not detected for other parameters.

The effect of temperature on phytoplankton physiology and metabolic processes is well known. First, under light-saturated conditions, higher temperature increases specific phytoplankton productivity by acting on photosynthetic carbon assimilation (Lewandowska et al. 2012; Falkowski and Raven 2013). In addition, under non-limiting nutrient conditions, an increase in water temperature increases phytoplankton nutrient uptake (Gillooly et al. 2001; Cross et al. 2015). Moreover, phytoplankton growth rates increases with increasing of temperature, almost doubling with each 10°C increase in temperature (Q_{10} temperature coefficient) (Rose and Caron 2007). Furthermore, the growth rate of phytoplankton is higher than that of herbivorous grazers at low temperatures (Huntley and Lopez 1992; Rose and Caron 2007). Thus, an increase in water temperature, particularly at relatively relative low *in situ* temperatures such as those in this study (6-14°C), can be more favorable for phytoplankton than for their grazers,

Discussion

allowing phytoplankton biomass accumulation, which starts the bloom. Therefore, the initiation of phytoplankton biomass accumulation can result from phytoplankton growth temporarily exceeding grazing-induced losses as a result of increasing temperature.

In previous studies, water temperature was identified as the main driver of blooms of particular species, especially cyanobacteria (Liu et al. 2011; Hunter-Cevera et al. 2016). However, the present study underlined that an increase in water temperature triggered blooms of all phytoplankton community blooms, not just a particular species. Furthermore, the spring blooms started at a temperature of 13.9°C in 2015 and 11.2°C in 2016, while the early spring bloom in 2015 began when the water temperature was 6.1°C. This wide water temperature range for bloom initiations indicates that there is not a threshold water temperature that triggers phytoplankton blooms; instead, blooms are initiated by an increase in water temperature.

Interannual comparison showed that winter 2015/2016 was the warmest winter recorded in France according to MétéoFrance (<http://www.meteofrance.fr/climat-passe-et-futur/bilans-climatiques/bilan-2016/hiver>), which led to exceptionally high winter water temperatures. In contrast in 2015, the winter cooling of the water was typical of this coastal site. As a result, the Chl *a* dynamics in 2016 were completely different from those in 2015 (Figure 1). The absence of an early spring bloom and the slower biomass accumulation during the 2016 spring bloom can be explained by the difference between the meteorological conditions. The abnormally high water temperature during the 2016 winter may have been the cause of biomass stagnation during the winter latency period, slowing phytoplankton biomass accumulation during the spring. The absence of significant winter cooling and the relatively mild water temperatures may have allowed predators (e.g., ciliates and copepods) as well as filter feeders (e.g., oyster and mussels) to remain active during this period and maintain grazing pressure on the phytoplankton (Peter and Sommer 2012; Sommer et al. 2017), in turn delaying the ecosystem disturbance required to start a bloom until mid-March, when the water temperature started to rise. Therefore, winter water temperature seems to be a crucial factor influencing the dynamics of the spring

bloom in temperate shallow coastal zones. The effect of the winter water temperature on the magnitude of the spring bloom has already been reported (Martens 2001; van Beusekom et al. 2009), with larger spring blooms and more phytoplankton biomass after cold winters and smaller spring blooms after mild winters in the Wadden Sea. With global warming, these mild winters could become more frequent (Solomon et al. 2007) and may reduce phytoplankton biomass accumulation during spring blooms. This modification of the bloom phenology might potentially change the structure of the plankton community assemblages and, therefore, directly affect the food web. Such modification is particularly important in shallow temperate coastal zones of economic interest as changes in bloom phenology and magnitude may affect fish and shellfish production.

There were short (2-3 weeks) winter blooms in both 2015 and 2016. Winter blooms are known to occur in marine ecosystems, but they are less common than spring blooms. Winter blooms can be rare, exceptional events (Wang et al. 2016), but they may occur regularly every year, as in the Bahia Blanca Estuary in Argentina (Guinder et al. 2015) or in tropical and subtropical seas (Madhupratap et al. 1996; Banse and English 2000; Tseng et al. 2005). Winter blooms in the coastal site of the present study were recorded once before, in December 1993 (Souchu et al. 2001; Collos et al. 2009), whereas the present study documented winter blooms of a magnitude similar to that of the spring bloom in two consecutive years. These winter blooms represent an important part of annual primary production (daily mean net growth rates of $0.055 \mu\text{g L}^{-1} \text{d}^{-1}$ in 2015 and $0.031 \mu\text{g L}^{-1} \text{d}^{-1}$ in 2016), providing food for the whole plankton food web, and can sometimes be the most important biomass accumulation event during the year (Guinder et al. 2015). Winter blooms in shallow coastal zones are generally triggered by a combination of forcing factors such as high nutrient concentrations due to autumn rains, an increase in light penetration into the water column due to a reduction in suspended matter or sediments and low grazing pressure due to low water temperature or tidal conditions (Guinder et al. 2015). In this study, water temperature was associated with the increase in Chl *a* fluorescence during the winter bloom of 2016. For 2015, however, the winter bloom had already been triggered when the monitoring started, and the link between water temperature and Chl *a* for this winter bloom could not be established as the time-

lag correlations could not be determined. Additional observations will be necessary to establish whether an annual winter bloom has become a rule, which might indicate that an ecological shift has occurred in this system. The winter bloom may also have been the result of particular climatic/environmental conditions that occurred during the study period. In fact, even though the impact of the El Niño-Southern Oscillation (ENSO) on the Mediterranean climate is still a source of discussion (Kalimeris et al. 2017), 2015 was a strong El Niño year with an ENSO Oceanic Niño Index (ONI) value of approximately 2, making it less important than that in 1997-1998 but more than that in 1991-1992 (Jacox et al. 2016), which could potentially explain the exceptional 2015-2016 winter climatic conditions.

4.2 Role of other environmental forcing factors in phytoplankton blooms

Nutrient input from runoff, rain events or sediment resuspension is widely considered a key factor triggering blooms in coastal zones. However, there was no direct link between nutrient concentrations and Chl *a* fluorescence in this study, suggesting that nutrients are not the sole driver of Chl *a* dynamics and that a more complex functioning drives blooms in this mesotrophic system (Figure 5). The absence of a link with nutrient concentrations could be explained by the meteorological conditions of this shallow coastal system, where the wind causes a fairly constant nutrient supply from sediment resuspension, which can maintain the necessary nutrient level for phytoplankton growth but does not produce inputs large enough to reveal show a direct link. The wind conditions (speed and direction) were correlated with Chl *a* fluorescence with 0- to 5-day lags throughout the study periods and during three bloom periods each (Table 2). These correlations may indicate that high-speed winds, generally from the northwest (the tramontane, Figure 3 and 4), reduce biomass accumulation, while low-speed winds, generally from the east and southeast increase biomass accumulation. Millet and Cecchi (1992) already reported this relationship between wind conditions and Chl *a* dynamics in this shallow coastal lagoon. They suggested that a wind speed of 4 m s⁻¹ was optimal for balancing the beneficial effect of vertical turbulent diffusion and the detrimental influence of horizontal advection dispersion. In our study, wind speed was significantly correlated with turbidity, which was probably caused by

sediment resuspension (in particular, peaks of wind speed coincided with those of turbidity, Figure 3), as has already been reported for shallow coastal zones (Souchu et al. 2001; Paphitis and Collins 2005; Constantin et al. 2017). This sediment resuspension, creating a fairly constant nutrient input to the water column, may have maintained phytoplankton production and biomass. With weekly nutrient sampling, the role of nutrient inputs in bloom dynamics may be masked because phytoplankton communities respond quickly to nutrient inputs (Kang et al. 2017). The use of high-sensitivity *in situ* nutrient sensors with high acquisition frequencies is crucial for improving our understanding of the effect of nutrient inputs on blooms in such dynamic systems. However, the present study revealed that wind conditions is an underestimated factor of bloom initiations, especially in shallow coastal zones.

There were some correlations between phytoplankton group abundances and nutrient dynamics, especially for PO_4 . Furthermore, the N:P ratio was almost 3 times the Redfield ratio of 16:1, suggesting that PO_4 could be a limiting factor for some phytoplankton groups during some periods of the year. This result is in agreement with that from a nutrient limitation study of French Mediterranean coastal lagoons (Souchu et al. 2010). In warmer conditions, as the metabolic demands per unit biomass increase, a higher nutrient supply is needed to support phytoplankton growth. As the nutrient demand increases, stress and competition for nutrients increase and smaller phytoplankton benefit (Daufresne et al. 2009; Peter and Sommer 2012). However, the PO_4 and NO_3 concentrations were higher in 2016, especially during the winter latency period. This result supports our hypothesis that the predators remain active because of mild water temperatures, in turn maintaining a high grazing pressure and leading to low levels of phytoplankton biomass and thus lower nutrient consumption.

Chl *a* fluorescence and salinity were correlated two times during blooms. Increases in salinity in the studied system can be due to warm and dry periods inducing high evaporation or the inflow of saltier water from the Mediterranean Sea via winds. Otherwise, a decrease in salinity is generally caused by freshwater inputs from rain, runoff or floods. When the salinity variations result from saltier water inflow or from freshwater inputs, nutrients may also be input (Pecqueur et al. 2011; Fouilland et al.

Discussion

2012). In this study, correlations between salinity and Chl *a* fluorescence were positive one time (for the early spring bloom in 2015) and negative one time (for the winter bloom in 2016), suggesting that there was an indirect effect on phytoplankton biomass through nutrient inputs rather than a direct physiological effect of salinity (Cloern 1996). Rain and consequent runoff events may have enriched the system with nutrients, providing a supply for phytoplankton growth. This may have been the case for the onset of the winter bloom in 2016, where a decrease in salinity was observed and corresponded to a 4-day rain event during the initiation of the bloom (<https://www.historique-meteo.net>). This rain event may have enriched the system with nutrients, facilitating phytoplankton growth. Additionally, saltier water inputs from the sea due to strong winds from the southeast may have led to upwelling of nutrient-rich waters or induced the transport and/or accumulation of phytoplankton in the lagoon by currents. These nutrient enrichments can benefit phytoplankton growth (Deininger et al. 2016; Fouilland et al. 2017); however, nutrients can be rapidly assimilated and thus may have not been detected by our weekly nutrient sampling. Saltier water inputs can also explain the strong positive link detected between salinity and Chl *a* fluorescence during the early spring bloom in 2015. The beginning of this period was characterized by winds coming from the southeast that may have input saltier and more nutrient-rich water from the Mediterranean Sea, in turn contributing to the phytoplankton bloom. The southeasterly wind may also have prevented the dispersion of the accumulated phytoplankton.

One other important result was the lack of correlations between incident light parameters (PAR, UVA and UVB irradiance) and Chl *a* dynamics (Table 2). This lack suggests that in the study system, light conditions are non-limiting for phytoplankton production, at least during winter and spring. The study site is a shallow lagoon in which light reaches a large part of the water column, with a mean attenuation coefficient of 0.35 m^{-1} (Deslous-Paoli 1996). In shallow temperate coastal systems, light is often non-limiting, as the light intensities in the water column are generally higher than the saturating light intensities for phytoplankton growth (Domingues et al. 2015). The non-limiting light was also supported by the occurrence of winter blooms with similar levels of Chl *a* fluorescence as the spring blooms, even though the light intensities were at their lowest level (Figure 2 and 3). Even though light

did not appear to have a direct impact on Chl *a* fluorescence in this study, day length may have played a role in bloom timing (Lambert et al. 2018). There were also some negative correlations between incident light and Chl *a* fluorescence with zero lag, probably due to the inhibition of phytoplankton under high light intensities, as mentioned in the literature (Takahashi et al. 1971; Worrest and Caldwell 2013). Where there were positive correlations between incident light and Chl *a* fluorescence, they exhibited a time lag of 1 to 3 days. One possible explanation for this result is that the phytoplankton responded, after a delay, to the high light conditions by first recovering from light inhibition and then increasing their biomass once acclimatized.

4.3 Small phytoplankton species benefit and diatoms lose out in warmer conditions

The dominant phytoplankton species in terms of carbon biomass in the 2015 winter bloom and the early spring bloom was the cryptophyte *P. prolonga* (6-12 μm). *Plagioselmis* is a widespread genus in Mediterranean coastal waters throughout the year and is sometimes considered the key primary producer in these systems (Novarino 2005; Šupraha et al. 2014). *Plagioselmis* and cryptophytes in general “high-quality food” (Sterner and Schulz 1998), ensuring efficient energy transfer to higher trophic levels. In 2016, there was a winter latency period but no early spring bloom. Nanoeukaryotes (3-6 μm) dominated in terms of carbon biomass during the winter latency period, with higher abundances than those observed in 2015, while the *P. prolonga* abundance was the same as that in 2015. Nanoeukaryotes (3-6 μm) and *P. prolonga* dominated in terms of biomass and were probably the main sources of available energy for grazers, at least from winter to early spring.

In both 2015 and 2016, the spring bloom was dominated in terms of abundance by chain-forming diatoms. *Chaetoceros* spp. and *Pseudo-nitzschia* sp., dominated the large-phytoplankton community (6–200 μm). Diatoms, including *Chaetoceros* spp. and *Pseudo-nitzschia* sp., are among the most frequent bloom-forming taxa, generally being dominant during spring blooms in coastal zones (Cloern, 1996; Carstensen et al., 2015). This is also the case at study sites where spring blooms are usually diatom dominated (Vaquer et al. 1996; Bec et al. 2005). This dominance is well known and is generally

Discussion

attributed to the fast growth rate of diatoms due to rapid nitrogen uptake (high nitrogen affinity; Lomas and Glibert (2000)), as confirmed by the correlation found between *Chaetoceros* spp. and NO_3 concentrations in 2015. This rapid response to nitrogen makes these species more competitive than others during the spring, when conditions are favorable (e.g., nutrients, light and temperature). These large cells with a high fatty acid content are known to be a preferential source food for metazooplankton (e.g., copepods) (Sommer et al. 2002; Irigoien et al. 2002), which are consumed by planktivorous fish. However, although *Chaetoceros* spp. dominated the biomass during the 2015 spring bloom, nanophytoplankton (3-6 μm) dominated the 2016 spring bloom. In addition, picophytoplankton (< 1 μm) and nanophytoplankton (3-6 μm) abundances were significantly higher in 2016 than in 2015, while *Chaetoceros* spp. abundances were significantly lower. We suggest that the meteorological conditions and in particular the warm winter of 2016 were probably the causes of these differences. Several experimental studies have also suggested that water warming induces a phytoplankton community shift to picoeukaryote and nanoeukaryote dominance in both fresh and marine waters (Sommer and Lengfellner 2008; Rasconi et al. 2015; Sommer et al. 2017). The first hypothesis for the shift in phytoplankton composition between 2015 and 2016 is that the relatively high water temperatures throughout winter and spring in 2016 promoted small phytoplankton (e.g., picophytoplankton) rather than larger ones (e.g., diatoms) due to the higher affinity for nutrients, gas uptake (CO_2 and O_2) and maximal growth rate under warmer conditions of the former. This advantage can be explained by the temperature-size relationship, which suggests that smaller organisms are more favored than larger ones in warmer conditions due to faster metabolic processes (Daufresne et al. 2009; Sommer et al. 2017). The second hypothesis is that the warmer winter of 2016 promoted grazers, especially larger ones (e.g., copepods). Heterotrophic protists and metazoans are more sensitive to low temperatures than phytoplankton are, and their grazing activity is higher under warmer conditions. The absence of cooling during the winter may have allowed larger grazers (those that fed on the larger phytoplankton) to remain abundant and active (Sommer and Sommer 2006; Vidussi et al. 2011; Sommer et al. 2017). Thus, these larger grazers may have reduced larger phytoplankton abundances and thereby made their ecological

niche more accessible to smaller phytoplankton. Moreover, large zooplankton feed on small protozooplankton that in turn graze on small phytoplankton, reducing the grazing pressure on small phytoplankton.

According to the first hypothesis, the shift from large phytoplankton to picophytoplankton and nanophytoplankton induced by warming will promote microzooplankton (mostly ciliates), creating an intermediate trophic link between primary producers and copepods. This link will lead to a reduction of the energy transfer from primary production to copepods and in turn to planktivorous fish (Sommer et al. 2002; Sommer and Lengfellner 2008b). Warmer water conditions, especially during the winter period, will certainly lead to changes in the plankton community that directly affect the whole food web and ecosystem functioning. In addition, one of the main differences between 2015 and 2016 was cyanobacterial abundance (here, mostly *Synechococcus*). During the winter and the early spring before the bloom, cyanobacterial abundances in 2016 were 10 times higher than those in 2015. Cyanobacteria are known to be strongly controlled by water temperature (and irradiance) and are more abundant during warmer months (Iriarte and Purdie 1994; Cloern 1996; Agawin et al. 1998). The relatively warm water during the winter and the early spring in 2016, without significant cooling, allowed cyanobacteria to maintain high abundances and compete with other phytoplankton. According to the second hypothesis, the small protozooplankton grazing on cyanobacteria would have been controlled via grazing by larger zooplankton facilitated by warmer conditions, further increasing the population of cyanobacteria. With the general spring water warming in both 2015 and 2016, cyanobacteria became more competitive. Their abundances started to increase when the water temperature was between 12 and 14°C. In some regions, including coastal waters and lakes, cyanobacterial blooms can cause hypoxia and nutrient limitation and can be both environmentally and economically damaging (Paerl and Fulton 2006; Vahtera et al. 2007). Furthermore, some cyanobacteria can produce toxins that are harmful to most vertebrates, including humans (Jakubowska and Szelaġ-Wasielewska 2015), and will cause health concerns if their high abundances become chronic with global warming. Fortunately, this is not the case for the cyanobacteria in our study, which were non-toxic unicellular taxa (e.g., *Synechococcus*).

Picoeukaryotes (< 1 μm) dominated the phytoplankton community in terms of abundance throughout the study, followed by picoeukaryotes (1-3 μm), even though they never dominated in terms of biomass (Figure 6 and Table 3). However, picoeukaryotes are known to have high biomass-specific primary production but are also targeted by microzooplankton grazers (e.g., ciliates), which prevents a major part of daily growth (Bec et al. 2005). This relationship suggests that despite the low standing stock of carbon, picoeukaryotes play an important role in transferring carbon to higher trophic levels in coastal zones such as the system studied here (Reckermann and Veldhuis 1997; Brown et al. 1999). As picoeukaryotes became more abundant in the water warming period in 2016, including the spring bloom, it is probable that, with global warming, they and small nanoeukaryotes (3-6 μm), will play a greater role in transferring carbon to higher trophic levels including species of commercial interest.

4.4 Toward a general explanation of bloom initiation in shallow coastal waters and general considerations

The disturbance recovery hypothesis (Behrenfeld et al. 2013b; Behrenfeld and Boss 2014) suggests that a disturbance factor disrupts the predator-prey interactions that allow phytoplankton growth to outpace grazing losses and thereby creates a bloom. Later, in response to the high phytoplankton biomass, the predator abundance and grazing pressure increase, re-establishing the new predator-prey equilibrium and hence ending the bloom. In the North Atlantic oceanic system, the disturbance factor disrupting predator-prey interactions is the deepening of the mixing layer. In shallow, coastal, non-oligotrophic systems such as Thau Lagoon, there is no deep mixing, and other forcing factors might be the major disturbance triggering phytoplankton blooms.

In these shallow coastal waters, previous studies reported that nutrient inputs via wind (sediment resuspension or water transport) and river inputs mainly drove phytoplankton production (Millet and Cecchi 1992; Cloern 1996). However, even if the role of these forcing factors is confirmed by the results presented here, this study highlights for the first time that water temperature seems to be the key factor triggering phytoplankton blooms. An increase in water temperature can stimulate phytoplankton

metabolic rates such as carbon assimilation and nutrient uptake (Gillooly et al. 2001; Cross et al. 2015). As the growth rates of phytoplankton can respond more rapidly than those of grazers (Rose and Caron 2007), phytoplankton growth outpaces the losses by grazing, leading to a net biomass gain and starting the bloom. The diverse sources of nutrient inputs (resuspension by winds, rain or freshwater inputs or seawater intake) with frequent pulses contribute to favorable phytoplankton growth conditions during periods of increasing water temperature. Rising water temperature enhances primary production and leads to biomass accumulation and phytoplankton blooms.

In contrast, there were no clear contemporaneous correlations between the environmental variables, including water temperature, and Chl *a* fluorescence during the post-bloom periods (except with wind speed for the post-winter bloom period in 2016). This lack of correlations suggested that the end of the blooms in these systems is regulated by biological processes, in particular zooplankton grazing activity (Banse 1994). After favorable conditions trigger the bloom, the increased phytoplankton biomass allows the predator abundances to increase until the grazing rate exceeds the phytoplankton growth rate, leading to phytoplankton biomass loss during the post-bloom period. This interaction supports the food web transfer of matter in these systems, which are also known to be productive in terms of secondary production.

Moreover, low winter water temperatures are important for conditioning the phytoplankton bloom phenology and composition. If there is no significant winter water cooling, then the blooms are delayed and reduced in magnitude, and the dominant phytoplankton in communities shift to smaller ones (cyanobacteria (< 1 μm), picoeukaryotes (< 1 μm) and nanoeukaryotes (3-6 μm)). Such a shift can affect primary production and the whole food web by reducing the energy transfer to higher trophic levels, promoting small predators over larger ones (microbial food web rather than the classic herbivorous food web; Legendre and Rassoulzadegan (1995)). With global warming, mild winters could become increasingly frequent and might potentially, in the midterm, totally change the structure of the plankton communities in the most reactive coastal ecosystems. These changes may propagate to upper

Discussion

trophic levels, especially those including fish and shellfish, and have a major impact on commercially exploited coastal systems such as like the studied site as these productive ecosystems are an essential economic resource for local populations. However, the mild winter effect on blooms and more generally the decadal water temperature increases due to global warming can be different according to the system. In some open or deep-coastal zones, phytoplankton blooms are triggered by upwelling, which provides nutrients from deep nutrient-rich water. As global warming heats more land than it heats ocean surface, it may strengthen alongshore winds favorable to upwelling, potentially increasing nutrient inputs and thus bloom events (García-Reyes and Largier 2010). In open-ocean systems of low and mid latitudes where blooms are not triggered by upwelling, surface temperature increases due to global warming might intensify ocean stratification, and potentially reduce mixing and thus the nutrient inputs from deep water that promote phytoplankton growth. This reduced nutrient supply could diminish the bloom amplitude, net primary production and phytoplankton biomass (Behrenfeld et al. 2006; Henson et al. 2013; Gittings et al. 2018) and modify bloom timing (Henson et al. 2018). However, at higher latitudes, where incident light is limiting, this stratification increase might improve light conditions favorable to phytoplankton growth in the mixing layer and thus increase net primary production and bloom events (Behrenfeld et al. 2006).

However, in the present study, the monitoring was conducted at only one sampling station in Thau Lagoon. In addition, only the winter and spring of two consecutive years were monitored, and 2015 was a “normal” climatic year while 2016 was an exceptional one with a particularly mild winter. Moreover, it is possible that 2015-2016 was influenced by ENSO or North Atlantic Oscillation (NAO) factors. Finally, the influence of tidal phases (spring/neap) on blooms was not studied as in Thau Lagoon the tidal amplitude is very low and frequently masked by climatic factors such as wind conditions (Audouin 1962). However, tidal phases can influence Chl *a* fluctuations and blooms in coastal waters with higher tidal amplitude (Blauw et al. 2012).

The crucial challenge concerning coastal waters, one of the most productive marine systems, is how these systems will respond to long-term climatic fluctuations such as those expected with global change. The results and conclusion of the present study are the first evidence of rising water temperature as a main driver of phytoplankton blooms in coastal waters. However, for the reasons mentioned above, to confirm our finding as a general rule, other diverse coastal waters should be investigated with adequate monitoring systems for several consecutive years.

Acknowledgments

This study was part of the Photo-Phyto project funded by the French National Research Agency (ANR-14-CE02-0018). We would like to thank Cecile Roques, Benjamin Sembeil, Océane Schenkels, Judith Duhaméeuw and Ludovic Pancin for their help with the sampling and analyses of samples. Sample handling and preservation were done at the Marine Station of the Observatoire de Recherche Méditerranéen de l'Environnement (OSU OREME) in Sète.

Chapitre 2

Fonctionnement du réseau d'interaction microbien en zone côtière peu profonde : différence entre périodes d'efflorescences et épisodes sans efflorescences

Avant-propos

Ce chapitre a pour objectif de présenter les travaux visant à déterminer le fonctionnement du réseau d'interactions microbien durant les périodes d'efflorescences et les épisodes sans efflorescences, ainsi que sa modification en fonction d'années climatiques contrastées, afin d'identifier le rôle potentiel des interactions dans l'initiation des efflorescences phytoplanctoniques en zone côtière peu profonde.

La compréhension du fonctionnement du réseau d'interactions microbien dans son ensemble nécessite une méthodologie d'échantillonnage et une analyse statistique adéquates. Pour répondre à cet objectif, le suivi présenté dans le chapitre 1 était accompagné d'un suivi hebdomadaire de l'abondance et de la diversité de la communauté microbienne, de l'hiver au printemps dans la lagune de Thau sur deux années consécutives, 2015 et 2016. En plus de la diversité et de l'abondance du phytoplancton utilisés dans le chapitre précédent, les organismes étudiés pendant ce suivi hebdomadaire allaient des virus jusqu'au ciliés avec lorica (tintinnides), en passant par les bactéries et les flagellés hétérotrophes. Comme indiqués dans le Chapitre 1, les analyses des échantillons de la communauté $< 6 \mu\text{m}$ ont été réalisées en cytométrie par Benjamin Sembeil (M2 en 2015) et Océane Schenkels (M2 en 2016) en majeure partie, le reste étant effectué par moi-même. L'analyse au microscope à fluorescence pour le comptage des flagellés hétérotrophes a été réalisé par Erika Gaudillère (L3 en 2015). L'analyse au

microscope inversé de l'abondance et de la diversité des ciliés et des tintinnides a été réalisée par Cécile Roques (AI MARBEC). J'ai personnellement réalisé l'analyse au microscope inversé de l'abondance et la diversité du phytoplancton 6 – 200 µm qui ont également servi pour le chapitre 1.

La compréhension du rôle des interactions dans le fonctionnement du réseau microbien dans son ensemble nécessite une analyse statistique rigoureuse et adaptée. Dans ce chapitre une méthode novatrice a été développée à partir de la modélisation des réseaux de corrélations entre groupes/taxons/espèces pour qualifier et quantifier statistiquement les interactions dominantes au sein du réseau microbien, et ainsi pouvoir comprendre plus en détail son fonctionnement. La procédure étape-par-étape de cette méthode est détaillée dans un encadré dédié, à la fin de ce chapitre.

Les résultats de ce chapitre mettent pour la première fois en évidence le fonctionnement des réseaux d'interactions microbiens et leurs différences entre les périodes avec ou sans efflorescences et entre les deux années climatiques contrastées étudiées. Ainsi, ils nous renseignent sur les voies majeures de la circulation de l'énergie pendant ces différentes périodes, et sur le rôle crucial des interactions dans l'initiation des efflorescences phytoplanctoniques en zone côtière peu profonde.

Ce chapitre a fait l'objet d'un manuscrit soumis à la revue *Frontiers in Microbiology* le 2 octobre 2019 intitulé : **Microbial Food Web Networks: Warming Favours Smaller Organism Interactions and Intensifies Trophic Cascade**. Seule la partie bibliographie de l'article soumis n'est pas présentée dans ce chapitre. Les références citées dans ce chapitre sont disponibles dans la bibliographie générale, à la fin du manuscrit. L'encadré de ce chapitre n'as pas été soumis à *Frontiers in Microbiology*.

Marine microbial food web networks: warming favors smaller organism interactions and intensifies trophic cascade

Thomas Trombetta^{1*}, Francesca Vidussi¹, Cécile Roques¹, Marco Scotti², Behzad Mostajir¹

¹MARBEC (Marine Biodiversity, Exploitation and Conservation), Centre National de la Recherche Scientifique, Université de Montpellier, Institut Français de Recherche pour l'Exploitation de la Mer, Institut de Recherche pour le Développement, Montpellier, France.

²GEOMAR Helmholtz Centre for Ocean Research Kiel, Kiel, Germany.

*** Correspondence:**

Corresponding Author: Thomas Trombetta; email: thomas.trombetta@cnrs.fr

Keywords: microorganism interactions, correlation networks, phytoplankton bloom, warming, microbial food web.

Abstract

Microbial food web organisms are at the base of the functioning of the pelagic ecosystems, and they support the whole marine food web. Because they are very reactive to environmental changes, their structures and interactions are modified in response to phytoplankton bloom. To study ecological interactions in the microbial food web, a weekly monitoring was carried out in the Thau Lagoon on the French Mediterranean coast. The monitoring lasted from winter to late spring and took place in two contrasting climatic years, a typical Mediterranean (2015) and a year with an extreme warm winter (2016). Correlation networks comprising 110 groups/taxa/species were constructed to identify and model interactions between the microorganisms during the two years and to characterize bloom and non-bloom periods. Interaction networks during bloom were complex and dominated by phytoplankton in the form of intraguild competition and mutualism with heterotrophic bacteria. In contrast, interaction networks during the non-bloom period were less complex and mostly dominated by ciliates bacterivory, which suggests a shift of biomass transfer from phytoplankton-dominated food webs during bloom to bacterioplankton-based food webs during non-bloom. Inter-annual climatic conditions significantly modified the structure of microbial food web interaction networks. The warmer year favored relationships among smaller group/taxa/species at the expense of large phytoplankton and ciliates, possibly due to an intensification of the trophic cascade. In the future, the prevalence of interactions among smaller microorganisms under global warming is expected to shift energy circulation towards the less productive microbial loop at the expense of the higher productive herbivory-dominated food web, potentially affecting the whole ecosystem functioning.

1 Introduction

The microbial food web plays a pivotal role in marine ecosystems as it controls energy as well as organic and inorganic matter transfer either to higher trophic levels or to the water-dissolved pool (e.g. dissolved organic carbon: DOC). Phytoplankton is the main primary producer, and it supports ecosystem productivity by providing carbon to higher trophic levels (Cloern 1996). Phytoplankton is

also considered as the most important source of DOC in marine environments through exudation, losses by cell damage, or lysis (Dafner and Wangersky 2002). In aquatic ecosystems, DOC is essential for the persistence and growth of bacteria. Consistent amounts of carbon can pass through bacteria to higher trophic levels, showing the relevance of the microbial loop to carbon circulation and ecosystem functioning (Azam et al. 1983; Mostajir et al. 2015). Besides, bacteria play a crucial role in nutrient cycling through remineralization of organic matter (Fasham 1984). Heterotrophic protists are the main consumers of both bacteria and phytoplankton, and they can actively transfer energy to higher trophic levels (Weisse et al. 1990; Calbet and Landry 2004; Calbet and Saiz 2005). Moreover, they contribute significantly to the dissolved pool through excretion as well as egestion and dissolution of fecal material (Fuhrman 1999). In addition, viruses often play an underestimated role in carbon cycling. They regulate matter circulation through cell lysis, thus supplying energy for bacterial production.

Interactions between microorganisms modulate microbial food web structure and performance by influencing the amount of circulating energy, intensity of nutrient cycling, and transfer efficiency to higher trophic levels. Microbial food webs embed diverse relationships that include predation, cross-feeding, competition, commensalism, mutualism, and parasitism. Predator-prey interactions transfer carbon from phytoplankton or bacterial biomass to higher trophic levels (Weisse et al. 1990; Calbet and Landry 2004; Calbet and Saiz 2005). In the microbial food web, this role is played by heterotrophic and mixotrophic protists such as flagellates, naked ciliates, and tintinnids, which strongly control and regulate the biomass of their resources (Weisse et al. 1990). The excretion of organic matter by grazers also contributes to the organic matter pool, and it facilitates the growth of microorganisms such as bacteria (Snyder and Hoch 1996) in a process known as cross-feeding (Morris et al. 2013). Besides, mixotrophic protists can be both predators and competitors (Mitra et al. 2016). They can shift their nutrition type from autotrophic to heterotrophic following the availability of resources, thus strongly modifying the microbial food web structure as it modulates the energy pathways to higher trophic levels (Mitra et al. 2014). Competition for nutrients can also occur among phytoplankton species or between phytoplankton and bacteria (Bratbak and Thingstad 1985). However, commensalism among

Introduction

phytoplankton and bacteria is not rare, especially at the end of the bloom when the availability of nutrients is low. In fact, phytoplankton produces exudates, notably DOC, that benefit bacterial productivity (Bratbak and Thingstad 1985; Gurung et al. 1999). This type of relationship can also become mutualistic when vitamin-synthesized or nutrient-remineralized products from bacteria supply phytoplankton with vitamins or macronutrients, supporting their growth (Paerl et al. 2017; Seymour et al. 2017; Mayali 2018). Mutualistic phytoplankton-bacteria interactions, along with competitive interactions for nutrients (Joint et al. 2002), strongly influence the microbial food web structure as they modulate the community composition and energy transfer (Rooney-Varga et al. 2005), and their effect can propagate to higher trophic levels. The community composition can also be modulated by other interactions, such as parasitism, which is considered a very common strategy in marine systems (Théodoridès 1989; Skovgaard and Saiz 2006). In particular, viral lysis of both bacteria and phytoplankton has been described as ubiquitous in marine waters (Wommack and Colwell 2000), and it is considered as one of the principal causes of microbial mortality, controlling its biomass and contributing to the dissolved pool (Suttle 1994, 2005). Moreover, parasitism is not restricted to viruses as protists can also be endo- or epibiotic parasites. So far, only a few parasites of planktonic hosts have been identified, and parasitism may be more important than reported (Skovgaard 2014).

Major stressors, such as global warming, modify the microbial food web structure and modulate the interactions between microorganisms. Warming benefits smaller phytoplankton cells (Peter and Sommer 2012) and smaller heterotrophic flagellates, thus reducing the energy transfer efficiency to higher trophic levels (Moustaka-Gouni et al. 2016). Experimental studies showed that warming directly impacts planktonic food webs as it alters the bottom-up/top-down balance in favor of top-down control (Kratina et al. 2012; Lewandowska et al. 2012; Shurin et al. 2012) and induces trophic cascades (Vidussi et al. 2011). Warmer waters also modify the metabolism of organisms by increasing microbial oxygen and carbon demand per unit production (Vázquez-Domínguez et al. 2007) and inducing higher microzooplankton grazing rates (Chen et al. 2012). Changes in the relative importance of functional traits, ecological interactions, and metabolic rates, which are caused by warmer temperatures, have the

potential to remodel the structure of the interaction network and can consequently jeopardize the provision of energy to higher trophic levels (Aberle et al. 2012).

Little is known about the interaction network structure of the microbial food web in marine waters, particularly in productive coastal areas, making it difficult to predict the functioning under future global warming conditions. In this study, the microbial food web of a Mediterranean coastal site (Thau Lagoon) was monitored. The microbial food web was composed of various groups, taxa or species (hereafter called groups/taxa/species) that include 1 virioplankton, 2 bacterioplankton (both Archaea and Bacteria), 46 phytoplankton, 4 heterotrophic flagellates, 28 naked ciliates, and 29 tintinnids. The survey lasted from winter to spring by encompassing the bloom and non-bloom periods, and it was carried out during a typical Mediterranean climatic year (2015) and an exceptionally warm year (2016). The winter of 2016 was the warmest on record, and it displayed abnormally high water temperature, absence of significant water cooling in winter, and slow temperature increase from winter to spring (Trombetta et al. 2019). The goals of the present study were: (1) to construct and analyze the interaction structure of the microbial food web during bloom and non-bloom periods, and (2) to investigate if the network structure in these two periods changes from a typical to a warm year. The broadest objective was to assess possible trends of change in the structure of the microbial food web of coastal waters under global warming.

2 Materials and methods

2.1 Study site

The Thau Lagoon (Supplementary Figure S1) is a productive marine ecosystem located on the French coast of the northwestern Mediterranean Sea (43°24'00" N, 3°36'00" E). It is a shallow coastal lagoon of 75 km² with a mean depth of 4 m and a maximum depth of 10 m (excluding deep depressions), which is connected to the sea by three channels. It is mesotrophic, with a mean turnover of 2 % (50 days), phosphorus- and nitrogen-limited (Souchu et al. 2010), and characterized by large seasonal water temperature variations (i.e. from 4 in the winter to 30 °C in the summer) throughout the year (Pernet et

al. 2012a). Apart from its ecological interest, it is a lagoon of economic relevance, mainly due to oyster farms representing 10 % of the French production.

2.2 Sampling design and planktonic diversity and abundance

To determine planktonic diversity and abundance, water samples were collected weekly at 1 m depth using a Niskin bottle. The sampling was carried out at a fixed station (Coastal Mediterranean Thau Lagoon Observatory: 43°24'53" N, 3°41'16" E) (Mostajir et al. 2018b) near the Mediterranean platform for Marine Ecosystem Experimental Research (MEDIMEER) in Sète. The water depth at the sampling station is 2.5–3 m. The station is located at less than 50 m from the main channel connecting the lagoon to the sea, where the water residence is at its lowest (less than 20 days) (Fiandrino et al. 2012). Water samples were taken from January 8 to May 12, 2015 and from January 12 to June 14, 2016. Hereafter, these two distinct periods are referred to as 2015 and 2016.

To estimate the abundance of virioplankton, 1.8 mL water samples were fixed with 0.02 μ m filtered buffered alkaline formalin (2 % final concentration) and stored at -80 °C until analysis. Next, subsamples (0.3–0.4 mL) were filtered through 0.02 μ m pore size Anodisc filters (Whatman). After staining with SYBR GOLD, the filters were air dried and mounted between a slide and glass cover slip with 30 μ L of antifadent mounting medium (Citifluor). Virus-like particles were enumerated using an Olympus AX-70 epifluorescence microscope.

The abundance of heterotrophic bacterioplankton (including both archaea and bacteria, hereafter called bacteria) and small size phytoplankton (< 6 μ m) was identified by flow cytometry. For heterotrophic bacteria and phytoplankton (< 6 μ m), duplicate 1.8 mL subsamples were taken and fixed with glutaraldehyde following the protocol described in Marie et al. (2001) and then stored at -80 °C until analysis. The abundance of High nucleic acid (HNA) and low nucleic acid (LNA) bacteria (Lebaron et al. 2001; Zubkov et al. 2001a; b), cyanobacteria < 1 μ m, picoeukaryotes < 1 μ m and 1–3 μ m and

nanoeukaryotes 3–6 μm was estimated using flow cytometry (FACSCalibur, Becton Dickinson) following the method described by Pecqueur et al. (2011).

The abundance and diversity of large size phytoplankton (6–200 μm) was estimated by microscopy as detailed in Trombetta et al. (2019). Duplicates of 125 mL subsamples were taken, fixed in 8 % formaldehyde and kept cold (4 °C) until analysis. Subsamples (50 mL) were settled for 24 h in an Utermöhl chamber and phytoplankton cells were identified and counted under an inverted microscope (Olympus IX-70). Phytoplankton was identified to the lowest possible taxonomic level (i.e. species or genus) using phytoplankton taxonomic key (Sournia et al. 1986; Tomas 1997).

To estimate the abundance of (microzooplankton) heterotrophic nanoflagellates (hereafter called HF), 30 mL aliquots were fixed with sterile filtered (0.2 μm pore size) formaldehyde (4 % final concentration). Samples were preserved at 4 °C in the dark until analysis. Subsamples (10 mL) were stained with 4',6'-diamidino-2-phenylindole hydrochloride (DAPI) and filtered with 25 mm black nucleopore polycarbonate membranes (0.8 μm pore size). Filters were placed on a microscope slide and HF were enumerated with an epifluorescence microscope (Olympus AX-70) using UV illumination; HF were grouped in four size classes of < 3, 3–5, 5–10, and >10 μm (hereafter named HF1, HF2, HF3, and HF4, respectively) (Mostajir et al., 2015b; Moustaka-Gouni et al., 2016).

To estimate the abundance and diversity of naked ciliates and tintinnids, 125 mL of the samples were fixed with 2 % Lugol's iodine acid solution. Samples were preserved in a cold dark room (4° C) until analysis. Subsamples (100 mL) were settled in an Utermöhl chamber for 24 h and the cells were identified and counted under an inverted microscope (Olympus IX70).

2.3 Microbial network construction and analysis

Correlation networks were constructed using abundance data of all microbial groups/taxa/species encompassing 1 node for virus, 2 nodes for bacteria, 46 nodes for phytoplankton, 4 nodes for HF, 28 nodes for naked ciliates, and 29 nodes for tintinnids. First, 2015 and 2016 data sets

Materials and methods

were divided into bloom and non-bloom periods as described by Trombetta et al. (2019). They defined blooms as periods (1) that started with at least two consecutive days of positive growth rates and (2) where the sum of the net growth rates over at least five consecutive days was positive. There were three bloom periods in 2015 and one in 2016, and two non-bloom periods in 2015 and one in 2016. Second, positive and negative correlations among groups/taxa/species were identified and used to represent network interactions. Third, network descriptors were calculated for each network. For each year (2015 and 2016), nine networks were produced: one positive, one negative, and one full (a merge of negative and positive) network for the bloom period; one positive, one negative, and one full network for the non-bloom period; and one positive, one negative and one full network for the full year period. In total, 18 networks were obtained.

Network nodes were defined using 1:1 correspondence with the microbial groups/taxa/species, and the network links between them were identified using the Spearman's rank correlation method. This method was chosen as it has been previously described as the best approach for weekly or higher frequency abundance data of microbial communities, which allows the identification of non-linear relationships without leading to conspicuous inflation of significant associations (Posch et al. 2015). A Monte-Carlo resample procedure was applied with 9999 iterations. Only correlations with estimated p -values < 0.05 were considered for network construction and analysis. The analysis focused on correlation networks illustrating bloom, non-bloom, and full year microbial communities in 2015 and 2016. Network links could either be negative or positive. Negative correlations indicate parasitism, predation, and competition, whereas the positive correlations indicate mutualism, commensalism, and cross-feeding (Faust and Raes 2012; Posch et al. 2015; Fuhrman et al. 2015). Various descriptors were used to characterize network structure and complexity. The numbers of groups/taxa/species (nodes, N) and the links between them (edges, E) indicate network size and total number of correlation relationships, respectively. The degree indicates the total number of interactions in which a node is involved. Mean number of edges per node (mean degree) and the degree distribution describe network complexity. Group/species/taxa with the higher degree are hubs and indicates key nodes for the structure

and functioning of the community (Domin et al. 2018). The proportions of negative and positive correlations provide information on the relative importance of various interaction types (i.e. parasitism, predation and competition vs. mutualism, commensalism, and cross-feeding). Network analysis was first applied on full networks (with negative and positive correlations) and then separately on negative-only and positive-only networks.

2.4 Statistical analysis

Differences in degree distribution shown by correlation networks during bloom and non-bloom periods for both years were investigated with Kruskal-Wallis test. When significant, the test was followed by post-hoc pairwise Wilcoxon signed-rank test. The tests were applied to compare the complexity of various networks (i.e. those based on all interactions and constructed using either positive or negative links only).

Next, we considered cell sizes to cluster the group/taxa/species. Such clustering served to perform a comparative analysis between networks and was also useful for the investigation of differences in the abundance of groups between the years. First, HNA and LNA were pooled into the bacteria group while different size classes of HF were lumped into the HF group. Second, the mean sizes of phytoplankton, naked ciliates, and tintinnids groups/taxa/species were identified using the literature and microscopy observations (Supplementary Table S1). For all the size classes, the groups/taxa/species were ordered according to their mean size and the Pruned Exact Linear Time (PELT) algorithm for optimal detection of changepoints was applied (Supplementary Figure S2) to identify size classes based on rupture points (Killick et al. 2012). This analysis detected: (1) four size classes for phytoplankton: < 20, 20–50, 50–100, and > 100 μm ; (2) four size classes for naked ciliates: < 30, 30–50, 50–80, and > 80 μm ; and (3) three size classes for tintinnids: < 100, 100–150, and >150 μm .

Paired Wilcoxon signed-rank test was used to compare the mean abundance of the various microbial groups and size classes between 2015 and 2016 (e.g. phytoplankton < 20 μm in 2015 vs.

phytoplankton < 20 μm in 2016). Sample dates were paired by week number (ISO 8601). For example, the sampling dates of January 8, 2015 and January 12, 2016 were paired as both correspond to the 2nd week of their respective year. As the sampling period in 2016 was 4 weeks longer than in 2015 (23 weeks against 19, respectively), the last four sampling dates were removed from the dataset for the comparison between mean abundances.

2.5 Novel approach to detect the statistical differences between empirical networks

A novel approach was introduced here to assess the statistical differences between empirical networks. Such approach is based on the use of random networks as null models and allows the indirect comparison between networks constructed using empirical data. For each network constructed using empirical data, 999 random networks with the same number of edges and nodes were assembled using the Erdős-Rényi model (Erdős and Rényi 1960). The results extracted from the random networks were used for a procedure analogous to permutation analysis. The distribution of the number of edges between functional groups in the 999 random networks was compared with the number of shared-edges observed in the empirical networks constructed with abundance data. When the number of shared interactions in empirical networks was outside the tails of distributions from random networks, the presence of a significant deviation was recorded. The thresholds for significance were set to 2.5 % and 97.5 % of distributions from random networks; values that lie either below the first or above the second limit corresponded to the numbers of shared links in empirical networks that were significantly lower or higher than in their random counterparts, respectively. Significant deviations from random models served first to detect the presence of non-trivial patterns. Where such significant deviations characterized one empirical network only (e.g. the 2015 network and not the 2016 network), differential responses in the comparison with random models were also interpreted as significant differences between the empirical networks.

3 Results

3.1 Microbial community phenology

Abundance dynamic of planktonic groups, classified on the basis of size classes, are visualized in Figure 1 for the years 2015 and 2016. The results of the Paired Wilcoxon signed-rank tests presented in this section are detailed in Supplementary Table S2. The mean abundances of phytoplankton < 20 μm and naked ciliates < 30 μm were significantly higher in 2016 than in 2015 (p -values < 0.05). Bacterial abundances were also higher in 2016 but marginally significant (p -value = 0.06). Conversely, the abundances of phytoplankton 20–50 μm , HF, and naked ciliates > 80 μm were significantly lower in 2016 than in 2015 (p -values < 0.05). There was no significant difference between 2015 and 2016 (p -values > 0.05) in terms of the abundances of all the other groups including viruses, phytoplankton 50–100 and > 100 μm , naked ciliates 30–50, 50–80, and > 80 μm and the three size classes of tintinnids.

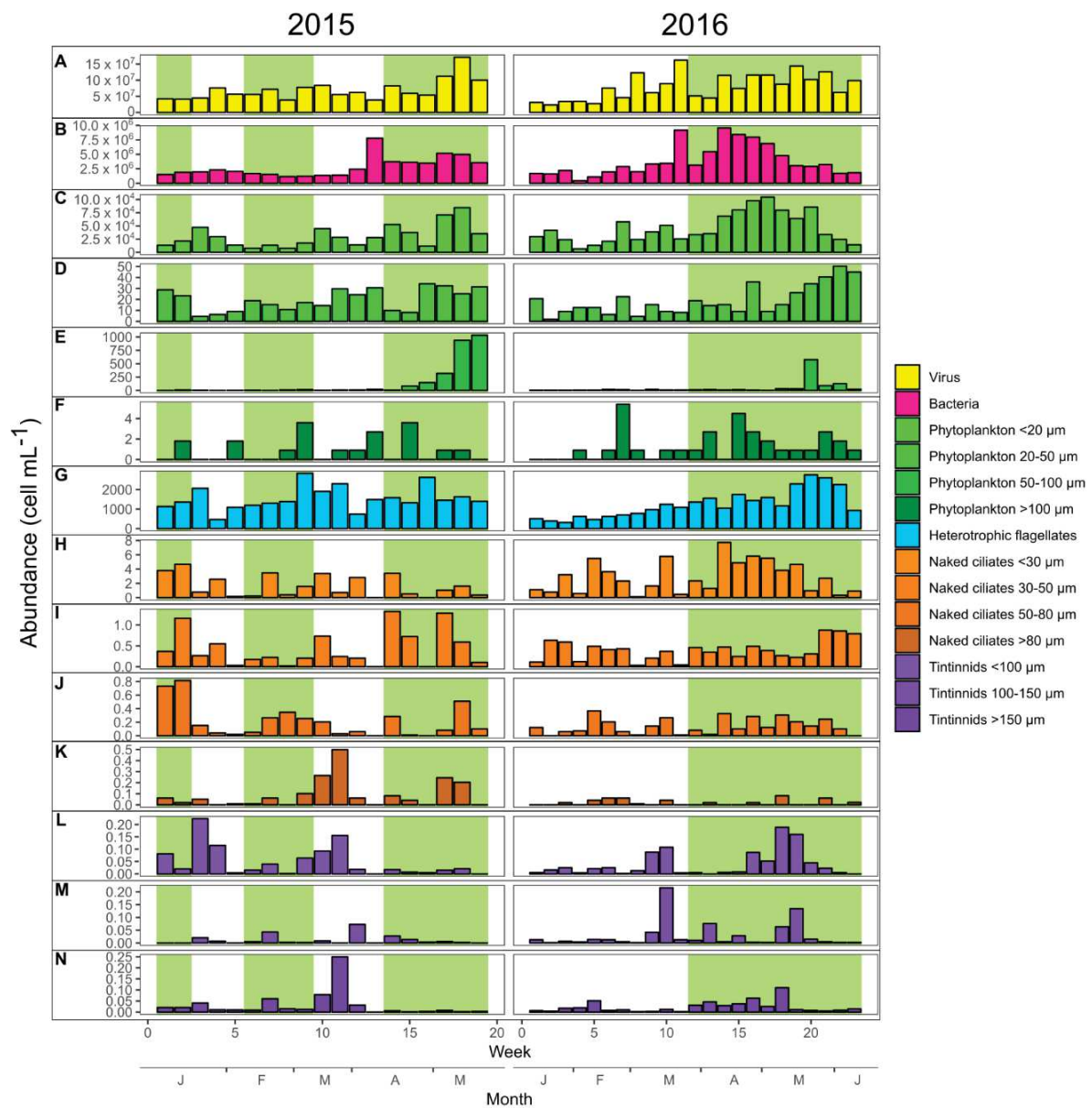


Figure 1 : Weekly abundances of the main microbial plankton groups during 2015 (left panels) and 2016 (right panels). The bloom periods have green background and the non-bloom periods have white background. Yellow bars are for viruses (A), pink for bacteria (B), and light blue for heterotrophic nanoflagellates (G). Bars of green gradient are for the different phytoplankton size classes (from C to F), orange gradient for naked ciliates (from H to K), and purple gradient for tintinnids (from L to N).

3.2 Correlation networks of the microbial communities

3.2.1 Comparison between 2015 and 2016 networks

In Table 1 the descriptors of the various networks, shown in Figure 2, are presented. Independently of the periods of bloom and non-bloom, all full, negative, and positive 2016 networks have higher numbers of nodes (N) and edges (E) than those in 2015, except for N in the 2016 negative network (Figure 2 and Table 1). A lower percentage of negative edges was observed in 2016 than in 2014 (26 % against 31 %, respectively). Mean degree was slightly higher in 2016 than in 2015 but the values were generally similar.

3.2.2 Comparison between bloom and non-bloom networks

In both years, the full networks (i.e. those including the full set of correlations) of the bloom period were more complex than those of non-bloom periods as they presented higher N, E, and mean degree (Figure 2 and Table 1). The proportion of negative E during the bloom period was 6 % higher in 2016 than in 2015 (36 % and 30 %, respectively) and higher than non-bloom periods (27 % and 29 %, respectively). The mean degree was higher for the bloom than the non-bloom in 2015 (7.91 and 2.92, respectively) and 2016 (7.30 and 4.94, respectively). For negative networks, bloom periods presented higher N, E, and mean degree than non-bloom networks both in 2015 and 2016. For positive networks, non-bloom periods presented higher N, E, and mean degree than during non-bloom both in 2015 and 2016.

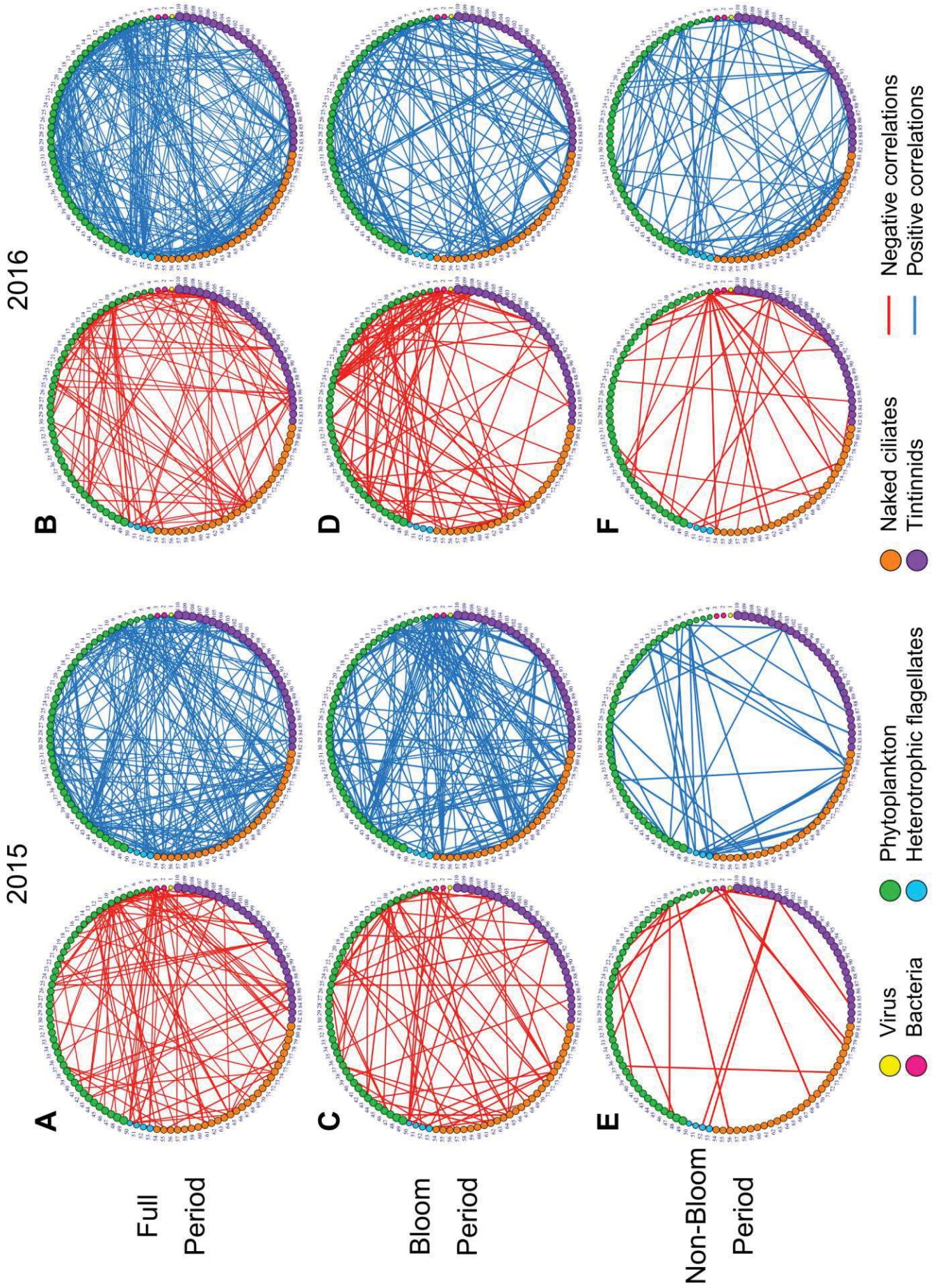


Figure 2 : Correlation networks of the microbial communities in 2015 (left) and 2016 (right). The different versions include correlations estimated for each year: (A, B) over the full period, (C, D) during the bloom, or (E, F) in the non-bloom periods. There were three blooms and two non-bloom periods in 2015, while in 2016 there were one bloom and one non-bloom intervals. Red and blue edges correspond to negative and positive correlations, respectively. Edge thickness is proportional to correlation strength. Node numbers correspond to groups/taxa/species IDs as reported in Supplementary Table S1. Nodes are ordered by groups—viruses (number 1), bacteria (numbers 2 and 3), phytoplankton (from number 4 to 49), heterotrophic nanoflagellates (from number 50 to 53), naked ciliates (from number 54 to 81) and tintinnids (from number 82 to 110), and mean cell size. Node size is proportional to the mean body size on a natural logarithm scale. Yellow node is for viruses, pink for bacteria, green for phytoplankton, light blue for heterotrophic nanoflagellates, orange for naked ciliates, and purple for tintinnids. The six networks combining both negative and positive correlations (full networks) are not presented in figures as they were obtained by simply merging the negative and positive correlations presented here. Consequently, only 12 networks out of the 18 produced are shown.

Table 1 : Network descriptors. The descriptors refer to (1) entire annual period (2015 and 2016), (2) bloom and (3) non-bloom periods (3), for the full, negative, and positive correlation networks. The descriptors are: the number of nodes (N), the number of edges (E), the percentage of negative correlations (for full networks) and the mean degree.

		Number of nodes (N)	Number of edges (E)	% Negative correlations	Mean degree
Full	2015	82	364	31%	8.88
	2016	94	461	26%	9.81
	Bloom 2015	69	273	30%	7.91
	Bloom 2016	79	288	36%	7.30
	Non-bloom 2015	48	70	29%	2.92
	Non-bloom 2016	62	153	27%	4.94
Negative	2015	71	112		3.16
	2016	62	120		3.87
	Bloom 2015	53	81		3.06
	Bloom 2016	59	103		3.50
	Non-bloom 2015	28	20		1.43
	Non-bloom 2016	43	41		1.91
Positive	2015	81	252		6.22
	2016	93	341		7.33
	Bloom 2015	64	192		6.00
	Bloom 2016	74	185		5.00
	Non-bloom 2015	39	50		2.56
	Non-bloom 2016	57	112		3.93

3.3 Network degree comparison

Degree distributions of various networks are presented in Figure 3. For complete year networks (i.e. with correlations inferred on the basis of the entire time series of each year), Wilcoxon signed-rank tests revealed no significant differences between 2015 and 2016 for full (Figure 3A), negative (Figure 3B), and positive (Figure 3C) networks. However, there were differences between bloom or non-bloom periods (Figure 3D, E, F). Kruskal-Wallis tests revealed significant differences between periods, irrespective of the year in the full ($\chi^2 = 38.8$, p -value < 0.001 , $df = 3$), negative ($\chi^2 = 26.2$, p -value < 0.001 , $df = 3$), and positive networks ($\chi^2 = 24.46$, p -value < 0.001 , $df = 3$).

Full, negative, and positive networks during bloom periods presented significantly higher median degree than in non-bloom periods in 2015 (p -values < 0.01 ; Figure 3D, E, F), whereas the median degree was significantly higher only for negative networks in 2016 (p -value < 0.001). Comparing 2015 and 2016, there was no significant difference in the median degrees of all the networks during the bloom periods (p -values > 0.05). However, during non-bloom periods, the median degree was higher in 2016 than in 2015 for full and positive networks (p -values < 0.05).

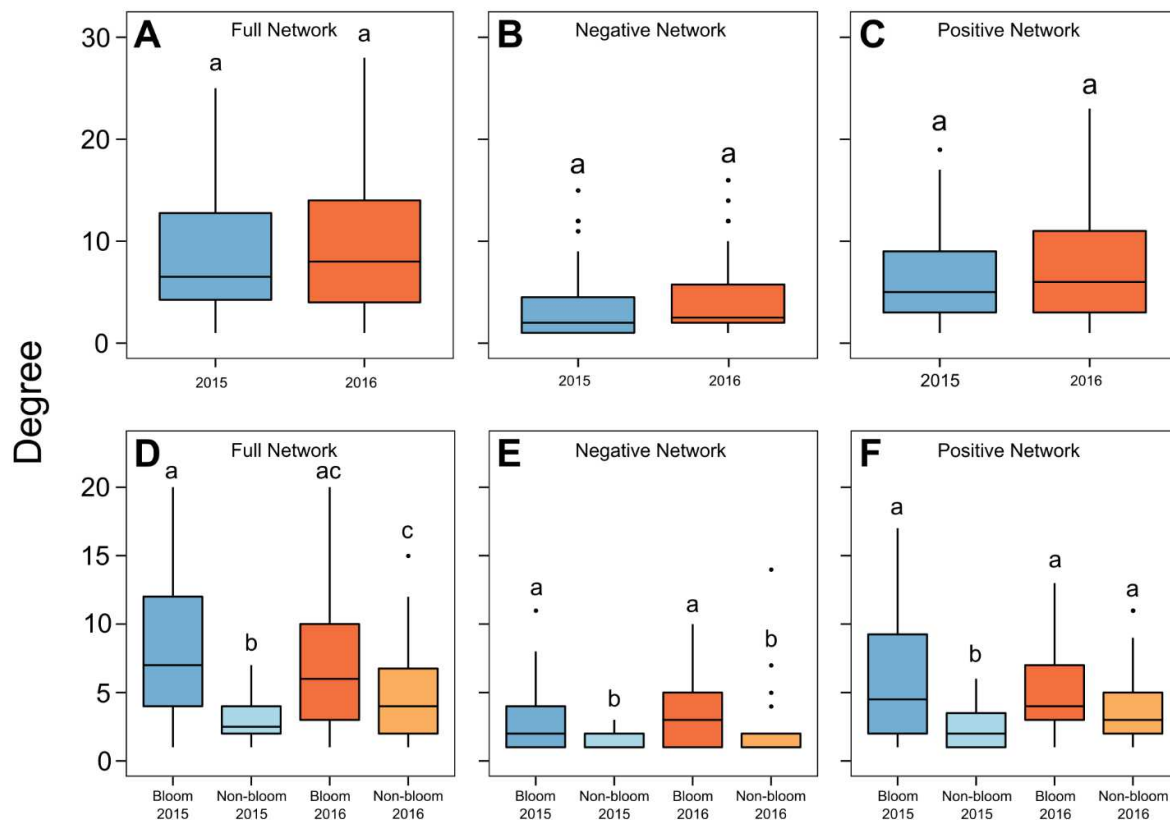


Figure 3 : Network degree distributions during 2015 and 2016. Degree centralities were computed for networks constructed using the full set of interactions (i.e. full stands (A) for both positive) or sign-specific correlations (i.e. either negative (B) or positive (C)). Networks were further separated depending on the period (i.e. either bloom or non-bloom D, E, and F). Lowercase letters indicate significant differences between groups based on pairwise Wilcoxon signed-rank test (p-value < 0.05). Boxplots that share the same letter were not significantly different.

3.4 Interactions between microbial groups

3.4.1 Comparison based on years 2015 and 2016

Figure 4 shows which edges in the networks constructed from empirical data significantly deviated from random expectations; differences were tested by knowing the cumulative number of correlations portrayed by each edge between nodes. All the relationships described here are those that significantly deviated from null models. The year 2015 was characterized by more negative relationships

Results

than random networks between bacteria and phytoplankton, within the phytoplankton groups, between bacteria and HF, and finally between bacteria and naked ciliates (Figure 4A, C, E). This pattern did not occur in 2016 (Figure 4B, D, F), as there were more negative relationships only for the connection between phytoplankton and bacteria. In 2015, positive relationships prevailed within the naked ciliates group, between viruses and naked ciliates, between bacteria and naked ciliates, and between HF and naked ciliates. On the contrary, in 2016, positive relationships among smaller microorganisms were overrepresented and observed between viruses and HF, between phytoplankton and HF, and among HF. In 2016, both negative and positive relationships between phytoplankton and naked ciliates, between phytoplankton and tintinnids, and between naked ciliates and tintinnids were less than those in random networks.

During the bloom periods of both years (Figure 4C, D), the relationships between bacteria and phytoplankton and within the phytoplankton group prevailed, whereas the positive correlations between phytoplankton and naked ciliates and between phytoplankton and tintinnids were less than in random networks. On the contrary, during non-bloom (Figure 4E, F), both negative and positive relationships prevailed between viruses and HF, between bacteria and naked ciliates, between HF and naked ciliates, and within the naked ciliates group, and the correlations linking phytoplankton to tintinnids were underrepresented.

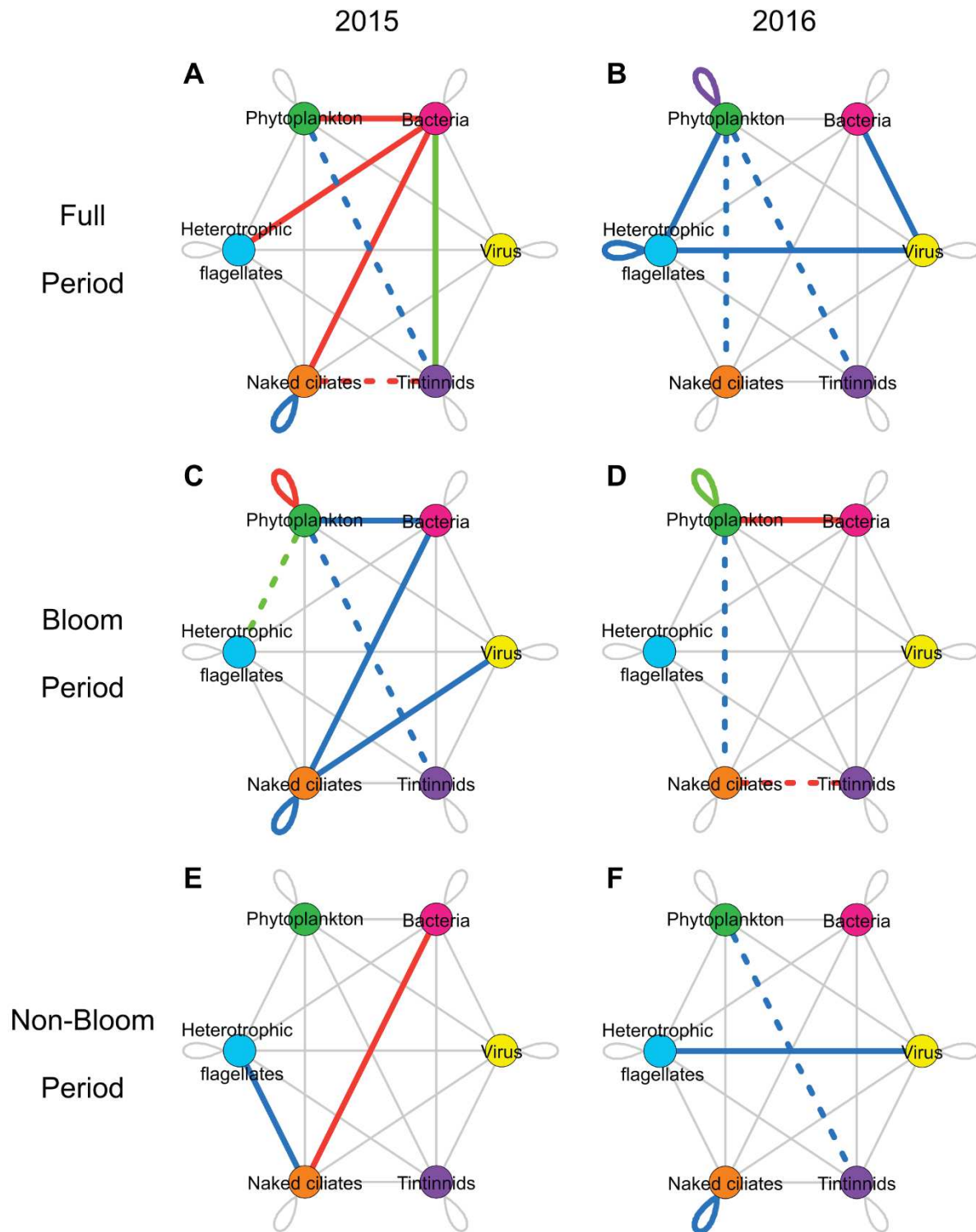


Figure 4 : Interactions between microbial food web groups. Networks of full periods (A, B), bloom periods (C, D), non-bloom periods (E, F) in 2015 (left panel) and 2016 (right panel). Yellow node is for viruses, pink for bacteria, green for phytoplankton, light blue for heterotrophic nanoflagellates, orange for naked ciliates, and purple for tintinnids. Edges are colored when the number of correlations in

networks constructed with empirical data significantly deviated from those in random models. Edge type corresponds to the direction of the significance: (1) solid lines indicate more correlations than in random networks; (2) dotted lines stand for fewer correlations than in random networks. Edge color provides information on the network type for which the significance was identified: (1) red edges correspond to negative correlation networks, (2) blue edges refer to positive correlation networks, (3) purple edges are for deviations in both negative and positive correlation networks (i.e. deviations found in both networks at the same time), and (4) green edges report about significant results in full networks (i.e. networks that include both correlation signs). Grey lines represent edges with numbers of correlations between groups that do not deviate from those in random networks.

3.5 Interactions between size classes of microbial groups

Edges between size classes of microbial groups that show the numbers of correlations that are significantly different in empirical networks compared to random models are summarized in Figure 5. Here, we describe the relationships that were found to be significantly different compared to null models. In 2015, irrespective of the period (Figure 5A, C, and E), negative correlations prevailed between the groups at the bottom of the microbial food web and those at the higher trophic levels—between bacteria and phytoplankton $< 20 \mu\text{m}$, between bacteria and HF, between bacteria and naked ciliates $30\text{--}80 \mu\text{m}$, between bacteria and naked ciliates $> 80 \mu\text{m}$, and between phytoplankton $20\text{--}50 \mu\text{m}$ and tintinnids $100\text{--}150 \mu\text{m}$. Positive relationships prevailed within naked ciliates size classes as well as between them and other groups: between HF and naked ciliates $30\text{--}50 \mu\text{m}$, between HF and naked ciliates $> 80 \mu\text{m}$, between bacteria and naked ciliates $30\text{--}50 \mu\text{m}$, between naked ciliates $< 30 \mu\text{m}$ and $30\text{--}50 \mu\text{m}$, and between naked ciliates $30\text{--}50 \mu\text{m}$ and tintinnids $100\text{--}150 \mu\text{m}$. In 2016 (Figure 5B, D, and F), both negative and positive relationships prevailed among the groups of the bottom of the microbial food web, especially for smaller size classes— between viruses and bacteria, between viruses and HF, between bacteria and HF, between phytoplankton $< 20 \mu\text{m}$ and HF, between phytoplankton $20\text{--}50 \mu\text{m}$ and HF, within the node of the group of phytoplankton $< 20 \mu\text{m}$, between phytoplankton $< 20 \mu\text{m}$ and $20\text{--}50 \mu\text{m}$ within HF. The numbers of positive and negative correlations found in empirical networks were instead below the expectations for the relationships linking the three smaller size classes of phytoplankton (i.e.

phytoplankton < 20, 20–50, and 50–100 μm) to large grazers (i.e. the two largest size classes of naked ciliates 50–80 and > 80 μm ; and the three size classes of tintinnids < 100, 100–150, and > 150 μm).

In bloom periods (Figure 5C, D), both positive and negative relationships prevailed at the bottom of the microbial food web—between bacteria and three size classes of phytoplankton < 20 μm , 20–50 μm , and 50–100 μm and within the group of phytoplankton < 20 μm . Positive relationships prevailed between the bottom of the microbial food web and the intermediate size class of naked ciliates (i.e. between bacteria and naked ciliates 30–50 μm and between phytoplankton 50–100 μm and naked ciliates 30–50 μm) and between naked ciliates and tintinnids (i.e. between naked ciliates and tintinnids 100–150 μm and between naked ciliates 50–80 μm and tintinnids <100 μm). During non-bloom (Figure 5E, F), positive relationships prevailed especially between protists groups smaller than 80 μm —between HF and naked ciliates 30–50 μm , within naked ciliates < 30 μm , between naked ciliates < 30 μm and 30–50 μm , and between ciliates < 30 μm and naked ciliates 50–80 μm . Negative relationships only prevailed between bacteria and the largest size class of tintinnids (tintinnids >150 μm).

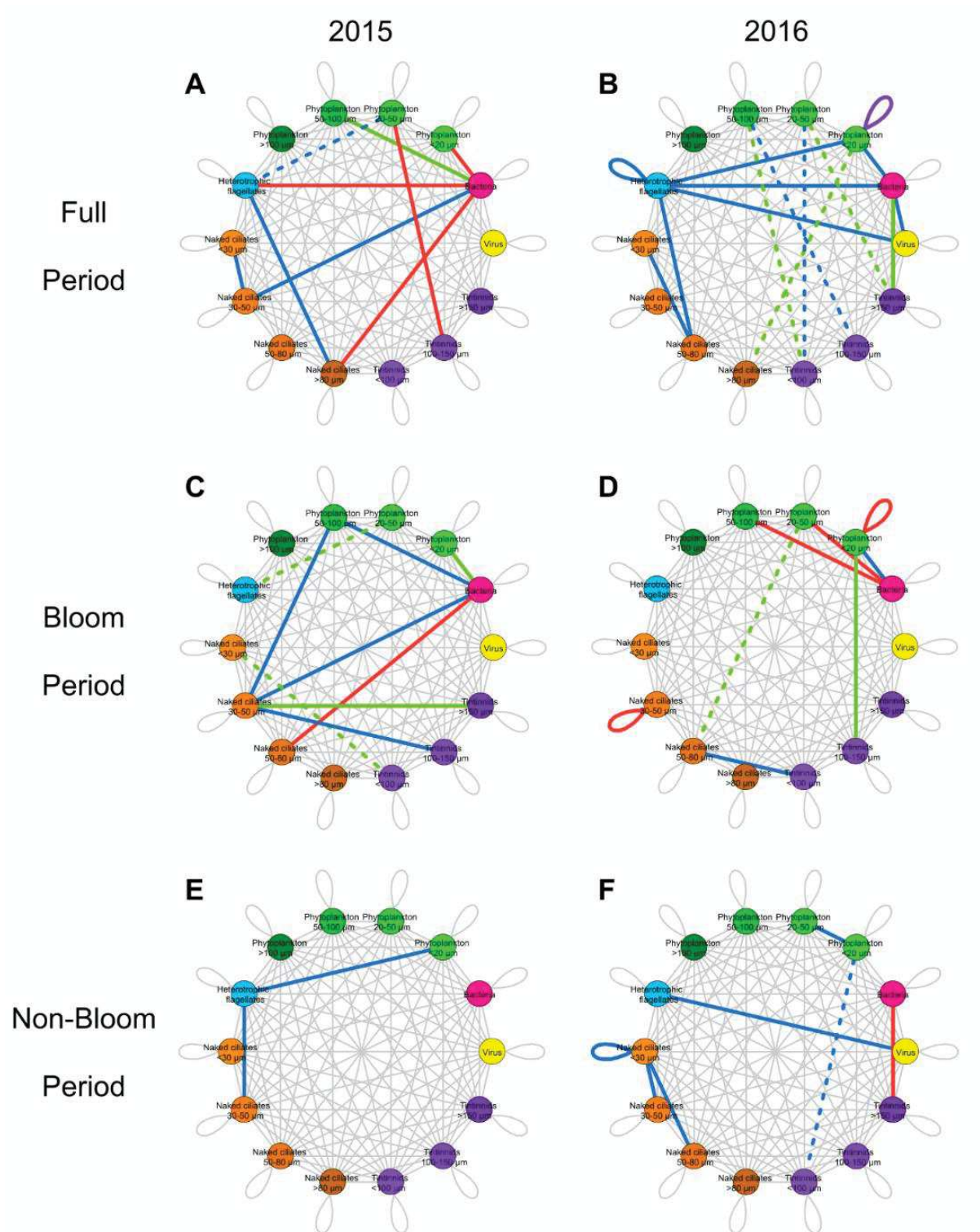


Figure 5 : Interactions between size classes of microbial food web groups. Networks of full periods (A, B), bloom periods (C, D), and non-bloom periods (E, F) in 2015 (left panel) and 2016 (right panel). Yellow node is for viruses, pink for bacteria, and light blue for heterotrophic nanoflagellates. Nodes of green gradient are for different phytoplankton size classes, orange gradient for naked ciliates, and purple

gradient for tintinnids. Edges are colored when the number of correlations in networks constructed with empirical data significantly deviated from those in random models. Edge type corresponds to the direction of the significance: (1) solid lines indicate more correlations than in random networks; (2) dotted lines stand for fewer correlations than in random networks. Edge color provide information about the network type for which the significance was identified: (1) red edges correspond to negative correlation networks, (2) blue edges refer to positive correlation networks, (3) purple edges are for deviations in both negative and positive correlation networks (i.e. deviations found in both networks at the same time), and (4) green edges provide information about significant results in full networks (i.e. networks that include both correlation signs). Grey lines represent edges with numbers of correlations between groups that do not deviate from those in random networks.

4 Discussion

In the present study, correlation networks were constructed to identify the ecological interactions linking microbial food web groups/taxa/species in coastal waters following the approach presented by Faust and Raes (2012) and Fuhrman et al. (2015). Correlation network analysis was applied so far to a few plankton communities in marine and freshwater systems (Posch et al. 2015; Tan et al. 2015; Needham and Fuhrman 2016; Xue et al. 2018). These studies had different objectives, such as identifying the daily succession of phytoplankton, bacteria, and archaea (Needham and Fuhrman 2016), unraveling the inter-specific association involved in a bloom formation (Tan et al. 2015), describing the role of rare and abundant eukaryotic plankton in networks (Xue et al. 2018), or comparing various correlation method (Posch et al. 2015). Previous works investigated microbial food web interactions analyzing single networks representative of the bloom period while the present study aims at detecting differences between bloom and non-bloom periods by taking into account the consequences of ocean warming through the comparison of various networks. It focuses on the comparison between several networks resulting from the interactions among 110 groups/taxa/species of planktonic microorganisms, including virioplankton, bacterioplankton, phytoplankton, and protozooplankton grazers. It analyses the structure of microbial food webs during bloom and non-bloom periods in 2015, a typical Mediterranean climatic year, and in 2016 which was characterized by an exceptionally warm winter. Our application shows that network analysis is a powerful method to identify: (1) dominant interactions in various

monitoring periods (e.g. bloom and non-bloom period), (2) most relevant sources for energy transfer to higher trophic levels (e.g. phytoplankton-based vs. bacterioplankton-based food webs), (3) grazers that represent bottlenecks to energy circulation in the microbial food web and shifts in their relative importance during different periods (bloom versus non-bloom), and (4) key groups/taxa/species that modulate microbial network dynamics (i.e. hubs with larger numbers of connections compared to other nodes) in each period. By applying a novel approach to detect significant differences, which is based on the comparison between empirical and random networks, we found that there is a significant intensification of both positive and negative interactions involving phytoplankton during bloom, which indicates increasing relevance of mutualism, grazing, and competition for resources. Non-bloom networks were dominated by negative interactions between bacteria and ciliates identified as bacterivory, which suggests a shift of biomass transfer from phytoplankton-dominated food webs during bloom to bacterioplankton-based food webs during non-bloom. The warmer year favored the relationships among smaller organisms and increased the relevance of the microbial-loop at the expense of the grazing chain.

4.1 Network complexity increases during phytoplankton bloom

Microbial interaction networks during the bloom and non-bloom periods differ and complexity increases during phytoplankton blooms. Trombetta et al. (2019) showed that in the same shallow coastal waters, increase in water temperature during spring triggers phytoplankton bloom. Here, we found that increases in phytoplankton biomass are responsible for profound modifications at the level of microbial interactions. Such changes are particularly clear when comparing microbial networks during bloom and non-bloom periods. Bloom networks were generally more complex than non-bloom networks. They displayed higher numbers of nodes, edges, and mean degree than non-bloom networks, both when considering all correlations and in the presence of either positive or negative edges only. Such pattern indicates that there were generally more relationships among microbial organisms during phytoplankton bloom. Negative correlations between groups/taxa/species stand for either predator-prey interactions or

competitions (Faust and Raes 2012). During bloom, the increase in phytoplankton abundance provided more resources to protozooplankton grazers, and the predator-prey interactions gained relevance. As an example, the degree of *Lohmaniella* sp. (**Supplementary Table S1**, species number 65: ID 65) was the 2nd highest in the group/taxa/species of naked ciliates in the negative networks during the 2015 and 2016 blooms (6 and 7 edges, respectively; Figure 2C, D). *Lohmaniella* sp. is a dominant naked ciliate in many marine ecosystems and mainly consumes phytoplankton (Chen and Chang 1999). This is confirmed by the negative edges shared by *Lohmaniella* sp. with chrysophyceae (ID 9), prymnesiophyceae (ID 12), and *Pyramimonas* sp. (ID 14). All these taxa belong to the size class of small phytoplankton and comprised the favorable predation size range of *Lohmaniella* sp. (Kivi and Setälä 1995; Tillmann 2004). During bloom, *Lohmaniella* sp. (ID 65), *Leegardiella* sp. (ID 68), and the small HF (ID 51) exhibited higher numbers of negative correlations than during non-bloom periods (Figure 2C, D, E, F). These protozooplankton grazers are hubs (Domin et al. 2018) that can modify microbial food web dynamics during phytoplankton bloom by consuming bacteria and small phytoplankton, and transferring relevant amounts of biomass to higher trophic levels. The present results also confirmed that HF are preferential grazers of bacteria (LNA, ID 2 and HNA, ID 3), cyanobacteria (ID 4), and picophytoeukaryotes $< 1 \mu\text{m}$ (ID 5), as shown previously by other investigations (Simek et al. 1997; Tophøj et al. 2018). Network analysis revealed increasing levels of complexity in the negative correlation networks during the bloom periods. This change can be related to predator-prey interactions, with high biodiversity of protozooplankton grazers that enable longer pathways for biomass transfer from the bottom of the food web to the higher trophic levels (Moustaka-Gouni et al. 2016). However, this higher complexity of the negative correlation network can also be attributed to the sharpening of competition. For example, increase in phytoplankton biodiversity during bloom may have amplified the competition for nutrients.

The increase in complexity in the 2015 correlation networks during bloom was also due to positive interactions. The higher number of positive interactions in the bloom compared to non-bloom period was the cause of the rising abundance of several phytoplankton groups/taxa/species. This might be

Discussion

explained by phytoplankton-produced exudates which benefit bacteria (Seymour et al. 2017), as there were more interactions between bacteria and phytoplankton compared to random expectations. Positive correlations between different groups/taxa/species of protozooplankton can also provide information about their similar response to the phytoplankton resource. For instance, during the 2015 bloom, there was a positive correlation between *Lohmaniella* sp. and *Leegardiella* sp. These two species are known to be grazers of small phytoplankton (Kivi and Setälä 1995; Gallegos et al. 1996) as confirmed by negative correlations between them and nanoeukaryotes 4–6 μm (ID 7), chrysophyceae (ID 9), prymnesiophyceae (ID 12), and *Pyramimonas* sp. (ID 14) (Figure 2C, D). The high abundance of phytoplankton < 20 μm (Figure 1C) during bloom allowed them to feed, develop, and coexist without competitive exclusion.

The degree distribution of the network reporting positive correlations during 2016 bloom was not significantly different from the one found for the non-bloom network of the same year. The cause of the relatively similar complexity between the bloom and non-bloom periods in 2016 could be (1) the abnormally high water temperature during the winter, (2) the absence of significant water cooling and (3) the slow increase in water temperature from the end of the winter to the spring (Trombetta et al. 2019). All these conditions may have contributed to the attenuation of the magnitude of environmental disturbance, and consequently the structure of the microbial interactions (Sommer 2002; Scheffer et al. 2003). Despite similarities between the general properties of the bloom and non-bloom 2016 networks, the structure of the microbial food web was highly dynamic and the hub species in the two periods were different. According to the degree centrality, the top five groups/taxa/species (i.e. the hubs of the microbial networks) differ between the bloom and non-bloom periods for full, negative, and positive networks. Various hubs prevail when moving from bloom to non-bloom periods and changes in dominance can be explained with the microbial succession related to bottom-up or top-down controls. Species can be controlled by (1) bottom-up forces such as physico-chemical parameters that directly affect physiology (e.g. temperature and salinity) or resources abundance (e.g. nutrients and prey availability) and (2) top-down forces such as predation or viral lysis. Both types of forces shape the

community structure and interactions within the microbial food web (Mostajir et al. 2015). For example, during the bloom, phytoplankton groups/taxa/species attained high abundance due to the availability of nutrient, light, and rupture of the bottom-up and top-down forces balance (grazing) in favor of bottom-up (Behrenfeld et al. 2013b). In this case, phytoplankton has higher chances of encountering and interacting with other groups/taxa/species (Seymour et al. 2017). In general, increased abundance is associated with higher probability of interactions with other cells, a mechanism common to autotrophic and heterotrophic microorganisms. For instance, during bloom, *Pseudo-nitzschia* sp. (ID 43), *Lohmaniella* sp. (ID 65), and *Strombidium* sp1 (ID 55) were involved in a large number of correlations/interactions (Figure 2C, D) whereas during non-bloom, the main interactors were *Licmophora* sp. (ID 47) and *Urotrichia* sp (ID 69; Figure 2E, F). Furthermore, hub species that engage in many interactions can indicate a more generalist trophic behavior (Faust and Raes, 2012; Díaz-Castelazo et al., 2013). *Lohmaniella* sp., which was found to be a hub during the 2015 bloom is known to be a generalist grazer (Mironova et al. 2009), and it correlated with seven groups/taxa/species in its prey size range (Kivi and Setälä 1995; Tillmann 2004). Although positive correlations do not necessarily stand for direct interactions, the presence of positive relationships between phytoplankton or bacteria and higher trophic level protists can provide feeding information. Such relationships can help to point out groups/taxa/species that play central roles in energy transfer through the grazing chain and the microbial loop. The existence of negative correlations among groups/taxa/species that share the same ecological role/occupy the same niche (e.g., protist grazers or phytoplankton taxa) most likely informs about competition.

4.2 Phytoplankton intraguild competition and interactions with bacteria dominate during bloom

The transition between bloom and non-bloom periods was accompanied by the modifications of the microbial network structure. Strong competition among phytoplankton groups/taxa/species was observed during 2015 and 2016 blooms (Figure 4). However, in 2015, the number of negative

Discussion

correlations among the various phytoplankton size classes was not significantly higher than what was observed using random models (Figure 5). Competition involved all phytoplankton groups/taxa/species irrespective of the size classes. On the contrary, in 2016, competitions mainly occurred among smaller size classes of phytoplankton (e.g., $< 20 \mu\text{m}$). It is well known that phytoplankton species compete for nutrient and light resources through physiological and biochemical adaptation (Margalef, 1978; Bratbak and Thingstad, 1985). Competition can manifest either indirectly through intrinsic physiological and biochemical adaptation, with the fittest species outcompeting the others (Krebs 2001; Morin 2009), or directly through allelopathy, mainly with species that produce chemical inhibitors (Rice 2012). Models revealed that competition is an important factor that regulates planktonic community structure during blooms (Huisman et al. 1999; Hashioka et al. 2013; Sourisseau et al. 2017). Furthermore, field and laboratory studies often identify competition among phytoplankton species during bloom (Sakshaug and Olsen 1986). However, this is the first time that *in situ* observations during bloom showed competition among phytoplankton groups/taxa/species as the predominant form of interaction shaping the microbial network. In the present study, diatom *Chaetoceros* sp1 bloomed in the spring (Trombetta et al. 2019), as it does in many other systems during the same period (Cloern 1996). This diatom species correlated negatively with five phytoplankton groups/taxa/species during the 2015 bloom (Figure 2C; i.e. two diatoms, one Chlorophyceae, one non-identified Cryptophyceae, and one non-identified Chrysophyceae) and three in 2016 (i.e. *Plagioselmis prolonga* and two non-identified Cryptophyceae). These negative correlations between different phytoplankton groups/taxa/species could be attributed to competition as diatoms are known to be strictly autotrophic (i.e. no mixotrophic predation). However, as cryptophytes are known to be mixotrophs and sometimes feed on bacteria and phytoplankton (Gast et al. 2014; Yoo et al. 2017), predation on *Chaetoceros* cannot be excluded despite the fact that their size is smaller compared to that of *Chaetoceros*.

During 2015 and 2016 blooms, the number of interactions between bacteria and phytoplankton in the networks accounting for all correlations, and also in those specific to negative or positive relations, was significantly higher than what was found using random models. Interactions between bacteria and

phytoplankton can indicate diverse relationships such as mutualism, commensalism, competition, or even predation in case of mixotrophic phytoplankton species (Danger et al. 2007; Mostajir et al. 2015). The high abundance and diversity attained by phytoplankton groups/taxa/species during bloom can explain the relevance gained by their interactions with bacteria through increase in the available phycosphere (Seymour et al. 2017). First, bacteria can satisfy part of their own carbon demand by consuming phytoplankton exudates (Bratbak and Thingstad 1985; Gurung et al. 1999). Phytoplankton exudation may be favored by the presence of exhausted nutrients, especially during bloom which is characterized by strong competition among phytoplankton groups/taxa/species (Bratbak and Thingstad 1985). Second, positive correlations can indicate mutualism between bacteria and phytoplankton. Recent studies highlighted that mutual associations between bacteria and phytoplankton may be more common than antagonistic interactions (Seymour et al. 2017). One of the most widely studied mutual interactions is between vitamin-synthesizing bacteria and phytoplankton. Many phytoplankton species require several vitamins such as B₁, B₇, and B₁₂ for their growth, which they are unable to synthesize (Seymour et al. 2017). Thus, vitamin-synthesizing bacteria provide vitamins to phytoplankton in exchange for organic carbon (Kazamia et al. 2012; Grant et al. 2014; Mayali 2018). Moreover, it cannot be concluded that positive relationships between bacteria and phytoplankton simply indicate common response to a forcing factor such as the spring rising temperature, nutrients inputs, or predation (Fuhrman et al. 2015). Third, competition can occur between bacteria and small phytoplankton cells for nutrient resources, especially under limiting conditions (Joint et al. 2002). Bacteria may limit phytoplankton primary production by depriving it of nutrients. Warming intensifies the metabolic demand per unit of biomass, which consequently increases nutrient demand (Daufresne et al. 2009) and exacerbates competition. During bloom in the warmer year (2016), the number of negative correlations between bacteria and two size classes of phytoplankton (20–50 and 50–100 µm) was higher than in random models (Figure 5). This result can be explained by the direct effect of higher nutrient demand induced by warmer conditions, which increased the competition between bacteria and phytoplankton. Under future global warming condition, the strengthening of negative interactions between bacteria and

phytoplankton observed here is expected to become more and more frequent. Finally, negative correlations can also indicate predation as some species, particularly cryptophytes and dinoflagellates, can be mixotrophic and feed on bacteria (Roberts and Laybourn-Parry 1999; Jeong et al. 2010). In the present study, the number of negative correlations between bacteria and phytoplankton 20–50 μm was significantly higher than in random models. This phytoplankton size class includes mostly dinoflagellates, such as *Gyrodinium* sp. and *Gymnodinium* sp., which are known to be bacterivorous (Jeong et al. 2010). These two species were found to be negatively correlated with both LNA and HNA during the bloom period in 2016 (but not in 2015), and their interactions most likely represent predation. Several studies reported that mixotrophic organisms, such as dinoflagellates, become more heterotrophic with rising temperature (Wilken et al. 2013). This study shows that during the warmer year of 2016, mixotrophic dinoflagellates may have shifted their feeding mode to mostly heterotrophic nutrition. Therefore, under future global warming conditions, the role of dinoflagellates in food webs could become more heterotrophic and contribute to the transfer of bacterial production to higher trophic levels.

4.3 Bacterivory of ciliates dominate during non-bloom

During the non-bloom period, the number of negative interactions between bacteria and naked ciliates (in 2015) and between bacteria and tintinnids $> 150 \mu\text{m}$ (in 2016) was significantly higher compared to expectations from random models. Because ciliates are important bacterivorous (Rassoulzadegan and Sheldon 1986), these negative correlations can mostly be interpreted as predation. Correlation networks also indicated a shift from the dominance of phytoplankton-based (autotrophic-based pathways) food web (Hlaili et al. 2014) during phytoplankton bloom to the prevalence of bacteria-based (heterotrophic-based pathways) food webs during non-bloom. Microzooplankton plays an important role in bacterial consumption, and recent studies suggested that it also takes part in phytoplankton grazing, thus challenging the dominance of mesozooplankton in the herbivorous food web. Therefore, microzooplankton provides substantial amounts of energy to higher trophic levels through two complementary sources. The balance between the different sources can vary; our dataset

shows that during the non-bloom periods, the phytoplankton biomass declined, thus impairing its capacity to sustain the growth of ciliates. Consequently, the ciliates shifted their feeding towards bacterivory. The shift to bacteria consumption allowed the maintenance of an efficient energy transfer from the bottom of the food web to higher trophic levels, as previously shown by Pomeroy and Wiebe (1988). Several studies have highlighted the relevance of bacterial production as an energy source in microbial food webs during pre- or post-bloom periods (Lignell et al. 1993; Christaki et al. 2014).

4.4 Warming favors interactions among smaller organisms

The interannual temperature changes deeply altered the structure of the interaction networks in the microbial food web. During the warmer year (2016), the interactions among small size groups/taxa/species were promoted at the expense of those involving large size classes. In the full and positive networks, the number of edges shared among phytoplanktons < 20 , $20\text{--}50$, and $50\text{--}100$ μm , larger heterotrophs microorganisms such as naked ciliates $50\text{--}80$ and > 80 μm , and all the three size classes of tintinnids was lower than that in the random models (Figure 5), whereas the number of edges between bacteria, small phytoplankton < 20 μm , and HF was higher compared to expectations from random networks. Supplementary Figure S3 shows that during 2016, there was a shift of dominance towards interactions among smaller microorganisms as shown by the significant negative relationship between mean body size and degree centrality. Indeed, in 2016, smaller phytoplankton groups/taxa/species such as pico- and nano-phytoeukaryotes were more abundant than large diatoms (Trombetta et al. 2019). The dominance of small plankton in response to warming has already been described by *in situ* and experimental studies for both freshwater and marine systems (Peter and Sommer 2012; Rasconi et al. 2015; Sommer et al. 2017). In microbial food web, warmer conditions promote the dominance of fast growing and r-trait species with small size and rapid development. Our *in situ* survey shows that, under warming conditions, both negative interactions (i.e. grazing, competition, and parasitism) and positive ones (i.e. mutualism, commensalism, and cross-feeding) are overrepresented. In 2016, phytoplankton and bacteria at the base of the food web display more interactions with HF than

with large grazers such as ciliates and tintinnids. HF species comprise a heterogeneous group due to the fact that they feed on diverse resources and exhibit intraguild predation (Moustaka-Gouni et al. 2016). Warmer conditions are unsuitable to larger HF groups/taxa/species, and they also modify the relevance of specific predator-prey interactions by supporting the prevalence of smaller species. In this *in situ* survey, warmer waters support a large spectrum of HF interactions possibly due to more favourable conditions for their metabolism. In 2016, the positive interactions between viruses and smaller heterotrophic organisms (bacteria and HF) were also overrepresented. Virioplankton abundance is tightly coupled with the abundance of its hosts because the lytic viral cycle is fast (i.e. less than 24 h) and produces up to 500 viruses per cycle per host (for bacteriophages) (Wommack and Colwell 2000). Thus, positive correlations can be interpreted as viral infections that follow the host abundance (Wommack and Colwell 2000; Bettarel et al. 2003). Our study identified positive correlations between viruses and their major hosts: bacteria (both HNA and LNA) as well as pico- and nano-eukaryotes (phytoplankton and HF) (Wommack and Colwell 2000). The predominance of interactions between bacteriophages and bacteria in 2016 can be explained by the high abundance of the host or by the probable positive effect of warmer conditions as temperature enhances viral infection and alters host susceptibility (Cottrell and Suttle 1995; Nagasaki and Yamaguchi 1998; Danovaro et al. 2011; Mojica et al. 2016).

4.5 Warming intensifies trophic cascade

The abundance of smaller microorganisms encompassing LNA and HNA bacteria, phytoplankton < 20 μm (mostly picophytoeukaryotes < 1 μm), and naked ciliates < 30 μm was higher in the warmer year (2016) than in 2015, whereas that of larger organisms including phytoplankton 20–50 μm (mostly diatoms and dinoflagellates), HF, and naked ciliates > 80 μm was lower. These trends suggest that a trophic cascade could have reshaped the microbial community during the warmer year, leading to higher abundance of smaller microorganisms such as bacteria and small phytoplankton (< 20 μm). The higher abundance of naked ciliates < 30 μm could have increased their grazing pressure above that of HF.

Grazing may have reduced HF abundance, thus releasing various prey (i.e. bacteria, cyanobacteria, and picophytoeukaryotes) from the top-down control of HF. The higher abundance of small naked ciliates ($< 30 \mu\text{m}$) could be explained by the reduction of abundance and thus grazing pressure of metazooplankton, especially copepods or rotifers. However, as the present investigation focuses on the microbial food web, copepods and rotifers were not adequately studied. The copepod-ciliate trophic link is a cornerstone relationship that transfers energy to higher trophic levels in several marine ecosystems (Calbet and Saiz 2005). The reduction of copepods abundance during warmer winters has been previously reported in the literature (Mackas et al. 2006; Garzke et al. 2015). The same mechanism might be involved in this survey, with small naked ciliates showing higher abundance due to the release of top-down control from copepods. However, this hypothesis was contradicted because the abundance of large ciliates ($> 80 \mu\text{m}$) in 2016, which are also potential preys of copepods, was lower than that in 2015. The evidence that warming enhanced the trophic cascade in plankton communities has been presented both for marine and freshwater ecosystems (Vidussi et al. 2011; Kratina et al. 2012; Shurin et al. 2012). These studies suggested that warming shifted the microorganism community control from bottom-up to top-down.

The mechanisms underlying such shift are yet to be properly understood, but they may reflect different physiological responses between autotrophs and heterotrophs under warming conditions. Warm conditions seem to increase the metabolism of heterotrophic protists above that of autotrophs; thus, heterotrophs display more pronounced increase of growth and grazing rates in response to warming (Rose and Caron 2007). These differential responses strengthen the trophic cascade (Vidussi et al. 2011) and benefit smaller microorganisms (Sommer and Lengfellner 2008; Peter and Sommer 2012). The temperature-size relationship can further explain why warmer conditions are more favorable for smaller organisms. In fact, increase in temperature makes smaller organisms more competitive than larger ones for the exploitation of resources, especially for CO_2 and nutrient uptakes, due to the higher surface to volume ratio (Sommer et al. 2017). The volume-mediated response to warming may have played a significant role in the prevalence of smaller microorganisms and their interactions in the present study.

Conclusions

Warming also allows predators to remain active during the winter and induces strong grazing pressure over the whole year (Sommer and Lengfellner 2008b). However, previous works on benthic systems showed that at intermediate temperatures, the strength of top-down control is stronger, whereas bottom-up force prevails at warmer temperatures. Such differential response is due to the regulation of metabolic processes by temperature (i.e. the optimal thermal performance and tolerance of macroalgae occurs at higher temperatures than that for their invertebrate mesograzers which exhibit highest consumption levels at intermediate temperatures; see Mertens et al. 2015). Global warming models predict an increase of 2.2–5.1 °C of the sea surface temperature by 2080 in the Mediterranean Sea, making it one of the most vulnerable regions in the world under future scenarios (IPCC 2013) and a cul-de-sac for endogenous species that could not shift their geographical range due to physical barriers in this enclosed basin (Lasram et al. 2010). Because mild winters are expected to become more frequent, the relevance of top-down control on primary production should also increase. The shift towards stronger top-down control will most likely lead to aquatic microbial communities dominated by small-size phytoplankton cells and bacteria (Morán et al. 2010; Peter and Sommer 2012). The present network analysis corroborates the hypothesis that future microbial communities in coastal ecosystems of temperate waters will be dominated by smaller organisms. Moreover, it shows that warmer waters will lead to the prevalence of relationships between smaller microorganisms over interactions involving larger cells (i.e. main interactors will belong to the following classes: bacteria, phytoplankton < 20 µm, and heterotrophic nanoflagellates).

5 Conclusions

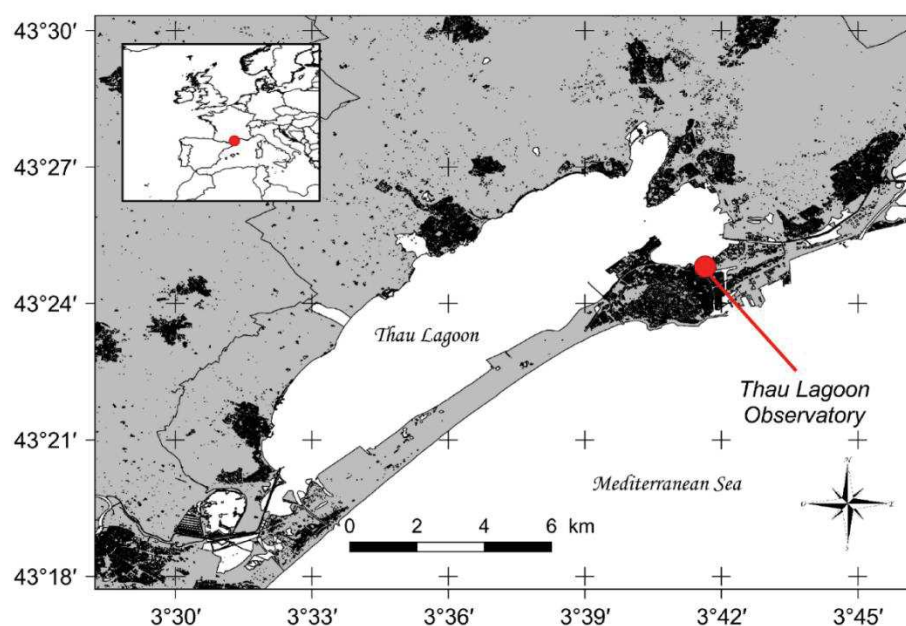
The present study unraveled that the structure of microbial interaction networks in coastal waters is highly dynamic and exhibits deep modifications following bloom and non-bloom periods. The abiotic environmental changes trigger low and high productive periods (i.e. non-bloom and bloom), thus shifting the dominance from microbial loop-dominated networks (i.e. bacteria-based) to communities where grazing prevails (i.e. herbivore feeding), respectively. Moreover, inter-annual climatic variations

deeply alter the arrangement of microbial interactions, and our results provide a snapshot of what could occur in coastal waters of western Mediterranean Sea under prospective global warming. Warmer waters enhance top-down control via the trophic cascade and support plankton communities where small-sized cells and microbial-loop interactions dominate. There is a pressing need to understand how variations in the interaction network modify the functioning of microbial communities in order to formulate reliable predictions about future global change scenarios. The analysis of correlation networks representing interactions among microbial groups/taxa/species in controlled experimental systems could help to elucidate the cause-effect mechanisms triggered by warmer temperatures (i.e. both constant increase and heat waves; see Pansch et al. 2018) and other factors related to climate change (e.g., ocean acidification and hypoxia).

6 Acknowledgments

We would like to appreciate Benjamin Sembeil, Océane Schenkels, Ludovic Pancin, and Erika Gaudillère for their help with the sampling and/or analyses of samples. Especially, we would like to acknowledge Sébastien Mas for the assistance during two years of monitoring. We thank Emilie Le Floc'h for helping during the sampling. Handling and preservation of samples were performed at the Marine Station of the Observatoire de Recherche Méditerranéen de l'Environnement (OSU OREME) in Sète. Microscopy and cytometry equipment were provided by the Microbex platform of MARBEC/Cemeb Labex. The manuscript was edited for English language by Editage (www.editage.com).

7 Supplementary material



Supplementary Figure 1 : Thau Lagoon and location of the sampling station.

Supplementary Table 1 : Groups/taxa/species used for the construction of the correlation networks. The following details are provided: group/taxa/species IDs, mean body size, taxonomic classification and size class.

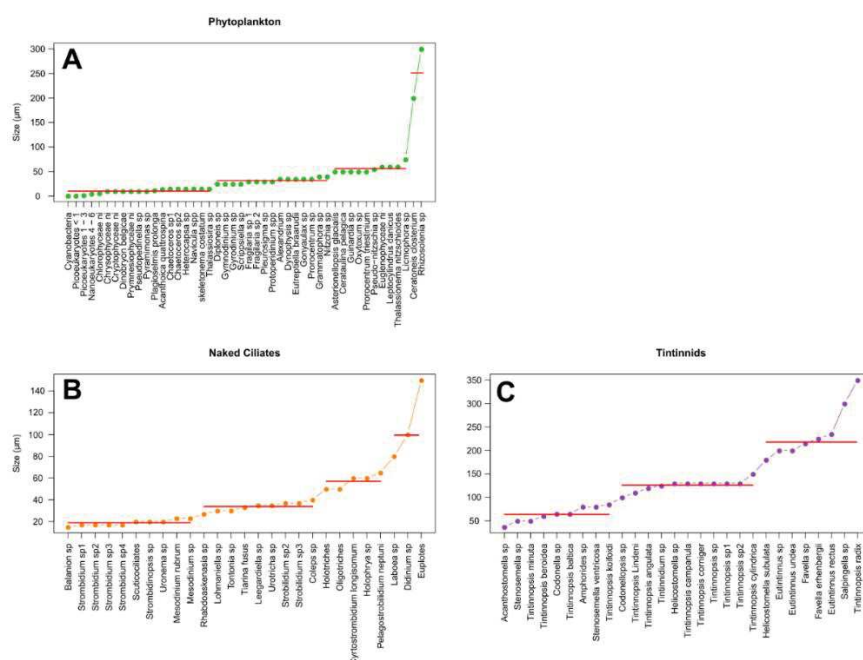
Groups/taxa/species	ID	Mean body size (μm)	Taxonomic classification	Size class
Virus	1		Virus	Virus
HNA	2	0.8	Bacteria	Bacteria
LNA	3	0.8	Bacteria	Bacteria
Cyanobacteria	4	0.8	Phytoplankton	<20 μm
Picoeukaryotes <1 μm	5	0.8	Phytoplankton	<20 μm
Picoeukaryotes 1 – 3 μm	6	2	Phytoplankton	<20 μm
Nano-eukaryotes 4 – 6 μm	7	5	Phytoplankton	<20 μm
<i>Chlorophyceae</i> ni.	8	6	Phytoplankton	<20 μm
<i>Chrysophyceae</i> ni.	9	10	Phytoplankton	<20 μm
<i>Cryptophyceae</i> ni.	10	10	Phytoplankton	<20 μm
<i>Dinobryon belgicæ</i>	11	10	Phytoplankton	<20 μm
<i>Prymnesiophyceae</i> ni.	12	10	Phytoplankton	<20 μm
<i>Pseudopedinella</i> sp.	13	10	Phytoplankton	<20 μm

<i>Pyramimonas</i> sp.	14	10	Phytoplankton	<20 µm
<i>Plagioselmis prolonga</i>	15	12	Phytoplankton	<20 µm
<i>Acanthoica quattropsina</i>	16	14	Phytoplankton	<20 µm
<i>Chaetoceros</i> sp1.	17	15	Phytoplankton	<20 µm
<i>Chaetoceros</i> sp2.	18	15	Phytoplankton	<20 µm
<i>Heterocapsa</i> sp.	19	15	Phytoplankton	<20 µm
<i>Navicula</i> spp.	20	15	Phytoplankton	<20 µm
<i>Skeletonema costatum</i>	21	15	Phytoplankton	<20 µm
<i>Thalassiosira</i> sp.	22	15	Phytoplankton	<20 µm
<i>Diploneis</i> sp.	23	25	Phytoplankton	20-50 µm
<i>Gymnodinium</i> sp.	24	25	Phytoplankton	20-50 µm
<i>Gyrodinium</i> sp.	25	25	Phytoplankton	20-50 µm
<i>Scrippsiella</i> sp.	26	25	Phytoplankton	20-50 µm
<i>Fragilaria</i> sp1.	27	30	Phytoplankton	20-50 µm
<i>Fragilaria</i> sp2.	28	30	Phytoplankton	20-50 µm
<i>Pleurosigma</i> sp.	29	30	Phytoplankton	20-50 µm
<i>Protoperidinium</i> spp.	30	30	Phytoplankton	20-50 µm
<i>Alexandrium</i> spp.	31	35	Phytoplankton	20-50 µm
<i>Dynophysis</i> sp.	32	35	Phytoplankton	20-50 µm
<i>Eutreptiella braarudii</i>	33	35	Phytoplankton	20-50 µm
<i>Gonyaulax</i> sp.	34	35	Phytoplankton	20-50 µm
<i>Prorocentrum</i> sp.	35	35	Phytoplankton	20-50 µm
<i>Grammatophora</i> sp.	36	40	Phytoplankton	20-50 µm
<i>Nitzschia</i> sp.	37	40	Phytoplankton	20-50 µm
<i>Asterionellopsis glacialis</i>	38	50	Phytoplankton	50-100 µm
<i>Cerataulina pelagica</i>	39	50	Phytoplankton	50-100 µm
<i>Guinardia</i> sp.	40	50	Phytoplankton	50-100 µm
<i>Oxytoxum</i> sp.	41	50	Phytoplankton	50-100 µm
<i>Prorocentrum triestinum</i>	42	50	Phytoplankton	50-100 µm
<i>Pseudo-nitzschia</i> sp.	43	55	Phytoplankton	50-100 µm
<i>Euglenophyceae</i> ni.	44	60	Phytoplankton	50-100 µm
<i>Leptocylindrus danicus</i>	45	60	Phytoplankton	50-100 µm
<i>Thalassionema nitzschioides</i>	46	60	Phytoplankton	50-100 µm
<i>Licmophora</i> sp.	47	75	Phytoplankton	50-100 µm
<i>Ceratoneis closterium</i>	48	200	Phytoplankton	>100 µm
<i>Rhizosolenia</i> sp.	49	300	Phytoplankton	>100 µm
Nanoflagellates <3µm	50	2	HF	HF
Nanoflagellates 3- 4 µm	51	3.5	HF	HF
Nanoflagellates 5 - 10 µm	52	7.5	HF	HF
Nanoflagellates >10 µm	53	12	HF	HF

Supplementary material

<i>Balanion</i> sp.	54	15	Naked ciliates	<30 µm
<i>Strombidium</i> sp1.	55	17	Naked ciliates	<30 µm
<i>Strombidium</i> sp2.	56	17	Naked ciliates	<30 µm
<i>Strombidium</i> sp3.	57	17	Naked ciliates	<30 µm
<i>Strombidium</i> sp4.	58	17	Naked ciliates	<30 µm
Scuticociliates	59	20	Naked ciliates	<30 µm
<i>Strombidinopsis</i> sp.	60	20	Naked ciliates	<30 µm
<i>Uronema</i> sp.	61	20	Naked ciliates	<30 µm
<i>Mesodinium rubrum</i>	62	23	Naked ciliates	<30 µm
<i>Mesodinium</i> sp.	63	23	Naked ciliates	<30 µm
<i>Rhabdoaskenasia</i> sp.	64	27	Naked ciliates	<30 µm
<i>Lohmaniella</i> sp.	65	30	Naked ciliates	30-50 µm
<i>Tontonia</i> sp.	66	30	Naked ciliates	30-50 µm
<i>Tiarina fusus</i>	67	33	Naked ciliates	30-50 µm
<i>Leegardiella</i> sp.	68	35	Naked ciliates	30-50 µm
<i>Urotricha</i> sp.	69	35	Naked ciliates	30-50 µm
<i>Strobilidium</i> sp2.	70	37	Naked ciliates	30-50 µm
<i>Strobilidium</i> sp3.	71	37	Naked ciliates	30-50 µm
Aloricate ciliates unidentified	72		Naked ciliates	
<i>Coleps</i> sp.	73	40	Naked ciliates	30-50 µm
Holotriches	74	50	Naked ciliates	50-80 µm
Oligotriches	75	50	Naked ciliates	50-80 µm
<i>Cyrtostrombidium longisomum</i>	76	60	Naked ciliates	50-80 µm
<i>Holophrya</i> sp.	77	60	Naked ciliates	50-80 µm
<i>Pelagostrobilidium neptuni</i>	78	65	Naked ciliates	50-80 µm
<i>Laboea</i> sp.	79	80	Naked ciliates	>80 µm
<i>Didinium</i> sp.	80	100	Naked ciliates	>80 µm
Euplotes	81	150	Naked ciliates	>80 µm
<i>Acanthostomella</i> sp.	82	37	Tintinnids	<100 µm
<i>Stenosemella</i> sp.	83	50	Tintinnids	<100 µm
<i>Tintinnopsis minuta</i>	84	50	Tintinnids	<100 µm
<i>Tintinnopsis beroidea</i>	85	60	Tintinnids	<100 µm
<i>Codonella</i> sp.	86	65	Tintinnids	<100 µm
<i>Tintinnopsis baltica</i>	87	65	Tintinnids	<100 µm
<i>Amphorides</i> sp.	88	80	Tintinnids	<100 µm
<i>Stenosemella ventricosa</i>	89	80	Tintinnids	<100 µm
<i>Tintinnopsis koifoidi</i>	90	85	Tintinnids	<100 µm
<i>Codonellopsis</i> sp.	91	100	Tintinnids	100-150 µm
<i>Tintinnopsis Lindeni</i>	92	110	Tintinnids	100-150 µm
<i>Tintinnopsis angulata</i>	93	120	Tintinnids	100-150 µm

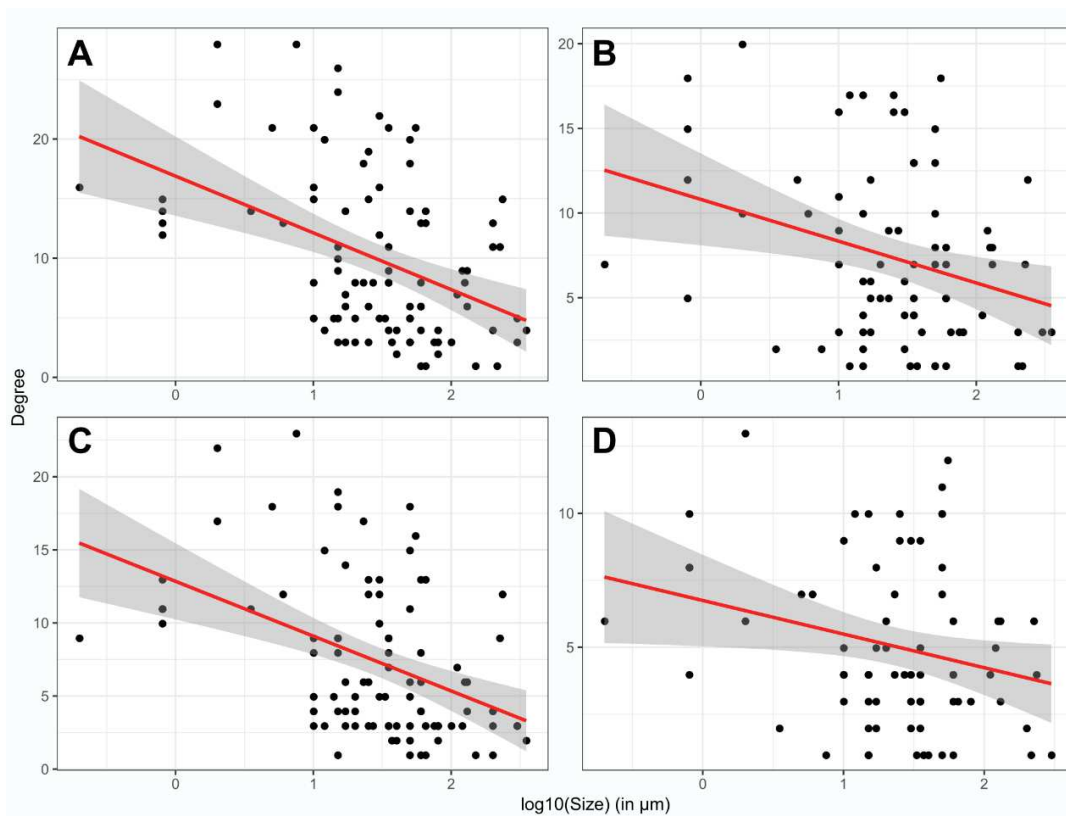
<i>Tintinnidium</i> sp.	94	125	Tintinnids	100-150 µm
<i>Helicostomella</i> sp.	95	130	Tintinnids	100-150 µm
Tintinnina unidentified	96		Tintinnids	
<i>Tintinnopsis campanula</i>	97	130	Tintinnids	100-150 µm
<i>Tintinnopsis corniger</i>	98	130	Tintinnids	100-150 µm
<i>Tintinnopsis</i> sp.	99	130	Tintinnids	100-150 µm
<i>Tintinnopsis</i> sp1.	100	130	Tintinnids	100-150 µm
<i>Tintinnopsis</i> sp2.	101	130	Tintinnids	100-150 µm
<i>Tintinnopsis cylindrica</i>	102	150	Tintinnids	>150 µm
<i>Helicostomella subulata</i>	103	180	Tintinnids	>150 µm
<i>Eutintinnus</i> sp.	104	200	Tintinnids	>150 µm
<i>Eutintinnus undea</i>	105	200	Tintinnids	>150 µm
<i>Favella</i> sp.	106	215	Tintinnids	>150 µm
<i>Favella erhenbergii</i>	107	225	Tintinnids	>150 µm
<i>Eutintinnus rectus</i>	108	235	Tintinnids	>150 µm
<i>Salpingella</i> sp.	109	300	Tintinnids	>150 µm
<i>Tintinnopsis radix</i>	110	350	Tintinnids	>150 µm



Supplementary Figure 2 : Mean body size of groups/taxa/species for (A) phytoplankton, (B) naked ciliates, and (C) tintinnids. Red horizontal lines represent the size class thresholds identified using the PELT algorithm.

Supplementary Table 2 : Mean abundance and results of the paired Wilcoxon tests on the weekly abundance of the different microbial groups and size classes (2015 vs. 2016). The term ‘Group’ indicates the various size classes of the different groups. The parameter V and the p -values refer to the tests performed. Asterisks indicate the significant tests at a 0.05 threshold. Details concerning abundance dynamics are provided in Figure 1.

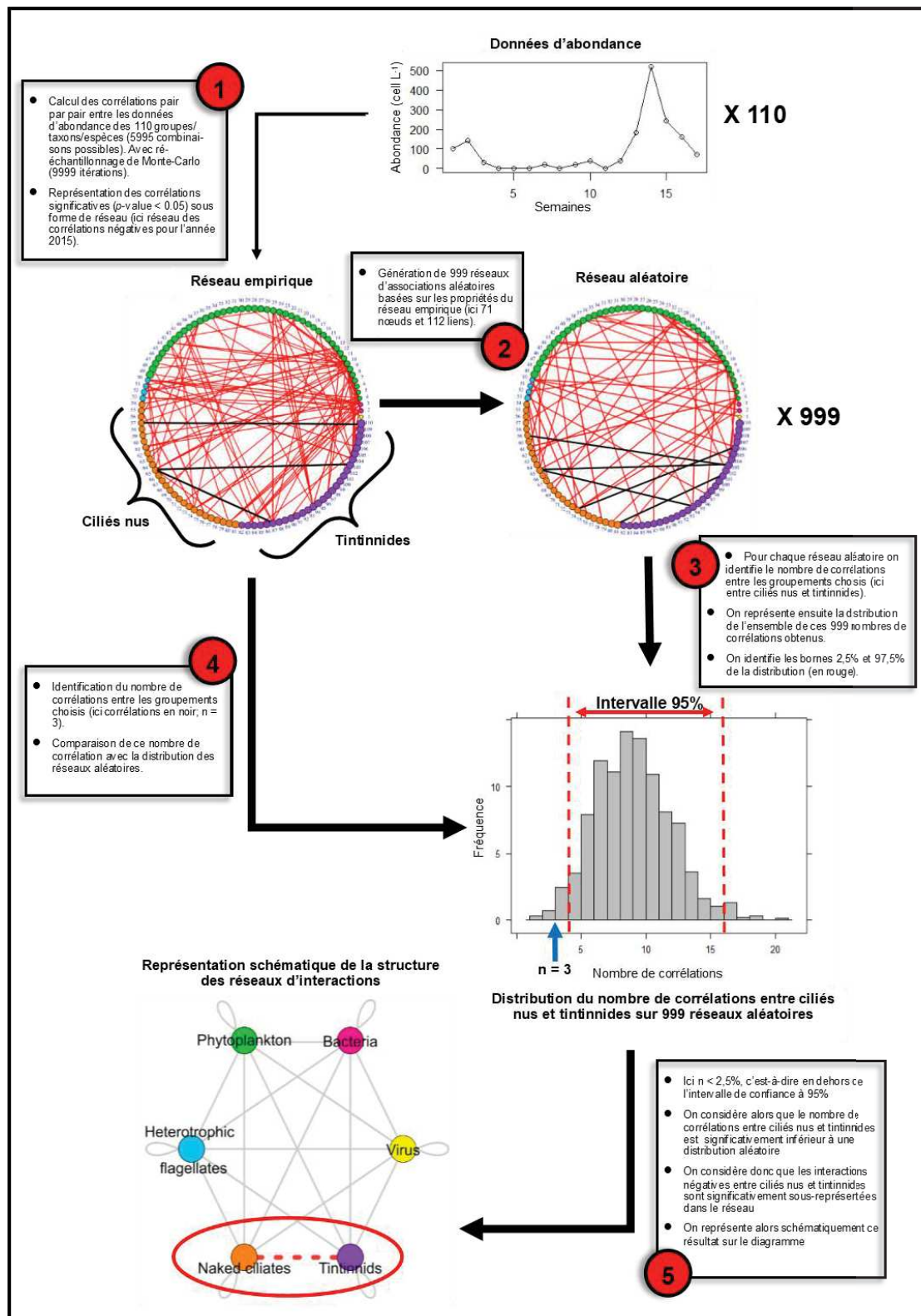
Group	Mean abundance in 2015 (cells mL ⁻¹)	Mean abundance in 2016 (cells mL ⁻¹)	V	p -value
Viruses	6.96×10^7	7.66×10^7	86	0.7381
Bacteria	2.77×10^6	4.15×10^6	48	0.0602
Phytoplankton <20 μm	3.04×10^4	4.71×10^4	33	0.0108 *
Phytoplankton 20-50 μm	19.67	13.00	150	0.0258 *
Phytoplankton 50-100 μm	137.23	11.40	92	0.4776
Phytoplankton >100 μm	0.95	1.28	25	0.4971
Heterotrophic flagellates	1.54×10^3	1.05×10^3	155	0.0141 *
Naked ciliates <30 μm	1.65	3.22	45	0.0446 *
Naked ciliates 30-50 μm	0.43	0.33	114	0.4653
Naked ciliates 50-80 μm	0.21	0.15	102	0.7983
Naked ciliates >80 μm	9.00×10^{-2}	1.87×10^{-2}	129	0.0138 *
Tintinnids <100 μm	4.73×10^{-2}	4.35×10^{-2}	82	0.8961
Tintinnids 100-150 μm	1.11×10^{-2}	3.42×10^{-2}	63	0.2049
Tintinnids >150 μm	3.05×10^{-2}	2.55×10^{-2}	91	0.8906



Supplementary Figure 3 : Regression analysis between \log_{10} mean body size and degree of groups/taxa/species. The significance of the relationship was investigated using general linear model (GLM) with gamma family and log link function. The best model was selected based on Akaike information criterion (AIC). After the model was applied, diagnostic plots were visualized and evaluated. Only networks that exhibited significant relationships are presented here: (A) 2016 full network for the whole year (with negative and positive correlations; $t = -3.18$, p -value < 0.01), (B) 2016 full network during bloom ($t = -2.48$, p -value < 0.05), (C) 2016 positive network ($t = -3.57$, p -value < 0.001), and (D) 2016 positive network during bloom ($t = -2.37$, p -value < 0.05).

Encadré

Méthode de représentation schématique de la structure des réseaux d'interactions.



Chapitre 3

Effet de l'élévation de la température et du zooplancton sur la dynamique des efflorescences phytoplanctoniques : une expérimentation *in situ*

Avant-propos

Ce chapitre présente les travaux effectués visant à déterminer, dans une expérimentation en mésocosmes *in situ*, l'influence de l'augmentation de la température, ainsi que des différentes fractions de taille du zooplancton (micro et mésozooplancton) sur la dynamique et la composition de la communauté phytoplanctonique.

Pour mieux comprendre les effets de la hausse des températures sur les efflorescences phytoplanctoniques, l'approche expérimentale par mésocosme s'est révélée être la plus pertinente car elle permet d'étudier l'effet d'un forçage en condition contrôlée à l'échelle de l'ensemble de la communauté planctonique naturelle. Cependant, comme vu précédemment, les interactions prédateurs-proies ont également un rôle primordial dans le contrôle de la dynamique et la composition phytoplanctonique, et ces interactions sont susceptibles d'être modifiées avec l'augmentation de la température. Ainsi, il s'est également révélé nécessaire de tamiser la communauté planctonique à différentes tailles de maille afin de démêler l'impact des différentes fractions zooplanctoniques, et notamment le microzooplancton, sur la dynamique et sur la composition du phytoplancton, ainsi que sa modification avec l'augmentation de la température. De ce fait, une expérience en mésocosmes simulant les prévisions de température à l'horizon 2080 (IPCC 2013) a été réalisée en avril 2018 dans les mésocosmes *in situ* de la plateforme MEDIMEER sur la lagune de Thau. Quatre traitements en triplicats ont été appliqués : (1) un traitement contrôle dans lequel la communauté planctonique naturelle est soumise à des conditions naturelles de température (C), (2) un traitement dans lequel la communauté

planctonique naturelle a été soumise à une augmentation de 3°C de la température par rapport aux conditions naturelles (T), (3) un traitement dans lequel le mesozooplancton (> 200 µm) a été retiré, dans des conditions naturelles de température et (4) un traitement dans lequel le mésozooplancton (> 200 µm) a été retiré, et la température augmentée 3°C par rapport aux conditions naturelles (TMicroZ).

L'élévation à + 3°C correspond aux prévisions moyennes de l'augmentation de la température de la Méditerranée à l'horizon 2080 (IPCC 2013). Le choix du retrait du zooplancton > 200 µm a été motivé par la nécessité de discerner l'influence des différentes fractions zooplanctoniques (< 200 µm ; microzooplancton et > 200 µm ; mésozooplancton). La concentration journalière en chlorophylle *a* a été utilisée pour identifier les différences de dynamique de l'efflorescence phytoplanctonique printanière en fonction des traitements. La diversité et la composition pigmentaire de la communauté phytoplanctonique ont également été analysées par la méthode de chromatographie en phase liquide à haute performance (*High performance pressure liquid chromatography*, HPLC), afin de déterminer les effets des différents traitements sur la dynamique des différentes composantes de la communauté phytoplanctonique. Cette expérimentation faisait partie du projet Photo-phyto et était ouverte aux participants extérieurs dans le cadre d'un *Transnational Access* du projet européen Aquacosm (<https://www.aquacosm.eu/>). Ainsi, de nombreux chercheurs et étudiants européens ont pu activement participer à cette expérimentation. La mise en place de l'expérience, l'échantillonnage et les analyses en laboratoire ont été réalisés par de nombreux étudiants, techniciens, ingénieurs et chercheurs dont je faisais partie. Les analyses pigmentaires par HPLC présentées dans ce chapitre ont été réalisées par Julien Dupont (L3 de l'IUT Chimie en 2018). Les analyses de nutriments ont été réalisées par Maxime Thibault (L3 de l'IUT Chimie en 2018), Ariadna Garcia-Astillero Honrado (M1, *Transnational Access* européenne) et Camille Suarez-Bazille (Apprentie IUT Chimie). Les analyses pigmentaires ont été réalisées par Julien Dupont et moi-même. Lors de cette expérimentation, j'ai conduit en parallèle des expérimentations d'incubation d'O₂ basées sur la méthode de Winkler (1888) modifiée par Carritt et Carpenter (1966), pour déterminer le statut métabolique de la communauté planctonique des différents mésocosmes. Cette expérimentation sera valorisée dans des articles en collaboration avec les partenaires européens impliqués dans cette expérimentation. Pour me former à la cytométrie en flux décrite dans le Chapitre 1, j'ai également analysé l'ensemble des échantillons issus du suivi journalier des mésocosmes pour l'abondance en phytoplancton et en bactérioplancton.

Les résultats de ce chapitre mettent en lumière les effets de la hausse des températures sur l'ensemble de la communauté phytoplanctonique lors d'une efflorescence printanière naturelle. Ils permettent notamment pour la première fois d'évaluer le rôle du micro- et du mésozooplancton dans la réponse de la communauté phytoplanctonique à l'élévation de la température. Ces résultats permettent

ainsi de mieux appréhender les modifications de la composition, du fonctionnement et de la circulation de l'énergie au sein du réseau planctonique dans un futur plus chaud.

Ce chapitre est la version la plus aboutie d'un futur article intitulé : **Warming reduces the phytoplankton bloom amplitude and induces shift in phytoplanktonic composition and succession : an *in situ* mesocosm experiment in marine coastal waters.**

**Warming reduces phytoplankton bloom amplitude and induces
shift in planktonic composition and succession: an *in situ*
mesocosm experiment in marine coastal waters**

Trombetta Thomas^{1*}, Francesca Vidussi¹, Sébastien Mas², Behzad Mostajir¹

¹MARBEC (Marine Biodiversity, Exploitation and Conservation), Centre National de la Recherche Scientifique, Université de Montpellier, Institut Français de Recherche pour l'Exploitation de la Mer, Institut de Recherche pour le Développement, Montpellier, France.

²MEDIMEER (Mediterranean platform for Marine Ecosystems Experimental Research), Observatoire de Recherche Méditerranéen de l'Environnement, Centre National de la Recherche Scientifique, Université de Montpellier, Institut de Recherche pour le Développement, Institut National de Recherche en Sciences et Technologies pour l'Environnement et l'Agriculture, Sète, France.

*** Correspondence:**

Corresponding Author: Thomas Trombetta; email: thomas.trombetta@cnrs.fr

Keywords: Mesocosm, phytoplankton pigments, phytoplankton composition, global warming.

Abstract

Spring phytoplankton bloom supports a consistent part of the annual marine ecosystems productivity contributing to CO₂ sequestration. To better understand the influence of micro and mesozooplankton and the response in warmer condition of the phytoplankton bloom and the dynamic of its different components as those expected in a climate change context, and, an *in situ* mesocosm experiment was carried out in a coastal Mediterranean area (Thau lagoon, south of France) in April 2018. Four treatments were applied: 1) natural planktonic community with natural water temperature (Control: C), 2) natural planktonic community with +3°C (T), 3) exclusion of larger zooplankton (> 200 µm; mesozooplankton) with natural water temperature (MicroZ), and 4) exclusion of larger zooplankton with +3°C (TMicroZ). To characterize the phytoplankton bloom and the composition dynamic, mesocosms were sampled daily at 09 AM for measurements of nutrients and phytoplankton pigment concentrations. The microzooplankton revealed to be the main grazer of the phytoplankton community whereas the mesozooplankton mainly plays the role of secondary consumer. Warmer conditions strongly modified the bloom biomass accumulation, amplitude, phytoplanktonic composition and succession. The bloom amplitude in warm conditions (T) was 2-times lower and the bloom lasted 1 day earlier compare to Control treatment. The concentration reduction of most of the taxonomic pigments was mostly due to a strengthening of the grazing pressure of both micro and mesozooplankton. Furthermore, warmer conditions induced a modification of the phytoplanktonic succession with an early bloom of small green algae and a late bloom of diatoms due to remineralization. At the end of the experiment, warmer conditions promoted smaller green algae and dinoflagellates at the expense of diatoms and prymnesiophytes. This study highlighted that in the future warmer ocean, the phytoplankton spring bloom will be weaker with predominance of the smaller phytoplankton taxa, causing a reduction of the carbon sequestration and transfer to higher trophic levels, and a modification of the nutrient cycling.

1 Introduction

Phytoplankton spring blooms provide most of the annual primary production in temperate and subpolar regions (Behrenfeld and Boss 2014). Phytoplankton blooms are characterized by a rapid phytoplankton biomass accumulation that supports the whole ecosystem productivity through the food web. Thus, in most of the ecosystems, including coastal waters, the system productivity is dependent of the amplitude, timing and duration of these spring blooms (Kjørboe 1993; Lignell et al. 1993; Brussaard et al. 1996; Tortajada et al. 2012). The initiation and development of phytoplankton bloom and in particular spring blooms have been explained by the increase of phytoplankton growth under favourable environmental conditions, so primary production depending on bottom-up forcing factors (nutrient concentration, light and temperature). However, top-down control leading to the disruption of the balance between phytoplankton growth and losses due to grazing, have been proposed as a new paradigm in the bloom initiation theory (Behrenfeld 2010; Behrenfeld et al. 2013b; Behrenfeld and Boss 2014). In fact, the phytoplankton biomass and dynamic are directly controlled by the herbivorous zooplankton grazing activity (Cloern 1996). Such top-down control on the initiation of phytoplankton bloom has been neglected for a long time. Phytoplankton world is wide, with a large diversity of size, taxonomic groups and functioning roles. Consequently, the phytoplankton response to physico-chemical forcing factors and to top-down control could be various depending on their sizes or groups. Especially water temperature revealed to be a crucial factor influencing metabolic processes of both autotrophs and heterotrophs (Rose and Caron 2007). Thus, it modifies the relationships within organisms susceptible to influence phytoplanktonic biomass and composition.

Increased water temperature due to global warming over the past century has been already supposed to be responsible of the ocean decrease of the phytoplankton biomass production (Behrenfeld et al. 2006; Boyce et al. 2010). Global warming models predict that the water temperature over the globe will continue to increase by 1.8 to 4 °C by the horizon 2080 (IPCC 2013), suggesting that the decrease of the phytoplankton production might continue. This global decrease is mainly driven by the open

ocean systems, as the surface warming increase the stratification, reducing the mixing and the nutrient import from depth supporting the phytoplankton production (Behrenfeld et al. 2006). However, recent *in situ* survey highlighted that warming occurring in shallow coastal water, especially during winter, could also reduce the spring phytoplankton biomass accumulation shifting the community toward the dominance of smaller phytoplankton species (Trombetta et al. 2019). Models and experimental studies based on metabolic theory of ecology highlighted that warmer conditions are more favorable to heterotrophic processes than autotrophic ones (Allen et al. 2005; López-Urrutia et al. 2006; Rose and Caron 2007) pointing out the potential of mismatch between predators and preys dynamics under warming. At the same time indoor mesocosm experiments put in advance a strengthening of the top-down control on phytoplankton under a temperature increase (Sommer and Lewandowska 2011; Peter and Sommer 2012) suggesting that the response of phytoplankton can be various depending its size and their potential predators. However, still little is known about the response of natural phytoplankton communities under warming conditions, in particular the extent of the effects on phytoplankton bloom dynamic and composition and also the influence of the different zooplankton size fraction on the phytoplankton community structure response.

The objectives of the present study were to investigate the response of phytoplankton communities under warming and highlight the influence of the larger zooplankton (mesozooplankton) compared to small one (microzooplankton) on its response. In this frame, a 12-mesocosm experiment was conducted on natural planktonic community ($< 1000 \mu\text{m}$) of a Mediterranean shallow coastal lagoon (Thau Lagoon in south of France) in spring 2018. Four treatments were applied: 1) natural planktonic community with natural water temperature (Control: C), 2) natural planktonic community with $+3^\circ\text{C}$ (T), 3) exclusion of larger zooplankton ($> 200 \mu\text{m}$; mesozooplankton) with natural water temperature (MicroZ), and 4) exclusion of larger zooplankton with $+3^\circ\text{C}$ (TMicroZ).

2 Material and Methods

2.1 Experimental design

An *in situ* mesocosm experiment was carried out in the Thau Lagoon, at the Mediterranean platform for marine Ecosystem Experimental Research (MEDIMEER). Mesocosms were 3 m high and 1.2 m wide and were held 1 m above the water surface by floating structures. Mesocosms were made of 200- μ m-thick vinylacetate mixed-polyethylene film (Insinööritoimisto Haikonen Ky) which transmitted 53% to the UVBR and 77% of the photosynthetically available radiations (PAR: 400-700 nm) (Nouguier et al. 2007) Mesocosms were moored *in situ* at the pontoon of MEDIMEER where the depth was around 3 m. The mesocosms water column depth was 2 m and contained 2260 L of Thau lagoon water. Thau Lagoon is a shallow coastal lagoon (mean depth: 4 m) located in the North western Mediterranean shore (43°24'00" N, 3°36'00" E). The Thau Lagoon is a productive Mediterranean lagoon hosting oyster farms experiencing a wide range of temperature from 4 to 29 °C. It's a mesotrophic lagoon generally described as phosphorus- and nitrogen-limited (Souchu et al. 2010). The *in situ* mesocosm experiment lasted 19 days from 5 to 23 April 2018. To prevent any contamination, the mesocosms were constantly covered by removable domes of polyethylene. The domes were openable with a zipper to perform any intervention when necessary.

Mescocosms were filled on April 5 2018 (hereafter call day 0). The lagoon water was pumped at 1.5 m depth near the MEDIMEER pontoon and screened throught 1000 μ m to remove large particles of the mesocoms water. Mesocosms were filled simultaneously from the water pool through filling tubes. The mesocosm water column was continually homogenized with a pump (Model 24, 12V, Xylem). The water was pumped at 1 m below the surface of the mesocosm and spewed near the bottom. A daily turnover of 3.5 mesocosm volume was set and adjusted in the course of the experiment following the remaining water after sampling.

2.2 Exclusion of mesozooplankton and increased water temperature treatments

Mesocosms were filled simultaneously through separated filling tubes with 1000 μm screened lagoon water (C and T) or to remove larger zooplankton with the same water passing through a 200 μm mesh size tissue (NITEX, SEFAR) placed tightly attached at the end of the filling tubes (MicroZ and TMicroZ).

Water temperature of Heated treatments (T and TMicroZ) was increased using an submersible heating element (Galvatec) immersed vertically at a depth of 1 m (Nouguier et al. 2007). The ΔT between Heated and Control treatments were controlled by an automated system based on a close-loop regulation according to Nouguier et al. (2007). To maintain the ΔT between Control and Heated mesocosms, the water temperature was monitored at 0.4, 0.8 and 1.2 m depth every 5 minutes using thermistor probes (Campbell Scientific 107) on all mesocosms. The mean of the three depths temperature of the Heated mesocosms was then compared to the mean temperature of the Control mesocosms using a Campbell Scientific data logger (CR1000) The heating elements started or stopped to reach or maintain the target ΔT value (for more detail see Nouguier et al. 2007). It should be noted that to avoid the thermal choc to organisms, the ΔT in both of the Heated treatments (T and TMicroZ) was increased $+1.5^{\circ}\text{C}$ between days 1 and 2 and 1.5°C more between days 2 and 3 to reach and maintain thereafter at $+3^{\circ}\text{C}$ relative to the natural water temperature of Control treatments until the end of the experiment.

2.3 Physico-chemical sampling and analysis

Mesocosms water temperature was monitored also at mid-depth every day between 9:00 AM and 10:00 AM with a multiparameter sensor (EC300, VWR International) from day 2 until the end of the experiment. Due to bad weather conditions, the mesocosms water temperatures were not monitored on days 6 and 7. Thus, water temperature data from the thermistor probes at 9:00 am were extracted at these days to provide the missing temperature data. Incident Photosynthetically Active Radiations (PAR, 400-700 nm) was recorded at a high frequency (every 15 min) using a Professional Weather Station (METPAK PRO, Gill instruments) with PAR sensor (Skye Instruments). PAR monitoring started from

day 6 (due to technical issues) at 06:45 PM until the end of the experiment. To identify the daily incident PAR dose received at the surface water, the Daily Light Integral (DLI) or daily dose, was calculated following the **Equation 1** where ΣPAR is the sum of PAR measured during the day (96 measures) and Δt the time interval between two measurements (900 s). As data of day 6 and day 18 were incomplete, the DLI was not calculated for these days.

$$DLI = \Sigma PAR \times \Delta t \quad (\text{Equation 1})$$

Samples (5 L) for nutrient analysis were taken daily using a Niskin bottle except for day 6 where due to bad weather conditions Niskin sampling was not performed. Mesocosm water was also sampled (10 L) daily between 8:30 and 10:00 AM using a low vacuum pump at mid-depth and stored in polycarbonates jerrycan pre-washed with acid and rinsed. Sub-samples aliquots were immediately taken from the later samples for pigment analysis.

To determine nitrates ($NO_2 + NO_3$), phosphates (PO_4) and silicates ($Si(OH)_4$) concentrations, two 13-mL aliquots were filtered on 3-times pre-washed PP 0.45 μm filters (25 mm, Agilent Technologies) and stored at $-20^\circ C$ until analysis. Samples were analyzed using Continuous Flow Analyzer (San⁺⁺, Skalar) following the standard nutrient analysis methods (Tréguer and Le Corre 1974). To measure ammonium (NH_4) concentrations 50 mL sub-samples from Niskin bottle were taken and were determined using fluorometric method (Holmes et al. 1999).

2.4 Phytoplankton pigment analysis and bloom identification

Sub-samples of 1 L were taken from the 10 L jerrycan to determine phytoplankton pigment concentrations. Sub-samples were filtered through glass-fiber filters (GF/F Whatman: 25 mm, nominal pore size: 0.7 μm) and stored at $-80^\circ C$ until analysis. Pigment concentrations were measured by high performance liquid chromatography (HPLC, Waters) following the method described by Zapata et al. (2000) with some modifications and the extraction protocol described in Vidussi et al. (2011).

In order to distinguish the different periods of the experiment, chlorophyll *a* (Chl *a*) concentration as a proxy for phytoplankton biomass was used. Blooms periods was identified by estimating the net phytoplankton growth rate using the phytoplankton biomass gain and loss (Behrenfeld 2010; Trombetta et al. 2019). Consequently, the phytoplankton daily net growth rate (*r*) was calculated for each mesocosm using Chl *a* concentration (**Equation 2**) and a daily mean and standard deviation of the *r* was calculated for each treatment.

$$r_{t+1} = C_{t+1} - C_t \quad (\text{Equation 2})$$

where C_t is the daily Chl *a* concentration. A bloom was identified as a period of at least two consecutive days of positive *r*.

Besides Chl *a*, some pigments are representative of particular taxa while others are ubiquitous and present in a large diversity of taxa and may be redundant with others. Therefore, a wise choice of pigments to investigate could capture the whole phytoplanktonic diversity. For statistical analysis, seven taxonomic pigments were chosen according to their signification as proxy of specific taxonomic groups, thus represent the phytoplankton taxonomic diversity, and their description in the literature to be relevant diagnostic pigments. The seven taxonomic pigments and their taxonomic signification reported in literature are presented in **Table 1**.

Table 1 : Taxonomic pigments, their abbreviations, taxonomic meaning and theoretical size class. Vidussi et al. (2001).

Pigments	Abbreviation	Presence in taxa	Size class
Chlorophyll <i>b</i>	Chl <i>b</i>	Green flagellates	Picophytoplankton ^a
Prasinoloxanthin	Prasi	Prasinophytes	Picophytoplankton ^a
Zeaxanthin	Zea	Cyanobacteria and prochlorophytes	Picophytoplankton ^a
Alloxanthin	Allo	Cryptophytes	Nanophytoplankton ^b
19'hexanoyloxyfucoxanthin	19HF	Haptophytes (prymnesiophyceae)	Nanophytoplankton ^b
Fucoxanthin	Fuco	Diatoms	Microphytoplankton ^c
Peridinin	Peri	Dinoflagellates	Microphytoplankton ^c

^aPicophytoplankton: cell size < 2 μm; ^bNanophytoplankton: cell size 2-20 μm; ^cMicrophytoplankton: cell size > 20 μm.

2.5 Statistical analysis

To test the effect of the different treatments (C, MicroZ, T and TMicroZ) on the nutrient, Chl *a*, and taxonomic pigments concentrations, one-way repeated-measures analyses of variance (RM-ANOVAs) were conducted. The ‘treatments’ were set as factors with 4 levels (C, MicroZ, T and TMicroZ) and ‘days’ were set as random effect to prevent from auto-correlation spurious effects. When significant, the RM-ANOVAs were followed by post-hoc pairwise tests to identify the effects of different treatments. These effects are susceptible to induce different responses on the various studied variables depending on the ecological phases of the mesocosms (pre-bloom, bloom and post-bloom). Thus, the RM-ANOVAs were conducted separately on the three different periods of pre-bloom, bloom and post-bloom. As the bloom periods could have occurred in different timing depending on the treatment, unified ‘pre-bloom’, ‘bloom’ and ‘post-bloom’ periods were identified using the common days of blooms between treatments. Due to technical issues, one mesocosm per treatments were removed from the analysis, consequently, “±” symbols in the text is for the range of observations. One mesocosm per treatment was removed from the analysis, consequently, only duplicates were presented in the present study

3 Results

3.1 Physico-chemical dynamic

At the beginning of the experiment, the water temperature in the Control treatments (C) was 13.2 °C at day 2 (**Figure 1**). The temperature in MicroZ treatments was the same. The ΔT of +3 °C in the Heated treatments (T and TMicroZ) was attained between day 2 and 4. The natural water temperature was almost stable in all treatments from the beginning of the experiment to the day 10 with a natural cooling period occurred between day 6 and 7 due to a short storm. Note that the natural cooling was mimicked also by the Heated treatments. The water temperature increased from day 10 to 17 to reach a maximum mean of 18.4 and 21.2 °C in the Control and Heated treatments, respectively. The temperature decreased by 1 °C the last day of the experiment.

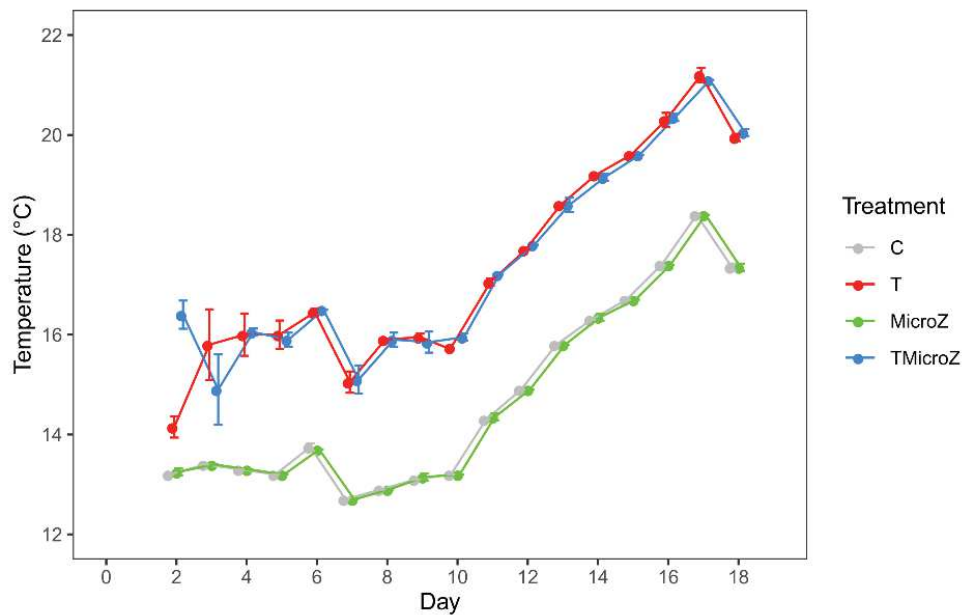


Figure 1 : Daily water temperature means (\pm range of the observations) for the different treatments. C is for the Control, T for the Heated treatment at +3°C, MicroZ for the mesozooplankton exclusion treatments and TMicroZ for the Heated at +3°C and mesozooplankton exclusion treatments.

The PAR DLI at the surface water was low due to a storm occurred between the day 7 and 9 (mean of $1.86 \pm 0.63 \times 10^7 \mu\text{mol m}^{-2} \text{d}^{-1}$, data not shown). The PAR DLI at day 10 and almost stable attaining high values until the end of the experiment, with a mean of $5.22 \pm 0.36 \times 10^7 \mu\text{mol m}^{-2} \text{d}^{-1}$.

At the beginning of the experiment nutrient concentrations were relatively high. Notably the mean NH_4 and NO_3 concentrations at day 0 in all mesocosms were 0.83 ± 0.24 and $1.22 \pm 0.40 \mu\text{mol L}^{-1}$, respectively, while that of NO_2 was $0.07 \pm 0.011 \mu\text{mol L}^{-1}$ (Figure 2). Moreover mean $\text{Si}(\text{OH})_4$ and PO_4 concentrations were 3.99 ± 0.80 and $0.84 \pm 0.14 \mu\text{mol L}^{-1}$, respectively. Nutrients showed three general trends with some exceptions according to the nutrient and the treatment: 1) a general initial decrease until the middle of the experiment followed by concentrations almost stable until the end of the experiment, 2) initially almost stable concentrations or a slow increase until the middle of the experiment followed by a decrease and 3) after an initial decrease an increase of concentrations in the middle of the

Results

experiment then in some case a final decrease. The NH_4 concentrations showed in general the first trend as for example in C concentrations decreased after a sporadic peak at day 4 to a plateau with low concentrations at day 8 (Figure 2A). In all the other treatments, NH_4 concentrations followed the same trend, except that the decrease was lower in T and that in TMicroZ after the decrease, concentrations increased until day 17. The concentrations of NO_2 and NO_3 showed the second trend but only for C and MicroZ treatments. Thus, concentration in C were stable at the beginning of the experiment and then decreased in the middle of the experiment (at days 8 and 7 in C, respectively) to reach concentration close to undetectable values until the end of the experiment (Figure 2B and C). The trend in the MicroZ treatment was the same, except that the concentration decrease started later for NO_2 and the value was higher for NO_3 . However, in the Heated treatments (T and TMicroZ) the trends were different, with an increase of both NO_2 and NO_3 concentrations until day 8, and even continuing until days 13 and 15, respectively, before a decrease at the end of the experiment for T. $\text{Si}(\text{OH})_4$ and PO_4 concentrations showed in general the third trend. In fact, $\text{Si}(\text{OH})_4$ concentrations decreased at the beginning of the experiment until day 6, then increased to reach a plateau at day 9, to decrease again at the end of the experiment at day 15 in C (Figure 2D). The other treatments followed the same trends, but the increase of concentration in T was stronger. PO_4 concentrations in C also decreased at the beginning of the experiment to reach a plateau at low concentrations at day 7 before increasing again at day 13 (Figure 2E). The other treatments followed the same trend, but with a stronger decrease in the non-Heated mesocosms (C and MicroZ).

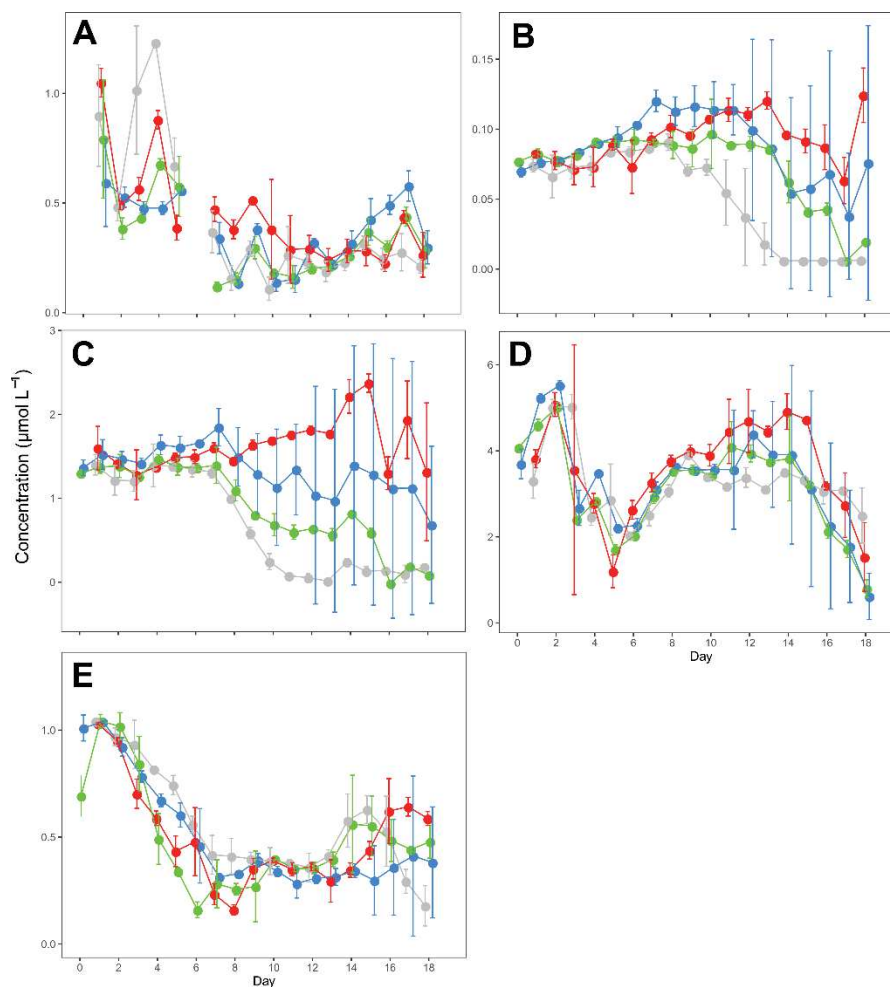


Figure 2 : The daily mean (\pm range of the observations) of nutrient concentrations in the mesocosms for the different treatments of the experiment. Nutrients are NH_4 (A), NO_2 (B), NO_3 (C), $\text{Si}(\text{OH})_4$ (D) and PO_4 (E). C is for the Control, T for the Heated treatments at $+3^\circ\text{C}$, MicroZ for the mesozooplankton exclusion treatments and TMicroZ for the Heated at $+3^\circ\text{C}$ and mesozooplankton exclusion treatments.

3.2 Bloom identification and Chl *a* dynamic and Bloom identification

The mean Chl *a* concentration at day 0 in all treatments was $0.84 \pm 0.04 \mu\text{g L}^{-1}$ (Figure 3). During the pre-bloom period, the Chl *a* concentrations slightly increased in all treatments, but above all in Heated treatments (T and TMicroZ) where a peak was observed at day 4 (Figure 3B and D). Then, a bloom was observed in all the mesocosms at day 6 characterized by a stronger Chl *a* concentration increase in C treatment compared to the others. The Chl *a* concentration peaked in day 10 in the Control

Results

(C; Figure 3A) while it was one day before, in day 9, for the other treatments (T, MicroZ and TMicroZ; Figure 3B, C and D). The mean Chl *a* concentration maximum attained $4.51 \pm 0.20 \mu\text{g L}^{-1}$ in C, while it was 48%, 39% and 25% lower in T ($2.33 \pm 0.15 \mu\text{g L}^{-1}$), MicroZ ($2.75 \pm 0.05 \mu\text{g L}^{-1}$) and TMicroZ ($3.39 \pm 0.43 \mu\text{g L}^{-1}$), respectively. After the peak, Chl *a* concentration decreased in all treatments. The concentrations fall to reach a plateau at day 14 of $< 1 \mu\text{g L}^{-1}$ in T and MicroZ (Figure 3B and C), and around $1.5 \mu\text{g L}^{-1}$ in TMicroZ (Figure 3D). The Chl *a* concentration in the C treatments did not showed the same plateau and continued to decrease until the end of the experiment (day 18, mean of $2.09 \pm 0.10 \mu\text{g L}^{-1}$; Figure 3A). Chl *a* concentration increased in treatments MicroZ and T during the last two days of the experiment (days 17 and 18).

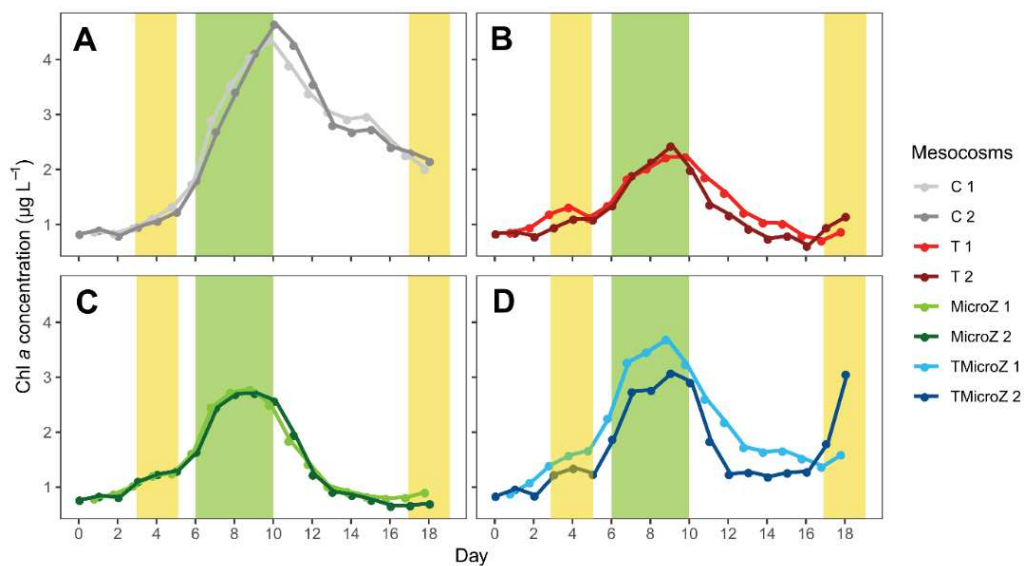


Figure 3 : Chl *a* concentrations in the different treatments. (A) represent the control (C) treatment, (B) the Heated at $+3^{\circ}\text{C}$ (T) treatment, (C) for the mesozooplankton exclusion treatment (MicroZ treatment), and (D) for the Heated at $+3^{\circ}\text{C}$ and mesozooplankton exclusion treatments (TMicroZ). Green background depicts main bloom period in all treatments and orange background the early and late blooms identified in MicroZ and TMicroZ treatments.

A period of several consecutive positive daily net growth rate (r ; Figure 4) identified as a bloom occurred from day 3 in C and MicroZ (Figure 4A and C). The bloom peaked at day 7, attaining r of $1.02 \pm 0.19 \text{ d}^{-1}$ and $0.82 \pm 0.03 \text{ d}^{-1}$, in C and MicroZ, respectively, while finished at days 11 and 10, respectively. These periods were followed by a period of post-bloom characterized by several consecutive negative daily r until day 14 and then a period of r close to 0. For the Heated treatments (T and TMicroZ) relatively high r (early bloom) was observed at days 3 and 4 followed by a day of negative r (day 5) (Figure 4B and D). From day 6 to 10 a period of positive high values of r occurred (bloom), followed by a period of negative r until day 14 (post-bloom). During the last two days (days 17 and especially 18), exceptional positive r was observed in T and TMicroZ treatments which can be considered as a late bloom. Thus, all treatments had a common bloom period with high positive r from day 6 to 10. Consequently, this period was hereafter called for all treatment ‘bloom’ period. The period before, from day 0 to 5, was called ‘pre-bloom’ and the period after, from day 11 to 18, ‘post-bloom’ period.

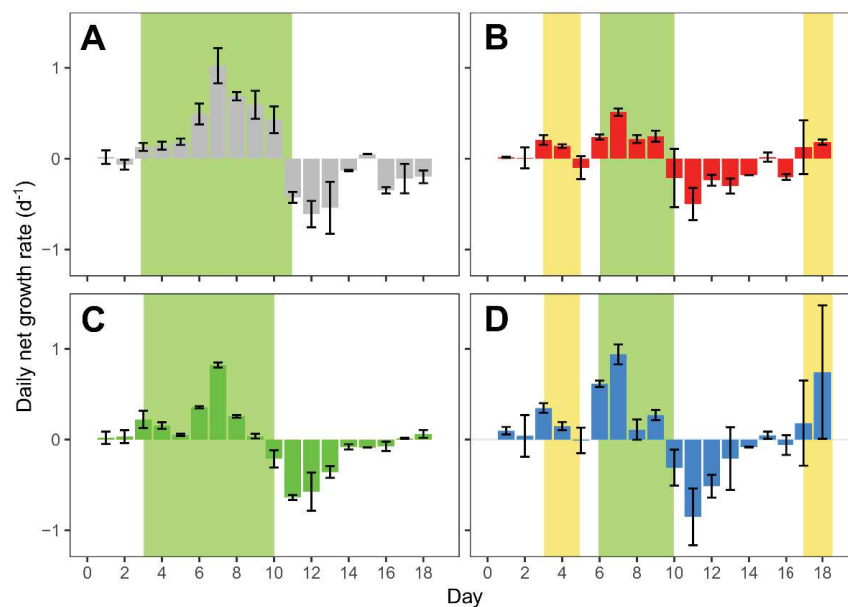


Figure 4 : Mean (\pm range of the observations) of daily net growth rates (r) of the different treatments. (A) represent the control (C) treatment, (B) the Heated at +3°C (T) treatment, (C) for the mesozooplankton exclusion treatment (MicroZ treatment), and (D) for the Heated at +3°C and mesozooplankton exclusion treatments (TMicroZ). Green and orange backgrounds depict the periods of

consecutive days of positive r . Green background is for the main bloom period and orange background for the early and late blooms identified.

3.3 Taxonomic pigments dynamic

The taxonomic pigment dynamics showed five different trends (Figure 5). (1) a similar trend as Chl *a*, this was the case of 19'HF that showed an initial increase attaining a maximum concentration in day 9 (for T and MicroZ) or 10 (for C and TMicroZ) and then a decrease (Figure 5A). (2) Fucoxanthin pigment has similar trend than Chl *a* but with a second increase at the end of the experiment in Heated mesocosms (T and TMicroZ; Figure 5B). (3) Peridinin and zeaxanthin had maximum peak of concentrations delayed of one or more days compared to Chl *a* (except for C; Figure 5C and D) and occurring during the phytoplankton post-bloom period. (4) Chlorophyll *b* (Chl *b*) and prasinoxanthin had two peaks of concentration, a first early peak during the pre-bloom period occurring in the Heated treatments (T and TMicroZ), and a second during the bloom period occurring in all treatments (**Figure 5E and F**). (5) Alloxanthin concentrations decreased all along the experiment (Figure 5G), especially in C treatment.

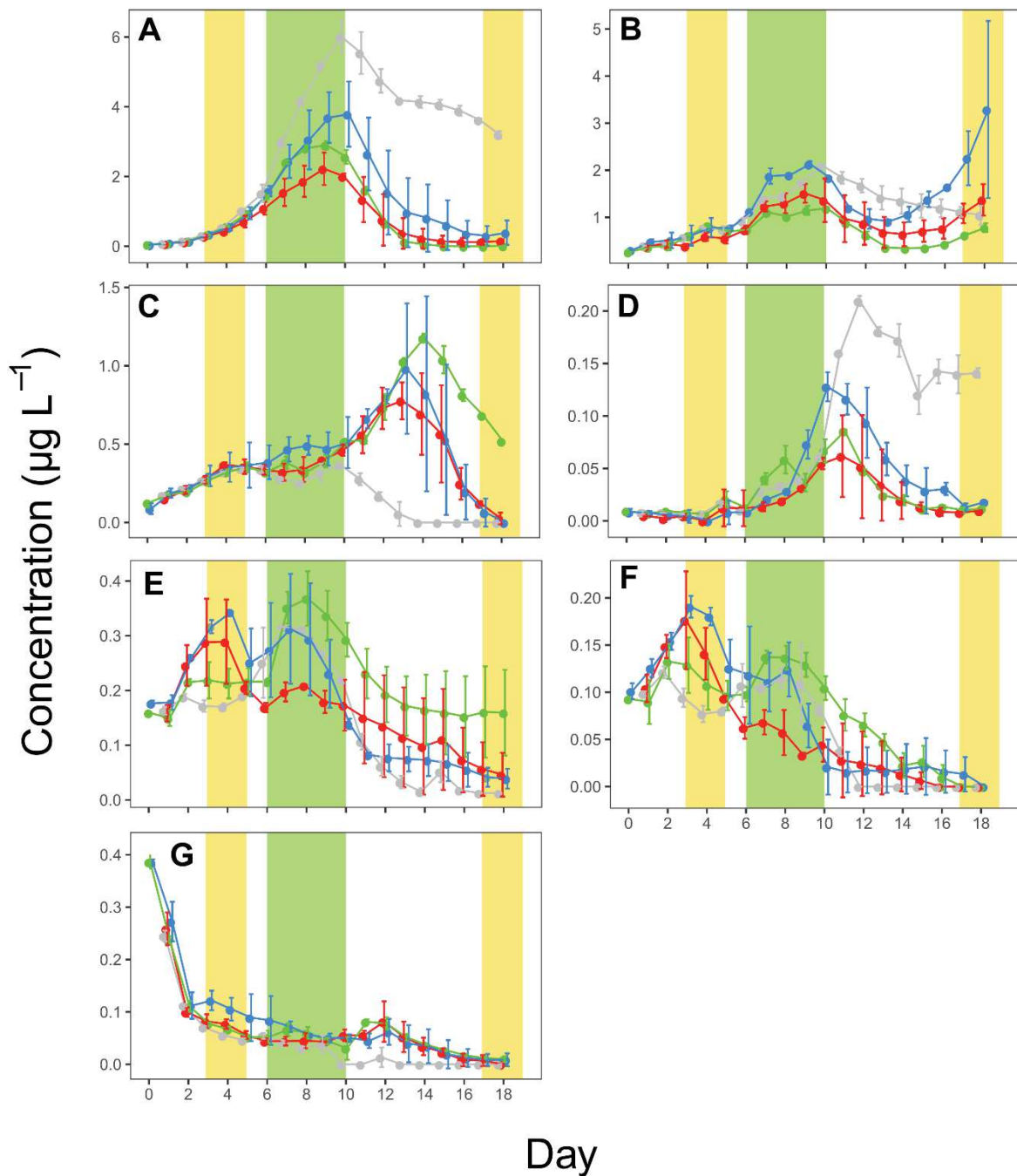


Figure 5 : Means of pigment concentrations (\pm range of the observations) in the different treatments. Pigments are (A) 19HF, (B) fucoxanthin, (C) peridinin, (D) zeaxanthin, (E) Chl *b*, (F) prasinoxanthin and (G) alloxanthin. C is for the Control, T for the Heated at +3°C treatments, MicroZ for the mesozooplankton exclusion treatments and TMicroZ for the Heated at +3°C and mesozooplankton exclusion treatments. Green background depicts main bloom period in all treatments and orange background the early and late blooms identified in MicroZ and TMicroZ treatments.

3.4 Treatments effects on nutrient, Chl *a* and taxonomic pigment concentrations during pre-bloom, bloom and post-bloom periods

3.4.1 Treatments effects on nutrient concentrations

The results of the RM-ANOVAs on nutrient concentrations are presented in Figure 6. All the results presented in the following sections are statistically significant.

In the T treatment, concentrations of NH_4 , NO_2 , NO_3 and $\text{Si}(\text{OH})_4$ were higher than in the C treatment (p -values < 0.05) during the bloom, and that of NO_2 and NO_3 during the post-bloom period (p -values < 0.001). On the opposite, PO_4 concentrations were lower than C during the pre-bloom and the bloom period, (p -values < 0.05 ; Figure 6).

In MicroZ treatment, NH_4 and PO_4 concentrations were lower than in the C treatment during the pre-bloom period (p -values < 0.01), while it was higher for NO_2 (p -value < 0.001). During the bloom period, PO_4 concentrations were lower in the MicroZ than in the C treatment (p -value < 0.05). During the post-bloom period, NO_2 concentrations were significantly higher in the MicroZ than in the C treatment (p -values < 0.001).

In the TMicroZ treatment, NO_2 concentrations were lower than in the T treatment during the pre-bloom period (p -value < 0.05). During the bloom period NH_4 and $\text{Si}(\text{OH})_4$ concentrations were significantly lower in the TMicroZ than in the T treatment (p -values < 0.01), while it was higher for NO_2 concentrations (p -value < 0.001). Only NO_3 concentrations were higher in the TMicroZ than in the MicroZ treatment during the bloom period (p -value < 0.01). During the post-bloom period, NO_3 and $\text{Si}(\text{OH})_4$ concentration were lower in the TMicroZ than in the T treatment (p -values < 0.05), while it was higher for NH_4 and NO_3 in the TMicroZ than in the MicroZ treatment (p -values < 0.05)

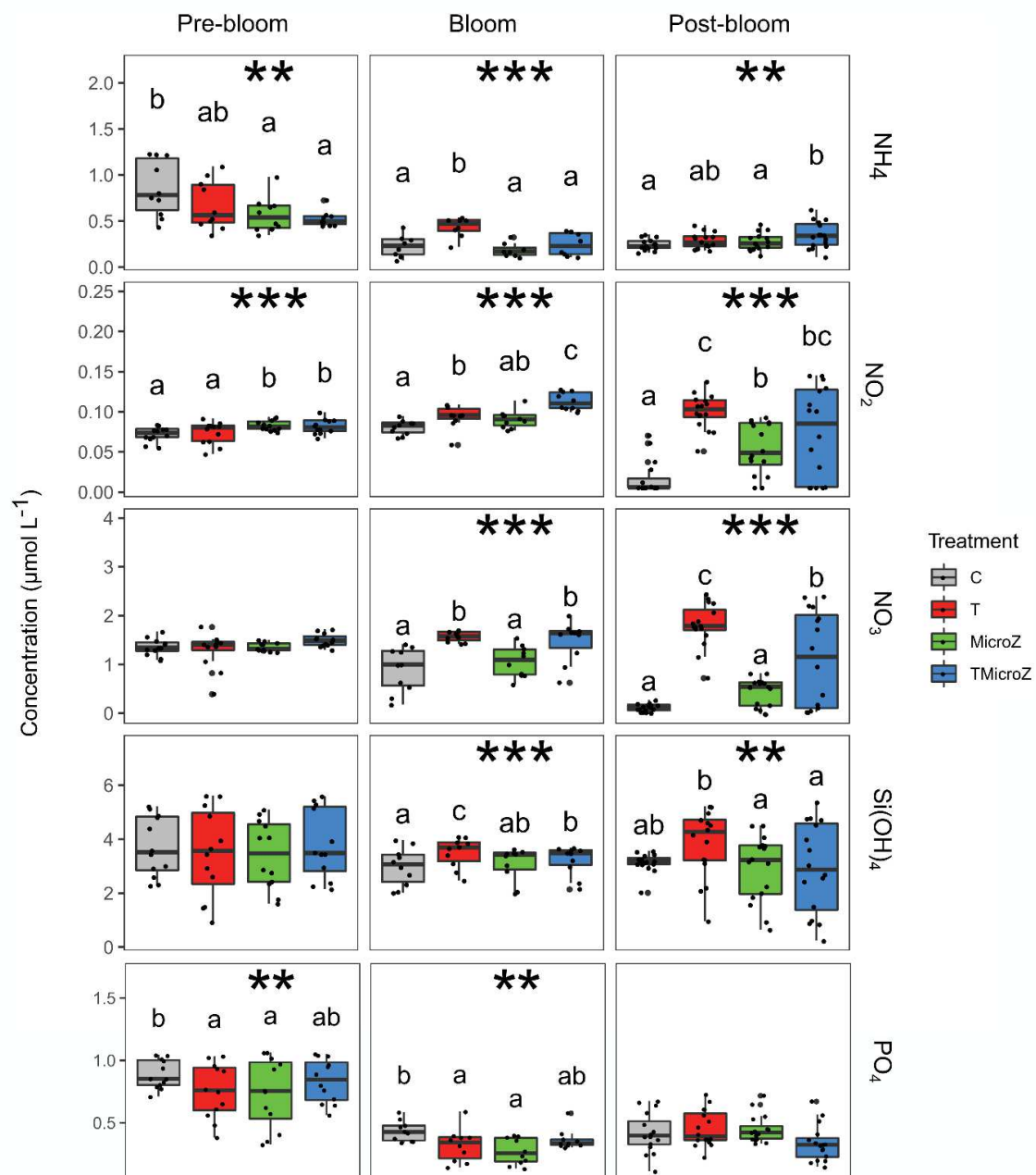


Figure 6 : Median of nutrient concentrations (NO_2 , NO_3 , NH_4 , $\text{Si}(\text{OH})_4$ and PO_4) in the mesocosms between the different treatments for pre-bloom, bloom and post-bloom periods. The grey colors indicate the Control treatment (C), the red the Heated treatment (T), the mesozooplankton exclusion treatment (MicroZ) and the Heated and mesozooplankton exclusion treatment (TMicroZ). The stars depict the significance level of RM-ANOVAs: * = p -value < 0.05; ** = p -value < 0.01; *** = p -value < 0.001. The letters indicate significant differences between treatments based on post-hoc pairwise tests. Boxplots that share the same letter were not significantly different. When the letters differ there were significantly different (p -value < 0.05).

3.4.2 Treatments effects on Chl *a* and taxonomic pigments concentrations

During the pre-bloom period, only concentrations in TMicroZ treatment were lower than those in the other treatments (p -values < 0.01 ; Figure 7). During the bloom period, concentrations in the C and in the TMicroZ treatments were not significantly different (Figure 7), but they were significantly higher than those in both the MicroZ and the T treatments (p -values < 0.01). The concentration in the MicroZ was also significantly higher than in the T treatment (p -value < 0.05). Chl *a* concentrations in the treatment C were significantly higher than all other treatments (p -values < 0.001) and it was also higher in the TMicroZ than in the T and MicroZ treatments (p -values < 0.001).

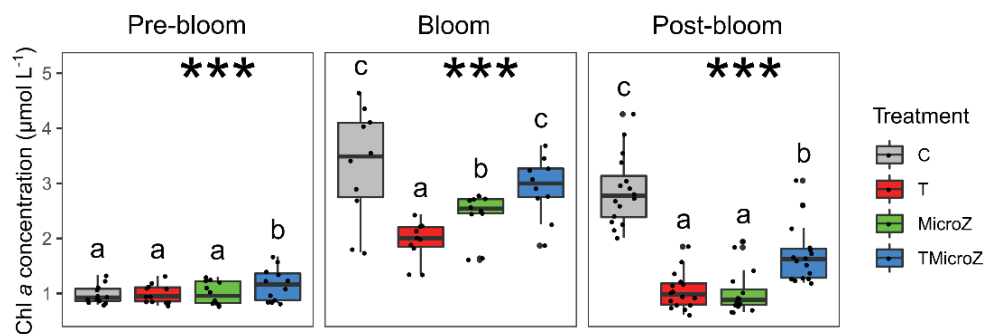


Figure 7 : Median of Chl *a* concentrations in the different treatments during pre-bloom, bloom and post-bloom periods. The grey colors indicate the Control treatment (C), the red the Heated treatment (T), the mesozooplankton exclusion treatment (MicroZ) and the Heated and mesozooplankton exclusion treatment (TMicroZ). The stars depict the significance level of RM-ANOVAs: * = p -value < 0.05 ; ** = p -value < 0.01 ; *** = p -value < 0.001 . The letters indicate significant differences between treatments based on post-hoc pairwise tests. Boxplots that share the same letter were not significantly different. When the letters differ there were significantly different (p -value < 0.05).

The results of the RM-ANOVAs on taxonomic pigments are presented in **Figure 8**. All the results presented in the following sections are statistically significant.

In the T treatment, Chl *b* and prasinoxanthin concentrations were lower than in the C treatment (p -value < 0.05), but it was lower for 19HF and fucoxanthin (p -values < 0.05). During the bloom period, concentrations of four out of the seven taxonomic pigments (Chl *b*, prasinoxanthin, 19HF and

fucoxanthin) were significantly lower in the T than in the C treatment (p -values < 0.01), while none of seven pigments was higher. During the post-bloom period, Chl *b* and peridinin concentrations were higher in the T than in the C treatment (p -values < 0.001), while it was lower for zeaxanthin, 19HF and fucoxanthin concentrations (p -values < 0.05).

In the MicroZ treatment, taxonomic pigments concentrations were not different than in the C treatment. However during the bloom period, 19HF and fucoxanthin concentrations were lower in the MicroZ than in the C treatment (p -values < 0.001), while it was higher for peridinin (p -values < 0.05). During the post-bloom period, Chl *b*, prasinoxanthin, alloxanthin and peridinin concentrations were higher in the MicroZ than in the C treatment (p -values < 0.001), while it was lower for zeaxanthin, 19HF and fucoxanthin (p -values < 0.001).

In the TMicroZ treatments, 19HF and fucoxanthin concentrations were higher than in the T for the pre-bloom period (p -values < 0.05), while Chl *b*, prasinoxanthin and alloxanthin concentrations were higher in the MicroZ (p -values < 0.01). During the bloom period, concentrations of six out of the seven pigments (Chl *b*, prasinoxanthin, zeaxanthin, 19HF, fucoxanthin and peridinin) were higher in the TMicroZ than in the T treatment (p -values < 0.05). On the other hand, fucoxanthin and peridinin concentrations were higher in the TMicroZ than in the MicroZ treatment during both bloom and post-bloom periods (p -values < 0.05), while it was lower for Chl *b* and prasinoxanthin during these periods (p -values < 0.05).

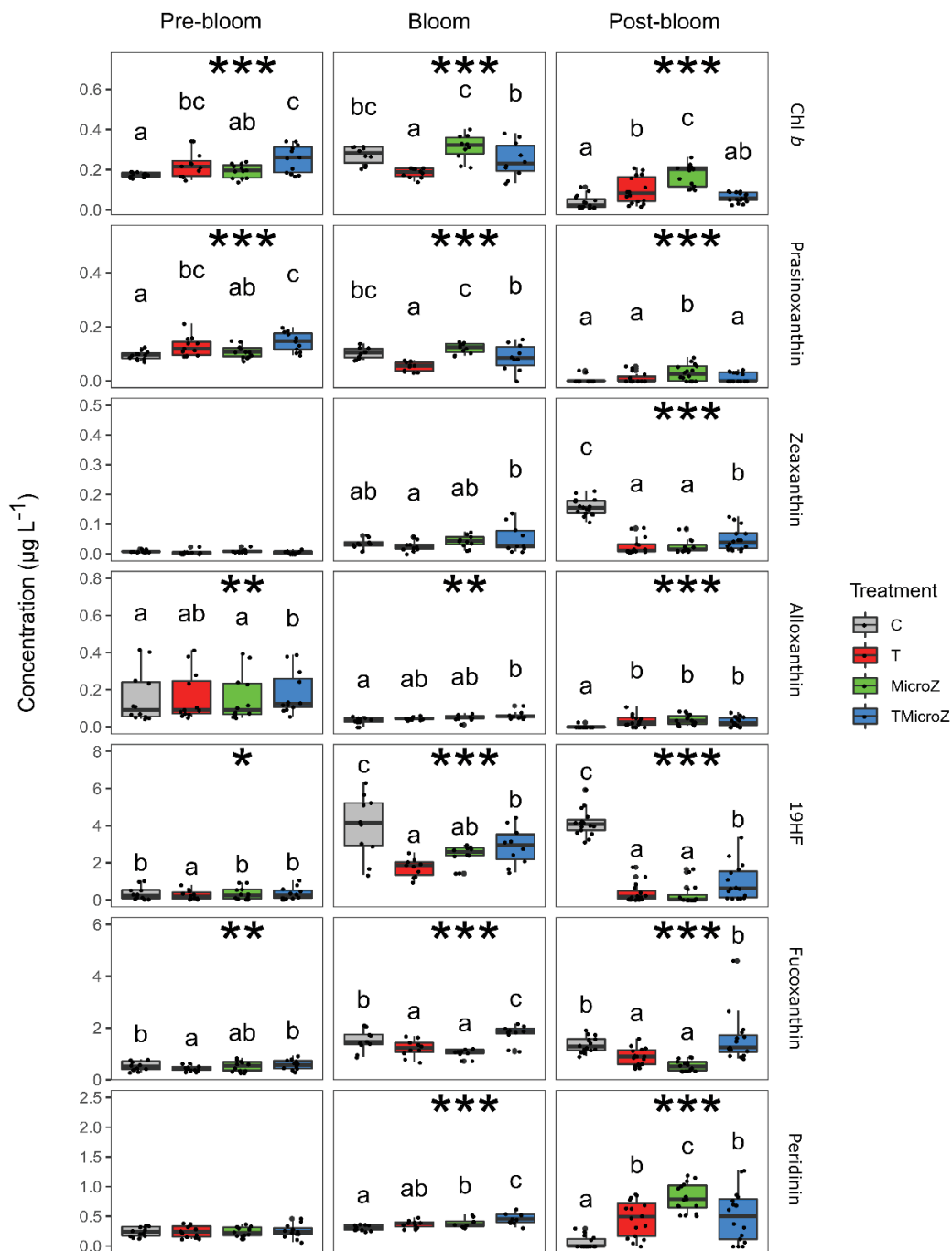


Figure 8 : Median concentrations of taxonomic pigments in the different treatments during pre-bloom, bloom and post-bloom periods. The grey colors indicate the Control treatment (C), the red the Heated treatment (T), the mesozooplankton exclusion treatment (MicroZ) and the Heated and mesozooplankton exclusion treatment (TMicroZ). The stars depict the significance level of RM-ANOVAs: * = p -value < 0.05; ** = p -value < 0.01; *** = p -value < 0.001. The letters indicate significant

differences between treatments based on post-hoc pairwise tests. Boxplots that share the same letter were not significantly different. When the letters differ there were significantly different (p -value < 0.05).

4 Discussion

4.1 Warming reduces the amplitude and the duration of the phytoplankton bloom

It is well known that water temperature impacts the phytoplankton directly through its thermodynamic control of metabolic process (Eppley 1972; Rose and Caron 2007) and the difference in temperature optimum for growth between species (Thomas et al. 2012). In parallel, water temperature can also indirectly influences the phytoplankton dynamic through the enhancement of inter-specific interactions such as predation, competition, etc. (Caron et al. 2000; Legrand et al. 2003). One of the major results of the present study was that the warming strongly reduced the amplitude of the phytoplankton bloom.

During the phytoplankton bloom period, maximum of Chl *a* concentration was 48% lower under Heated treatment (T) than in control (C) (Figure 4). Thus, clearly warmer water conditions reduced the phytoplankton bloom amplitude, resulting in half of the phytoplankton biomass. The whole phytoplanktonic community was negatively affected by warmer temperature. During the bloom, the concentration of 4 out of the 7 chemotaxonomic pigments were lower in T than in C treatment (Figure 5 and 8). For instance, 19HF (mainly prymnesiophytes) and fucoxanthin (mainly diatoms) concentrations were respectively 57% and 19% lower in the T relative to C treatment. To our best knowledge, this is the first time that such biomass reduction of all phytoplanktonic community was observed under warmer regardless the taxonomic groups or size classes. A phytoplankton biomass reduction could be the result of a decrease in phytoplanktonic abundance or an inter- or intra-specific cell size reduction. A reduction of the phytoplankton abundance could be related to intensification of grazing as in-depth investigations revealed that warmer water favored the grazers, such as copepods or ciliates that could largely feed on phytoplankton reducing its abundance (Aberle et al. 2007; Rose and

Discussion

Caron 2007; Sommer and Lengfellner 2008a; Vidussi et al. 2011). This could have been occurred in the present study because when removing the mesozooplankton ($> 200 \mu\text{m}$) with potential large copepods grazers, the Chl *a* concentrations in the TMicroZ treatment was higher than that observed in the T treatment with the same temperature conditions but with the whole community including the mesozooplankton. As the nutrients concentrations were higher in the T and TMicroZ treatments during the bloom (except PO_4 ; Figure 2 and 6), the phytoplankton biomass reduction was not the consequence of nutrient limitation of phytoplankton due to a potential faster nutrient depletion in the T relative to C treatment. Indeed, the NO_2 concentrations in TMicroZ and the NO_2 and NO_3 concentrations in T increased during the bloom, while they were stable or decreased in the C and MicroZ treatments. In the T treatment, an increase of NO_3 concentration was also observed after the bloom period which could be attributed to a potential nitrification process under warming, due to a potential increase in bacterial activity. The phytoplankton biomass reduction observed in the Heated treatment could also be the result of phytoplankton cell size reduction at inter- and/or intra-specific levels. Inter-specific cell size modification can be due to a higher competitiveness of smaller cells at higher temperature (Sommer et al. 2017) or to the higher grazing rates of copepods that feed preferentially on larger phytoplankton such as diatoms (Peter and Sommer 2012). Several *in situ* and experimental studies reported that warming also have a strong effect of intra-specific size reduction within the phytoplankton (Peter and Sommer 2012; Jung et al. 2013; Sommer et al. 2017). This is known as ‘the temperature-size rule’ and it was observed in a wide diversity of ectotherms in general. On clonal culture, warming leads to a cell size reduction of 2.5% per $^\circ\text{C}$ on average on aquatic protists (Atkinson et al. 2003), but it can be higher in natural communities (Peter and Sommer 2012). This temperature-size rule can be explained by two hypotheses. (1) Warming reduces the ratio of supply to potential consumption of limiting resources, thus, smaller cell size compensates this by increasing the uptake per volume unit (Margalef 1954; Raven 1998). (2) To be more competitive in warmer conditions that generally increase the growth rates, species tend to complete faster their cell cycle, dividing earlier to increase their fitness, at the expense of their cell size (Stearns 1976).

Warming reduced not only the amplitude of the bloom, but also its duration (Figure 3 and 4), as the phytoplankton bloom ended one day earlier in T (day 10) compared to C (day 11). A decrease in the phytoplankton biomass at the end of the bloom was due to a shift in the balance between growth and losses which was in favor of losses, resulting in a negative r . In the C treatment this shift could be due to a reduction of the growth resulting in nutrient depletion. Indeed, the NH_4 , NO_2 and NO_3 concentrations were nearly to 0 at day 11 and could not sustain the phytoplankton growth. Consequently, in the C treatment nutrient depletion could have been the main factor leading to the end of the bloom. However, this was not the case under warm condition (T) because as previously mentioned, NO_2 , NO_3 , $\text{Si}(\text{OH})_4$ concentrations in T treatments were high and even increased at day 10 when the bloom ended (Figure 2), suggesting that they were not limiting and did not contributed to phytoplankton decrease leading to the end of the bloom. A decrease of growth in warmed treatments due to the temperature level is unlikely, because mid temperatures as those applied in this experiment are known to stimulate phytoplankton growth (Rose and Caron 2007) and not the contrary. Thus, the end of the bloom under warmer conditions (T and T_{MicroZ}) could have been the consequence of an increase in the losses. The potential increase in the losses could mainly be due to a more important grazing activity over phytoplankton because heterotrophic metabolic rates increases faster with the temperature than that of autotrophic ones (Allen et al. 2005; López-Urrutia et al. 2006; Sommer and Lengfellner 2008a; Yvon-Durocher Gabriel et al. 2010).

During the bloom period the incident daily dose of PAR was low. This was due to a high cloud cover caused by a storm occurring from day 6 to 9. It is suggested that the light is not a major limiting factor for phytoplankton growth in this study as the Chl *a* concentration strongly increased and the r was high during these days. This result was already suggested in Trombetta et al. (2019), as they found strong phytoplankton blooms in Thau lagoon during winter when the PAR is at its lowest, and no correlations between the daily dose of PAR and the Chl *a* concentration were found.

4.2 Warming modifies the phytoplankton succession inducing an early bloom of small green flagellates and a late bloom of diatoms

In the C treatment, every phytoplanktonic taxa bloomed at the same time, inducing a strong Chl *a* concentrations and was dominated by prymnesiophytes and diatoms (Figure 4 and 5). However, the warming had an impact on the phytoplankton bloom succession modifying timing of blooming species and even inducing bloom that not occurred under control conditions. In fact, warming induces different responses among taxa leading to an early bloom of small green algae (Figure 5E and F), and a late bloom occurred after the main bloom, that was mainly dominated by diatoms (Figure 5B).

Warming induced two days of positive r at day 3 and 4 in the T and T_{MicroZ} treatments (Figure 3B and D). However, it was immediately followed by a day of negative r (day 5) inducing a rupture in the biomass accumulation process characterizing a bloom. Pigment analysis revealed that this 2-days early bloom was due to green algae including prasinophyceae, as Chl *b* and prasinoxanthin showed enhanced concentrations during these two days under warmed treatments (T and T_{MicroZ}). Previous studies (Rose and Caron 2007; Sommer et al. 2017) reported that higher water temperature favored small phytoplankton which is in concordance with the results of the present study. Temperature allowed small phytoplankton, in this case green flagellates, to increase their growth outpacing temporarily the losses due to the grazing or other mortality causes, at day 3 and 4. Later in the course of the experiment, at day 5, the losses recovered probably due to the catch-up of their predators grazing activity, as small microzooplankton is well known to tightly control its preys (Sherr and Sherr 2002).

Larger phytoplankton such as diatoms and did not seem to be affected by the warming in their main bloom timing as it was occurred at the same time in the T and C (Figure 5B). This can be explained by the temperature levels occurred during this study (between 13 and 21°C) as it was reported that the Q_{10} for growth primary production between 10 and 20°C is lower for micro- and nano- than for pico-phytoplankton (Andersson et al. 1994). Therefore, an increase of 3°C during this study induced a strong

response of picophytoplankton producing an early bloom, while it was not at all the case for diatoms, as no significant modification was observed in their bloom timing.

At the end of the experiment, a late bloom of diatoms (Chl *a* and fucoxanthin) was observed in the Heated treatments (T and TMicroZ; Figure 5B). This bloom can be attributed to regenerate production based on NH₄ concentrations. After the main bloom and the dinoflagellates bloom in the Heated treatments, enhancement of NH₄ concentrations at the end of the experiment was due to the potential increase of particulate and dissolved organic matter related to zooplankton excretion and defecation. A part this process, NH₄ could also come from enhanced heterotrophic bacteria activity through remineralization of the organic matter (Nixon 1981). In fact, warmer conditions are known to increase the bacterial metabolic rates (Rivkin and Legendre 2001; López-Urrutia et al. 2006) and could have caused an intensification of the remineralization in the Heated treatments supporting the regenerated primary production of diatoms.

The effects of warming in the modification of the phytoplankton succession are diverse as it can be due to a differential modification of the intrinsic phytoplankton metabolism depending on the species, a modification of the activity of the various grazers and an intensification of the remineralization cycles.

4.3 Small green algae and dinoflagellates benefit from warming

The concentrations of the most taxonomic pigments in the present study were significantly lower in the T than in the C treatment (Figure 5 and 8). However, after the bloom the concentration of specific pigments of the small green algae (Chl *b*) were higher in the T than in the C treatment. This confirms that warmer conditions are favorable to these groups as explained before. The bloom of the small green algae (Chl *b*) occurred earlier in the warmer conditions (between days 0 and 5) than in the non-Heated treatments. This corroborates to what explained before that warmer conditions being favorable to smaller phytoplankton species is a widely known phenomenon. It has been already described in controlled experimental studies (Peter and Sommer 2012; Sommer et al. 2017) *in situ* in open ocean (Morán et al. 2010). In addition, Trombetta et al. (2019) highlighted for the first time that in the shallow

Discussion

coastal waters, this pattern also occurred, with higher picophytoplankton abundances observed in a warmer year, confirming the present experimental findings. As previously mentioned, warmer conditions being favorable to smaller phytoplanktonic species could be explained mostly by the direct temperature-size metabolic effects increasing their competitiveness to nutrient access (Sommer et al. 2017) or by the increase of the grazing pressure over larger phytoplankton making their niche more accessible to smaller phytoplankton (Peter and Sommer 2012).

Peridinin concentrations were also higher in the T than in the C treatment during the post-bloom, suggesting that dinoflagellates containing peridinin were favored in warmer conditions as it was also the case for the smaller phytoplanktonic species. Previous studies pointed out the high thermal tolerance of dinoflagellates supporting the results obtained in this study (Kibler et al. 2015; Xiao et al. 2018; Brandenburg et al. 2019). Dinoflagellates were favored in warmer conditions compared to their common competitors (as diatoms) due to an higher thermal tolerance in low nutrient concentrations, while diatoms are only thermal tolerant at higher nutrient concentrations (Xiao et al. 2018). However, in the present study, Peridinin concentrations were high in the T when the nutrients concentrations were high, while fucoxanthin (mainly attributed to diatoms) concentrations were low. The present results also indicate that the situation is more complex than a simple temperature-nutrient-phytoplankton relationship. Indeed, when removing mesozooplankton ($> 200 \mu\text{m}$), this pattern was reversed, with higher Peridinin concentrations in MicroZ (non-Heated) than in TMicroZ (Heated). This suggested that biotic interactions (such as copepod or ciliate predations) were crucial in the fitness of dinoflagellates in the present study. The higher Peridinin concentrations in the T than in the C treatment could be also a results of the warming being more favorable to heterotrophic than autotrophic organisms (Wilken et al. 2013). Dinoflagellates, known as one of the groups with the higher number of constitutive mixotrophs (Stoecker 1999), the higher temperature in the T could have been an advantage for the dinoflagellate growth, by increasing their phagotrophy activity. This shift toward phagotrophy activity could also contributed to the reduction of the Chl *a* concentration in the T treatment as they could have predated phytoplanktonic cells.

Warming disadvantages larger phytoplanktonic organisms as the concentration of some of their characteristic taxonomic pigments were lower in the T relative to C treatment during some or all of the periods of the experiment (Figure 5 and 8). In particular, fucoxanthin concentration was lower in pre-bloom, bloom and post-bloom period in the T than in the C treatment. This result is in agreement with an *in situ* observations reported by Trombetta et al. (2019) that observed in the same system as the present study that the abundance of *Chaetoceros spp.*, the most abundant diatom during the spring bloom, was significantly lower during a warm year (2016) than a normal year (2015). The present results could be interpreted otherwise that the promotion of smaller phytoplankton suggesting that warmer temperature induced (1) a stronger competitiveness of smaller phytoplankton outcompeting larger ones or (2) a stronger grazing pressure on larger phytoplankton. The present results tend to highlight that those two hypotheses occurred in synergy as when removing the mesozooplankton ($> 200 \mu\text{m}$), diatoms benefited from the temperature effect on primary production, leading to higher fucoxanthin concentrations.

The phytoplankton of this particular lagoon are adapted to important thermal amplitude that can vary by several degree per days due to its shallowness (Trombetta et al 2019). Diatoms such as *Chaetoceros sp.* in this lagoon are well adapted to the high temperatures and bloomed at temperatures such as those experienced in T during bloom periods. Consequently, it is unlikely that these organisms exceeded their optimal temperature during the bloom, inducing a growth reduction or an increase in mortality, especially with the 2-days thermic adaptation.

4.4 The influence of mesozooplankton on the phytoplankton dynamic and composition and its modification under warming

The removal of the mesozooplankton ($> 200 \mu\text{m}$) in the MicroZ treatments helped to better understand their role in phytoplankton abundance and diversity control, and their potential modification in warmer conditions.

Discussion

In the MicroZ treatment where the mesozooplankton $> 200 \mu\text{m}$ was removed, the Chl *a* bloom amplitude was 39% lower than in C condition (Figure 7). The removal of potential grazers such as copepods could have reduced their grazing pressure on phytoplankton, especially larger ones, thus enhancing the bloom. However, it was the opposite that was observed, with larger phytoplankton such as diatoms (fucoxanthin) and prymnesiophytes (19HF) which were reduced, while smaller phytoplankton such as small green algae (Chl *b*, prasinoxanthin) which their concentrations were slightly higher in the MicroZ relative to C treatment (Figure 8). These results reveal a modification of the trophic cascade due to the removal of the mesozooplankton $> 200 \mu\text{m}$. Copepods are considered as the main grazers of diatoms, but in the present study, the role of the protists microzooplankton, especially ciliates, revealed to be pivotal as they were the main contributors to the diatoms abundance control. In this system, smaller diatoms such as *Chaetoceros* spp. are dominant (Bec et al. 2005; Trombetta et al. 2019) and could be potentially grazed by ciliates (Verity and Villareal 1986). In this study it is suggested that mesozooplankton mainly plays the role of secondary consumers. Indeed, in MicroZ treatment, the absence of copepod predators that can be ciliates predators, could have allowed ciliates to develop free from predation, thus exerting a stronger grazing pressure on these diatoms and on prymnesiophytes reducing their biomass, despite the absence of herbivorous copepods that can also predate on the same prey (diatoms and prymnesiophytes). In addition without mesozooplankton, a small part of ciliate community, the carnivorous ones, could also have increased the grazing pressure on smaller heterotrophic flagellates that slightly reduced their pressure on small phytoplankton, resulting in an increase of the biomass of small green algae.

In the warmer treatment in absence of mesozooplankton (TMicroZ), the bloom amplitude, mostly attributed to higher diatom biomass, increased by 23% compared to natural water temperature conditions with the presence of microzooplankton (MicroZ), (Figure 5 and 8). In this case, warmer condition could have favored diatoms allowing their growth to exceed the losses due to microzooplankton such as ciliates predation. The biomass of small green algae (Chl *b*, prasinoxanthin) was reduced by 25 % in TMicroZ compared to MicroZ (Figure 5 and 8) suggesting that the warmer water temperature increased

the grazing pressure of microzooplankton on small phytoplankton, in accordance with (Rose and Caron 2007) that pointed out the differential temperature effects on phytoplankton and protozooplankton metabolism. In the hypothesis that warming only affect the predator-prey interactions, a +3°C increase in water temperature increases by 25% the impact of microzooplankton grazing on small green algae.

4.5 Warming disrupts the balance between bottom-up and top-down control of phytoplankton dynamic

The warming effect on the bloom amplitude, composition and succession are the witnesses of a more general ecological process of the warming effect on phytoplankton dynamic. This process is the modification of the balance between environmental and biotic interactions controlling phytoplankton dynamic. In the C treatment, the phytoplankton biomass was strongly controlled by nutrient limitation as the phytoplankton biomass started to decrease once the nutrient exhausted (Figure 2, 4 and 6). It is widely known that warming increases the nutrient or CO₂ uptakes and thus, increases phytoplankton growth rate (Rose and Caron 2007). Consequently, a higher phytoplankton biomass in the T treatment relative to the C could have been expected, with a faster nutrient depletion. However, totally the opposite trend was observed as Chl *a* concentrations in the T were 48% lower and nutrients concentrations were higher (and even increased) than what measured in the C treatment (Figure 2 and 4) during the bloom and post-bloom periods. Thus, the phytoplankton biomass was not directly controlled by nutrient availability under temperature. We put in advance the hypothesis that in the present experiment, the phytoplankton dynamic was controlled indirectly by warmer conditions through enhancement of the biotic interactions. Few other studies as well suggested that warmer water increases the trophic cascade and shift the bottom-up versus top-down balance toward a top-down control of the primary production (Kratina et al., 2012; Shurin et al., 2012; Lewandowska et al., 2014). These observations were explained by the metabolic theory of ecology predicting that the temperature affects more strongly heterotrophic than autotrophic processes (Allen et al. 2005; López-Urrutia et al. 2006; Rose and Caron 2007). The high temperatures above 15°C induced on the protist grazers faster growth rates than their phytoplankton

Discussion

autotrophic preys (Rose and Caron 2007), thus exerting a strong control on the preys. Consequently, as already pointed out, in the TMicroZ treatment with warmer conditions and in absence of mesozooplankton, their potential prey, ciliates, could have been developed more and therefore grazed more on small phytoplankton. , the absence of mesozooplankton realizing the predator pressure on the ciliates, resulted to the higher grazing pressure of the ciliates on their prey which consequently the lower green algae concentration (Chl *b* and Prasinolaxanthin; Figure 5 and 8) in the TMicroZ relative to the MicroZ treatment. In addition, free from the grazing of mesozooplankton, larger phytoplankton (diatoms) increased their growth under increase of temperature, resulting in higher fucoxanthin concentrations in the TMicroZ relative to the MicroZ treatment. In the T relative to C treatment, the presence of both micro- and mesozooplankton induced a stronger grazing pressure on all phytoplankton functional groups belong to different size classes. In fact, comparing the T and C treatments, temperature directly or indirectly via trophic cascade leaded to a reduction of the pigment concentrations of green algae including those of prasinophytes (Chl *b*, Prasinolaxanthin), of prymnesiophytes (19HF) and the major pigment mainly attributed to diatoms (fucoxanthin). Besides, metazoan copepods are known to develop faster at higher temperatures but not enough as their preys, inducing a predator/prey mismatch (Edwards and Richardson, 2004). However, it was pointed out that this rule cannot be always the case and that in productive temperate waters, as in the Mediterranean metazoan copepods, that are generally of small size, can develop faster (faster hatching and development), tightly controlling their preys at higher temperatures (Vidussi et al. 2011). The results of the present study and those of Vidussi et al. (2011) realized in the same system tends to support the idea that no mismatch occurred between copepods and their preys in this system as the pigment concentrations during bloom were lower in the T than in C treatment, suggesting a strong control of predators on phytoplankton dynamic in warm conditions. This is supported by the fact that increase of water temperature by +3°C enhanced by 48% the impact of zooplankton grazing on phytoplankton biomass (based on the observation of Chl *a* maximum).

However, other kind of biotic interaction than predation could have been strengthened under warmer conditions, enhancing the biotic control on phytoplankton biomass. For example, warmer conditions have been reported to increase the production of allelopathic algal proteases or cell division inhibitors by heterotrophic bacteria in order to be more competitive against phytoplankton (Seymour et al. 2017). Viral infection and lysis can also be strengthened by warmer conditions that could have caused additional phytoplankton losses (Danovaro et al. 2011; Mojica et al. 2016). However, these explanations are only hypothetical as this study mainly focused on the role of top-down control grazers (micro- and mesozooplankton) on phytoplankton community biomass.

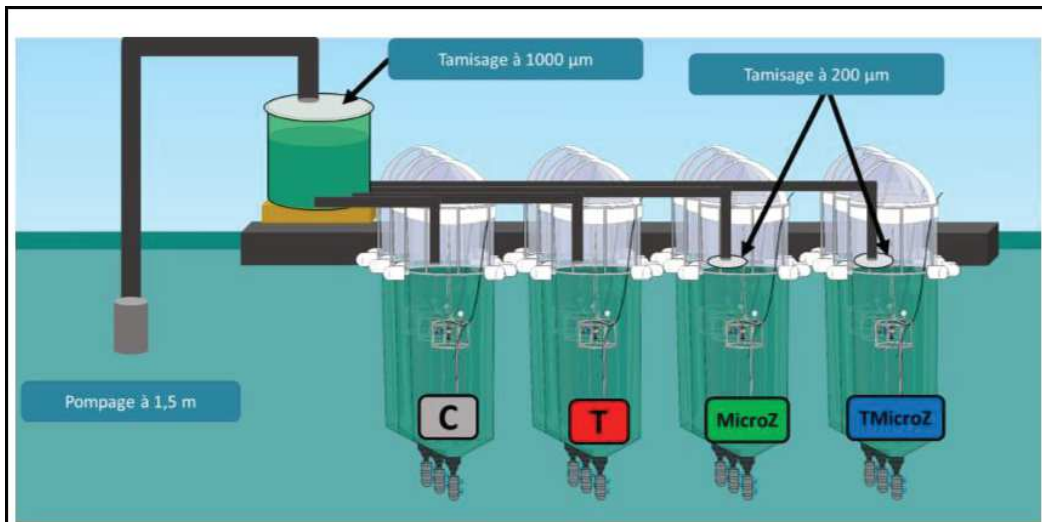
The results of the present study put in evidence a strengthening of the top-down control in the warm conditions. In the global warming context, the results of the present study along with a potential increase in heterotrophy, grazing, along with the increase of other biotic interactions like viral lysis could lead to a strong modification of the biochemical cycles. In the global warming context, the rising temperature could strongly alter the carbon cycling (Sarmiento et al. 1998). The phytoplankton biomass reduction, the shift of mixotrophy to heterotrophy (Wilken et al. 2013), the increase of the respiration compares to primary production (Wohlers et al. 2009), and the increase of by-production from viral lysis could all result in a reduction of the oceanic carbon sequestration (Joos et al. 1999).

5 Acknowledgments

We would like to thank the numerous students who participated in this experiment performing the sampling and analyses and more generally helping to run this experiment. We are grateful to David Parin, Solenn Soriano and Remy Valdès for their precious technical implications in the experiment set up, sampling and analysis. We would acknowledge specially Julien Dupont for the HPLC analysis. We thank Maxime Thibault, Ariadna Garcia-Astillero Honrado and Camille Suarez-Bazille for the nutrient analysis.

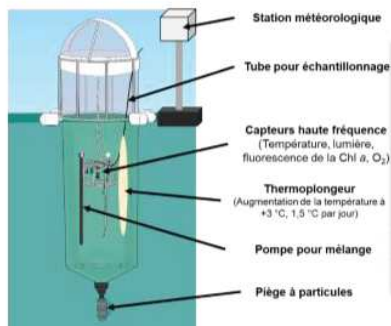
Encadré

Dispositif de l'expérimentation en mésocosmes.



Tamissage et remplissage simultané des 12 mésocosmes.

- L'eau de la lagune est pompée à 1,5 m de la surface dans un réservoir équipée d'un tamis en tissu (1000 µm).
- Les mésocosmes sont remplis par gravité et en simultané par 12 tuyaux les connectant au réservoir.
- Un tamis en tissu de 200 µm est installée à l'extrémité des tuyaux de remplissage pour chaque mésocosme des traitements MicroZ et TMicroZ.



Équipement des mésocosmes.

Les mésocosmes sont équipés :

- D'un tube d'échantillonnage.
- De capteurs haute fréquence (bouquet différent en fonction des mésocosmes).
- D'une pompe pour le mélange de la colonne d'eau.
- D'un piège à particules.
- D'un thermoplongeur (pour les traitements T et TMicroZ).

Une station météorologique est installée sur le ponton.

Photos du site expérimental (droite) et d'un mésocosme isolé (gauche)



Discussion générale

Les objectifs de cette thèse étaient d'identifier les forçages responsables de l'initiation des efflorescences phytoplanctoniques en zone côtière, notamment le rôle de la température et des interactions biologiques au sein du réseau trophique microbien, ainsi que de tester expérimentalement l'effet de l'augmentation de la température et des différentes fractions de taille de la communauté zooplanctonique sur la dynamique des efflorescences printanières dans le contexte du réchauffement climatique.

Les travaux de cette thèse ont contribué à la progression de la recherche, 1) sur le plan méthodologique, par le développement et l'application d'outils et méthodes novatrices dans l'étude de la dynamique des écosystèmes et des processus écologiques intrinsèques ainsi que 2) sur le plan écologique, par la compréhension des mécanismes responsables de l'initiation des efflorescences phytoplanctoniques dans les milieux côtiers peu profonds, du rôle des réseaux d'interactions microbiens dans la dynamique des organismes et la circulation de l'énergie au sein du réseau trophique microbien, ainsi que de l'influence de la température sur la dynamique et la composition de ces efflorescences.

1 Approche de la thèse et apport des différentes méthodes développées.

La lagune de Thau s'est révélée être un laboratoire à ciel ouvert parfait pour la compréhension des mécanismes physiques, chimiques et écologiques responsables de l'initiation des efflorescences phytoplanctoniques en zone côtière. En effet, la lagune de Thau, comme la majorité des lagunes côtières est sous l'intense influence de forçages multiples et divers tels que les vents, les flux de chaleur, la balance évaporation/précipitation, l'apport de masses d'eau externes, etc. (Kjerfve 1994). Du fait de sa faible profondeur, ce système réagit très vite aux forçages divers qu'il subit. Le moindre coup de vent

peut augmenter radicalement la turbidité, le moindre coup de chaleur augmenter significativement la salinité et l'évaporation, et le moindre apport d'eau du bassin versant enrichir le milieu en nutriments. De ce fait, les organismes, notamment microbiens planctoniques subissent continuellement des changements de conditions environnementales qui influencent leur croissance, leur mortalité et les interactions qu'ils entretiennent avec le reste de la communauté. De plus, le site d'échantillonnage et d'étude choisi se situe à l'entrée du principal canal reliant la lagune à la mer. Ce site est donc sous forte influence marine avec un temps de résidence moyen des masses d'eau plus faible qu'ailleurs dans la lagune. Ainsi, ce multi-forçage et cette forte réactivité systémique prédisposent la lagune de Thau à l'étude de l'effet des forçages physico-chimiques sur la dynamique écologique des communautés microbiennes, notamment quant à l'initiation des efflorescences phytoplanctoniques en zone côtière. De plus, la Méditerranée est l'une des zones qui seront le plus impactées par la hausse des températures dans le monde dans le contexte du changement global, et il est donc crucial de comprendre le fonctionnement des efflorescences dans ces zones pour mieux anticiper les changements à venir.

Cependant, ces influences multiples et cette forte dynamique nécessitent une méthodologie d'étude rigoureuse et adaptée pour répondre à ces objectifs. Ainsi, une triple approche a été nécessaire pour prendre en compte tous les aspects et les facettes de cette problématique. Ces approches consistaient en 1) un suivi à haute fréquence (< 15 min) des paramètres météorologiques (température de l'air, vents, irradiance, etc.), hydrologiques (température de l'eau, salinité, turbidité, etc.) susceptibles d'influencer la dynamique de la biomasse phytoplanctonique (fluorescence de la chlorophylle *a*), sur deux années climatiques différentes, associé à un suivi hebdomadaire effectué en parallèle, de l'abondance et la diversité de la communauté microbienne, 2) une approche de modélisation sous forme de réseau de corrélations des données obtenues *in situ* pour comprendre la dynamique de succession microbienne et de structuration des réseaux d'interactions entre groupes/taxons/espèces, et 3) une approche expérimentale dans des conditions contrôlées, en mésocosme *in situ* immergés dans la colonne d'eau, pour tester l'effet de l'augmentation de la température et des différentes fractions zooplanctoniques sur la dynamique et la composition de l'efflorescence printanière.

1.1 Apport des données hautes fréquences dans la compréhension des processus écologiques.

L'apport de la haute fréquence dans l'étude ce type de système a été crucial dans l'identification des facteurs d'initiations des efflorescences. Les zones côtières peu profondes sont des systèmes très dynamiques répondant extrêmement rapidement aux forçages environnementaux tels que l'augmentation de la température, les vents, les apports de masses d'eaux, etc. Particulièrement, le métabolisme du phytoplancton répond très rapidement (de l'ordre de la dizaine de minutes à la journée) aux forçages, tels que les changements de température, de lumière (Abbott et al. 1982) ou de nutriments (Goldman et al. 1981). De ce fait, nous avons observé que les efflorescences phytoplanctoniques sont initiées très rapidement, avec des temps de réponses de l'ordre de la journée. De plus, ces efflorescences étaient souvent sous forme de séries de pulses durant quelques jours, moins d'une semaine en général (Chapitre 1, Figure 2). Si l'hypothèse de l'augmentation de la température a déjà été émise comme facteur d'initiation potentiel dans ces zones (Kirk, 1994; Bec et al. 2005), c'est bien l'apport du suivi à haute fréquence qui nous a permis de le démontrer (Trombetta et al. 2019). C'était le cas également en zone côtière de la mer du Nord sous forte influence des marées, où l'hypothèse de l'initiation des efflorescences déclenchée par l'augmentation de l'irradiance et de la réduction de la quantité de matière en suspension a été émise, avant d'être validée par la méthode du suivi haute fréquence (Blauw et al. 2012).

Le Chapitre 1 de cette thèse démontre bien le caractère crucial du choix de la fréquence d'acquisition des données pour comprendre les phénomènes écologiques. Plus particulièrement dans le cas des écosystèmes côtiers peu profonds, très réactifs et dynamiques, l'étude des processus d'accumulation de biomasse phytoplanctonique lors des efflorescences nécessite une fréquence d'acquisition de données quotidienne. Une fréquence d'acquisition plus faible, par exemple hebdomadaire n'aurait pas permis d'identifier la température comme facteur d'initiation avec la méthode statistique de corrélation utilisée, étant donné que la plupart des phases d'accumulation de

biomasse durai^{ent} moins d'une semaine. Sur notre jeu de données à haute fréquence issu du suivi de 2015 et 2016, en extrayant chaque semaine une seule valeur de température et de fluorescence de la chlorophylle *a* pour simuler un échantillonnage hebdomadaire, ces deux variables ne sont pas corrélées entre elles. En revanche, l'utilisation d'une fréquence plus grande pour l'analyse, par exemple de l'ordre de 15 min comme dans ce suivi, aurait engendré un biais statistique du fait des importantes variations journalières de température et de chlorophylle *a* (forte auto-corrélation des données). C'est pour cela qu'un lissage des données sur une fréquence journalière (moyenne journalière) a été utilisé pour l'identification statistique des facteurs d'initiation des efflorescences phytoplanctoniques.

Les hautes fréquences d'échantillonnage de 15 min se révèlent idéales pour comprendre la dynamique et les mécanismes circadiens du phytoplancton, ainsi que l'influence des paramètres environnementaux. Par exemple, une intensité lumineuse trop importante au courant de la journée peut être délétère, dans le cas où l'énergie lumineuse absorbée est supérieure à la capacité d'utilisation pour la photosynthèse. Dans ce cas le phytoplancton met en place un mécanisme d'inhibition temporaire de la photosynthèse par dissipation thermique de l'énergie reçue par les molécules de chlorophylle, qui peut être détectée par analyse de la fluorescence de la chlorophylle et connue sous le nom d'extinction non photochimique (Non-photochemical quenching ; Krause and Jahns 2004). Cependant, en dehors de la fluorescence de la chlorophylle *a*, la haute fréquence ne permet pas à l'heure actuelle de mesurer un grand nombre de paramètres biologiques. Il est donc nécessaire de coupler ce type d'approche avec un échantillonnage classique, par exemple hebdomadaire pour comprendre l'effet des forçages physico-chimiques sur la diversité et la dynamique de la communauté planctonique.

1.2 Apport et perspectives de l'approche réseau

L'approche réseau a été cruciale dans cette thèse pour comprendre de façon précise comment les interactions et les associations entre les composantes du réseau microbien influencent la dynamique des organismes et la circulation de l'énergie dans l'écosystème. Cette approche a été rendue possible grâce à l'échantillonnage hebdomadaire de la lagune, afin de déterminer la diversité et l'abondance de la communauté microbienne. L'utilisation des réseaux d'associations en écologie, pour appréhender les interactions entre organismes au sein des communautés est très récente, moins de dix ans, et trouve son origine dans le développement de la métagénomique et du pyroséquençage (Faust and Raes 2012). Cette approche est de plus en plus utilisée en écologie et en microbiologie, car elle se révèle être un excellent outil pour la prédiction du fonctionnement de communautés, et se base sur de simples données d'abondance pour la modélisation des interactions biologiques. Cependant, les communautés microbiennes présentent une forte diversité d'espèces et de fonctions, et par conséquent une multitude de relations d'interactions sont possibles. L'application de la méthode des réseaux basée sur les corrélations offre un tableau très complexe des interactions entre organismes au sein de la communauté (Chapitre 1, Figure 2), difficilement interprétable écologiquement parlant. Ainsi, il s'est révélé nécessaire de développer une nouvelle méthode d'analyse des réseaux permettant de mieux appréhender le fonctionnement de ces derniers.

Par l'utilisation de la nouvelle méthode développée au cours de cette thèse, basée sur le groupement des groupes/taxons/espèces en fonction de traits fonctionnels et la comparaison de réseaux de corrélation empiriques avec des réseaux générés aléatoirement, nous avons été en mesure de déterminer les types d'interactions statistiquement dominantes au sein des réseaux microbiens. De ce fait, il est désormais possible de comparer indirectement les différents réseaux et d'observer des modifications de la structure des réseaux d'interactions entre les différentes périodes de production et les différentes années au sein d'un même écosystème. Cela permet de mieux percevoir le rôle de ces interactions dans la dynamique de l'écosystème et de ses composantes, ainsi que de prédire le

fonctionnement et la circulation de la matière au sein des réseaux trophiques microbiens. Les travaux de cette thèse apportent de nouvelles perspectives méthodologiques qui peuvent être appliquées à différentes échelles de résolution temporelle et spatiale, et spécifiques dans l'optique de mieux comprendre le fonctionnement des réseaux d'interactions et leur influence sur la dynamique des écosystèmes.

Cependant, ces réseaux sont des modèles statiques représentant une image instantanée des associations entre organismes et le fonctionnement d'un écosystème à un moment donné (Faust and Raes 2012). Un des enjeux majeurs de l'analyse des réseaux d'interactions est de pouvoir prévoir l'évolution des associations dans ces réseaux au cours du temps, notamment dans la perspective du changement global. Une des pistes est l'utilisation des nouvelles méthodes d'« apprentissage automatique » (*Machine-learning*; Recknagel 2001) basées sur l'intelligence artificielle tel que les algorithmes de « réseaux de neurones artificiels » (*Neural network*) ou des « forêts d'arbres aléatoires » (*Random forest*). Ces méthodes se basent sur l'intelligence artificielle pour « apprendre » de façon automatisée, à partir d'importantes bases de données, à reconnaître des schémas plus ou moins complexes. Avec l'essor des bases de données libres d'accès et participatives incluant des données environnementales, d'abondance, de diversité, de séquençage, de statuts écologiques, etc., l'utilisation de ces méthodes peut se révéler être un vrai atout pour comprendre le fonctionnement des systèmes microbiens et prévoir leur devenir et leur fonctionnement dans le contexte du changement global. Par exemple, avec ces méthodes il est possible de prédire la structure d'un réseau en fonction des paramètres environnementaux (Larsen et al. 2012). De plus, ces méthodes peuvent également permettre de déterminer le fonctionnement (flux de matière, productivité, etc.) et l'état (écologique, métabolique, etc.) d'un système avec des données d'assemblage de communauté (Thompson et al. 2019).

1.3 Apport et perspectives de l'approche mésocosme

Comme vu auparavant, l'approche d'observation *in situ* permet d'étudier les communautés dans leur ensemble, mais est fortement dépendante de multiples et complexes forçages environnementaux. L'approche en microcosme quant à elle, permet de tester l'effet d'un forçage en particulier mais uniquement sur une espèce isolée ou sur un assemblage réduit d'espèces. L'approche en mésocosme, à mi-chemin entre observation *in situ* et expérimentation en microcosme, permet de tester l'effet d'un forçage au niveau des communautés (composition, abondance, turnover, interactions, distribution des traits, etc.), mais également au niveau spécifique (croissance, mortalité, etc.) au sein des communautés (Fordham 2015). Elle permet aussi de valider ou pas les hypothèses faites par l'observations *in situ* et d'en émettre d'autres. Dans cette thèse, l'approche en mésocosme *in situ* pour tester l'effet de la hausse des températures et donc les effets potentiels, dans un contexte du réchauffement climatique, sur la communauté phytoplanctonique au sein de la communauté planctonique s'est révélée être un atout majeur dans la compréhension de la réponse du phytoplancton face au réchauffement climatique. Cette approche a permis de valider les hypothèses émises suite aux observations *in situ* faites en 2015 et 2016, notamment sur l'effet des fortes températures sur la réduction de la biomasse et de la taille des communautés phytoplanctoniques. Elle a également permis de déterminer l'influence des différentes fractions zooplanctoniques en conditions plus chaude sur la dynamique et la composition du phytoplancton pendant les périodes d'efflorescences et au-delà. Cela nous a ensuite permis d'établir des hypothèses sur la composition des communautés et la circulation de la matière et de l'énergie dans un avenir plus chaud.

A terme, l'analyse de l'ensemble des données issues de cette expérimentation, tel que la diversité et l'abondance de l'ensemble de la communauté planctonique, les paramètres métaboliques de production, de croissance et de mortalité, les concentrations en nutriments, en matière organique dissoute, etc. pourra permettre de paramétrer et calibrer des modèles. Par exemple, la paramétrisation d'un modèle de métacommunauté couplé à un modèle climatique pourrait permettre de comprendre et

de prédire la modification de la structure des communautés microbiennes dans le contexte du réchauffement climatique. Également, l'application des modèles statiques de réseaux de corrélations tels que vu plus haut permettraient de comprendre l'effet de l'augmentation expérimentale de la température sur la structure des réseaux d'interactions entre espèces.

2 Apport de la thèse à la connaissance des processus écologiques

2.1 Mécanisme d'initiation des efflorescences phytoplanctoniques en zone côtière

Les objectifs des chapitres 1 et 2 de cette thèse ont été de démêler le rôle des forçages physico-chimiques dans l'initiation des efflorescences phytoplanctoniques en zone côtière peu profonde, et de comprendre le fonctionnement du réseau d'interactions microbien pendant ces périodes. Une analyse couplée entre 1) une observation *in situ* des paramètres hydrologiques, météorologiques et biologiques à haute fréquence et 2) un suivi hebdomadaire de l'abondance et la diversité de la communauté microbienne modélisé par une approche de réseau de corrélation, cette thèse a permis de déterminer le fonctionnement complexe, et jusqu'alors inconnu, de l'initiation des efflorescences phytoplanctoniques en zone côtière mésotrophe, peu profonde, sous faible influence des marées et dans une zone telle que la Méditerranée.

Comme décrit dans l'introduction de cette thèse l'initiation des efflorescences phytoplanctoniques de façon générale serait due à un facteur de perturbation menant à la rupture de la balance entre la croissance et les pertes (essentiellement dues au broutage) du phytoplancton, en faveur de la croissance, entraînant une accumulation de la biomasse phytoplanctonique (Behrenfeld 2010; Behrenfeld et al. 2013b). Ce facteur peut être diverse en fonction des systèmes. En Atlantique Nord c'est le plongement de la couche de mélange qui fournit la perturbation nécessaire à l'écosystème pour rompre cette balance, en diluant les prédateurs dans la colonne d'eau réduisant ainsi le taux de rencontre entre proie et prédateur et donc la pression de prédation. Dans le cas des upwellings par exemple, c'est la remonté des eaux profondes chargées en nutriments qui jouent ce rôle de facteur de perturbation, en fournissant au phytoplancton les ressources nécessaires pour que la croissance excède les pertes (Wilkerson et al.

2006). A l'inverse, dans les zones côtières sous forte influence des cycles de marées, comme c'est le cas dans la mer du Nord, c'est l'augmentation de la pénétration de la lumière dans la colonne d'eau due à l'augmentation de l'irradiance et à la réduction de la matière en suspension, qui est responsable de l'initiation des efflorescences phytoplanctoniques (May et al. 2003; Tian et al. 2009; Blauw et al. 2012).

En milieu côtier peu profond, mésotrophe, sous faible influence des marées et dans une zone telle que la Méditerranée, il n'y a pas de variation de profondeur de la couche de mélange de l'ordre de celle de l'océan profond, la concentration en nutriment n'est généralement pas limitante, du moins pour la période qui précède les efflorescences printanières, la marée ne semble pas exercer un contrôle significatif sur la croissance phytoplanctonique et l'irradiance est généralement élevée, même en hiver. Jusqu'à ce jour, le facteur de perturbation qui pourrait permettre de rompre la balance entre la croissance phytoplanctonique et les pertes dues au broutage à l'origine de l'initiation des efflorescences dans ces zones étaient inconnu. Ainsi, le chapitre 1 de cette thèse met en évidence que dans ces zones, c'est essentiellement l'augmentation de la température qui joue ce rôle de perturbation (Trombetta et al. 2019). De plus, les résultats confirment que la concentration en nutriments et l'irradiance solaire ne sont pas des facteurs limitants et ne sont donc pas responsables de la perturbation à l'origine des efflorescences phytoplanctoniques dans cette zone côtière. L'hypothèse de la température, entre autre, comme initiateur des efflorescences phytoplanctoniques a déjà été émise dans plusieurs études, mais aucune jusqu'alors n'a été en mesure de le démontrer, du fait d'une fréquence de suivi inadaptée (Kirk, 1994; Bec et al. 2005).

L'augmentation de la température lagunaire, notamment à la sortie de l'hiver, permet de rompre temporairement la balance entre la croissance et les pertes du phytoplancton due au broutage, initiant ainsi les efflorescences. Une augmentation de la température peut agir sur la croissance ou les pertes du phytoplancton par stimulation directe de son métabolisme. Il est bien connu que l'augmentation de la température stimule à la fois l'activité métabolique du phytoplancton et du zooplancton. En revanche, la croissance des protistes autotrophes est plus importante que celle des protistes brouteurs quand la

température est inférieure à 15°C (Eppley 1972; Rose and Caron 2007). De plus, pendant les périodes sans efflorescences (appelées « *non-bloom periods* » dans les chapitres 1 et 2), le réseau microbien est dominé par les interactions prédateurs-proies entre les ciliés et les bactéries, au détriment de celles entre ciliés et phytoplancton (chapitre 2, Figure 4 et 5). Ceci suggère que pendant ces périodes, le bactérioplancton subit une intense pression de prédation contrairement au phytoplancton. Ainsi, en période de pré-efflorescence, la faible pression de prédation sur le phytoplancton, associée à une augmentation de la température favorisant sa croissance par rapport à celle des brouteurs est à l'origine de l'initiation des efflorescences phytoplanctoniques dans l'écosystème étudié.

Le chapitre 2 met en évidence que les interactions de type prédateur-proie ne sont pas les seules interactions dominantes au sein du réseau microbien. De ce fait, l'initiation des efflorescences phytoplanctoniques peut être facilitée par d'autres interactions biologiques en contribuant à la croissance phytoplanctonique. Par exemple, durant les périodes d'efflorescences, les principales interactions dans lesquelles le phytoplancton est impliqué sont les interactions de mutualisme avec les bactéries (Chapitre 2, Figure 4 et 5). Ainsi, nous pouvons supposer que l'augmentation de la température en tant que facteur de perturbation initiant les efflorescences pourrait également renforcer les interactions mutualistes entre le phytoplancton et les bactéries hétérotrophes, favorisant la croissance du phytoplancton. Des études récentes supportant cette hypothèse démontrent que l'augmentation de la température favoriserait les échanges de carbone et d'azote entre le phytoplancton et les bactéries. Une augmentation de 4°C de la température a augmenté de 50% en moyenne le transfert d'ammonium des bactéries vers le phytoplancton, ayant eu comme effet de stimuler significativement la croissance phytoplanctonique (Arandia-Gorostidi et al. 2017). Ainsi, l'augmentation de la température, en tant que facteur de perturbation, pourrait également modifier les interactions au sein du réseau microbien, permettant à la croissance du phytoplancton d'excéder ses pertes.

Dans les systèmes côtiers peu profonds, mésotrophes, tempérés et sous faible influence des marées tels que la lagune de Thau, l'augmentation de la température agit en synergie avec les

modifications des interactions biologiques sur l'accumulation de la biomasse. Dans ces systèmes, d'autres facteurs venant enrichir le milieu en nutriments tels que le vent qui remet en resuspension du sédiment, les pluies ou le transport de masses d'eau, viennent supporter la croissance phytoplanctonique pendant les périodes d'augmentation de température (chapitre 1).

Nous pouvons émettre l'hypothèse que ce mécanisme d'initiation des efflorescences identifié dans la lagune de Thau pourrait être le même dans d'autres systèmes similaires. Une des suites à donner à ces travaux de thèse serait de tester ces hypothèses d'initiation des efflorescences dans d'autres systèmes peu profonds, mésotrophes, sous faible influence des marées et sous climat de type Méditerranéen, dans un premier temps par la méthode du suivi multi-paramétrique *in situ* à haute fréquence. Par exemple, il existe un nombre important de lagunes mésotrophes et sous faible influence des marées sur le pourtour de la Méditerranée. La validation de nos résultats dans ces autres systèmes, et l'identification des différences majeures avec ce qui a été observé, pourraient permettre de comprendre plus facilement les mécanismes et la dynamique des efflorescences dans ses zones, cruciales pour les populations locales en raison des importants services écosystémiques rendus.

2.2 Importance des interactions microbiennes dans la dynamique du phytoplancton et dans le fonctionnement du réseau microbien

2.2.1 Fonctionnement des réseaux d'interactions microbiens

De nombreuses études se sont intéressées à l'effet des interactions entre micro-organismes sur la dynamique et la diversité des composantes impliquées, ainsi que sur l'impact sur la circulation de la matière (Tillmann 2004; Skovgaard 2014; Seymour et al. 2017). Cependant, ces études ont généralement traité une seule interaction à chaque fois (e.g. prédation) ou sur uniquement deux espèces en particulier (e.g. phytoplancton – brouteurs protistes). De ce fait, il existe une lacune importante dans la mise en évidence concrète d'interactions au sein d'un réseau, les rétroactions et interaction multiples possibles, ainsi que sur leur influence sur le fonctionnement, la dynamique et la diversité des communautés microbiennes. En fait, une poignée d'études traitent de ce sujet, (Steele et al. 2011; Posch et al. 2015;

Tan et al. 2015; Needham and Fuhrman 2016; Xue et al. 2018), mais ne s'attardent pas sur la comparaison de la structure de ces réseaux entre les différentes périodes écologiques du système (e.g. périodes d'efflorescences et sans efflorescences) ou différentes années climatiques contrastées. De plus, quand ces études se basaient sur des données d'abondance et de diversité microbienne (Posch et al. 2015) elles ne le faisaient pas sur un nombre important de groupes/taxons/espèces tels qu'étudiés dans le chapitre 2, limitant ainsi la compréhension du fonctionnement des réseaux d'interactions.

Le chapitre 2 de cette thèse (Trombetta et al., soumis), par contre, démontre bien les différences nettes en termes de structure des réseaux d'interactions microbiens entre les différentes périodes de production étudiées, ainsi qu'entre les deux années climatiquement contrastées. Ces différences structurelles entre périodes, que ce soit sur la complexité du réseau ou sur les types d'interactions dominants, attestent de la forte dynamique des interactions entre micro-organismes et de leurs modifications dans le temps. Cette grande variabilité suggère le rôle important de la structuration des réseaux d'interactions dans le fonctionnement des réseaux trophiques microbiens. En effet, cette variabilité peut moduler la dynamique de l'écosystème dans son ensemble puisque les interactions entre micro-organismes témoignent notamment du transfert et donc le devenir de la matière (nutriments, carbone, etc.) au sein du réseau (Sherr et al. 1988; Azam and Malfatti 2007). Par exemple, en période d'efflorescence, les corrélations positives entre bactéries et phytoplancton dominant, suggérant des interactions mutualistes privilégiées entre ces deux groupes et donc un transfert potentiellement important de carbone du phytoplancton vers les bactéries, et de nutriments des bactéries vers le phytoplancton potentiellement important (Seymour et al. 2017). Comme vu plus haut, ce type d'interaction favorise la production et l'accumulation de biomasse à la base de l'écosystème et donc les efflorescences et le transfert d'énergie aux niveaux trophiques supérieurs. Également, en 2016, pendant l'année avec l'hiver le plus chaud jamais enregistré par Météofrance, les interactions entre les virus et les bactéries ainsi que les flagellés hétérotrophes indiquent une augmentation potentielle de l'infection virale, suggérant une plus grande mortalité de ces derniers et un plus grand apport de matière organique par lyse virale dans le système (Fuhrman 1999). En outre, les interactions de prédation modulent la

dynamique des organismes impliqués et sont témoins directs de la circulation de l'énergie au sein du réseau (*cf* section suivante).

Cette thèse révèle que les forçages physico-chimiques dans le fonctionnement des réseaux trophiques microbiens induisent de profondes restructurations des réseaux d'interaction microbiens par l'intermédiaire d'actions, de réactions et de rétroactions en chaîne. Au sein d'un réseau d'interaction, les paramètres physico-chimiques peuvent influencer les organismes directement, par l'intermédiaire de leurs performances physiologiques et métaboliques intrinsèques, comme par exemple l'effet de la température sur l'optimum de croissance d'une espèce (Thomas et al. 2012), mais également indirectement en affectant les interactions biotiques. Les forçages physico-chimiques affectent la valeur sélective des organismes, c'est-à-dire leur capacité de survie, de reproduction et de transmission des gènes à leur descendance. Ainsi, dans le cas où les forçages affectent les organismes directement, la modification de leur valeur sélective fait varier le poids de leurs interactions et donc influencent directement la valeur sélective des autres organismes (Aránguiz-Acuña et al. 2011; Pajk et al. 2012). De plus, les forçages environnementaux affectent également les interactions entre les organismes, modifiant de ce fait la valeur sélective des organismes impliqués, et en conséquence leur dynamique d'abondance et leur capacité d'interaction avec des tiers (Arandia-Gorostidi et al. 2017). Par exemple, nous avons vu dans cette thèse que pendant l'initiation des efflorescences phytoplanctoniques, l'augmentation de la température augmente la valeur sélective (croissance et donc division) du phytoplancton (chapitre 1), mais renforce également leurs liens mutualistes avec les bactéries (chapitre 2 ; Arandia-Gorostidi et al., 2017). Ainsi, la valeur sélective de ces deux types d'organismes est derechef augmentée par échange de composés essentiels à leur croissance, menant *in fine* à une augmentation de leur biomasse caractéristique d'une efflorescence. En conséquence, cela favorise les interactions de type proie-prédateur de broutage des bactéries ou du phytoplancton, mais également la compétition pour l'accès aux nutriments entre les différents groupes phytoplanctoniques (chapitre 2, Figure 4 et 5). Cependant, l'effet des conditions physico-chimiques sur les réseaux d'interactions microbiens en milieu marin est

encore peu étudié, bien qu'en parallèle de cette thèse, de récentes études ont démontré qu'elles ont une influence fondamentale sur leur structuration (Hemraj et al., 2017).

2.2.2 Circulation de l'énergie pendant les périodes d'efflorescences phytoplanctoniques et comparaison avec les périodes de non efflorescence.

Les travaux de cette thèse nous ont permis d'identifier les voies privilégiées de transfert de l'énergie au sein du réseau microbien vers les niveaux trophiques supérieurs, et leurs modifications en fonction des périodes d'efflorescences ou de non efflorescences. Il est à noter que nous n'avons pas quantifié les taux de transferts, cependant les résultats obtenus sur les réseaux d'interactions nous permettent d'avoir une idée de leurs modifications en fonction des différentes périodes.

Pendant les périodes d'efflorescences, on observe une importante abondance des différentes classes de taille du phytoplancton ainsi que des bactéries hétérotrophes (Chapitre 1, Figure 6 ; Chapitre 2, Figure 1), en raison des conditions environnementales favorables (température, nutriments et lumière) et des interactions mutualistes entre ces organismes qui favorisent leur croissance. Cette diversité de la taille des proies pour les consommateurs est favorable à la fois à la voie de transfert autotrophe et hétérotrophe de l'énergie vers les niveaux trophiques supérieurs (Figure 1A). Ainsi, les organismes plus petits tels que les bactéries hétérotrophes, le pico- et le nanophytoplancton, rejoignent la voie de transfert hétérotrophe en étant consommés par le protozooplancton (flagellés hétérotrophes, ciliés et tintinnides), qui sont à leur tour consommés par le métazooplancton (copépodes, larves de poisson, etc.). Les plus gros producteurs primaires, comme les diatomées par exemple, rejoignent quant à eux la voie autotrophe en étant directement consommés par le métazooplancton. Ce type de fonctionnement assure pendant les périodes d'efflorescence la productivité de l'écosystème par un transfert efficace de l'énergie vers les niveaux trophiques supérieurs. Cependant, le chapitre 3 de cette thèse met en évidence que dans ce système, la voie hétérotrophe est dominante au sein du réseau microbien car une partie non négligeable des diatomées est consommées par le protozooplancton.

En revanche, pendant les périodes sans efflorescences phytoplanctoniques, les interactions négatives entre bactéries et ciliés dominant, indiquant une prépondérance des interactions bactérivore des ciliés (Chapitre 2, Figure 1). Les faibles abondances en phytoplancton pendant ces périodes-là font des bactéries la source principale d'énergie pour les niveaux trophiques supérieurs. Ainsi, pendant les périodes sans efflorescences phytoplanctoniques, le transfert de l'énergie se fait essentiellement par la voie hétérotrophe bactéries – protozooplancton – métazooplancton (Figure 1B). La voie de transfert autotrophe classique phytoplancton - métazooplancton est potentiellement réduite pendant ces périodes-là. Par réduction de l'une des deux voies, le transfert global de l'énergie vers les niveaux trophiques supérieurs est donc réduit. De plus, comme la voie hétérotrophe présente un ou plusieurs intermédiaires de plus (flagellés et ciliés hétérotrophes) que la voie autotrophe classique, elle est moins efficace dans le transfert de l'énergie du fait de ces maillons intermédiaires supplémentaires (Fenchel 1988; Sherr and Sherr 1988; Hairston and Hairston 1993). De ce fait, pendant les périodes sans efflorescences phytoplanctoniques, le transfert de l'énergie vers les niveaux trophiques supérieurs est grandement réduit, entraînant une réduction potentielle de la production de ces derniers.

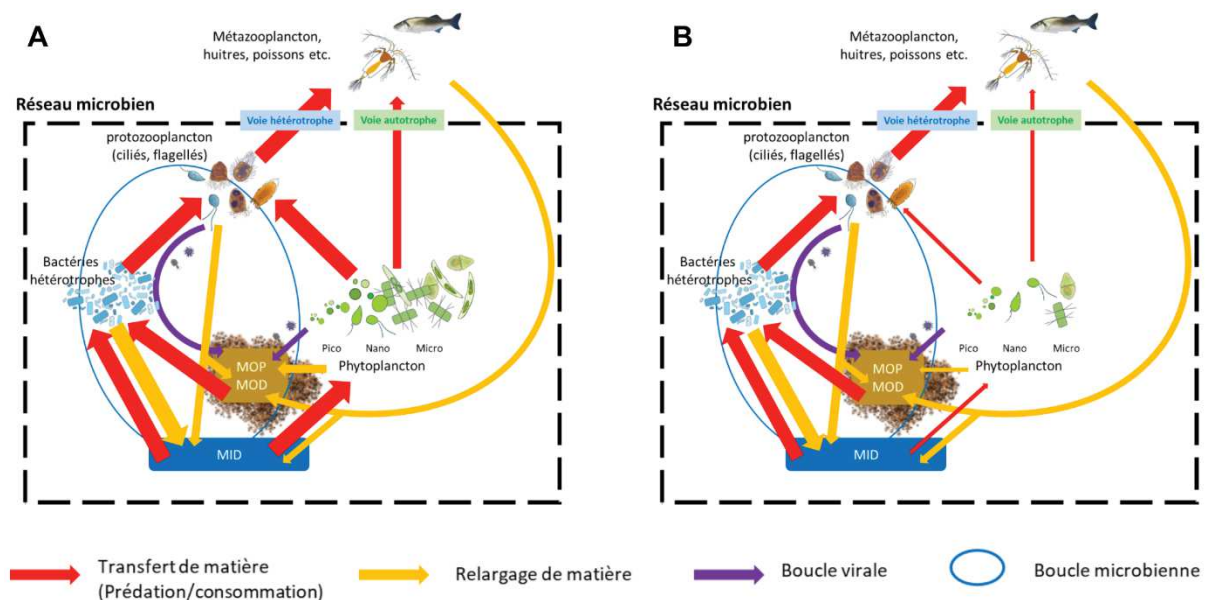


Figure 1 : Représentation du réseau trophique microbien et de la circulation de la matière et de l'énergie entre ses différentes composantes. (A) Période d'efflorescence phytoplanctonique et (B) période de non efflorescence. MOP : Matière organique particulaire ; MOD : Matière organique dissoute ; MID : Matière inorganique dissoute. Le sens des flèches représente le sens du transfert de

l'énergie ou de la matière organique. Les flèches violettes indiquent une recharge de MOP/MOD par lyse virale. La taille des organismes n'est pas proportionnelle à leur taille réelle. La variation de l'épaisseur des flèches par rapport à la Figure 2 de l'Introduction générale représente l'amplification ou la réduction de la voie de transfert dans les conditions d'efflorescence ou non.

2.2.3 Étude des réseaux d'interactions, vers une meilleure compréhension des processus modulant les communautés

Cette thèse révèle clairement les répercussions de la modification des interactions entre les organismes sur l'ensemble du réseau d'interactions, et donc sur le fonctionnement des réseaux trophiques microbiens et la circulation de matière et de d'énergie dans les systèmes étudiés. Les interactions entre organismes qui opèrent au sein d'un réseau complexe d'actions, de réactions en chaîne et de rétroactions, influencées par les forçages physico-chimiques. Dans l'optique de comprendre l'influence des interactions biotiques sur le fonctionnement des écosystèmes en général, il s'avère primordial d'étudier ces interactions sous la forme d'un réseau complexe, composé d'organismes diversifiés. Cependant, la compréhension de la structure et du fonctionnement des réseaux d'interaction microbiens en est encore à son balbutiement, et de plus amples efforts sont nécessaires pour y parvenir. L'importance du rôle des forçages environnementaux dans la structuration de ces réseaux, ainsi que leur impact sur les écosystèmes de façon générale est encore une voie à explorer dans la compréhension du fonctionnement des écosystèmes marins, mais peut permettre de mettre en évidence de nouveaux concepts et paradigmes écologiques.

Dans ces travaux de thèse, la taille des organismes ainsi que leur comportement trophique (producteur primaire, bactérien, consommateur primaire, etc.) ont été utilisées comme type de traits pouvant expliquer les fonctions écologiques et le rôle des organismes au sein du réseau (Chapitre 2). Cette approche a été motivée par la volonté de mieux comprendre les interactions modulant la circulation de l'énergie au sein des réseaux trophiques. Cependant les organismes peuvent être groupés en fonction d'autres types de traits (histoire de vie, trait comportementaux, physiologiques ou morphologiques). Par

exemple, l'application de l'approche réseau regroupant les organismes en fonction de la composition cellulaire et des besoins stœchiométriques du mode de reproduction (sexuée, asexuée) et de la durée de génération pourrait permettre de comprendre le rôle des interactions biologiques dans la croissance et la reproduction des organismes.

2.3 Avenir des efflorescences phytoplanctoniques et du transfert de l'énergie en zone côtière peu profonde face au réchauffement climatique

2.3.1 Modification de la phénologie des efflorescences phytoplanctoniques

Les chapitres 1 et 3 de cette thèse ont montré des effets clairs des températures anormalement élevées sur la dynamique des efflorescences phytoplanctoniques. Lors d'observations *in situ* (chapitre 1) en 2015, l'année avec la température hivernale normale pour la région, une efflorescence printanière précoce à la mi-février (« *early spring bloom* ») due à l'augmentation de la température lagunaire à la sortie de l'hiver a été observée avant l'efflorescence printanière majeure d'avril. En 2016, l'année avec l'hiver le plus chaud jamais enregistré en France, la biomasse phytoplanctonique a stagné, sans efflorescence à proprement parler jusqu'à fin mars. Ensuite, une efflorescence phytoplanctonique printanière s'est développée, mais avec une plus faible accumulation journalière de biomasse qu'en 2015. En conditions contrôlées (chapitre 3), l'augmentation de 3°C de la température a également entraîné une plus faible accumulation journalière de la biomasse phytoplanctonique, réduisant ainsi l'amplitude de l'efflorescence de moitié. De plus, la biomasse de l'ensemble de la communauté phytoplanctonique a été réduite pendant l'efflorescence. La date du maximum de biomasse de l'efflorescence semble également avoir été avancée de 1 jour en condition plus chaude.

La température s'est révélée être un facteur crucial responsable de l'initiation des efflorescences phytoplanctoniques en zone côtière peu profonde, tempérée, mésotrophe et sous faible influence des marées. Ainsi, nous pouvons émettre certaines hypothèses sur la modification de l'initiation des efflorescences, plus particulièrement de leur date d'initiation dans le contexte du réchauffement climatique. Les lagunes et les zones côtières peu profondes présentent de très importantes variations

saisonniers de température, pouvant aller de 4°C à l'hiver jusqu'à 30°C au plus chaud de l'été dans la lagune de Thau par exemple (Pernet et al. 2012b; a). Dans le contexte du réchauffement climatique les projections prévoient que la Méditerranée sera l'une des zones les plus sujettes à la hausse des températures (IPCC 2013), avec une hausse des températures par rapport aux actuelles de l'ordre de 2°C pendant l'hiver et de 4°C pendant l'été, à l'horizon 2030 (Giannakopoulos et al. 2009). Ces travaux de thèse révèlent que les conditions de température hivernale sont importantes dans la phénologie des efflorescences et l'accumulation de biomasse au printemps. Ainsi dans le cadre du réchauffement climatique, nous pouvons supposer que les températures hivernales plus chaudes n'entraîneront pas d'initiation des efflorescences précoces dès la sortie de l'hiver, en accord avec ce qui a été observé en 2016. En revanche, une plus forte augmentation de la température au printemps et en l'été devrait avancer les efflorescences printanières dans la saison. La modification de la phénologie et notamment de la période d'initiation des efflorescences printanières, a déjà été reportée dans la littérature en tant que conséquence du réchauffement climatique dans des systèmes plus profonds (Straile and Adrian 2000; Gerten and Adrian 2001). La plupart de ces études reportent des efflorescences printanières initiées plus tôt dans la saison, attribuées à l'effet de l'augmentation de la température sur la stratification précoce de la colonne d'eau, entraînant une concentration précoce des organismes en surface avec des conditions de lumière et de nutriments favorables à leur croissance (Straile and Adrian 2000; Gerten and Adrian 2001).

2.3.2 Réduction de l'ampleur des efflorescences phytoplanctoniques

Cette thèse met en évidence de façon claire que de la hausse de la température se traduit une plus faible accumulation de biomasse, et réduit l'amplitude des efflorescences phytoplanctoniques. Les effets de la hausse de la température sur l'amplitude des efflorescences ont déjà été rapportés dans des études précédentes, et son effet peut être variable en fonction des écosystèmes (*cf* chapitre 1). En revanche, à notre connaissance, c'est la première fois qu'un effet d'une telle ampleur est décrit, avec notamment une réduction de la moitié de la biomasse chlorophyllienne et affectant ainsi négativement l'ensemble

de la communauté phytoplanctonique. Ces résultats suggèrent que sous un climat plus chaud, avec des hivers également plus doux (IPCC 2013), il est probable que la production primaire nette des systèmes côtiers tempérés et peu profonds soit significativement réduite. Il a été émis l'hypothèse que ceci puisse être en partie due à un effet plus important des températures $> 15\text{ °C}$ sur les métabolismes des organismes hétérotrophes que sur celui des autotrophes (Rose and Caron 2007). Cela favoriserait ainsi le contrôle top-down sur la production primaire par intensification du broutage (Peter and Sommer 2012) ou par renforcement de l'effet de cascade trophique (Kratina et al. 2012), en accord avec ce qui a été mis en évidence dans les chapitres 2 et 3. Cette hypothèse est également supportée par les données de concentrations en nutriments, qui ne montrent aucune forme de limitation pour la production primaire à la fois *in situ* (chapitre 1) et en condition expérimentale (chapitre 3), malgré les conditions de température favorisant l'assimilation des nutriments. Les résultats du chapitre 3 ont permis d'établir, pour la première fois à notre connaissance, les effets d'une augmentation de $+3\text{ °C}$ de la température sur la magnitude de la réduction de la biomasse des différents groupes phytoplanctoniques, ainsi que l'implication des différentes fractions zooplanctoniques. Une augmentation de 3 °C a réduit la biomasse chlorophyllienne de 48% pendant l'efflorescence, impactant notablement les prymnesiophytes et les diatomées avec une réduction de 57% et 19% de leur biomasse respective pendant l'efflorescence. La suppression du zooplancton $> 200\text{ }\mu\text{m}$ a révélé que cette fraction (principalement des copépodes) était à l'origine de 48% de la réduction de la biomasse phytoplanctonique due au réchauffement, par broutage direct ou par cascade trophique suite à la consommation du zooplancton $< 200\text{ }\mu\text{m}$ (ciliés et flagellés hétérotrophes). Cependant, il n'est pas à exclure que la hausse des températures ait induit également une augmentation de la mortalité autre que la prédation, telle que la mortalité par la lyse virale ou par le parasitisme (Danovaro et al. 2011; Domis et al. 2013; Alves-de-Souza et al. 2015; Frenken et al. 2016; Mojica et al. 2016).

Ainsi, dans le contexte du réchauffement climatique, le transfert de l'énergie issue de la production primaire aux niveaux trophiques supérieurs serait toujours assuré par une importante activité de broutage. Cependant à une échelle saisonnière, des températures plus hautes pourraient entraîner un

mismatch avec les métazoaires au cycle de vie plus long, comme pour les plus gros copépodes ou les larves de poissons planctonivores (Edwards and Richardson 2004; Cury et al. 2008). Ce décalage entre la production du réseau microbien et le développement des métazoaires pourrait entraîner à court terme une réduction du transfert d'énergie entre ces deux composantes, au profit de la matière organique dissoute et donc de la boucle microbienne, ou un changement d'intermédiaires dans le transfert vers les niveaux supérieurs (Cury et al. 2008). A plus long terme, cela pourrait entraîner un changement des communautés planctonivores au profit d'espèces au cycle de vie plus adapté à des conditions plus chaudes, comme par exemple des espèces invasives thermorésistantes, favorisant ainsi le phénomène de *tropicalisation de la Méditerranée* (Raitsos et al. 2010).

2.3.3 Vers une dominance du phytoplancton de plus petite taille au détriment des diatomées

Un des résultats les plus marquants de cette thèse est la modification de la communauté phytoplanctonique vers la dominance d'espèces et de groupes de plus petite taille, comme les cyanobactéries, les pico- ou les nanophytoeucaryotes $< 6 \mu\text{m}$, au détriment des diatomées, quand la température de l'eau est plus élevée. Ce phénomène, observé *in situ* (chapitre 1), se traduit par la dominance des interactions entre organismes de petite taille au sein du réseau microbien (chapitre 2), ainsi qu'en conditions expérimentales (chapitre 3). De plus, une augmentation de l'abondance bactérienne a été observée *in situ* pendant l'année la plus chaude (chapitre 2).

Il a déjà été observé expérimentalement (Peter and Sommer 2012) et *in situ* (Morán et al. 2010) qu'une augmentation de température entraîne une réduction intra- et interspécifique de taille du phytoplancton. Cependant c'est la première fois que des observations couplées *in situ* et expérimentales sur un même système visent à expliquer les mécanismes liés à une réduction de taille du phytoplancton. Par cette approche couplée, nous sommes en mesure de mieux comprendre les mécanismes écologiques sous-jacents à cette modification, et ainsi de mieux anticiper le fonctionnement des écosystèmes et le transfert d'énergie dans le contexte du réchauffement climatique. Une réduction de la taille de la communauté est le résultat d'un métabolisme plus actif des cellules plus petites. Ceci est expliqué par

la règle écologique, qui favorise les petites tailles cellulaires à haute température par une plus forte affinité pour les nutriments, et une plus forte croissance due à leur plus grand ratio taille-volume (Sommer et al. 2017). Dans notre cas, c'est ce qui a causé l'efflorescence précoce des petites algues vertes en conditions expérimentales et *in situ*, et entraîné la plus forte biomasse lors du traitement chauffé (T) par rapport au contrôle (C) en période de post-efflorescence en condition expérimentale, malgré la plus grande pression de broutage exercé par les brouteurs protistes avec l'augmentation de la température (comparaison des traitements MicroZ et TMicroZ, chapitre 3).

La favorisation des espèces plus petites se fait au détriment d'espèces plus grosses tels que les diatomées du fait de leur compétitivité réduite en conditions plus chaudes. En effet, il a été démontré que les plus hautes températures intensifient le broutage des plus grosses cellules du phytoplancton par le proto- et le mézozooplancton, notamment les diatomées (Peter and Sommer 2012). En plus d'être l'acteur phytoplanctonique majeur à la base du transfert d'énergie vers les niveaux trophiques supérieurs (zooplancton, bivalves, poissons, etc.) dans de nombreux écosystèmes (Cloern 1996; Carstensen et al. 2015), les diatomées sont considérées comme les premiers exportateurs de carbone vers les fonds marins en raison de leur relativement faible flottabilité comparée à celle d'autres organismes (Tréguer et al. 2018; Boyd et al. 2019). De ce fait, elles participent activement à la séquestration du CO₂ atmosphérique. La réduction des diatomées dans un avenir plus chaud, en zone côtière peu profonde, comme dans l'océan mondial de façon générale (Armbrust 2009) réduirait l'effet tampon des océans sur les émissions de gaz à effet de serre via une réduction importante de la séquestration du CO₂ (Behrenfeld et al. 2013b). Ces résultats sont d'autant plus importants qu'ils montrent que les importantes concentrations en nutriments, favorables à la croissance des diatomées (Lomas and Glibert 2000) ne leur permettent pas de contrer les effets couplés de l'intense compétition avec les espèces plus petites et la forte pression de broutage.

En milieu côtier peu profond tel que la lagune de Thau, les diatomées sont une des sources principales d'alimentation des huîtres, du fait de leur taille appropriée à leur filtration et de leur

importante abondance (Dupuy et al. 2000; Cugier et al. 2010). Dans de nombreux systèmes côtiers, l'ostréiculture présente un fort enjeu économique, et un déclin des diatomées (50% pendant l'efflorescence pour *Chaetoceros* spp. dans les conditions *in situ*, chapitre 1 ; et 19% dans les conditions expérimentales, chapitre 3) au profit du picoplancton, non retenu directement par les huitres, pourrait à terme réduire la production ostréicole. Cependant, il se pourrait également que cela n'affecte pas significativement cette production étant donné que le picophytoplancton et les bactéries peuvent être retenus indirectement via la filtration de leurs prédateurs par les huitres (Le Gall et al. 1997).

2.3.4 Fonctionnement du réseau trophique microbien et avenir du transfert de l'énergie face au réchauffement climatique

Une réduction de la taille de la communauté phytoplanctonique (chapitres 1, 2 et 3), une augmentation de la biomasse bactérienne (chapitre 2), ainsi qu'une prépondérance des interactions entre micro-organismes à la base du réseau trophique (chapitre 2) modifierait fondamentalement le transfert d'énergie vers les niveaux trophiques supérieurs. Cela induirait une modification du transfert d'énergie par amplification de la voie hétérotrophe (Figure 2). Les bactéries ainsi que le pico et nanophytoplancton sont majoritairement broutés par les flagellés hétérotrophes et les petits ciliés (Johansson et al. 2004; Moustaka-Gouni et al. 2016). Ces micro-organismes sont eux même prédatés par des copépodes carnivores, assurant le transfert d'énergie vers les niveaux trophiques supérieurs. Ainsi, comme vu plus haut, la voie hétérotrophe est moins efficace en terme de transfert d'énergie du fait de l'intermédiaire prédateur protozooplanctonique en plus par rapport à la voie autotrophe, réduisant de ce fait l'efficacité du transfert d'énergie par la présence d'une étape supplémentaire dans la voie trophique (Fenchel 1988). Une stimulation du transfert hétérotrophe au détriment de la chaîne herbivore dite classique dans un climat plus chaud, entraînerait alors une déperdition d'énergie plus importante entre la production primaire et les niveaux supérieurs, impactant directement la productivité des écosystèmes. De plus, les résultats du chapitre 2 montrent que les interactions entre les virus et les bactéries et ainsi qu'entre les virus et les flagellés hétérotrophes, sont surreprésentés en conditions de plus fortes températures. Ces

résultats suggèrent une augmentation potentielle de l'infection virale, et donc une plus grande mortalité induisant un plus grand apport de MOP par lyse virale dans le système dans un avenir plus chaud, favorisant de ce fait la boucle microbienne.

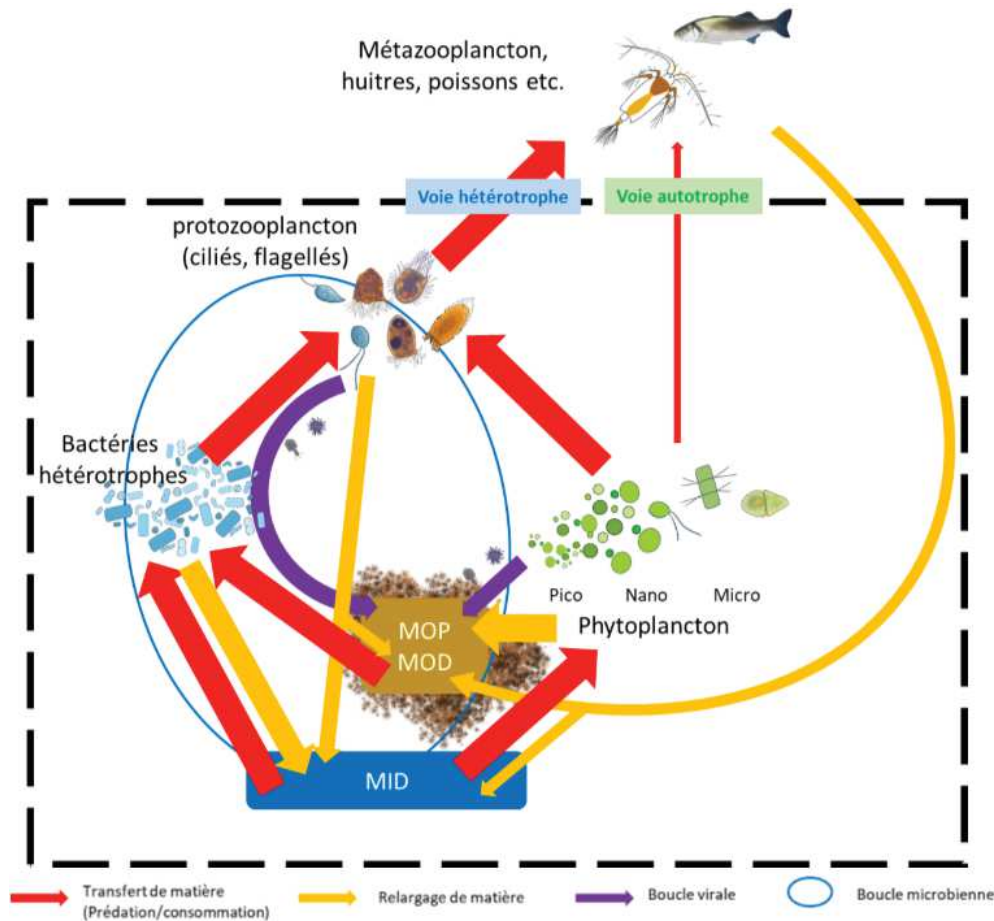


Figure 2 : Représentation du réseau trophique microbien et de la circulation de la matière et de l'énergie entre ses différentes composantes pendant les efflorescences en conditions de fortes températures. MOP : Matière organique particulaire ; MOD : Matière organique dissoute ; MID : Matière inorganique dissoute. Le sens des flèches représente le sens du transfert de l'énergie ou de la matière organique. Les flèches violettes indiquent une recharge de MOP/MOD par lyse virale. Les tailles des organismes ne sont pas proportionnelles à leur taille réelle. La variation de l'épaisseur des flèches par rapport à la Figure 4 de l'Introduction générale représente l'amplification ou la réduction de la voie de transfert dans des conditions plus chaudes.

3 Conclusion

L'objectif principal de cette thèse était d'identifier les forçages responsables de l'initiation et la dynamique des efflorescences phytoplanctoniques en zone côtière. Plus particulièrement, nous avons mis en évidence le rôle de la température et des interactions biologiques au sein du réseau microbien dans ces processus. Nous avons également identifié l'effet de l'augmentation de la température sur la dynamique et la composition des efflorescences dans le contexte du réchauffement climatique.

Les travaux de cette thèse ont permis de mettre en évidence le rôle crucial de l'augmentation de la température dans l'initiation des efflorescences phytoplanctoniques en zone côtière peu profonde. Elle agit en tant que facteur de perturbation venant stimuler la croissance phytoplanctonique et les interactions mutualistes, les pertes devenant plus importantes que la pression de prédation. La modification du réseau d'interactions entre groupes/taxons/espèces au sein du réseau microbien s'est révélée être primordiale dans l'initiation de ces efflorescences, la dynamique des micro-organismes et la circulation de l'énergie, par un complexe jeu d'actions, de réactions et de rétroactions en chaîne. Nous avons démontré qu'en réponse à l'augmentation de la température de l'eau, les efflorescences phytoplanctoniques étaient plus faibles et dominées par des espèces phytoplanctoniques de petite taille, au détriment des diatomées notamment, ce qui pourrait être semblable dans le futur dans le contexte du réchauffement climatique. La circulation et le transfert de l'énergie serait de ce fait modifiés, avec une favorisation de la voie à la base hétérotrophe, moins efficace, au détriment de la voie à la base autotrophe classique.

En plus d'une meilleure compréhension des mécanismes d'initiation des efflorescences en zone côtière peu profonde, les travaux de cette thèse proposent également des avancées méthodologiques dans l'étude des processus écologiques, à travers l'utilisation de mesures à haute fréquence, de l'approche réseau et de l'expérimentation en mésocosme dans des conditions contrôlées pour tester des hypothèses issues des observations *in situ*.

Pour conclure, les travaux de cette thèse s'inscrivent au sein d'un environnement de travail bâti à Sète et à Montpellier depuis bientôt deux décennies, visant à qualifier et quantifier les effets des forçages physiques, chimiques et biologiques sur la diversité, la physiologie et les interactions des organismes marins au sein de leurs réseaux planctoniques dans l'objectif de mieux comprendre le fonctionnement et la dynamique des écosystèmes marins côtiers. Inscrit au sein des UMR ECOLAG, ECOSYM puis MARBEC, et dans le développement de la plateforme MEDIMEER depuis 2002, cet environnement de travail a été fondé, bâti et enrichi par une multitude de chercheurs, ingénieurs, techniciens et étudiants au fil des années, au travers de collaborations nationales, européennes et internationales. Ainsi les travaux de cette thèse ont été soutenus par l'ensemble de cet environnement favorable. Ils sont venus apporter quelques pierres à cet édifice, et viendront à leur tour soutenir les travaux futurs, enrichissant encore et toujours la "Connaissance".

Bibliographie

-A-

- Abbott, M. R., P. J. Richerson, and T. M. Powell. 1982. In situ response of phytoplankton fluorescence to rapid variations in light. *Limnology and Oceanography* **27**: 218–225. doi:10.4319/lo.1982.27.2.0218
- Aberle, N., B. Bauer, A. Lewandowska, U. Gaedke, and U. Sommer. 2012. Warming induces shifts in microzooplankton phenology and reduces time-lags between phytoplankton and protozoan production. *Mar Biol* **159**: 2441–2453. doi:10.1007/s00227-012-1947-0
- Aberle, N., K. Lengfellner, and U. Sommer. 2007. Spring bloom succession, grazing impact and herbivore selectivity of ciliate communities in response to winter warming. *Oecologia* **150**: 668–681. doi:10.1007/s00442-006-0540-y
- Agawin, N. S. R., C. M. Duarte, and S. Agustí. 1998. Growth and abundance of *Synechococcus* sp. in a Mediterranean Bay: seasonality and relationship with temperature. *Marine Ecology Progress Series* **170**: 45–53.
- Albaina, A., and X. Irigoien. 2006. Fecundity limitation of *Calanus helgolandicus*, by the parasite *Ellobiopsis* sp. *J Plankton Res* **28**: 413–418. doi:10.1093/plankt/fbi129
- Allredge, A. L., and B. M. Jones. 1973. *Hastigerina pelagica*: Foraminiferal habitat for planktonic dinoflagellates. *Mar. Biol.* **22**: 131–135. doi:10.1007/BF00391777
- Allen, A. P., J. F. Gillooly, and J. H. Brown. 2005. Linking the global carbon cycle to individual metabolism. *Functional Ecology* **19**: 202–213. doi:10.1111/j.1365-2435.2005.00952.x
- Alpine, A. E., and J. E. Cloern. 1992. Trophic interactions and direct physical effects control phytoplankton biomass and production in an estuary. *Limnology and Oceanography* **37**: 946–955. doi:10.4319/lo.1992.37.5.0946
- Alves-de-Souza, C., D. Pecqueur, E. L. Floc'h, and others. 2015. Significance of Plankton Community Structure and Nutrient Availability for the Control of Dinoflagellate Blooms by Parasites: A Modeling Approach. *PLOS ONE* **10**: e0127623. doi:10.1371/journal.pone.0127623

- Amin, S. A., L. R. Hmelo, H. M. van Tol, and others. 2015. Interaction and signalling between a cosmopolitan phytoplankton and associated bacteria. *Nature* **522**: 98–101. doi:10.1038/nature14488
- Andersson, A., P. Haecky, and Å. Hagström. 1994. Effect of temperature and light on the growth of micro- nano- and pico-plankton: impact on algal succession. *Marine Biology* **120**: 511–520. doi:10.1007/BF00350071
- Aragon, Y. 2011. *Séries temporelles avec R: Méthodes et cas*, Springer-Verlag.
- Arandia-Gorostidi, N., P. K. Weber, L. Alonso-Sáez, X. A. G. Morán, and X. Mayali. 2017. Elevated temperature increases carbon and nitrogen fluxes between phytoplankton and heterotrophic bacteria through physical attachment. *The ISME Journal* **11**: 641–650. doi:10.1038/ismej.2016.156
- Aránguiz-Acuña, A., R. Ramos-Jiliberto, and R. O. Bustamante. 2011. Experimental assessment of interaction costs of inducible defenses in plankton. *J Plankton Res* **33**: 1445–1454. doi:10.1093/plankt/fbr023
- Armbrust, E. V. 2009. The life of diatoms in the world's oceans. *Nature* **459**: 185–192. doi:10.1038/nature08057
- Atkinson, D., B. J. Ciotti, and D. J. S. Montagnes. 2003. Protists decrease in size linearly with temperature: ca. 2.5% degrees C(-1). *Proc Biol Sci* **270**: 2605–2611. doi:10.1098/rspb.2003.2538
- Audouin, J. 1962. Hydrologie de l'étang de Thau. *Revue des Travaux de l'Institut des Pêches Maritimes* **26**: 5–104.
- Azam, F., T. Fenchel, J. G. Field, J. S. Gray, L. A. Meyer-Reil, and F. Thingstad. 1983. The Ecological Role of Water-Column Microbes in the Sea. *Marine Ecology Progress Series* **10**: 257–263.
- Azam, F., and F. Malfatti. 2007. Microbial structuring of marine ecosystems. *Nature Reviews Microbiology* **5**: 782–791. doi:10.1038/nrmicro1747

-B-

- Bacher, C., P. Duarte, J. G. Ferreira, M. Héral, and O. Raillard. 1998. Assessment and comparison of the Marennes-Oléron Bay (France) and Carlingford Lough (Ireland) carrying capacity with ecosystem models. *Aquatic Ecology* **31**: 379–394. doi:10.1023/A:1009925228308

- Bakun, A. 1990. Global Climate Change and Intensification of Coastal Ocean Upwelling. *Science* **247**: 198–201. doi:10.1126/science.247.4939.198
- Banse, K. 1994. Grazing and Zooplankton Production as Key Controls of Phytoplankton Production in the Open Ocean. *Oceanography* **7**: 13–20.
- Banse, K., and D. C. English. 2000. Geographical differences in seasonality of CZCS-derived phytoplankton pigment in the Arabian Sea for 1978–1986. *Deep Sea Research Part II: Topical Studies in Oceanography* **47**: 1623–1677. doi:10.1016/S0967-0645(99)00157-5
- Bec, B., J. Hussein Ratrema, Y. Collos, P. Souchu, and A. Vaquer. 2005. Phytoplankton seasonal dynamics in a Mediterranean coastal lagoon: emphasis on the picoeukaryote community. *Journal of plankton research* **27**: 881–894. doi:10.1093/plankt/fbi061
- Behrenfeld, M. J. 2010. Abandoning Sverdrup’s Critical Depth Hypothesis on phytoplankton blooms. *Ecology* **91**: 977–989. doi:10.1890/09-1207.1
- Behrenfeld, M. J., and E. S. Boss. 2014. Resurrecting the Ecological Underpinnings of Ocean Plankton Blooms. *Annu. Rev. Mar. Sci.* **6**: 167–194. doi:10.1146/annurev-marine-052913-021325
- Behrenfeld, M. J., S. C. Doney, I. Lima, E. S. Boss, and D. A. Siegel. 2013a. Annual cycles of ecological disturbance and recovery underlying the subarctic Atlantic spring plankton bloom. *Global Biogeochem. Cycles* **27**: 526–540. doi:10.1002/gbc.20050
- Behrenfeld, M. J., S. C. Doney, I. Lima, E. S. Boss, and D. A. Siegel. 2013b. Annual cycles of ecological disturbance and recovery underlying the subarctic Atlantic spring plankton bloom. *Global Biogeochem. Cycles* **27**: 526–540. doi:10.1002/gbc.20050
- Behrenfeld, M. J., S. C. Doney, I. Lima, E. S. Boss, and D. A. Siegel. 2013c. Reply to a comment by Stephen M. Chiswell on: “Annual cycles of ecological disturbance and recovery underlying the subarctic Atlantic spring plankton bloom” by M. J. Behrenfeld et al. (2013). *Global Biogeochemical Cycles* **27**: 1294–1296. doi:10.1002/2013GB004720
- Behrenfeld, M. J., R. T. O’Malley, D. A. Siegel, and others. 2006. Climate-driven trends in contemporary ocean productivity. *Nature* **444**: 752–755. doi:10.1038/nature05317
- Behrenfeld, M. J., T. K. Westberry, E. S. Boss, and others. 2009. Satellite-detected fluorescence reveals global physiology of ocean phytoplankton. *Biogeosciences* **6**: 779–794. doi:10.5194/bg-6-779-2009

- Bettarel, Y., T. Sime-Ngando, C. Amblard, J.-F. Carrias, and C. Portelli. 2003. Virioplankton and microbial communities in aquatic systems: a seasonal study in two lakes of differing trophy. *Freshwater Biology*. doi:10.1046/j.1365-2427.2003.01064.x
- van Beusekom, J. E. E., M. Loebel, and P. Martens. 2009. Distant riverine nutrient supply and local temperature drive the long-term phytoplankton development in a temperate coastal basin. *Journal of Sea Research* **61**: 26–33. doi:10.1016/j.seares.2008.06.005
- Blauw, A. N., E. Benincà, R. W. P. M. Laane, N. Greenwood, and J. Huisman. 2012. Dancing with the Tides: Fluctuations of Coastal Phytoplankton Orchestrated by Different Oscillatory Modes of the Tidal Cycle. *PLOS ONE* **7**: e49319. doi:10.1371/journal.pone.0049319
- Boyce, D. G., M. R. Lewis, and B. Worm. 2010. Global phytoplankton decline over the past century. *Nature* **466**: 591–596. doi:10.1038/nature09268
- Boyd, P. W., H. Claustre, M. Levy, D. A. Siegel, and T. Weber. 2019. Multi-faceted particle pumps drive carbon sequestration in the ocean. *Nature* **568**: 327–335. doi:10.1038/s41586-019-1098-2
- Brandenburg, K. M., M. Velthuis, and D. B. V. de Waal. 2019. Meta-analysis reveals enhanced growth of marine harmful algae from temperate regions with warming and elevated CO₂ levels. *Global Change Biology* **25**: 2607–2618. doi:10.1111/gcb.14678
- Bratbak, G., and T. F. Thingstad. 1985. Phytoplankton-bacteria interactions: an apparent paradox? Analysis of a model system with both competition and commensalism. *Marine Ecology Progress Series* **25**: 23–30.
- Brown, S. L., M. R. Landry, R. T. Barber, L. Campbell, D. L. Garrison, and M. M. Gowing. 1999. Picophytoplankton dynamics and production in the Arabian Sea during the 1995 Southwest Monsoon. *Deep Sea Research Part II: Topical Studies in Oceanography* **46**: 1745–1768. doi:10.1016/S0967-0645(99)00042-9
- Brussaard, C. P. D., G. J. Gast, F. C. van Duyl, and R. Riegman. 1996. Impact of phytoplankton bloom magnitude on a pelagic microbial food web. *Marine Ecology Progress Series* **144**: 211–221.

-C-

- Calbet, A., and M. R. Landry. 2004. Phytoplankton growth, microzooplankton grazing, and carbon cycling in marine systems. *Limnology and Oceanography* **49**: 51–57. doi:10.4319/lo.2004.49.1.0051

- Calbet, A., and E. Saiz. 2005. The ciliate-copepod link in marine ecosystems. *Aquatic Microbial Ecology* **38**: 157–167. doi:10.3354/ame038157
- Calbet, A., A. F. Sazhin, J. C. Nejstgaard, and others. 2014. Future Climate Scenarios for a Coastal Productive Planktonic Food Web Resulting in Microplankton Phenology Changes and Decreased Trophic Transfer Efficiency. *PLOS ONE* **9**: e94388. doi:10.1371/journal.pone.0094388
- del Campo, J., F. Not, I. Forn, M. E. Sieracki, and R. Massana. 2013. Taming the smallest predators of the oceans. *ISME J* **7**: 351–358. doi:10.1038/ismej.2012.85
- Caron, D. A., M. R. Dennett, D. J. Lonsdale, D. M. Moran, and L. Shalapyonok. 2000. Microzooplankton herbivory in the Ross Sea, Antarctica. *Deep Sea Research Part II: Topical Studies in Oceanography* **47**: 3249–3272. doi:10.1016/S0967-0645(00)00067-9
- Carritt, D. E., and J. H. Carpenter. 1966. Comparison and evaluation of currently employed modifications of Winkler method for determining dissolved oxygen in seawater: a NASCO report. *Journal of Marine Research* **24**: 286–318.
- Carstensen, J., R. Klais, and J. E. Cloern. 2015. Phytoplankton blooms in estuarine and coastal waters: Seasonal patterns and key species. *Estuarine, Coastal and Shelf Science* **162**: 98–109. doi:10.1016/j.ecss.2015.05.005
- Case, T. J., and M. E. Gilpin. 1974. Interference Competition and Niche Theory. *PNAS* **71**: 3073–3077. doi:10.1073/pnas.71.8.3073
- Chen, B., M. R. Landry, B. Huang, and H. Liu. 2012. Does warming enhance the effect of microzooplankton grazing on marine phytoplankton in the ocean? *Limnology and Oceanography* **57**: 519–526. doi:10.4319/lo.2012.57.2.0519
- Chen, K.-M., and J. Chang. 1999. Short communication. Influence of light intensity on the ingestion rate of a marine ciliate, *Lohmaniella* sp. *J Plankton Res* **21**: 1791–1798. doi:10.1093/plankt/21.9.1791
- Chisholm, S. W. 1992. Phytoplankton Size, p. 213–237. *In* P.G. Falkowski, A.D. Woodhead, and K. Vivirito [eds.], *Primary Productivity and Biogeochemical Cycles in the Sea*. Springer US.
- Chiswell, S. M. 2013. Comment on “Annual cycles of ecological disturbance and recovery underlying the subarctic Atlantic spring plankton bloom.” *Global Biogeochemical Cycles* **27**: 1291–1293. doi:10.1002/2013GB004681

- Christaki, U., D. Lefèvre, C. Georges, and others. 2014. Microbial food web dynamics during spring phytoplankton blooms in the naturally iron-fertilized Kerguelen area (Southern Ocean). *Biogeosciences* **11**: 6739–6753. doi:<https://doi.org/10.5194/bg-11-6739-2014>
- Cloern, J. E. 1991. Tidal stirring and phytoplankton bloom dynamics in an estuary. *Journal of Marine Research* **49**: 203–221. doi:[10.1357/002224091784968611](https://doi.org/10.1357/002224091784968611)
- Cloern, J. E. 1996. Phytoplankton bloom dynamics in coastal ecosystems: A review with some general lessons from sustained investigation of San Francisco Bay, California. *Rev. Geophys.* **34**: 127–168. doi:[10.1029/96RG00986](https://doi.org/10.1029/96RG00986)
- Colijn, F., and G. C. Cadée. 2003. Is phytoplankton growth in the Wadden Sea light or nitrogen limited? *Journal of Sea Research* **49**: 83–93. doi:[10.1016/S1385-1101\(03\)00002-9](https://doi.org/10.1016/S1385-1101(03)00002-9)
- Collos, Y., B. Bec, C. Jauzein, and others. 2009. Oligotrophication and emergence of picocyanobacteria and a toxic dinoflagellate in Thau lagoon, southern France. *Journal of Sea Research* **61**: 68–75. doi:[10.1016/j.seares.2008.05.008](https://doi.org/10.1016/j.seares.2008.05.008)
- Constantin, S., Ștefan Constantinescu, and D. Doxaran. 2017. Long-term analysis of turbidity patterns in Danube Delta coastal area based on MODIS satellite data. *Journal of Marine Systems* **170**: 10–21. doi:[10.1016/j.jmarsys.2017.01.016](https://doi.org/10.1016/j.jmarsys.2017.01.016)
- Costanza, R., R. d'Arge, R. de Groot, and others. 1997. The value of the world's ecosystem services and natural capital. *Nature* **387**: 253. doi:[10.1038/387253a0](https://doi.org/10.1038/387253a0)
- Costanza, R., R. de Groot, P. Sutton, S. van der Ploeg, S. J. Anderson, I. Kubiszewski, S. Farber, and R. K. Turner. 2014. Changes in the global value of ecosystem services. *Global Environmental Change* **26**: 152–158. doi:[10.1016/j.gloenvcha.2014.04.002](https://doi.org/10.1016/j.gloenvcha.2014.04.002)
- Cottrell, M. T., and C. A. Suttle. 1995. Dynamics of lytic virus infecting the photosynthetic marine picoflagellate *Micromonas pusilla*. *Limnology and Oceanography* **40**: 730–739. doi:[10.4319/lo.1995.40.4.0730](https://doi.org/10.4319/lo.1995.40.4.0730)
- Croft, M. T., A. D. Lawrence, E. Raux-Deery, M. J. Warren, and A. G. Smith. 2005. Algae acquire vitamin B12 through a symbiotic relationship with bacteria. *Nature* **438**: 90–93. doi:[10.1038/nature04056](https://doi.org/10.1038/nature04056)
- Crofton, H. D. 1971. A quantitative approach to parasitism. *Parasitology* **62**: 179–193. doi:[10.1017/S0031182000071420](https://doi.org/10.1017/S0031182000071420)

- Cross, W. F., J. M. Hood, J. P. Benstead, A. D. Huryn, and D. Nelson. 2015. Interactions between temperature and nutrients across levels of ecological organization. *Global Change Biology* **21**: 1025–1040. doi:10.1111/gcb.12809
- Cugier, P., C. Struski, M. Blanchard, J. Mazurié, S. Pouvreau, F. Olivier, J. R. Trigui, and E. Thiébaud. 2010. Assessing the role of benthic filter feeders on phytoplankton production in a shellfish farming site: Mont Saint Michel Bay, France. *Journal of Marine Systems* **82**: 21–34. doi:10.1016/j.jmarsys.2010.02.013
- Cury, P. M., Y.-J. Shin, B. Planque, and others. 2008. Ecosystem oceanography for global change in fisheries. *Trends in Ecology & Evolution* **23**: 338–346. doi:10.1016/j.tree.2008.02.005
- Cushing, D. H. 1959. The seasonal variation in oceanic production as a problem in population dynamics. *ICES J Mar Sci* **24**: 455–464. doi:10.1093/icesjms/24.3.455
- Cushing, D. H. 1989. A difference in structure between ecosystems in strongly stratified waters and in those that are only weakly stratified. *J Plankton Res* **11**: 1–13. doi:10.1093/plankt/11.1.1

-D-

- Dafner, E. V., and P. J. Wangersky. 2002. A brief overview of modern directions in marine DOC studies part II--recent progress in marine DOC studies. *J Environ Monit* **4**: 55–69.
- Danger, M., J. Leflaive, C. Oumarou, L. Ten-Hage, and G. Lacroix. 2007. Control of phytoplankton–bacteria interactions by stoichiometric constraints. *Oikos* **116**: 1079–1086. doi:10.1111/j.0030-1299.2007.15424.x
- Danovaro, R., C. Corinaldesi, A. Dell’Anno, J. A. Fuhrman, J. J. Middelburg, R. T. Noble, and C. A. Suttle. 2011. Marine viruses and global climate change. *FEMS Microbiol Rev* **35**: 993–1034. doi:10.1111/j.1574-6976.2010.00258.x
- Daufresne, M., K. Lengfellner, and U. Sommer. 2009. Global warming benefits the small in aquatic ecosystems. *PNAS* **106**: 12788–12793. doi:10.1073/pnas.0902080106
- Deininger, A., C. L. Faithfull, K. Lange, T. Bayer, F. Vidussi, and A. Liess. 2016. Simulated terrestrial runoff triggered a phytoplankton succession and changed seston stoichiometry in coastal lagoon mesocosms. *Marine Environmental Research* **119**: 40–50. doi:10.1016/j.marenvres.2016.05.001
- Deslous-Paoli, J.-M. 1996. Programme OXYTHAU: le bassin de Thau : relation milieu- ressources dans les secteurs conchylicoles. Importance des mécanismes d’échanges verticaux, IFREMER.

- Díaz-Castelazo, C., I. R. Sánchez-Galván, P. R. Guimarães, R. L. G. Raimundo, and V. Rico-Gray. 2013. Long-term temporal variation in the organization of an ant–plant network. *Ann Bot* **111**: 1285–1293. doi:10.1093/aob/mct071
- Dolan, J. R., M. R. Landry, and M. E. Ritchie. 2013. The species-rich assemblages of tintinnids (marine planktonic protists) are structured by mouth size. *ISME J* **7**: 1237–1243. doi:10.1038/ismej.2013.23
- Domin, H., Y. H. Zurita-Gutiérrez, M. Scotti, J. Buttlar, U. Hentschel Humeida, and S. Fraune. 2018. Predicted Bacterial Interactions Affect in Vivo Microbial Colonization Dynamics in *Nematostella*. *Front Microbiol* **9**: 728. doi:10.3389/fmicb.2018.00728
- Domingues, R. B., C. C. Guerra, A. B. Barbosa, and H. M. Galvão. 2015. Are nutrients and light limiting summer phytoplankton in a temperate coastal lagoon? *Aquat Ecol* **49**: 127–146. doi:10.1007/s10452-015-9512-9
- Domis, L. N. D. S., J. J. Elser, A. S. Gsell, and others. 2013. Plankton dynamics under different climatic conditions in space and time. *Freshwater Biology* **58**: 463–482. doi:10.1111/fwb.12053
- Dupuy, C., A. Vaquer, T. Lam-Höai, C. Rougier, N. Mazouni, J. Lautier, Y. Collos, and S. Le Gall. 2000. Feeding rate of the oyster *Crassostrea gigas* in a natural planktonic community of the Mediterranean Thau Lagoon. *Marine Ecology Progress Series* **205**: 171–184.

-E-

- Edwards, M., and A. J. Richardson. 2004. Impact of climate change on marine pelagic phenology and trophic mismatch. *Nature* **430**: 881–884. doi:10.1038/nature02808
- Eppley, R. W. 1972. Temperature and phytoplankton growth in the sea. *Fishery bulletin* **70**: 1063–85.
- Erdős, P., and A. Rényi. 1960. On the Evolution of Random Graphs. *Publication of the Mathematical Institute of the Hungarian Academy of Sciences*. 17–61.

-F-

- Falkowski, P. G., M. E. Katz, A. H. Knoll, A. Quigg, J. A. Raven, O. Schofield, and F. J. R. Taylor. 2004. The Evolution of Modern Eukaryotic Phytoplankton. *Science* **305**: 354–360. doi:10.1126/science.1095964
- Falkowski, P. G., and J. A. Raven. 2013. *Aquatic Photosynthesis: Second Edition*, Princeton University Press.

- Fasham, M. J. R. 1984. *Flows of Energy and Materials in Marine Ecosystems: Theory and Practice*, Springer US.
- Faust, K., and J. Raes. 2012. Microbial interactions: from networks to models. *Nature Reviews Microbiology* **10**: 538–550. doi:10.1038/nrmicro2832
- Fenchel, T. 1988. Marine Plankton Food Chains. *Annual Review of Ecology and Systematics* **19**: 19–38. doi:10.1146/annurev.es.19.110188.000315
- Ferrari, R., S. T. Merrifield, and J. R. Taylor. 2015. Shutdown of convection triggers increase of surface chlorophyll. *Journal of Marine Systems* **147**: 116–122. doi:10.1016/j.jmarsys.2014.02.009
- Fiandrino, A., A. Giraud, S. Robin, and C. Pinatel. 2012. Validation d'une méthode d'estimation des volumes d'eau échangés entre la mer et les lagunes et définition d'indicateurs hydrodynamiques associés.
- Field, C. B., M. J. Behrenfeld, J. T. Randerson, and P. Falkowski. 1998. Primary Production of the Biosphere: Integrating Terrestrial and Oceanic Components. *Science* **281**: 237–240. doi:10.1126/science.281.5374.237
- Foissner, W., A. Chao, and L. A. Katz. 2009. Diversity and geographic distribution of ciliates (Protista: Ciliophora), p. 111–129. *In* W. Foissner and D.L. Hawksworth [eds.], *Protist Diversity and Geographical Distribution*. Springer Netherlands.
- Fordham, D. A. 2015. Mesocosms Reveal Ecological Surprises from Climate Change. *PLOS Biology* **13**: e1002323. doi:10.1371/journal.pbio.1002323
- Foster, R. A., M. M. M. Kuypers, T. Vagner, R. W. Paerl, N. Musat, and J. P. Zehr. 2011. Nitrogen fixation and transfer in open ocean diatom–cyanobacterial symbioses. *ISME J* **5**: 1484–1493. doi:10.1038/ismej.2011.26
- Fouilland, E., A. Trottet, C. Alves-de-Souza, and others. 2017. Significant Change in Marine Plankton Structure and Carbon Production After the Addition of River Water in a Mesocosm Experiment. *Microb. Ecol.* **74**: 289–301. doi:10.1007/s00248-017-0962-6
- Fouilland, E., A. Trottet, C. Bancon-Montigny, and others. 2012. Impact of a river flash flood on microbial carbon and nitrogen production in a Mediterranean Lagoon (Thau Lagoon, France). *Estuarine Coastal and Shelf Science* **113**: 192–204. doi:10.1016/j.ecss.2012.08.004
- Frederiksen, M., M. Edwards, A. J. Richardson, N. C. Halliday, and S. Wanless. 2006. From plankton to top predators: bottom-up control of a marine food web across four trophic levels. *Journal of Animal Ecology* **75**: 1259–1268. doi:10.1111/j.1365-2656.2006.01148.x

Frenken, T., M. Velthuis, L. N. de S. Domis, S. Stephan, R. Aben, S. Kosten, E. van Donk, and D. B. V. de Waal. 2016. Warming accelerates termination of a phytoplankton spring bloom by fungal parasites. *Global Change Biology* **22**: 299–309. doi:10.1111/gcb.13095

Fuhrman, J. A. 1999. Marine viruses and their biogeochemical and ecological effects. *Nature* **399**: 541. doi:10.1038/21119

Fuhrman, J. A., J. A. Cram, and D. M. Needham. 2015. Marine microbial community dynamics and their ecological interpretation. *Nature Reviews Microbiology* **13**: 133–146. doi:10.1038/nrmicro3417

Fuhrman, J. A., and R. T. Noble. 1995. Viruses and protists cause similar bacterial mortality in coastal seawater. *Limnology and Oceanography* **40**: 1236–1242. doi:10.4319/lo.1995.40.7.1236

-G-

Gallegos, C. L., W. N. Vant, and K. A. Safi. 1996. Microzooplankton grazing of phytoplankton in Manukau Harbour, New Zealand. *New Zealand Journal of Marine and Freshwater Research* **30**: 423–434. doi:10.1080/00288330.1996.9516730

García-Reyes, M., and J. Largier. 2010. Observations of increased wind-driven coastal upwelling off central California. *Journal of Geophysical Research: Oceans* **115**. doi:10.1029/2009JC005576

Garzke, J., S. M. H. Ismar, and U. Sommer. 2015. Climate change affects low trophic level marine consumers: warming decreases copepod size and abundance. *Oecologia* **177**: 849–860. doi:10.1007/s00442-014-3130-4

Gast, R. J., Z. M. McKie-Krisberg, S. A. Fay, J. M. Rose, and R. W. Sanders. 2014. Antarctic mixotrophic protist abundances by microscopy and molecular methods. *FEMS Microbiol Ecol* **89**: 388–401. doi:10.1111/1574-6941.12334

Gerten, D., and R. Adrian. 2001. Differences in the persistency of the North Atlantic Oscillation signal among lakes. *Limnology and Oceanography* **46**: 448–455. doi:10.4319/lo.2001.46.2.0448

Giannakopoulos, C., P. Le Sager, M. Bindi, M. Moriondo, E. Kostopoulou, and C. M. Goodess. 2009. Climatic changes and associated impacts in the Mediterranean resulting from a 2 °C global warming. *Global and Planetary Change* **68**: 209–224. doi:10.1016/j.gloplacha.2009.06.001

Gillooly, J. F., J. H. Brown, G. B. West, V. M. Savage, and E. L. Charnov. 2001. Effects of Size and Temperature on Metabolic Rate. *Science* **293**: 2248–2251. doi:10.1126/science.1061967

- Gittings, J. A., D. E. Raitsos, G. Krokos, and I. Hoteit. 2018. Impacts of warming on phytoplankton abundance and phenology in a typical tropical marine ecosystem. *Scientific Reports* **8**: 2240. doi:10.1038/s41598-018-20560-5
- Glé, C., Y. Del Amo, B. Bec, and others. 2007. Typology of environmental conditions at the onset of winter phytoplankton blooms in a shallow macrotidal coastal ecosystem, Arcachon Bay (France). *J Plankton Res* **29**: 999–1014. doi:10.1093/plankt/fbm074
- Goldman, J. C., C. D. Taylor, and P. M. Glibert. 1981. Nonlinear Time-Course Uptake of Carbon and Ammonium by Marine Phytoplankton. *Marine Ecology Progress Series* **6**: 137–148.
- Grant, M. A. A., E. Kazamia, P. Cicuta, and A. G. Smith. 2014. Direct exchange of vitamin B12 is demonstrated by modelling the growth dynamics of algal-bacterial cocultures. *ISME J* **8**: 1418–1427. doi:10.1038/ismej.2014.9
- Gregg, W. W., N. W. Casey, and C. R. McClain. 2005. Recent trends in global ocean chlorophyll. *Geophysical Research Letters* **32**. doi:10.1029/2004GL021808
- Guinder, V. A., M. C. López-Abbate, A. A. Berasategui, V. L. Negrin, G. Zapperi, P. D. Pratolongo, M. D. Fernández Severini, and C. A. Popovich. 2015. Influence of the winter phytoplankton bloom on the settled material in a temperate shallow estuary. *Oceanologia* **57**: 50–60. doi:10.1016/j.oceano.2014.10.002
- Guixa-Boixereu, N., K. Lysnes, and C. Pedrós-Alió. 1999. Viral Lysis and Bacterivory during a Phytoplankton Bloom in a Coastal Water Microcosm. *Appl. Environ. Microbiol.* **65**: 1949–1958.
- Gurung, T. B., J. Urabe, and M. Nakanishi. 1999. Regulation of the relationship between phytoplankton *Scenedesmus acutus* and heterotrophic bacteria by the balance of light and nutrients. *Aquatic Microbial Ecology* **17**: 27–35. doi:10.3354/ame017027

-H-

- Hairton, Nelson G., and Hairton Nelson G. 1993. Cause-Effect Relationships in Energy Flow, Trophic Structure, and Interspecific Interactions. *The American Naturalist* **142**: 379–411. doi:10.1086/285546
- Hansen, B., P. K. Bjornsen, and P. J. Hansen. 1994. The size ratio between planktonic predators and their prey. *Limnology and Oceanography* **39**: 395–403. doi:10.4319/lo.1994.39.2.0395

- Hashioka, T., M. Vogt, Y. Yamanaka, and others. 2013. Phytoplankton competition during the spring bloom in four plankton functional type models. doi:10.5194/bg-10-6833-2013
- Hemraj, D. A., A. Hossain, Q. Ye, J. G. Qin, and S. C. Leterme. 2017. Anthropogenic shift of planktonic food web structure in a coastal lagoon by freshwater flow regulation. *Scientific Reports* **7**: 44441. doi:10.1038/srep44441
- Henson, S. A., H. S. Cole, J. Hopkins, A. P. Martin, and A. Yool. 2018. Detection of climate change-driven trends in phytoplankton phenology. *Global Change Biology* **24**: e101–e111. doi:10.1111/gcb.13886
- Henson, S., H. Cole, C. Beaulieu, and A. Yool. 2013. The impact of global warming on seasonality of ocean primary production. *Biogeosciences* **10**: 4357–4369. doi:10.5194/bg-10-4357-2013
- Hlaili, A. S., N. Niquil, and L. Legendre. 2014. Planktonic food webs revisited: Reanalysis of results from the linear inverse approach. *Progress in Oceanography* **120**: 216–229. doi:10.1016/j.pocean.2013.09.003
- Hobbie, J. E., R. J. Daley, and S. Jasper. 1977. Use of nuclepore filters for counting bacteria by fluorescence microscopy. *Appl. Environ. Microbiol.* **33**: 1225–1228.
- Holmes, R. M., A. Aminot, R. K erouel, B. A. Hooker, and B. J. Peterson. 1999. A simple and precise method for measuring ammonium in marine and freshwater ecosystems. *Can. J. Fish. Aquat. Sci.* **56**: 1801–1808. doi:10.1139/f99-128
- Hopkinson, C. S., and E. M. Smith. 2005. *Estuarine respiration: an overview of benthic, pelagic, and whole system respiration*, Oxford University Press.
- Houde, E. D., and E. S. Rutherford. 1993. Recent trends in estuarine fisheries: Predictions of fish production and yield. *Estuaries* **16**: 161–176. doi:10.2307/1352488
- Huisman, J., P. van Oostveen, and F. J. Weissing. 1999. Critical depth and critical turbulence: Two different mechanisms for the development of phytoplankton blooms. *Limnol. Oceanogr.* **44**: 1781–1787. doi:10.4319/lo.1999.44.7.1781
- Hunt, G. L., K. O. Coyle, L. B. Eisner, and others. 2011. Climate impacts on eastern Bering Sea foodwebs: a synthesis of new data and an assessment of the Oscillating Control Hypothesis. *ICES J Mar Sci* **68**: 1230–1243. doi:10.1093/icesjms/fsr036
- Hunter-Cevera, K. R., M. G. Neubert, R. J. Olson, A. R. Solow, A. Shalapyonok, and H. M. Sosik. 2016. Physiological and ecological drivers of early spring blooms of a coastal phytoplankton. *Science* **354**: 326–329. doi:10.1126/science.aaf8536

Huntley, M. E., and M. D. Lopez. 1992. Temperature-dependent production of marine copepods: a global synthesis. *Am. Nat.* **140**: 201–242. doi:10.1086/285410

-I-

IPCC. 2013. *Climate Change 2013: The Physical Science Basis. Contribution of Working Group I to the Fifth Assessment Report of the Intergovernmental Panel on Climate Change* [Stocker, T.F., D. Qin, G.-K. Plattner, M. Tignor, S.K. Allen, J. Boschung, A. Nauels, Y. Xia, V. Bex and P.M. Midgley (eds.)]. Cambridge University Press.

Iriarte, A., and D. A. Purdie. 1994. Size distribution of chlorophyll a biomass and primary production in a temperate estuary (Southampton Water): the contribution of photosynthetic picoplankton. *Marine Ecology Progress Series* **115**: 283–297.

Irigoiien, X., R. P. Harris, H. M. Verheye, and others. 2002. Copepod hatching success in marine ecosystems with high diatom concentrations. *Nature* **419**: 387–389. doi:10.1038/nature01055

-J-

Jacox, M. G., E. L. Hazen, K. D. Zaba, D. L. Rudnick, C. A. Edwards, A. M. Moore, and S. J. Bograd. 2016. Impacts of the 2015–2016 El Niño on the California Current System: Early assessment and comparison to past events. *Geophysical Research Letters* **43**: 7072–7080. doi:10.1002/2016GL069716

Jakubowska, N., and E. Szelaĝ-Wasielewska. 2015. Toxic Picoplanktonic Cyanobacteria—Review. *Mar Drugs* **13**: 1497–1518. doi:10.3390/md13031497

Jeong, H. J., Y. D. Yoo, J. S. Kim, K. A. Seong, N. S. Kang, and T. H. Kim. 2010. Growth, feeding and ecological roles of the mixotrophic and heterotrophic dinoflagellates in marine planktonic food webs. *Ocean Sci. J.* **45**: 65–91. doi:10.1007/s12601-010-0007-2

Jiang, L., and P. J. Morin. 2004. Temperature-dependent interactions explain unexpected responses to environmental warming in communities of competitors. *Journal of Animal Ecology* **73**: 569–576. doi:10.1111/j.0021-8790.2004.00830.x

Johansson, M., E. Gorokhova, and U. Larsson. 2004. Annual variability in ciliate community structure, potential prey and predators in the open northern Baltic Sea proper. *J Plankton Res* **26**: 67–80. doi:10.1093/plankt/fbg115

- Joint, I., P. Henriksen, G. A. Fonnes, D. Bourne, T. F. Thingstad, and B. Riemann. 2002. Competition for inorganic nutrients between phytoplankton and bacterioplankton in nutrient manipulated mesocosms. *Aquatic Microbial Ecology* **29**: 145–159. doi:10.3354/ame029145
- Joos, F., G.-K. Plattner, T. F. Stocker, O. Marchal, and A. Schmittner. 1999. Global Warming and Marine Carbon Cycle Feedbacks on Future Atmospheric CO₂. *Science* **284**: 464–467. doi:10.1126/science.284.5413.464
- Jung, S. W., S. J. Youn, H. H. Shin, S. M. Yun, J.-S. Ki, and J. H. Lee. 2013. Effect of temperature on changes in size and morphology of the marine diatom, *Ditylum brightwellii* (West) Grunow (Bacillariophyceae). *Estuarine, Coastal and Shelf Science* **135**: 128–136. doi:10.1016/j.ecss.2013.05.007

-K-

- Kahru, M., R. Kudela, M. Manzano-Sarabia, and B. G. Mitchell. 2009. Trends in primary production in the California Current detected with satellite data. *Journal of Geophysical Research: Oceans* **114**. doi:10.1029/2008JC004979
- Kalimeris, A., E. Ranieri, D. Founda, and C. Norrant. 2017. Variability modes of precipitation along a Central Mediterranean area and their relations with ENSO, NAO, and other climatic patterns. *Atmospheric Research* **198**: 56–80. doi:10.1016/j.atmosres.2017.07.031
- Kang, Y., R. M. Kudela, and C. J. Gobler. 2017. Quantifying nitrogen assimilation rates of individual phytoplankton species and plankton groups during harmful algal blooms via sorting flow cytometry. *Limnol. Oceanogr. Methods* **15**: 706–721. doi:10.1002/lom3.10193
- Kazamia, E., H. Czesnick, T. T. V. Nguyen, and others. 2012. Mutualistic interactions between vitamin B12 -dependent algae and heterotrophic bacteria exhibit regulation. *Environ. Microbiol.* **14**: 1466–1476. doi:10.1111/j.1462-2920.2012.02733.x
- Kazamia, E., K. E. Helliwell, S. Purton, and A. G. Smith. 2016. How mutualisms arise in phytoplankton communities: building eco-evolutionary principles for aquatic microbes. *Ecology Letters* **19**: 810–822. doi:10.1111/ele.12615
- Kemp, P. F., J. J. Cole, B. F. Sherr, and E. B. Sherr. 1993. *Handbook of Methods in Aquatic Microbial Ecology*, CRC Press.
- Kibler, S. R., P. A. Tester, K. E. Kunkel, S. K. Moore, and R. W. Litaker. 2015. Effects of ocean warming on growth and distribution of dinoflagellates associated with ciguatera fish poisoning in the Caribbean. *Ecological Modelling* **316**: 194–210. doi:10.1016/j.ecolmodel.2015.08.020

- Killick, R., P. Fearnhead, and I. A. Eckley. 2012. Optimal Detection of Changepoints With a Linear Computational Cost. *Journal of the American Statistical Association* **107**: 1590–1598. doi:10.1080/01621459.2012.737745
- Kjørboe, T. 1993. Turbulence, Phytoplankton Cell Size, and the Structure of Pelagic Food Webs, p. 1–72. *In* J.H.S. Blaxter and A.J. Southward [eds.], *Advances in Marine Biology*. Academic Press.
- Kirchman, D. L. 1994. The uptake of inorganic nutrients by heterotrophic bacteria. *Microb Ecol* **28**: 255–271. doi:10.1007/BF00166816
- Kirk, J. T. (1994). *Light and photosynthesis in aquatic ecosystems*. Cambridge University Press.
- Kivi, K., and O. Setälä. 1995. Simultaneous measurement of food particle selection and clearance rates of planktonic oligotrich ciliates (Ciliophora: Oligotrichina). *Marine Ecology Progress Series* **119**: 125–137. doi:10.3354/meps119125
- Kjerfve, B. 1994. Chapter 1 Coastal Lagoons, p. 1–8. *In* B. Kjerfve [ed.], *Elsevier Oceanography Series*. Elsevier.
- Koeller, P., C. Fuentes-Yaco, T. Platt, and others. 2009. Basin-scale coherence in phenology of shrimps and phytoplankton in the North Atlantic Ocean. *Science* **324**: 791–793. doi:10.1126/science.1170987
- Kopp, R. E., J. L. Kirschvink, I. A. Hilburn, and C. Z. Nash. 2005. The Paleoproterozoic snowball Earth: a climate disaster triggered by the evolution of oxygenic photosynthesis. *Proc. Natl. Acad. Sci. U.S.A.* **102**: 11131–11136. doi:10.1073/pnas.0504878102
- Kratina, P., H. S. Greig, P. L. Thompson, T. S. A. Carvalho-Pereira, and J. B. Shurin. 2012. Warming modifies trophic cascades and eutrophication in experimental freshwater communities. *Ecology* **93**: 1421–1430. doi:10.1890/11-1595.1
- Krause, G. H., and P. Jahns. 2004. Non-photochemical Energy Dissipation Determined by Chlorophyll Fluorescence Quenching: Characterization and Function, p. 463–495. *In* G.C. Papageorgiou and Govindjee [eds.], *Chlorophyll a Fluorescence: A Signature of Photosynthesis*. Springer Netherlands.
- Krebs, C. J. 2001. *Ecology: The Experimental Analysis of Distribution and Abundance: Hands-On Field Package*, 5 edition. Benjamin Cummings.
- Kühn, S. F., G. Drebes, and E. Schnepf. 1996. Five new species of the nanoflagellate *Pirsonia* in the German Bight, North Sea, feeding on planktic diatoms. *Helgolander Meeresunters* **50**: 205–222. doi:10.1007/BF02367152

-L-

- Lambert, S., M. Tragin, J.-C. Lozano, J.-F. Ghiglione, D. Vaultot, F.-Y. Bouget, and P. E. Galand. 2018. Rhythmicity of coastal marine picoeukaryotes, bacteria and archaea despite irregular environmental perturbations. *ISME J.* doi:10.1038/s41396-018-0281-z
- Larsen, P. E., D. Field, and J. A. Gilbert. 2012. Predicting bacterial community assemblages using an artificial neural network approach. *Nat Methods* **9**: 621–625. doi:10.1038/nmeth.1975
- Lasram, F. B. R., F. Guilhaumon, C. Albouy, S. Somot, W. Thuiller, and D. Mouillot. 2010. The Mediterranean Sea as a ‘cul-de-sac’ for endemic fishes facing climate change. *Global Change Biology* **16**: 3233–3245. doi:10.1111/j.1365-2486.2010.02224.x
- Le Gall, S., M. Bel Hassen, and P. Le Gall. 1997. Ingestion of a bacterivorous ciliate by the oyster *Crassostrea gigas*: protozoa as a trophic link between picoplankton and benthic suspension-feeders. *Marine Ecology Progress Series* **152**: 301–306.
- Lebaron, P., P. Servais, H. Agogue, C. Courties, and F. Joux. 2001. Does the high nucleic acid content of individual bacterial cells allow us to discriminate between active cells and inactive cells in aquatic systems? *Appl. Environ. Microbiol.* **67**: 1775–1782. doi:10.1128/AEM.67.4.1775-1782.2001
- Legendre, L., and F. Rassoulzadegan. 1995. Plankton and nutrient dynamics in marine waters. *Ophelia* **41**: 153–172. doi:10.1080/00785236.1995.10422042
- Legrand, C., E. Granéli, and P. Carlsson. 1998. Induced phagotrophy in the photosynthetic dinoflagellate *Heterocapsa triquetra*. *Aquatic Microbial Ecology* **15**: 65–75. doi:10.3354/ame015065
- Legrand, C., K. Rengefors, G. O. Fistarol, and E. Granéli. 2003. Allelopathy in phytoplankton - biochemical, ecological and evolutionary aspects. *Phycologia* **42**: 406–419. doi:10.2216/i0031-8884-42-4-406.1
- Lemos, M. L., C. P. Dopazo, A. E. Toranzo, and J. L. Barja. 1991. Competitive dominance of antibiotic-producing marine bacteria in mixed cultures. *Journal of Applied Bacteriology* **71**: 228–232. doi:10.1111/j.1365-2672.1991.tb04452.x
- Lewandowska, A. M., D. G. Boyce, M. Hofmann, B. Matthiessen, U. Sommer, and B. Worm. 2014. Effects of sea surface warming on marine plankton. *Ecology Letters* **17**: 614–623. doi:10.1111/ele.12265

- Lewandowska, A. M., P. Breithaupt, H. Hillebrand, H.-G. Hoppe, K. Jürgens, and U. Sommer. 2012. Responses of primary productivity to increased temperature and phytoplankton diversity. *Journal of Sea Research* **72**: 87–93. doi:10.1016/j.seares.2011.10.003
- Lidicker, W. Z. 1979. A Clarification of Interactions in Ecological Systems. *BioScience* **29**: 475–477. doi:10.2307/1307540
- Lignell, R., A.-S. Heiskanen, H. Kuosa, K. Gundersen, P. Kuuppo-Leinikki, R. Pajuniemi, and A. Uitto. 1993. Fate of a phytoplankton spring bloom: sedimentation and carbon flow in the planktonic food web in the northern Baltic. *Marine Ecology Progress Series* **94**: 239–252.
- Litchman, E., and C. A. Klausmeier. 2008. Trait-Based Community Ecology of Phytoplankton. *Annual Review of Ecology, Evolution, and Systematics* **39**: 615–639. doi:10.1146/annurev.ecolsys.39.110707.173549
- Liu, X., X. Lu, and Y. Chen. 2011. The effects of temperature and nutrient ratios on *Microcystis* blooms in Lake Taihu, China: An 11-year investigation. *Harmful Algae* **10**: 337–343. doi:10.1016/j.hal.2010.12.002
- Lomas, M. W., and P. M. Glibert. 2000. Comparisons of Nitrate Uptake, Storage, and Reduction in Marine Diatoms and Flagellates. *Journal of Phycology* **36**: 903–913. doi:10.1046/j.1529-8817.2000.99029.x
- López-Urrutia, Á., E. S. Martin, R. P. Harris, and X. Irigoien. 2006. Scaling the metabolic balance of the oceans. *PNAS* **103**: 8739–8744. doi:10.1073/pnas.0601137103
- López-Urrutia, Á., and X. A. G. Morán. 2007. Resource Limitation of Bacterial Production Distorts the Temperature Dependence of Oceanic Carbon Cycling. *Ecology* **88**: 817–822. doi:10.1890/06-1641

-M-

- Mackas, D. L., W. T. Peterson, M. D. Ohman, and B. E. Lavaniegos. 2006. Zooplankton anomalies in the California Current system before and during the warm ocean conditions of 2005. *Geophysical Research Letters* **33**. doi:10.1029/2006GL027930
- Madhupratap, M., S. P. Kumar, P. M. A. Bhattathiri, M. D. Kumar, S. Raghukumar, K. K. C. Nair, and N. Ramaiah. 1996. Mechanism of the biological response to winter cooling in the northeastern Arabian Sea. *Nature* **384**: 549–552. doi:10.1038/384549a0

- Mahadevan, A., E. D'Asaro, C. Lee, and M. J. Perry. 2012. Eddy-Driven Stratification Initiates North Atlantic Spring Phytoplankton Blooms. *Science* **337**: 54–58. doi:10.1126/science.1218740
- Margalef, R. 1954. Modifications induced by different temperatures on the cells of *Scenedesmus obliquus* (Chlorophyceae). *Hydrobiologia* **6**: 83–91. doi:10.1007/BF00039412
- Margalef, R. 1978. Life-forms of phytoplankton as survival alternatives in an unstable environment. *Oceanologica Acta* **1**: 493–509.
- Marie, D., F. Partensky, D. Vaultot, and C. Brussaard. 2001. Enumeration of Phytoplankton, Bacteria, and Viruses in Marine Samples, *In* Current Protocols in Cytometry. John Wiley & Sons, Inc.
- Marra, J., and R. T. Barber. 2005. Primary productivity in the Arabian Sea: A synthesis of JGOFS data. *Progress in Oceanography* **65**: 159–175. doi:10.1016/j.pocean.2005.03.004
- Martens, P. 2001. Effects of the severe winter 1995/96 on the biological oceanography of the Sylt-Rømø tidal basin. *Helgol Mar Res* **55**: 166–169. doi:10.1007/s101520100078
- May, C. L., J. R. Koseff, L. V. Lucas, J. E. Cloern, and D. H. Schoellhamer. 2003. Effects of spatial and temporal variability of turbidity on phytoplankton blooms. *Marine Ecology Progress Series* **254**: 111–128. doi:10.3354/meps254111
- Mayali, X. 2018. Editorial: Metabolic Interactions Between Bacteria and Phytoplankton. *Front. Microbiol.* **9**. doi:10.3389/fmicb.2018.00727
- Menden-Deuer, S., and E. J. Lessard. 2000. Carbon to volume relationships for dinoflagellates, diatoms, and other protist plankton. *Limnol. Oceanogr.* **45**: 569–579. doi:10.4319/lo.2000.45.3.0569
- Menge, B. A., and J. P. Sutherland. 1976. Species Diversity Gradients: Synthesis of the Roles of Predation, Competition, and Temporal Heterogeneity. *The American Naturalist* **110**: 351–369. doi:10.1086/283073
- Mertens, N. L., B. D. Russell, and S. D. Connell. 2015. Escaping herbivory: ocean warming as a refuge for primary producers where consumer metabolism and consumption cannot pursue. *Oecologia* **179**: 1223–1229. doi:10.1007/s00442-015-3438-8
- Mignot, A., R. Ferrari, and K. A. Mork. 2016. Spring bloom onset in the Nordic Seas. Copernicus Publications.
- Millet, B., and P. Cecchi. 1992. Wind-induced hydrodynamic control of the phytoplankton biomass in a lagoon ecosystem. *Limnol. Oceanogr.* **37**: 140–146. doi:10.4319/lo.1992.37.1.0140

- Mironova, E. I., I. V. Telesh, and S. O. Skarlato. 2009. Planktonic ciliates of the Baltic Sea (a review). *Inland Water Biol* **2**: 13–24. doi:10.1134/S1995082909010039
- Mitra, A., K. J. Flynn, J. M. Burkholder, and others. 2014. The role of mixotrophic protists in the biological carbon pump. *Biogeosciences* **11**: 995–1005. doi:10.5194/bg-11-995-2014
- Mitra, A., K. J. Flynn, J. M. Burkholder, J. M. Berge, T.; Calbet, A.; Raven, J.A.; Granéli, E.; Glibert, P.M.; Hansen, P.J.; Stoecker, D.K.; Thingstad, F.; Tillmann, U.; Våge, S.; Wilken, S.; Zubkov, M.V.. 2014 The role of mixotrophic protists in the biological carbon pump. *Biogeosciences*, 11 (4). 995-1005. <https://doi.org/10.5194/bg-11-995-2014> <<https://doi.org/10.5194/bg-11-995-2014>>
- Mitra, A., K. J. Flynn, U. Tillmann, and others. 2016. Defining Planktonic Protist Functional Groups on Mechanisms for Energy and Nutrient Acquisition: Incorporation of Diverse Mixotrophic Strategies. *Protist* **167**: 106–120. doi:10.1016/j.protis.2016.01.003
- Moal, J., V. Martin-Jezequel, R. Harris, J.-F. Samain, and S. Poulet. 1987. Interspecific and intraspecific variability of the chemical-composition of marine-phytoplankton. *Oceanologica Acta* **10**: 339–346.
- Mojica, K. D. A., J. Huisman, S. W. Wilhelm, and C. P. D. Brussaard. 2016. Latitudinal variation in virus-induced mortality of phytoplankton across the North Atlantic Ocean. *The ISME Journal* **10**: 500–513. doi:10.1038/ismej.2015.130
- Morán, X. A. G., Á. López-Urrutia, A. Calvo-Díaz, and W. K. W. Li. 2010. Increasing importance of small phytoplankton in a warmer ocean. *Global Change Biology* **16**: 1137–1144. doi:10.1111/j.1365-2486.2009.01960.x
- Moreau, S., B. Mostajir, S. Bélanger, I. R. Schloss, M. Vancoppenolle, S. Demers, and G. A. Ferreyra. 2015. Climate change enhances primary production in the western Antarctic Peninsula. *Global Change Biology* **21**: 2191–2205. doi:10.1111/gcb.12878
- Morin, P. J. 2009. *Community Ecology*, John Wiley & Sons.
- Morris, B., R. Henneberger, H. Huber, and C. Moissl-Eichinger. 2013. Microbial syntrophy: interaction for the common good. *FEMS microbiology reviews* **37**: 384–406. doi:10.1111/1574-6976.12019
- Mostajir, B., C. Amblard, E. Buffan-Dubau, R. D. Wit, R. Lensi, and T. Sime-Ngando. 2015. Microbial Food Webs in Aquatic and Terrestrial Ecosystems, p. 485–509. *In Environmental Microbiology: Fundamentals and Applications*. Springer, Dordrecht.

Mostajir, B., S. Mas, D. Parin, and F. Vidussi. 2018a. High-Frequency physical, biogeochemical and meteorological data of Coastal Mediterranean Thau Lagoon Observatory. SEANOE. doi:10.17882/58280

Mostajir, B., S. Mas, D. Parin, and F. Vidussi. 2018b. High-Frequency physical, biogeochemical and meteorological data of Coastal Mediterranean Thau Lagoon Observatory. SEANOE

Moustaka-Gouni, M., K. A. Kormas, M. Scotti, E. Vardaka, and U. Sommer. 2016. Warming and Acidification Effects on Planktonic Heterotrophic Pico- and Nanoflagellates in a Mesocosm Experiment. *Protist* **167**: 389–410. doi:10.1016/j.protis.2016.06.004

-N-

Nagasaki, K., and M. Yamaguchi. 1998. Effect of temperature on the algicidal activity and the stability of HaV (Heterosigma akashiwo virus). *Aquatic Microbial Ecology* **15**: 211–216. doi:10.3354/ame015211

Needham, D. M., and J. A. Fuhrman. 2016. Pronounced daily succession of phytoplankton, archaea and bacteria following a spring bloom. *Nature Microbiology* **1**: 16005. doi:10.1038/nmicrobiol.2016.5

Nixon, S. W. 1981. Remineralization and Nutrient Cycling in Coastal Marine Ecosystems, p. 111–138. *In* B.J. Neilson and L.E. Cronin [eds.], *Estuaries and Nutrients*. Humana Press.

Nouguier, J., B. Mostajir, E. L. Floc'h, and F. Vidussi. 2007. An automatically operated system for simulating global change temperature and ultraviolet B radiation increases: application to the study of aquatic ecosystem responses in mesocosm experiments. *Limnology and Oceanography: Methods* **5**: 269–279. doi:10.4319/lom.2007.5.269

Novarino, G. 2005. Nanoplankton protists from the western Mediterranean Sea. II. Cryptomonads (Cryptophyceae = Crptomonadea). *Scientia Marina* **69**: 47–74. doi:10.3989/scimar.2005.69n147

-P-

Paerl, H. W., and R. S. Fulton. 2006. Ecology of Harmful Cyanobacteria, p. 95–109. *In* *Ecology of Harmful Algae*. Springer, Berlin, Heidelberg.

Paerl, R. W., F.-Y. Bouget, J.-C. Lozano, V. Vergé, P. Schatt, E. E. Allen, B. Palenik, and F. Azam. 2017. Use of plankton-derived vitamin B1 precursors, especially thiazole-related precursor, by

- key marine picoeukaryotic phytoplankton. *The ISME Journal* **11**: 753. doi:10.1038/ismej.2016.145
- Pajk, F., E. von Elert, and P. Fink. 2012. Interaction of changes in food quality and temperature reveals maternal effects on fitness parameters of a keystone aquatic herbivore. *Limnology and Oceanography* **57**: 281–292. doi:10.4319/lo.2012.57.1.0281
- Pansch, C., M. Scotti, F. R. Barboza, and others. 2018. Heat waves and their significance for a temperate benthic community: A near-natural experimental approach. *Global Change Biology* **24**: 4357–4367. doi:10.1111/gcb.14282
- Paphitis, D., and M. B. Collins. 2005. Sediment resuspension events within the (microtidal) coastal waters of Thermaikos Gulf, northern Greece. *Continental Shelf Research* **25**: 2350–2365. doi:10.1016/j.csr.2005.08.028
- Park, M. G., W. Yih, and D. W. Coats. 2004. Parasites and Phytoplankton, with Special Emphasis on Dinoflagellate Infections I. *Journal of Eukaryotic Microbiology* **51**: 145–155. doi:10.1111/j.1550-7408.2004.tb00539.x
- Pauly, D., and V. Christensen. 1995. Primary production required to sustain global fisheries. *Nature* **374**: 255–257. doi:10.1038/374255a0
- Pecqueur, D., F. Vidussi, E. Fouilland, and others. 2011. Dynamics of microbial planktonic food web components during a river flash flood in a Mediterranean coastal lagoon. *Hydrobiologia* **673**: 13–27. doi:10.1007/s10750-011-0745-x
- Peierls, B. L., N. S. Hall, and H. W. Paerl. 2012. Non-monotonic Responses of Phytoplankton Biomass Accumulation to Hydrologic Variability: A Comparison of Two Coastal Plain North Carolina Estuaries. *Estuaries and Coasts* **35**: 1376–1392. doi:10.1007/s12237-012-9547-2
- Pernet, F., J. Barret, P. Le Gall, C. Corporeau, L. Degremont, F. Lagarde, J.-F. Pepin, and N. Keck. 2012a. Mass mortalities of Pacific oysters *Crassostrea gigas* reflect infectious diseases and vary with farming practices in the Mediterranean Thau lagoon, France. *Aquaculture Environment Interactions* **2**: 215–237. doi:10.3354/aei00041
- Pernet, F., N. Malet, A. Pastoureaud, A. Vaquer, C. Quéré, and L. Dubroca. 2012b. Marine diatoms sustain growth of bivalves in a Mediterranean lagoon. *Journal of Sea Research* **68**: 20–32. doi:10.1016/j.seares.2011.11.004
- Peter, K. H., and U. Sommer. 2012. Phytoplankton Cell Size: Intra- and Interspecific Effects of Warming and Grazing. *PLOS ONE* **7**: e49632. doi:10.1371/journal.pone.0049632

- Platt, T., C. Caverhill, and S. Sathyendranath. 1991. Basin-scale estimates of oceanic primary production by remote sensing: The North Atlantic. *J. Geophys. Res.* **96**: 15147–15159. doi:10.1029/91JC01118
- Platt, T., C. Fuentes-Yaco, and K. T. Frank. 2003. Marine ecology: Spring algal bloom and larval fish survival. *Nature* **423**: 398–399. doi:10.1038/423398b
- Polovina, J. J., E. A. Howell, and M. Abecassis. 2008. Ocean's least productive waters are expanding. *Geophysical Research Letters* **35**. doi:10.1029/2007GL031745
- Pomeroy, L. R. 1974. The Ocean's Food Web, A Changing Paradigm. *BioScience* **24**: 499–504. doi:10.2307/1296885
- Pomeroy, L. R., and W. J. Wiebe. 1988. Energetics of microbial food webs. *Hydrobiologia* **159**: 7–18. doi:10.1007/BF00007363
- Posch, T., B. Eugster, F. Pomati, J. Pernthaler, G. Pitsch, and E. M. Eckert. 2015. Network of Interactions Between Ciliates and Phytoplankton During Spring. *Front. Microbiol.* **6**. doi:10.3389/fmicb.2015.01289
- Proctor, L. M., and J. A. Fuhrman. 1990. Viral mortality of marine bacteria and cyanobacteria. *Nature* **343**: 60–62. doi:10.1038/343060a0
- Pyper, B. J., and R. M. Peterman. 1998. Comparison of methods to account for autocorrelation in correlation analyses of fish data. *Can. J. Fish. Aquat. Sci.* **55**: 2127–2140. doi:10.1139/f98-104
- R-**
- Rabalais, N. N., R. E. Turner, R. J. Díaz, and D. Justić. 2009. Global change and eutrophication of coastal waters. *ICES J Mar Sci* **66**: 1528–1537. doi:10.1093/icesjms/fsp047
- Raitsos, D. E., G. Beaugrand, D. Georgopoulos, A. Zenetos, A. M. Pancucci-Papadopoulou, A. Theocharis, and E. Papathanassiou. 2010. Global climate change amplifies the entry of tropical species into the eastern Mediterranean Sea. *Limnology and Oceanography* **55**: 1478–1484. doi:10.4319/lo.2010.55.4.1478
- Rasconi, S., A. Gall, K. Winter, and M. J. Kainz. 2015. Increasing Water Temperature Triggers Dominance of Small Freshwater Plankton. *PLOS ONE* **10**: e0140449. doi:10.1371/journal.pone.0140449
- Rasmussen, B., I. R. Fletcher, J. J. Brocks, and M. R. Kilburn. 2008. Reassessing the first appearance of eukaryotes and cyanobacteria. *Nature* **455**: 1101–1104. doi:10.1038/nature07381

- Rassoulzadegan, F., and R. W. Sheldon. 1986. Predator-prey interactions of nanozooplankton and bacteria in an oligotrophic marine environment. *Limnology and Oceanography* **31**: 1010–1029. doi:10.4319/lo.1986.31.5.1010
- Raven, J. A. 1998. The twelfth Tansley Lecture. Small is beautiful: the picophytoplankton. *Functional Ecology* **12**: 503–513. doi:10.1046/j.1365-2435.1998.00233.x
- Raven, J. A., and P. G. Falkowski. 1999. Oceanic sinks for atmospheric CO₂. *Plant, Cell & Environment* **22**: 741–755. doi:10.1046/j.1365-3040.1999.00419.x
- Reckermann, M., and M. J. W. Veldhuis. 1997. Trophic interactions between picophytoplankton and micro- and nanozooplankton in the western Arabian Sea during the NE monsoon 1993. *Aquatic Microbial Ecology* **12**: 263–273. doi:10.3354/ame012263
- Recknagel, F. 2001. Applications of machine learning to ecological modelling. *Ecological Modelling* **146**: 303–310. doi:10.1016/S0304-3800(01)00316-7
- Rice, E. L. 2012. *Allelopathy*, Academic Press.
- Rivkin, R. B., and L. Legendre. 2001. Biogenic Carbon Cycling in the Upper Ocean: Effects of Microbial Respiration. *Science* **291**: 2398–2400. doi:10.1126/science.291.5512.2398
- Roberts, E. C., and J. Laybourn-Parry. 1999. Mixotrophic cryptophytes and their predators in the Dry Valley lakes of Antarctica. *Freshwater Biology* **41**: 737–746. doi:10.1046/j.1365-2427.1999.00401.x
- Roesler, C., J. Uitz, H. Claustre, and others. 2017. Recommendations for obtaining unbiased chlorophyll estimates from in situ chlorophyll fluorometers: A global analysis of WET Labs ECO sensors. *Limnology and Oceanography: Methods* **15**: 572–585. doi:10.1002/lom3.10185
- Rooney-Varga, J. N., M. W. Giewat, M. C. Savin, S. Sood, M. LeGresley, and J. L. Martin. 2005. Links between Phytoplankton and Bacterial Community Dynamics in a Coastal Marine Environment. *Microb Ecol* **49**: 163–175. doi:10.1007/s00248-003-1057-0
- Rose, J. M., and D. A. Caron. 2007. Does low temperature constrain the growth rates of heterotrophic protists? Evidence and implications for algal blooms in cold waters. *Limnology and Oceanography* **52**: 886–895. doi:10.4319/lo.2007.52.2.0886
- Rose, J. M., Y. Feng, C. J. Gobler, R. Gutierrez, C. E. Hare, K. Leblanc, and D. A. Hutchins. 2009. Effects of increased pCO₂ and temperature on the North Atlantic spring bloom. II. Microzooplankton abundance and grazing. *Marine Ecology Progress Series* **388**: 27–40. doi:10.3354/meps08134

Rousseeuw, K. 2014. Modélisation de signaux temporels hautes fréquences multicateurs à valeurs manquantes : Application à la prédiction des efflorescences phytoplanctoniques dans les rivières et les écosystèmes marins côtiers. PhD Thesis. Université du Littoral Côte d'Opale.

-S-

Sakshaug, E., and Y. Olsen. 1986. Nutrient Status of Phytoplankton Blooms in Norwegian Waters and Algal Strategies for Nutrient Competition. *Can. J. Fish. Aquat. Sci.* **43**: 389–396. doi:10.1139/f86-049

Sarmiento, H., J. M. Montoya, E. Vázquez-Domínguez, D. Vaqué, and J. M. Gasol. 2010. Warming effects on marine microbial food web processes: how far can we go when it comes to predictions? *Philosophical Transactions of the Royal Society B: Biological Sciences* **365**: 2137–2149. doi:10.1098/rstb.2010.0045

Sarmiento, J. L., T. M. C. Hughes, R. J. Stouffer, and S. Manabe. 1998. Simulated response of the ocean carbon cycle to anthropogenic climate warming. *Nature* **393**: 245–249. doi:10.1038/30455

Scheffer, M., S. Rinaldi, J. Huisman, and F. J. Weissing. 2003. Why plankton communities have no equilibrium: solutions to the paradox. *Hydrobiologia* **491**: 9–18. doi:10.1023/A:1024404804748

Schnepf, E., G. Drebes, and M. Elbrächter. 1990. *Pirsonia guinardiae*, gen. et spec. nov.: A parasitic flagellate on the marine diatom *Guinardia flaccida* with an unusual mode of food uptake. *Helgolander Meeresunters* **44**: 275–293. doi:10.1007/BF02365468

Seymour, J. R., S. A. Amin, J.-B. Raina, and R. Stocker. 2017. Zooming in on the phycosphere: the ecological interface for phytoplankton–bacteria relationships. *Nature Microbiology* **2**: 17065. doi:10.1038/nmicrobiol.2017.65

Sherr, B. F., E. B. Sherr, and C. S. Hopkinson. 1988. Trophic interactions within pelagic microbial communities: Indications of feedback regulation of carbon flow. *Hydrobiologia* **159**: 19–26. doi:10.1007/BF00007364

Sherr, E. B., and B. F. Sherr. 1994. Bacterivory and herbivory: Key roles of phagotrophic protists in pelagic food webs. *Microb Ecol* **28**: 223–235. doi:10.1007/BF00166812

Sherr, E. B., and B. F. Sherr. 2002. Significance of predation by protists in aquatic microbial food webs. *Antonie Van Leeuwenhoek* **81**: 293–308. doi:10.1023/A:1020591307260

- Sherr, E., and B. Sherr. 1988. Role of microbes in pelagic food webs: A revised concept. *Limnology and Oceanography* **33**: 1225–1227. doi:10.4319/lo.1988.33.5.1225
- Shurin, J. B., J. L. Clasen, H. S. Greig, P. Kratina, and P. L. Thompson. 2012. Warming shifts top-down and bottom-up control of pond food web structure and function. *Philos. Trans. R. Soc. Lond., B, Biol. Sci.* **367**: 3008–3017. doi:10.1098/rstb.2012.0243
- Sieburth, J. M., V. Smetacek, and J. Lenz. 1978. Pelagic ecosystem structure: Heterotrophic compartments of the plankton and their relationship to plankton size fractions 1. *Limnology and Oceanography* **23**: 1256–1263. doi:10.4319/lo.1978.23.6.1256
- Simek, K., P. Hartman, J. Nedoma, J. Pernthaler, D. Springmann, J. Vrba, and R. Psenner. 1997. Community structure, picoplankton grazing and zooplankton control of heterotrophic nanoflagellates in a eutrophic reservoir during the summer phytoplankton maximum. *SCSIO OpenIR* **12**.
- Skovgaard, A. 2014. Dirty Tricks in the Plankton: Diversity and Role of Marine Parasitic Protists. *Acta Protozoologica* **2014**: 51–62. doi:10.4467/16890027AP.14.006.1443
- Skovgaard, A., and E. Saiz. 2006. Seasonal occurrence and role of protistan parasites in coastal marine zooplankton. *Marine Ecology Progress Series* **327**: 37–49. doi:10.3354/meps327037
- Snyder, R. A., and M. P. Hoch. 1996. Consequences of protist-stimulated bacterial production for estimating protist growth efficiencies. *Hydrobiologia* **341**: 113–123. doi:10.1007/BF00018115
- Solomon, S., D. Qin, M. Manning, M. Marquis, K. Averyt, M. M. B. Tignor, H. L. Miller Jr., and Z. Chen. 2007. *Climate Change 2007 - The Physical Science Basis: Working Group I Contribution to the Fourth Assessment Report of the IPCC*, Cambridge University Press.
- Sommer, U. 2002. Competition and Coexistence in Plankton Communities, p. 79–108. *In* U. Sommer and B. Worm [eds.], *Competition and Coexistence*. Springer Berlin Heidelberg.
- Sommer, U. 2012. *Plankton Ecology: Succession in Plankton Communities*, Springer Science & Business Media.
- Sommer, U., and K. Lengfellner. 2008a. Climate change and the timing, magnitude, and composition of the phytoplankton spring bloom. *Global Change Biology* **14**: 1199–1208. doi:10.1111/j.1365-2486.2008.01571.x
- Sommer, U., and K. Lengfellner. 2008b. Climate change and the timing, magnitude, and composition of the phytoplankton spring bloom. *Global Change Biology* **14**: 1199–1208. doi:10.1111/j.1365-2486.2008.01571.x

- Sommer, U., and A. Lewandowska. 2011. Climate change and the phytoplankton spring bloom: warming and overwintering zooplankton have similar effects on phytoplankton. *Global Change Biology* **17**: 154–162. doi:10.1111/j.1365-2486.2010.02182.x
- Sommer, U., K. H. Peter, S. Genitsaris, and M. Moustaka-Gouni. 2017. Do marine phytoplankton follow Bergmann's rule sensu lato? *Biol Rev* **92**: 1011–1026. doi:10.1111/brv.12266
- Sommer, U., and F. Sommer. 2006. Cladocerans versus copepods: the cause of contrasting top-down controls on freshwater and marine phytoplankton. *Oecologia* **147**: 183–194. doi:10.1007/s00442-005-0320-0
- Sommer, U., H. Stibor, A. Katschik, F. Sommer, and T. Hansen. 2002. Pelagic food web configurations at different levels of nutrient richness and their implications for the ratio fish production:primary production, p. 11–20. *In Sustainable Increase of Marine Harvesting: Fundamental Mechanisms and New Concepts*. Springer, Dordrecht.
- Souchu, P., B. Bec, V. H. Smith, and others. 2010. Patterns in nutrient limitation and chlorophyll a along an anthropogenic eutrophication gradient in French Mediterranean coastal lagoons. *Can. J. Fish. Aquat. Sci.* **67**: 743–753. doi:10.1139/F10-018
- Souchu, P., A. Vaquer a, Y. Collos, S. Landrein, J.-M. Deslous-Paoli, and B. Bibent. 2001. Influence of shellfish farming activities on the biogeochemical composition of the water column in Thau lagoon. *Marine Ecology Progress Series* **218**: 141–152.
- Sourisseau, M., V. Le Guennec, G. Le Gland, M. Plus, and A. Chapelle. 2017. Resource Competition Affects Plankton Community Structure; Evidence from Trait-Based Modeling. *Front. Mar. Sci.* **4**. doi:10.3389/fmars.2017.00052
- Sournia, A., M. Ricard, and M.-J. Chrétiennot-Dinet, eds. 1986. *Atlas du phytoplancton marin*, Editions du Centre national de la recherche scientifique : Diffusion, Presses du CNRS.
- Spero, H. J., and D. L. Angel. 1991. Planktonic Sarcodines: Microhabitat for Oceanic Dinoflagellates. *Journal of Phycology* **27**: 187–195. doi:10.1111/j.0022-3646.1991.00187.x
- Stearns, S. C. 1976. Life-History Tactics: A Review of the Ideas. *The Quarterly Review of Biology* **51**: 3–47. doi:10.1086/409052
- Steele, J. A., P. D. Countway, L. Xia, and others. 2011. Marine bacterial, archaeal and protistan association networks reveal ecological linkages. *ISME J* **5**: 1414–1425. doi:10.1038/ismej.2011.24

- Sterner, R. W., and K. L. Schulz. 1998. Zooplankton nutrition: recent progress and a reality check. *Aquatic Ecology* **32**: 261–279. doi:10.1023/A:1009949400573
- Stoecker, D. K. 1999. Mixotrophy among Dinoflagellates1. *Journal of Eukaryotic Microbiology* **46**: 397–401. doi:10.1111/j.1550-7408.1999.tb04619.x
- Straile, D., and R. Adrian. 2000. The North Atlantic Oscillation and plankton dynamics in two European lakes — two variations on a general theme. *Global Change Biology* **6**: 663–670. doi:10.1046/j.1365-2486.2000.00350.x
- Šupraha, L., S. Bosak, Z. Ljubešić, H. Mihanović, G. Olujić, I. Mikac, and D. Viličić. 2014. Cryptophyte bloom in a Mediterranean estuary: High abundance of *Plagioselmis* cf. *prolonga* in the Krka River estuary (eastern Adriatic Sea). *Scientia Marina* **78**: 329–338.
- Suttle, C. A. 1994. The significance of viruses to mortality in aquatic microbial communities. *Microb Ecol* **28**: 237–243. doi:10.1007/BF00166813
- Suttle, C. A. 2005. Viruses in the sea. *Nature* **437**: 356–361. doi:10.1038/nature04160
- Sverdrup, H. U. 1953. On Conditions for the Vernal Blooming of Phytoplankton. *ICES J Mar Sci* **18**: 287–295. doi:10.1093/icesjms/18.3.287

-T-

- Takahashi, M., S. Shimura, Y. Yamaguchi, and Y. Fujita. 1971. Photo-inhibition of phytoplankton photosynthesis as a function of exposure time. *Journal of the Oceanographical Society of Japan* **27**: 43–50. doi:10.1007/BF02109329
- Tan, S., J. Zhou, X. Zhu, S. Yu, W. Zhan, B. Wang, and Z. Cai. 2015. An association network analysis among microeukaryotes and bacterioplankton reveals algal bloom dynamics. *Journal of Phycology* **51**: 120–132. doi:10.1111/jpy.12259
- Taylor, J. R., and R. Ferrari. 2011. Shutdown of turbulent convection as a new criterion for the onset of spring phytoplankton blooms. *Limnol. Oceanogr.* **56**: 2293–2307. doi:10.4319/lo.2011.56.6.2293
- Théodoridès, J. 1989. Parasitology of Marine Zooplankton, p. 117–177. *In* J.H.S. Blaxter and A.J. Southward [eds.], *Advances in Marine Biology*. Academic Press.
- Thomas, M. K., C. T. Kremer, C. A. Klausmeier, and E. Litchman. 2012. A Global Pattern of Thermal Adaptation in Marine Phytoplankton. *Science* **338**: 1085–1088. doi:10.1126/science.1224836

- Thompson, J., R. Johansen, J. Dunbar, and B. Munsky. 2019. Machine learning to predict microbial community functions: An analysis of dissolved organic carbon from litter decomposition. *PLOS ONE* **14**: e0215502. doi:10.1371/journal.pone.0215502
- Tian, T., A. Merico, J. Su, J. Staneva, K. Wiltshire, and K. Wirtz. 2009. Importance of resuspended sediment dynamics for the phytoplankton spring bloom in a coastal marine ecosystem. *Journal of Sea Research* **62**: 214–228. doi:10.1016/j.seares.2009.04.001
- Tian, T., J. Su, G. Flöser, K. Wiltshire, and K. Wirtz. 2011. Factors controlling the onset of spring blooms in the German Bight 2002–2005: Light, wind and stratification. *Continental Shelf Research* **31**: 1140–1148. doi:10.1016/j.csr.2011.04.008
- Tillmann, U. 2004. Interactions between Planktonic Microalgae and Protozoan Grazers. *Journal of Eukaryotic Microbiology* **51**: 156–168. doi:10.1111/j.1550-7408.2004.tb00540.x
- Tillmann, U., K.-J. Hesse, and A. Tillmann. 1999. Large-scale parasitic infection of diatoms in the Northfrisian Wadden Sea. *Journal of Sea Research* **42**: 255–261. doi:10.1016/S1385-1101(99)00029-5
- Tilman, D. (1982). *Resource competition and community structure*. Princeton university press.
- Tomas, C. R. 1997. *Identifying Marine Phytoplankton*, Elsevier.
- Tophøj, J., R. D. Wollenberg, T. E. Sondergaard, and N. T. Eriksen. 2018. Feeding and growth of the marine heterotrophic nanoflagellates, *Procrystobia sorokini* and *Paraphysomonas imperforata* on a bacterium, *Pseudoalteromonas* sp. with an inducible defence against grazing. *PLOS ONE* **13**: e0195935. doi:10.1371/journal.pone.0195935
- Tortajada, S., N. Niquil, H. Blanchet, and others. 2012. Network analysis of the planktonic food web during the spring bloom in a semi enclosed lagoon (Arcachon, SW France). *Acta Oecologica* **40**: 40–50. doi:10.1016/j.actao.2012.02.002
- Townsend, D. W., L. M. Cammen, P. M. Holligan, D. E. Campbell, and N. R. Pettigrew. 1994. Causes and consequences of variability in the timing of spring phytoplankton blooms. *Deep Sea Research Part I: Oceanographic Research Papers* **41**: 747–765. doi:10.1016/0967-0637(94)90075-2
- Townsend, D. W., M. D. Keller, M. E. Sieracki, and S. G. Ackleson. 1992. Spring phytoplankton blooms in the absence of vertical water column stratification. *Nature* **360**: 59–62. doi:10.1038/360059a0
- Tréguer, P., C. Bowler, B. Moriceau, and others. 2018. Influence of diatom diversity on the ocean biological carbon pump. *Nature Geosci* **11**: 27–37. doi:10.1038/s41561-017-0028-x

Tréguer, P., and P. Le Corre. 1974. Manuel d'analyse des sels nutritifs dans l'eau de mer (utilisation de l'autoanalyzer II Technicon R), UBO.

Tréguer, P., and P. Le Corre. 1975. Manuel d'analyse des sels nutritifs dans l'eau de mer (utilisation de l'autoanalyzer II Technicon R), UBO.

Trombetta, T., F. Vidussi, S. Mas, D. Parin, M. Simier, and B. Mostajir. 2019. Water temperature drives phytoplankton blooms in coastal waters. *PLOS ONE* **14**: e0214933. doi:10.1371/journal.pone.0214933

Tseng, C.-M., G. T. F. Wong, I.-I. Lin, C.-R. Wu, and K.-K. Liu. 2005. A unique seasonal pattern in phytoplankton biomass in low-latitude waters in the South China Sea. *Geophysical Research Letters* **32**. doi:10.1029/2004GL022111

-V-

Vadstein, O. 2000. Heterotrophic, Planktonic Bacteria and Cycling of Phosphorus, p. 115–167. *In* B. Schink [ed.], *Advances in Microbial Ecology*. Springer US.

Vahtera, E., D. J. Conley, B. G. Gustafsson, and others. 2007. Internal ecosystem feedbacks enhance nitrogen-fixing cyanobacteria blooms and complicate management in the Baltic Sea. *Ambio* **36**: 186–194.

Vaquer, A., M. Troussellier, C. Courties, and B. Bibent. 1996. Standing stock and dynamics of picophytoplankton in the Thau Lagoon (northwest Mediterranean coast). *Limnol. Oceanogr.* **41**: 1821–1828. doi:10.4319/lo.1996.41.8.1821

Vázquez-Domínguez, E., D. Vaqué, and J. M. Gasol. 2007. Ocean warming enhances respiration and carbon demand of coastal microbial plankton. *Global Change Biology* **13**: 1327–1334. doi:10.1111/j.1365-2486.2007.01377.x

Verity, P. G., and T. A. Villareal. 1986. The Relative Food Value of Diatoms, Dinoflagellates, Flagellates, and Cyanobacteria for Tintinnid Ciliates. *Archiv für Protistenkunde* **131**: 71–84. doi:10.1016/S0003-9365(86)80064-1

Vernadsky, V. I. 2012. *The Biosphere*, Springer Science & Business Media.

Vidussi, F., H. Claustre, B. B. Manca, A. Luchetta, and J.-C. Marty. 2001. Phytoplankton pigment distribution in relation to upper thermocline circulation in the eastern Mediterranean Sea during winter. *Journal of Geophysical Research: Oceans* **106**: 19939–19956. doi:10.1029/1999JC000308

Vidussi, F., B. Mostajir, E. Fouilland, and others. 2011. Effects of experimental warming and increased ultraviolet B radiation on the Mediterranean plankton food web. *Limnol. Oceanogr.* **56**: 206–218. doi:10.4319/lo.2011.56.1.0206

Voigt, W., J. Perner, A. J. Davis, and others. 2003. Trophic Levels Are Differentially Sensitive to Climate. *Ecology* **84**: 2444–2453. doi:10.1890/02-0266

-W-

Walsh, J. J., G. T. Rowe, R. L. Iverson, and C. P. McRoy. 1981. Biological export of shelf carbon is a sink of the global CO₂ cycle. *Nature* **291**: 196–201. doi:10.1038/291196a0

Wang, J., H. Hong, and Y. Jiang. 2016. A coupled physical–biological modeling study of the offshore phytoplankton bloom in the Taiwan Strait in winter. *Journal of Sea Research* **107**: 12–24. doi:10.1016/j.seares.2015.11.004

Weisse, T. 2002. The significance of inter- and intraspecific variation in bacterivorous and herbivorous protists. *Antonie Van Leeuwenhoek* **81**: 327–341. doi:10.1023/A:1020547517255

Weisse, T., H. Müller, R. M. Pinto-Coelho, A. Schweizer, D. Springmann, and G. Baldringer. 1990. Response of the microbial loop to the phytoplankton spring bloom in a large prealpine lake. *Limnology and Oceanography* **35**: 781–794. doi:10.4319/lo.1990.35.4.0781

Wetzel, R. G., and G. E. Likens. 2000. Composition and Biomass of Phytoplankton, p. 147–174. *In* *Limnological Analyses*. Springer, New York, NY.

Wilhelm, S. W., and C. A. Suttle. 1999. Viruses and Nutrient Cycles in the Sea Viruses play critical roles in the structure and function of aquatic food webs. *BioScience* **49**: 781–788. doi:10.2307/1313569

Wilken, S., J. Huisman, S. Naus-Wiezer, and E. V. Donk. 2013. Mixotrophic organisms become more heterotrophic with rising temperature. *Ecology Letters* **16**: 225–233. doi:10.1111/ele.12033

Wilkerson, F. P., A. M. Lassiter, R. C. Dugdale, A. Marchi, and V. E. Hogue. 2006. The phytoplankton bloom response to wind events and upwelled nutrients during the CoOP WEST study. *Deep Sea Research Part II: Topical Studies in Oceanography* **53**: 3023–3048. doi:10.1016/j.dsr2.2006.07.007

Wohlert, J., A. Engel, E. Zöllner, P. Breithaupt, K. Jürgens, H.-G. Hoppe, U. Sommer, and U. Riebesell. 2009. Changes in biogenic carbon flow in response to sea surface warming. *PNAS* **106**: 7067–7072. doi:10.1073/pnas.0812743106

Wommack, K. E., and R. R. Colwell. 2000. Virioplankton: Viruses in Aquatic Ecosystems. *Microbiol. Mol. Biol. Rev.* **64**: 69–114. doi:10.1128/MMBR.64.1.69-114.2000

Worrest, R. C., and M. M. Caldwell. 2013. *Stratospheric Ozone Reduction, Solar Ultraviolet Radiation and Plant Life*, Springer Science & Business Media.

-X-

Xiao, W., X. Liu, A. J. Irwin, E. A. Laws, L. Wang, B. Chen, Y. Zeng, and B. Huang. 2018. Warming and eutrophication combine to restructure diatoms and dinoflagellates. *Water Research* **128**: 206–216. doi:10.1016/j.watres.2017.10.051

Xue, Y., H. Chen, J. R. Yang, M. Liu, B. Huang, and J. Yang. 2018. Distinct patterns and processes of abundant and rare eukaryotic plankton communities following a reservoir cyanobacterial bloom. *The ISME Journal* **12**: 2263. doi:10.1038/s41396-018-0159-0

-Y-

Yoo, Y. D., K. A. Seong, H. J. Jeong, W. Yih, J.-R. Rho, S. W. Nam, and H. S. Kim. 2017. Mixotrophy in the marine red-tide cryptophyte *Teleaulax amphioxieia* and ingestion and grazing impact of cryptophytes on natural populations of bacteria in Korean coastal waters. *Harmful Algae* **68**: 105–117. doi:10.1016/j.hal.2017.07.012

Yvon-Durocher Gabriel, Jones J. Iwan, Trimmer Mark, Woodward Guy, and Montoya Jose M. 2010. Warming alters the metabolic balance of ecosystems. *Philosophical Transactions of the Royal Society B: Biological Sciences* **365**: 2117–2126. doi:10.1098/rstb.2010.0038

-Z-

Zapata, M., F. Rodríguez, and J. L. Garrido. 2000. Separation of chlorophylls and carotenoids from marine phytoplankton: a new HPLC method using a reversed phase C8 column and pyridine-containing mobile phases. *Marine Ecology Progress Series* **195**: 29–45.

Zubkov, M. V., B. M. Fuchs, S. D. Archer, R. P. Kiene, R. Amann, and P. H. Burkill. 2001a. Linking the composition of bacterioplankton to rapid turnover of dissolved dimethylsulphoniopropionate in an algal bloom in the North Sea. *Environ. Microbiol.* **3**: 304–311.

Zubkov, M. V., B. M. Fuchs, P. H. Burkill, and R. Amann. 2001b. Comparison of cellular and biomass specific activities of dominant bacterioplankton groups in stratified waters of the Celtic Sea. *Appl. Environ. Microbiol.* **67**: 5210–5218. doi:10.1128/AEM.67.11.5210-5218.2001

Annexe 1 : Article du Chapitre 1 version Plos One

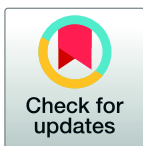
Trombetta, T., F. Vidussi, S. Mas, D. Parin, M. Simier, and B. Mostajir. 2019. Water temperature drives phytoplankton blooms in coastal waters. PLOS ONE 14: e0214933. doi:10.1371/journal.pone.0214933.

RESEARCH ARTICLE

Water temperature drives phytoplankton blooms in coastal waters

Thomas Trombetta^{1*}, Francesca Vidussi¹, Sébastien Mas², David Parin², Monique Simier³, Behzad Mostajir¹

1 MARBEC (Marine Biodiversity, Exploitation and Conservation), Centre National de la Recherche Scientifique, Université de Montpellier, Institut Français de Recherche pour l'Exploitation de la Mer, Institut de Recherche pour le Développement, Montpellier, France, **2** MEDIMEER (Mediterranean Platform for Marine Ecosystems Experimental Research), Observatoire de Recherche Méditerranéen de l'Environnement, Centre National de la Recherche Scientifique, Université de Montpellier, Institut de Recherche pour le Développement, Institut National de Recherche en Sciences et Technologies pour l'Environnement et l'Agriculture, Sète, France, **3** MARBEC (Marine Biodiversity, Exploitation and Conservation), Institut de Recherche pour le Développement, Centre National de la Recherche Scientifique, Université de Montpellier, Institut Français de Recherche pour l'Exploitation de la Mer, Sète, France

* thomas.trombetta@cnrs.fr

OPEN ACCESS

Citation: Trombetta T, Vidussi F, Mas S, Parin D, Simier M, Mostajir B (2019) Water temperature drives phytoplankton blooms in coastal waters. PLoS ONE 14(4): e0214933. <https://doi.org/10.1371/journal.pone.0214933>

Editor: Adrianna Ianora, Stazione Zoologica Anton Dohrn, ITALY

Received: August 24, 2018

Accepted: March 24, 2019

Published: April 5, 2019

Copyright: © 2019 Trombetta et al. This is an open access article distributed under the terms of the [Creative Commons Attribution License](https://creativecommons.org/licenses/by/4.0/), which permits unrestricted use, distribution, and reproduction in any medium, provided the original author and source are credited.

Data Availability Statement: All relevant data are within the manuscript and its Supporting Information files. High-frequency data are also available from SEANOE, <https://doi.org/10.17882/58280>.

Funding: This study was part of the Photo-Phyto project funded by the French National Research Agency (ANR-14-CE02-0018). The funders had no role in study design, data collection and analysis, decision to publish, or preparation of the manuscript.

Abstract

Phytoplankton blooms are an important, widespread phenomenon in open oceans, coastal waters and freshwaters, supporting food webs and essential ecosystem services. Blooms are even more important in exploited coastal waters for maintaining high resource production. However, the environmental factors driving blooms in shallow productive coastal waters are still unclear, making it difficult to assess how environmental fluctuations influence bloom phenology and productivity. To gain insights into bloom phenology, Chl *a* fluorescence and meteorological and hydrological parameters were monitored at high-frequency (15 min) and nutrient concentrations and phytoplankton abundance and diversity, were monitored weekly in a typical Mediterranean shallow coastal system (Thau Lagoon). This study was carried out from winter to late spring in two successive years with different climatic conditions: 2014/2015 was typical, but the winter of 2015/2016 was the warmest on record. Rising water temperature was the main driver of phytoplankton blooms. However, blooms were sometimes correlated with winds and sometimes correlated with salinity, suggesting nutrients were supplied by water transport via winds, saltier seawater intake, rain and water flow events. This finding indicates the joint role of these factors in determining the success of phytoplankton blooms. Furthermore, interannual variability showed that winter water temperature was higher in 2016 than in 2015, resulting in lower phytoplankton biomass accumulation in the following spring. Moreover, the phytoplankton abundances and diversity also changed: cyanobacteria (< 1 µm), picoeukaryotes (< 1 µm) and nanoeukaryotes (3–6 µm) increased to the detriment of larger phytoplankton such as diatoms. Water temperature is a key factor affecting phytoplankton bloom dynamics in shallow productive coastal waters and could become crucial with future global warming by modifying bloom phenology and changing phytoplankton community structure, in turn affecting the entire food web and ecosystem services.

Competing interests: The authors have declared that no competing interests exist.

Introduction

Ocean phytoplankton generate almost half of global primary production [1], making it one of the supporting pillars of marine ecosystems, controlling both diversity and functioning. Phytoplankton in temperate and subpolar regions are characterized by spring blooms, a seasonal phenomenon with rapid phytoplankton biomass accumulation due to a high net phytoplankton growth rate [2]. This peak biomass of primary producers in the spring supports the marine food web through carbon transfer to higher trophic levels from zooplankton to fishes. Spring phytoplankton blooms are a common phenomenon in all aquatic systems, from open oceans to coastal waters and from transient waters to inland freshwaters. The magnitude, timing and duration of blooms are as diverse as the ecosystems in which they occur.

For more than half a century, several paradigms and theories have been developed to explain the general mechanism of bloom initiation; however from the earliest critical depth hypothesis of Sverdrup in 1953 [3] they have been, and still are, subject to scientific debate. The critical depth hypothesis is a bottom-up model based on abiotic drivers and proposes that a bloom starts when there is sufficient solar radiation and the surface mixing layer becomes shallower. This change induces stratification [4–7], allowing phytoplankton to remain in the surface layer, such that their growth rates overcome their losses (i.e., mostly by zooplankton grazing). This hypothesis has been questioned several times, as observations have shown that blooms can occur in the absence of stratification. The mixing layer is defined by density, and since the critical depth hypothesis was put forth, other bottom-up mixing models have been proposed to explain bloom onset. These models are based on actively mixed layers that may occur in turbulence windows (the critical turbulence hypothesis [8]) or under deep convection shutdown (the convection shutdown hypothesis [7]), allowing the phytoplankton to remain in the surface layer long enough to benefit from favorable light conditions and start a bloom.

Recently, the disturbance recovery hypothesis of Behrenfeld et al. [9,10] formalized a new theory based on biotic drivers (top-down control) that had already been suggested several years before [11,12]. This biotic driver theory proposes that a disturbance factor, such as environmental forcing, disrupts zooplankton-phytoplankton predator-prey interactions, allowing the prey (phytoplankton) to grow rapidly, creating a bloom. Later, when the predator-prey interactions recover, the bloom ends as the losses by predation overwhelm the gains in prey biomass. This general ecological theory was proposed for the North Atlantic, where the establishment of deep-water mixing provides the ecosystem disturbance that disrupts predator-prey interactions. In other systems, different sources of disturbance can play this role, such as monsoon forcing in the Arabian Sea [13] or upwelling in coastal systems [11]. However, the role played by bottom-up and top-down drivers in phytoplankton spring blooms is still a source of debate [14,15].

Coastal waters and lakes are highly dynamic and productive ecosystems where phytoplankton blooms are common [16,17]. Coastal phytoplankton blooms are a major ecological event providing a substantial part of the annual primary production and energy transfer supporting the entire marine food web. These highly productive periods in coastal systems occur mainly in spring and autumn and are believed to be influenced by several factors such as increasing irradiance, anticyclones and nutrient inputs [18–20]. However, clear links between general theories and field observations in coastal waters have not yet been established. In particular, the factors that might disturb predator-prey relationships in these shallow systems have been neglected. Coastal waters, including estuaries, sea grass beds, coral reefs and continental shelves, cover only 6% of the world's surface but provide between 22% and 43% of the

estimated value of the world's ecosystem services [21]. In addition to hosting major biochemical and ecological processes, such as nutrient cycling and biological control, and providing habitats and refugia, coastal waters are of great economic importance for local populations because they provide food, raw materials and recreational activities [22]. Coastal waters can be strongly affected by climatic events due to their higher reactivity and lower inertia compared to open-ocean waters, making them highly sensitive to environmental forcing fluctuations [23].

Nevertheless, in open oceans, increasing water temperature due to global warming changes the start and end timing of the blooms, and reduces their amplitude, affecting the survival and hatching time of commercially important species [24,25]. Furthermore, experimental studies have shown that warmer conditions change the composition and trophic interactions of plankton communities, propagating the effects to higher trophic levels [26–28]. However, the impact of environmental forcing factors on spring bloom phenology in shallow waters is not well studied, making it difficult to assess the future of coastal water ecosystems in a global climate change context.

The objective of the present study was to investigate spring bloom dynamics and the associated phytoplankton diversity in a typical shallow coastal system to identify the environmental factors triggering the blooms. The study combined high-frequency monitoring of chlorophyll *a* (Chl *a*) fluorescence as a proxy of phytoplankton biomass, high-frequency monitoring of environmental parameters in the air and water and weekly water sampling of the phytoplankton community and nutrients in the water. The study was undertaken during winter and spring of 2015 and 2016 in Thau Lagoon, a typical productive coastal site on the edge of the Mediterranean Sea.

Materials and methods

Study site

The study site, Thau Lagoon (Fig 1), was chosen as it is a productive coastal site of economic interest (principally oyster farms representing 10% of French production) characterized by large seasonal temperature variation (from approximately 4 to 30°C throughout the year [29]). Thau Lagoon is located on the French coast of the northwestern Mediterranean Sea (43°24'00" N, 3°36'00" E). It is a shallow lagoon with a mean depth of 4 m, a maximum depth of 10 m (excluding deep depressions) and an area of 75 km² and is connected to the Mediterranean Sea by three channels. Thau Lagoon is a mesotrophic lagoon with a turnover rate of 2% (50 days), mostly through the Sète channel [30]. Recent studies have suggested that the lagoon is a phosphorus- and nitrogen-limited system [31]. The water column was monitored at a high frequency (at mid-depth, approximately 1.5 m below the surface) using several sensors at a fixed station (Coastal Mediterranean Thau Lagoon Observatory 43°24'53" N, 3°41'16" E) [32] near the Mediterranean platform for Marine Ecosystem Experimental Research (MEDIMEER), in the city of Sète. This fixed station was also used for weekly water sampling. The depth of the station is 2.5–3 m, and the station is situated less than 50 m from the entrance of the major channel where the water residence time is the lowest (20 days) [30]; therefore, the station is mostly influenced by seawater intake rather than inland freshwater. Meteorological data were also collected at a high frequency on the MEDIMEER pontoon less than 5 m from the location of high-frequency water monitoring. The study was carried out from January 7 to May 19, 2015, and from December 1, 2015, to July 6, 2016. Hereafter, these two periods are referred to as 2015 and 2016 for simplicity. No specific permissions were required for the sampling site for the present research activities as the study site is not protected. No endangered or protected species were involved in this work.

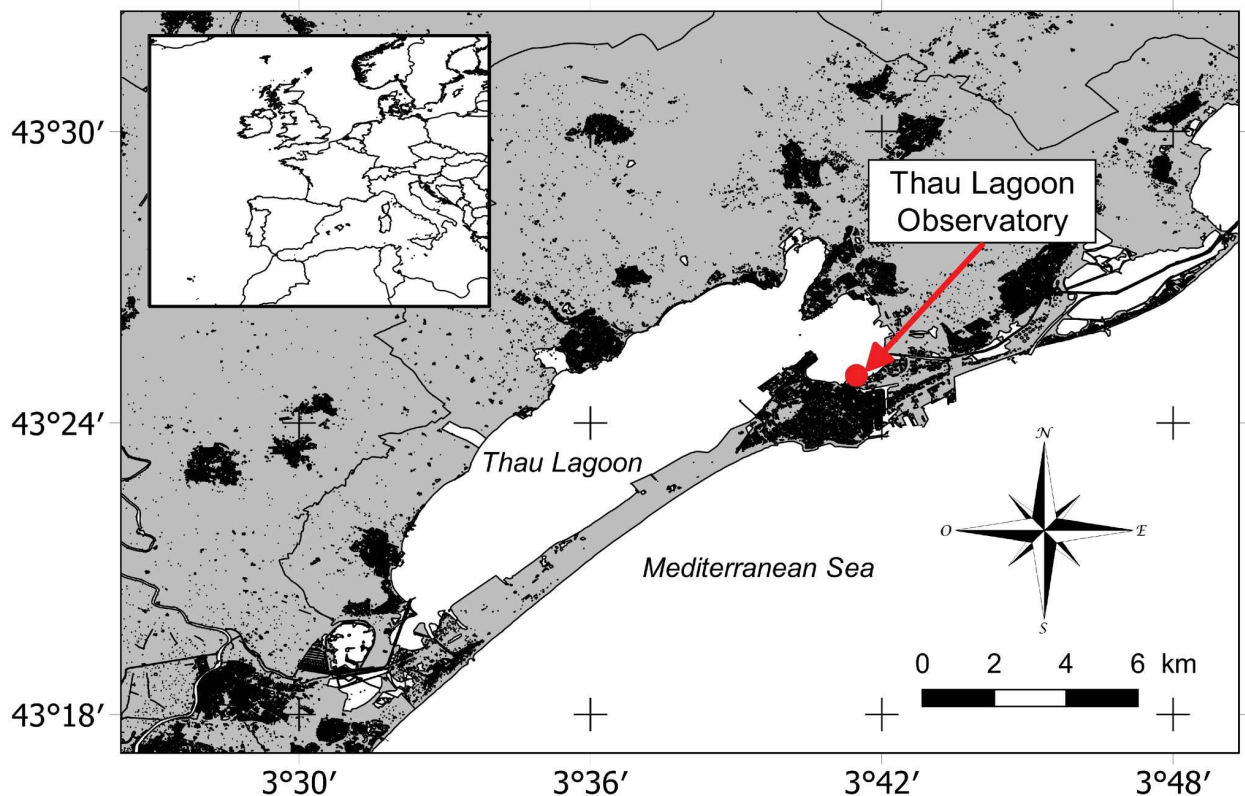


Fig 1. Location of the sampling station.

<https://doi.org/10.1371/journal.pone.0214933.g001>

High-frequency monitoring of the meteorological data, Chl *a* fluorescence and physical and chemical properties of the water

For the meteorological parameters (Table 1), air temperature, wind speed and direction, photosynthetically active radiation (PAR, 400–700 nm) and ultraviolet radiation A and B (UVA, 320–400 nm, and UVB, 280–320 nm) were recorded at a high frequency (every 15 min) using a Professional Weather Station (METPAK PRO, Gill instruments) with PAR, UVA and UVB sensors (Skye Instruments).

For the water properties at mid-depth (Table 1), the water temperature and salinity were recorded with an NKE STPS sensor (Table 1). The dissolved O₂ concentration and saturation were recorded using an optical sensor (AADI Oxygen Optode, Aanderaa). The turbidity and the *in situ* Chl *a* fluorescence were recorded with an ECO FLNTU fluorometer (Wetlabs). Water properties were recorded at the same frequency and over the same periods as the meteorological parameters, except for water temperature and conductivity in 2016, where the monitoring started ten days later (from December 11, 2015, to July 6, 2016). All sensors were calibrated before deployment. The temperature sensor was calibrated from 5 to 25°C in 5°C steps using a reference thermometer and thermostatic bath. The salinity sensor was calibrated at 25°C using seawater standards of 10, 30, 35 and 38 (Linearity Pack, OSIL, UK). The 0 standard was made with ultrapure water (MilliQ). The oxygen sensor was calibrated at 0% and 100% O₂ saturation using the Winkler method [33] for measuring the O₂ concentration. The Chl *a* fluorescence sensor was calibrated using several types of phytoplankton cultures at various concentrations, with the concentrations measured by spectrofluorometry. All sensors were

Table 1. Type and acquisition characteristics of the studied variables.

Type of data	Acquisition frequency	Variable	Type of instrument
Meteorological	High frequency: every 15 min	Air temperature	Sensor: Professional Weather Station (METPAK PRO, Gill instruments)
		Wind speed	
		Wind direction	
		PAR (400–700 nm)	Light sensors: Skye Instruments
		UVA (320–400 nm)	
		UVB (280–320 nm)	
Hydrological	High frequency: every 15 min	Water temperature	Sensors: NKE STPS
		Salinity	Sensors: AADI Oxygen Optode (Andraaa)
		O ₂ concentration	
		O ₂ saturation	Sensor: ECO FLNTU fluorometer (Wetlabs)
		Turbidity	
Biological	High frequency: every 15 min	Chl <i>a</i> fluorescence	Sensor: ECO FLNTU fluorometer (Wetlabs)
Biological	Weekly	Chl <i>a</i> concentrations	Water sample collected by a Niskin bottle and analyzed using high performance liquid chromatography (Waters)
		Phytoplankton abundances (cell diameter: < 6 μm)	Water sample collected by a Niskin bottle and analyzed using flow cytometry (FACSCalibur, Becton Dickinson)
		Phytoplankton abundances (cell diameter: 6–200 μm)	Water sample collected by a Niskin bottle and analyzed using optical microscopy (Olympus IX-70)
Chemical	Weekly	Nutrient concentrations (NO ₃ , NO ₂ , PO ₄ and Si(OH) ₄)	Water sample collected by a Niskin bottle and analyzed using an automated colorimeter (Seal Analytical)

PAR: photosynthetically active radiation; UVA and UVB: ultraviolet A and B, respectively; O₂: dioxygen, Chl *a*: chlorophyll *a*; NO₃: nitrate; NO₂: nitrite; PO₄: phosphate and Si(OH)₄: silicate.

<https://doi.org/10.1371/journal.pone.0214933.t001>

cleaned weekly to prevent biofouling, and measurement drift was checked after each measurement campaign using the same methods as those used to calibrate each sensor.

Weekly monitoring of nutrients, Chl *a* concentrations, phytoplankton abundance and diversity

In addition to high-frequency monitoring, water samples were collected weekly to determine nutrient and Chl *a* concentrations and phytoplankton abundances and diversity (Table 1). Samples were collected using a Niskin bottle 1 m below the surface from January 15 to May 12, 2015, and from January 12 to July 6, 2016, between 09:00 and 10:00 am.

To determine the nutrient concentrations, 50 mL seawater subsamples were taken using acid-precleaned polycarbonate bottles and then filtered through Gelman 0.45 μm filters that had been prewashed three times. Then, 13 mL of the filtrate was stored at -20°C until analysis. Nitrate (NO₃), nitrite (NO₂), phosphate (PO₄) and silicate (Si(OH)₄) concentrations were measured using an automated colorimeter (Seal Analytical) following standard nutrient analysis methods [34].

To determine Chl *a* concentrations, 1 L subsamples were taken, filtered through glass fiber filters (GF/F Whatman: 0.25 mm, nominal pore size: 0.7 μm), and stored at -80°C until analysis. Pigment concentrations, including Chl *a* concentrations, were measured by high performance liquid chromatography (HPLC, Waters) following the extraction protocol described in Vidussi et al. (2011) [34] and the HPLC method described by Zapata et al. (2000) [35].

Phytoplankton (< 6 μm) abundances were estimated by flow cytometry (FACSCalibur, Becton Dickinson), and phytoplankton (6–200 μm) abundances and diversity, by optical

microscopy (Olympus IX-70). For the phytoplankton ($< 6 \mu\text{m}$) abundances, duplicate 1.8 mL subsamples were taken, fixed with glutaraldehyde following the protocol described in Marie et al. (2001) [36] and then stored at -80°C until analysis. Cyanobacteria ($< 1 \mu\text{m}$), picoeukaryotes ($< 3 \mu\text{m}$) and nanoeukaryotes (in this study, $3\text{--}6 \mu\text{m}$ cell diameter; see Results) abundances were estimated using the flow cytometry method described by Pecqueur et al. (2011) [37]. Phytoplankton ($6\text{--}200 \mu\text{m}$) abundance and diversity were estimated by microscopy. Duplicate 125 mL subsamples were taken, fixed in 8% formaldehyde and then settled for 24 h in an Utermöhl chamber. Cells of each identified phytoplankton taxon were counted under an inverted microscope. Phytoplankton were identified to the lowest possible taxonomic level (species or genus) using standard keys for phytoplankton taxonomy [38]. Carbon biomasses of phytoplankton analyzed by flow cytometry were estimated using the conversion factors of $0.21 \text{ pgC cell}^{-1}$ for cyanobacteria and $0.22 \text{ pgC } \mu\text{m}^{-3}$ for picoeukaryotes and nanoeukaryotes [39]. For microscopic observations, phytoplankton biovolumes were estimated for the most common taxa using the best shape [40], and carbon biomasses were then calculated using the conversion factors [41,42].

Chl *a* fluorescence correction and bloom identification

Chl *a* fluorescence is commonly used as a proxy for phytoplankton biomass. Chl *a* fluorescence data from the fluorometer were corrected using the weekly measurements of Chl *a* concentrations by HPLC to provide coherent high-frequency Chl *a* fluorescence data [43].

Bloom periods were identified by estimating the net phytoplankton growth rate (Eq 1) using the biomass gain or loss [5,9]. The high-frequency Chl *a* fluorescence data over 24 h were used to calculate the daily mean phytoplankton biomass (C_t). The daily net growth rate (r_t) was the difference in phytoplankton biomass between two consecutive days. A negative value indicates a biomass loss, whereas a positive r value indicates a biomass gain.

$$r_{t+1} = C_{t+1} - C_t \quad (1)$$

A bloom was identified as a period 1) that started with at least 2 consecutive days of positive growth rates and 2) where the sum of net growth rates over at least 5 consecutive days was positive. The end of the bloom was the day before 5 consecutive days with negative growth. A 1-day peak of net growth was considered a “sporadic event” and not a bloom. When close successions of 5-day blooms were identified, they were coalesced into “bloom periods” followed by “post-bloom periods” to identify key events. The means of the daily net growth rates were calculated for bloom periods to compare the mean growth rates among the different periods.

Data analysis

Some of the operations required to maintain the quality of the high-frequency sampling, such as sensor recalibration and cleaning or drift correction, occasionally induced single or multiple missing measurements or outliers, which were removed from the data set. In our study, the fraction of missing values for each variable was generally low, i.e., between 0.06% (water temperature, 2015) and 23.48% (O_2 saturation, 2016). Only the UVA data in 2016 had a higher rejection rate (61.96%), due to a technical problem. Consequently, UVA data were not included in the data analysis for 2016 but were included in the 2015 analysis. All the other missing high-frequency data were estimated using a moving average in a 480 data point window (5 days) [44].

The daily mean of the high-frequency data except for PAR, UVA and UVB was calculated to remove daily variation patterns; for the three exceptions, the daily cumulative value was calculated. The whole data set (i.e., daily values of biological, meteorological and hydrological

data) was kept as a separate set for each study period. The two resulting data sets were divided into separate data sets for each period as bloom periods (winter, early spring and spring), post-bloom periods (post-winter bloom and post-early spring bloom) and a winter latency period. The winter latency period was defined as a period where the daily net growth rate was low, with a mean daily net growth rate close to zero. A post-spring bloom in 2015 and a pre-winter bloom in 2016 were identified. However, these blooms were too short to perform a strong statistical test; therefore, we did not keep them in the analysis of identified periods. These separations between different periods therefore provided therefore 5 data sets for 2015 and 4 data sets for 2016. Then, autoregressive and moving average (ARMA) models were used for each time series in each data set to identify ARMA processes [45] before first-differencing the fitted series to remove stationarity [46]. Principal component analysis (PCA) was used on the fitted and first-differenced time series in the 2015 and 2016 data sets to identify the relationships between environmental variables graphically. Then, Spearman's rank correlation tests were applied pairwise to highlight significant correlations in the 2015 and 2016 data sets. As Chl *a* may exhibit a delayed response to environmental forcing factors, time-lag correlation tests were performed on the 11 different data sets. Time-lag correlations are based on simple Spearman's rank correlation tests between two variables repeated with time-shifted data to identify the delayed influence of a variable on the Chl *a* dynamics.

The weekly data (nutrient concentrations and phytoplankton abundances and diversity) were kept as a separate data set for each study period but were not divided into identified periods because the quantity of data would have been insufficient (19 data points for 2015 and 23 data points for 2016). For the high-frequency data, ARMA models were used for each time series in each data set when needed. Paired Wilcoxon signed-rank tests were used to compare the mean values of the phytoplankton abundances and diversity and the nutrient concentrations between the 2015 and 2016 data sets. Sample dates were paired by week number (ISO 8601). For example, the sampling dates of January 8, 2015, and January 12, 2016, both corresponding to the 2nd week of the year, were paired. To identify correlations between weekly data and high-frequency environmental data, daily means of the environmental data for the sampling days were added to the weekly data sets before using ARMA models and first-differencing each time series. Spearman's rank correlation tests were then performed pairwise on the 2015 and 2016 data sets.

Results

Bloom identification based on Chl *a* fluorescence data

Three blooms were identified in 2015, while only two blooms were identified in 2016 (Fig 2A and 2B). Blooms were defined as consecutive days of biomass gain (positive values of daily net growth rates), while post-bloom periods were consecutive days of biomass loss (negative values; Fig 2C and 2D, respectively). There were winter blooms in January for 2015 and one month earlier, in December 2015, for 2016 (Fig 2A and 2B). The 2016 winter bloom was stronger, with Chl *a* concentrations reaching $3.64 \mu\text{g L}^{-1}$ in 2016 and $2.77 \mu\text{g L}^{-1}$ in 2015 (Fig 2A and 2B) and maximum daily net growth rates of $0.54 \mu\text{g L}^{-1}$ in 2016 and $0.49 \mu\text{g L}^{-1}$ in 2015 (Fig 2C and 2D). The mean daily net growth rate was $0.055 \mu\text{g L}^{-1} \text{d}^{-1}$ in 2016, almost double the $0.031 \mu\text{g L}^{-1} \text{d}^{-1}$ in 2015. However, it should be noted that the 2015 winter bloom had already started at the beginning of the monitoring. The winter blooms in 2015 and 2016 were followed by post-bloom periods, with the Chl *a* concentration falling to $0.54 \mu\text{g L}^{-1}$ in 2015 and $0.62 \mu\text{g L}^{-1}$ in 2016. In 2015, there was an early spring bloom between February 11 and March 11 that was weaker than the preceding winter bloom (maximum Chl *a*: $2.01 \mu\text{g L}^{-1}$ and mean daily net growth rate: $0.023 \mu\text{g L}^{-1} \text{d}^{-1}$). This early spring bloom was followed by a post-bloom period,

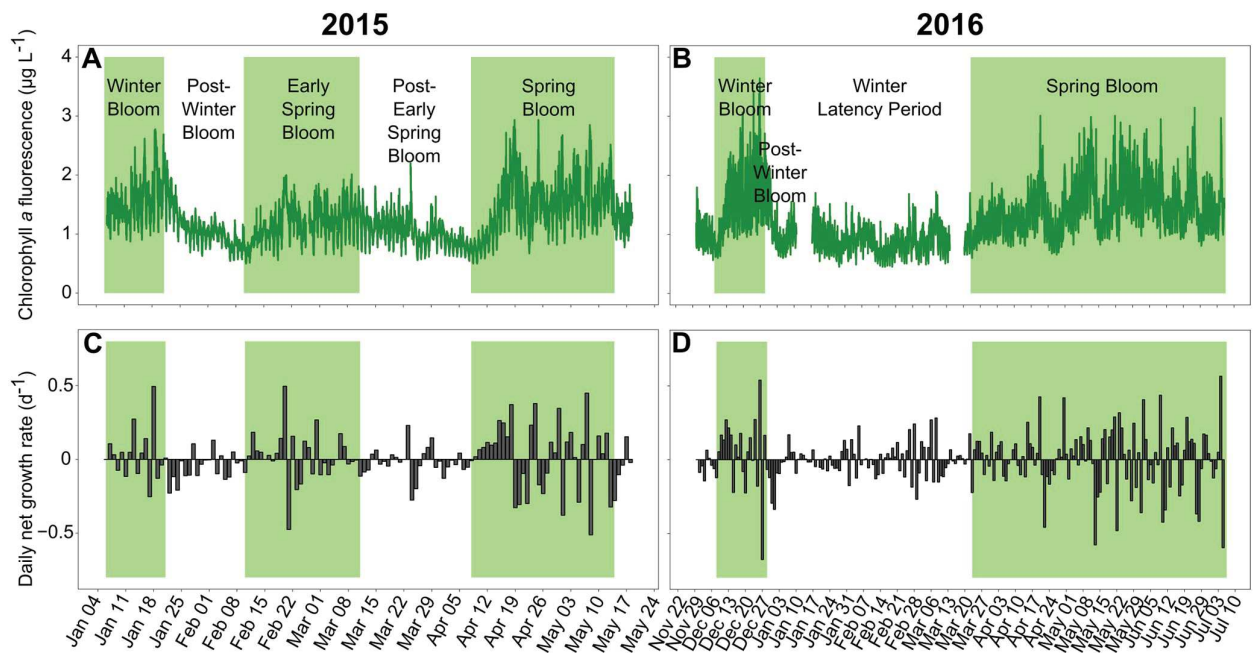


Fig 2. Chlorophyll *a* fluorescence and daily net growth rates. *In situ* Chl *a* fluorescence in 2015 (A) and 2016 (B) and daily net growth rates in 2015 (C) and 2016 (D), indicating daily biomass gains (positive values) and losses (negative values). The bloom periods have a green background, and the post-bloom periods and winter latency period have a white background.

<https://doi.org/10.1371/journal.pone.0214933.g002>

with the Chl *a* concentration falling to $0.54 \mu\text{g L}^{-1}$. In 2016, however, instead of an early spring bloom, there was a winter latency period from January 6 to March 11. During this period, the daily net growth rates were low (Fig 2D), with a mean daily net growth rate close to zero. Then, the main spring blooms occurred from April 9 to May 14 (36 days) in 2015 and from March 24 to July 05 (104 days) in 2016. Notably, the monitoring periods had been planned to end on May 19, 2015, and July 6, 2016; therefore the spring blooms might have continued after these dates. In 2016, the spring bloom showed a maximum Chl *a* concentration of $3.16 \mu\text{g L}^{-1}$, which was higher than the value of $2.93 \mu\text{g L}^{-1}$ recorded in 2015, but with a mean daily net growth rate ($0.010 \mu\text{g L}^{-1} \text{d}^{-1}$) lower than that ($0.022 \mu\text{g L}^{-1} \text{d}^{-1}$) recorded in 2015.

High-frequency meteorological and hydrological data

The PAR was lowest when the winter blooms occurred in both 2015 and 2016 (Fig 2A and 2B). Then, the PAR slowly increased to reach its maximum of $2688 \mu\text{mol m}^{-2} \text{s}^{-1}$ on April 19, 2015, and $2865 \mu\text{mol m}^{-2} \text{s}^{-1}$ on June 18, 2016.

Two dominant winds were identified. Dominance of wind was based on the frequency of occurrence of wind directions over the two studied periods (Fig 3C and 3D). The first wind was from the northwest (49.5% of the data between 270° and 359°), and the second was from the southeast (21% of the data between 90° and 180°). There were three windy periods with northwesterly winds (median of 302°) in 2015 (Fig 3E) during the post-winter bloom period (max = 16.6 m s^{-1}), the early spring bloom period (max = 17.4 m s^{-1}) and the post-early spring bloom period (max = 16.5 m s^{-1}). The wind speed was lower during the winter bloom, the onset of the early spring bloom and the spring bloom (means of 3.3, 1.9 and 3.1 m s^{-1} , respectively). In 2016 (Fig 3F), the wind speeds were low during the winter bloom (mean = 1.8

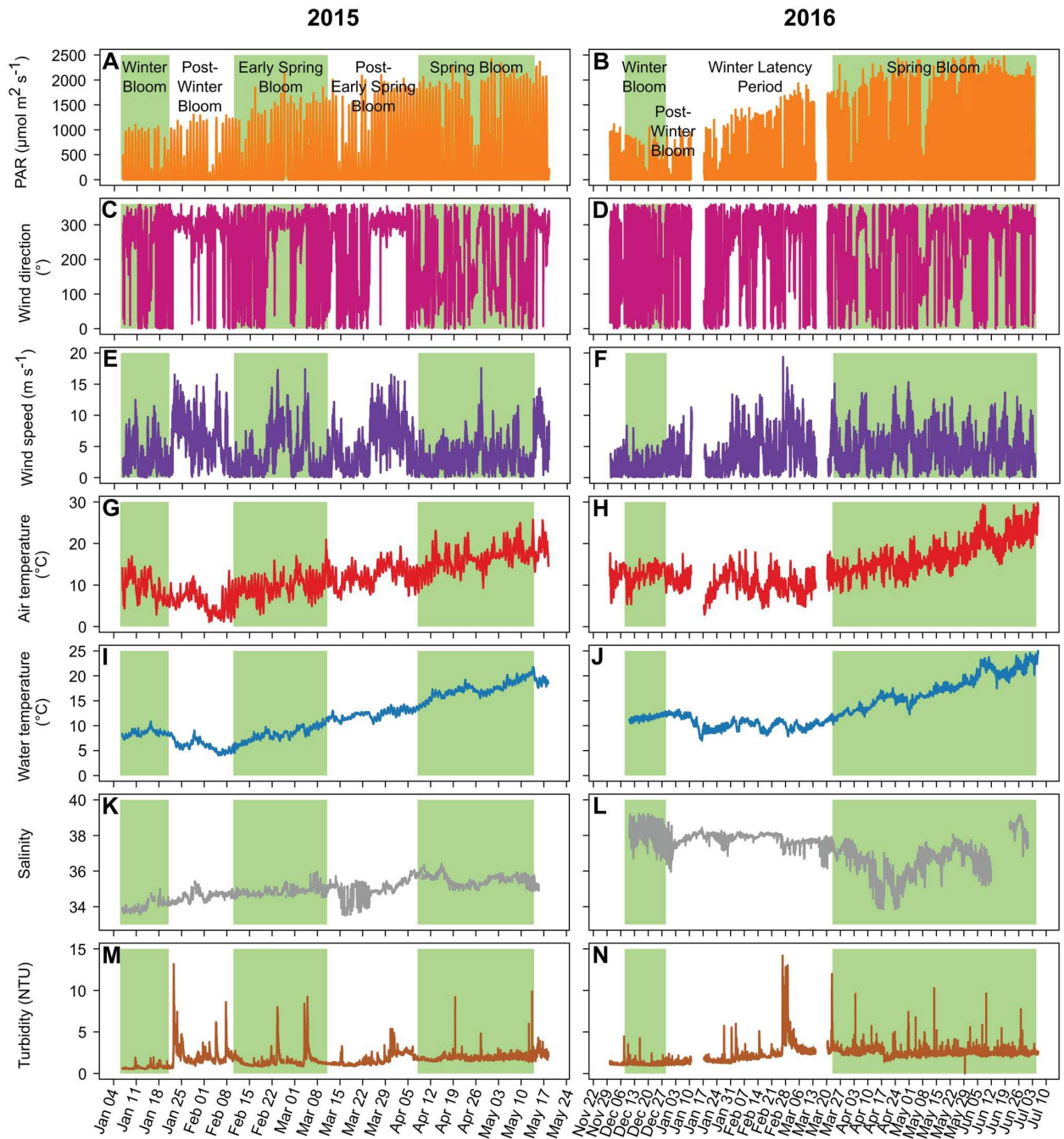


Fig 3. Environmental variables. Main environmental variables for 2015 (left) and 2016 (right). A to H are the meteorological data: PAR (A and B), wind direction (C and D), wind speed (E and F) and air temperature (G and H); and I to N are the hydrological variables: water temperature (I and J), salinity (K and L) and turbidity (M and N). The background colors for the various periods are the same as in Fig 2.

<https://doi.org/10.1371/journal.pone.0214933.g003>

m s^{-1}); otherwise, the wind was erratic, with numerous short windy events exhibiting mean wind speed values higher than those observed during the winter bloom.

During the 2015 study period, the mean air temperature dropped from 19.9°C in early January to 1.1°C in early February (Fig 3G). It then increased until the end of the study period,

with a maximum of 25.7°C on May 14. During the 2016 study period, the air temperature was stable from early December to mid-March (mean: 10.9±2.7°C, minimum: 2.9°C and maximum: 18.5°C) with a quick chill in early January (Fig 3H). Then the air temperature increased from mid-March until the end of the study period, with a maximum of 30.8°C on July 7.

The water temperature was less variable than the air temperature (Fig 3I and 3J). In 2015, the water temperature was stable during January (8.5±0.6°C), decreased to a minimum of 4.0°C on February 6 and then increased to 21.7°C on May 14. In 2016, the water temperature was 11.8±0.5°C from December 12 to January 11, followed by a quick chill to a minimum of 7.0°C on January 17. Then, the water temperature was stable until March 10 (9.9±0.8°C), followed by an increase until the end of the study period, reaching a maximum of 25.1°C on July 6.

The salinity was also different between 2015 and 2016 (Fig 3K and 3L). In 2015, the salinity was 34.95±0.56, while in 2016, it was higher (37.34±0.95) and more variable and exhibited a large decrease during April, reaching a minimum value of 33.85 on April 18.

The turbidity (Fig 3M and 3N) was 1.69±0.87 NTU in 2015, which was lower than the 2.25±1.06 NTU observed in 2016, with sporadic peaks reaching 13.15 NTU in 2015 and 14.19 NTU in 2016.

Relationships between Chl *a* fluorescence, meteorological and hydrological data

The general relationships between Chl *a*, meteorological and hydrological data in 2015 and 2016 based on PCA are shown in Fig 4A and 4B. For both data sets, there was a group on the second axis, comprising the wind conditions (speed and direction) and turbidity. Spearman's rank correlations were strong between wind speed and wind direction for both data sets (2015: $\rho = 0.38$, p -value < 0.001; 2016: $\rho = 0.48$, p -value < 0.001). However, the turbidity was correlated with the wind conditions in 2015 (speed: $\rho = 0.41$, p -value < 0.001; direction: $\rho = 0.19$, p -value < 0.05) but not in 2016. Another group, on the first PCA axis of both data sets, comprised the light parameters, i.e., PAR, UVA (only in 2015) and UVB, and oxygen concentration and saturation. Spearman's rank correlations were significant between light conditions and oxygen (2015: all p -values < 0.01; 2016: all p -values < 0.001). Chl *a* fluorescence was opposed to both these groups in both 2015 and 2016, with significant negative correlations with the wind conditions (all p -values < 0.05) and the light conditions (all p -values < 0.05). The PCA for both data sets also showed a positive correlation between water temperature and air temperature (2015: $\rho = 0.36$, p -value < 0.001; 2016: $\rho = 0.29$, p -value < 0.001). The water temperature was positively correlated with Chl *a* fluorescence in 2015 ($\rho = 0.25$, p -value < 0.01) but not in 2016.

Time-lag correlations between high-frequency Chl *a* fluorescence, meteorological and hydrological data

As Chl *a* fluorescence may have exhibited a delayed response to environmental forcing factors, the time series were tested for time-lag correlations (Table 2). Chl *a* fluorescence was positively correlated with the water temperature (0- and 5-day lags, strong p -values < 0.01) as well as salinity (1- and 3-day lags, p -values < 0.05) in both the 2015 and 2016 data sets. As found using PCA, Chl *a* fluorescence was negatively correlated with the light conditions (PAR, UVA and UVB), with a 0-day lags in both 2015 and 2016. However, there was a positive correlation between Chl *a* fluorescence and light conditions with a 1-day lag, but only in 2015. There were negative correlations between Chl *a* fluorescence and wind conditions (speed and direction) with a lag of 0 to 2 days in both 2015 and 2016 (p -values < 0.05).

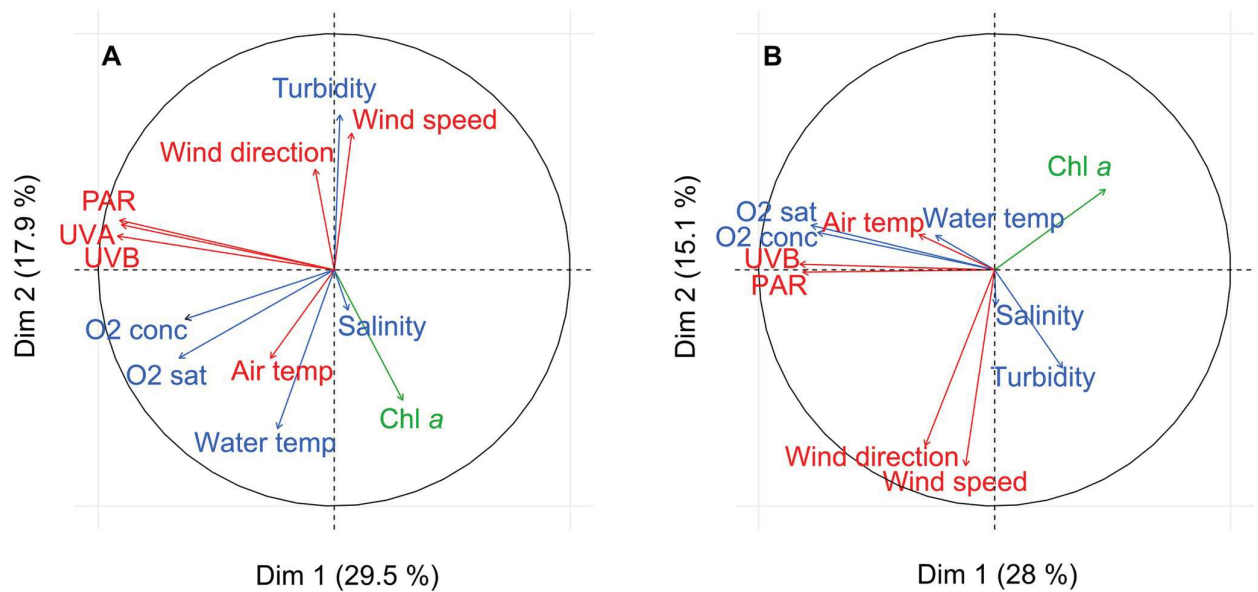


Fig 4. Principal component analysis (PCA) of environmental variables. PCA of Chl *a*, meteorological and hydrological data for the 2015 data set (A) and 2016 data set (B). PCA allows the variables to be projected in multidimensional space to highlight the relationships between them. Here, only two dimensions are represented as they explain the environmental dynamic well. The arrows represent the variables. When arrows are far from the center and close to each other, they are positively correlated, whereas when they are symmetrically opposed, they are negatively correlated. If the arrows are orthogonal, they are not correlated. Finally, when the variables are close to the center, they are not well projected in the dimensions represented; consequently, it is hard to conclude that a relationship occurs between these variables. In this last case, to highlight masked links, we coupled the PCA with pairwise Spearman's rank correlations as described in the Material and methods.

<https://doi.org/10.1371/journal.pone.0214933.g004>

For the separate periods (bloom, post-bloom and winter latency periods), Chl *a* fluorescence was positively correlated with water temperature, with a lag of from 0 to 5 days during four of the five bloom periods (*p*-values from < 0.05 to < 0.001). Chl *a* fluorescence was negatively correlated with the wind conditions (speed and/or direction), with a range of lags between 0 and 4 days for four blooms (*p*-values from < 0.05 to < 0.001). Salinity was positively correlated with Chl *a* fluorescence during the early spring bloom in 2015 (*p*-value < 0.001) and negatively correlated with Chl *a* fluorescence during the winter bloom in 2016 (*p*-value < 0.001). Chl *a* fluorescence was negatively correlated with light conditions for 3 blooms with 0-day lags (*p*-values from < 0.05 to < 0.001), while for the spring bloom in 2015, they were positively correlated with a 1-day lag (*p*-value < 0.05). There was little correlation during the post-bloom periods. Chl *a* fluorescence was negatively correlated with PAR and UVA during the post-winter bloom in 2015 (5-day lags, *p*-value < 0.05) as well as with the wind speed in for 2016 (0-day lag, *p*-value < 0.05) and was positively correlated with the wind direction (5-day lags, *p*-value < 0.05) during the post-early spring bloom period in 2015.

Nutrient dynamics

During the winter bloom and the post-winter bloom periods, the PO₄, NO₂ and NO₃ concentrations were on average 3 to 9 times lower in 2015 (0.01±0.00, 0.07±0.03 and 0.72±0.24 μmol L⁻¹, respectively) (Fig 5A, 5E and 5G) than in 2016 (0.09±0.05, 0.20±0.05 and 2.26±0.63 μmol L⁻¹, respectively) (Fig 5B, 5F and 5H). The Si(OH)₄ concentration (Fig 5C and 5D) in 2015 (8.67±2.05 μmol L⁻¹) was, however, twice that in 2016 (3.86±0.57 μmol L⁻¹) over the same period. In 2015, the Si(OH)₄ concentrations then gradually decreased until the end of the early spring bloom, reaching a mean of 2.14±0.29 μmol L⁻¹ in March.

Table 2. Time-lag correlations between meteorological and hydrological data.

Year	Period	PAR	UVA	UVB	Wind speed	Wind direction	Air temperature	Water temperature	Salinity	Turbidity
2015	Whole	-- (0;0.27) +++ (1;0.31)	-- (0;0.24) +++ (1;0.32)	-(0;0.22) +++ (1;0.31)	-(0;0.17) -- (1;0.28)	-- (0;0.24)		++ (0;0.25)	+(3;0.18)	
	Winter Bloom					++ (0;0.71) -- (4;0.79)				
	Post-Winter Bloom	-(5;0.56)	-(5;0.55)							+(3;0.54)
	Early Spring Bloom	-(0;0.40)	-(0;0.39)		+(5;0.43)			+++ (0;0.60)	+++ (0;0.56) -- (4;0.43)	-(0;0.38)
	Post-Early Spring Bloom					+(5;0.54)				
	Spring Bloom	-(0;0.41) +(1;0.39)	-- (0;0.43) +(1;0.41)	-(0;0.41) +(1;0.39)	+(2;0.40)	-- (0;0.53)		+(2;0.35)		
2016	Whole	--- (0;0.38)		--- (0;0.36)	-(0;0.17) -(2;0.30)	-- (0;0.30) -(2;0.15)		++ (5;0.17)	+(1;0.15) ++ (3;0.21)	+(0;0.16)
	Winter Bloom					-- (0;0.57)		+(0;0.54)	--- (0;0.72)	
	Post-Winter Bloom				-(0;0.86)					
	Winter Latency Period	-(0;0.25) ++ (3;0.32)		-- (0;0.31) ++ (3;0.34)		-(0;0.24) ++ (4;0.32)			++ (3;0.32)	++ (0;0.35) -- (1;0.32)
	Spring Bloom	--- (0;0.44)		--- (0;0.44)	--- (0;0.35) +(5;0.21)	-- (0;0.27) -(1;0.22) +(5;0.23)		-(0;0.25) -(2;0.20) +(5;0.21)		

Spearman’s rank time-lag correlations between Chl *a* fluorescence and environmental variables in 2015 and 2016. Whole: tests performed on the whole data set for a study period. Only significant results are shown. The signs + and—represent significant positive and negative correlations, respectively; a single sign represents *p*-value < 0.05; ++ or—represents *p*-value < 0.01; and +++ or—represents *p*-value < 0.001. The time lag (in days) and coefficient of the correlations are in parentheses. For example, +(2;0.40) represents a positive correlation with a *p*-value < 0.05, 2-day lag and coefficient of 0.40. The bloom periods have a green background.

<https://doi.org/10.1371/journal.pone.0214933.t002>

In 2015, from the early spring bloom to the end of the spring bloom, the PO₄, NO₂ and NO₃ concentrations remained at the same levels as in the winter, even though there were peaks in the PO₄ (0.08 μmol L⁻¹) and NO₃ (6.01 μmol L⁻¹) concentrations on March 12. In 2016, over the same period, the PO₄, NO₂ and NO₃ concentrations fluctuated more than in 2015, but the mean values were similar (0.04±0.06, 0.04±0.02 and 1.24±0.83 μmol L⁻¹, respectively). The mean Si(OH)₄ concentration during the spring bloom in 2015 (1.62 ±1.00 μmol L⁻¹) was approximately half that in 2016 (2.74±0.80 μmol L⁻¹).

Wilcoxon signed-rank tests showed that the PO₄ and NO₃ concentrations were significantly higher in 2016 than in 2015 (*p*-values < 0.05). The N:P ratios (Redfield ratios) were between 11 and 94 (mean: 45±25) in 2015 and between 6 and 124 (mean: 46±35) in 2016. Spearman’s rank correlations showed significant correlations between Chl *a* and nutrient concentrations in neither 2015 nor 2016.

Dynamics of phytoplankton abundances

Three groups of picophytoplankton, namely, cyanobacteria (< 1 μm diameter), picoeukaryotes (< 1 μm diameter) and picoeukaryotes (1–3 μm diameter), and one group of nanoeukaryotes (3–6 μm diameter) were enumerated by flow cytometry (Fig 6A to 6D). The abundances of picoeukaryotes (< 1 μm and 1–3 μm) and nanoeukaryotes were similar between 2015 and 2016: the total abundance of these three groups was 2.14±1.30 × 10⁴ cells mL⁻¹ in 2015 and 2.84±1.41 × 10⁴ cells mL⁻¹ in 2016. However, the mean abundance of picoeukaryotes and

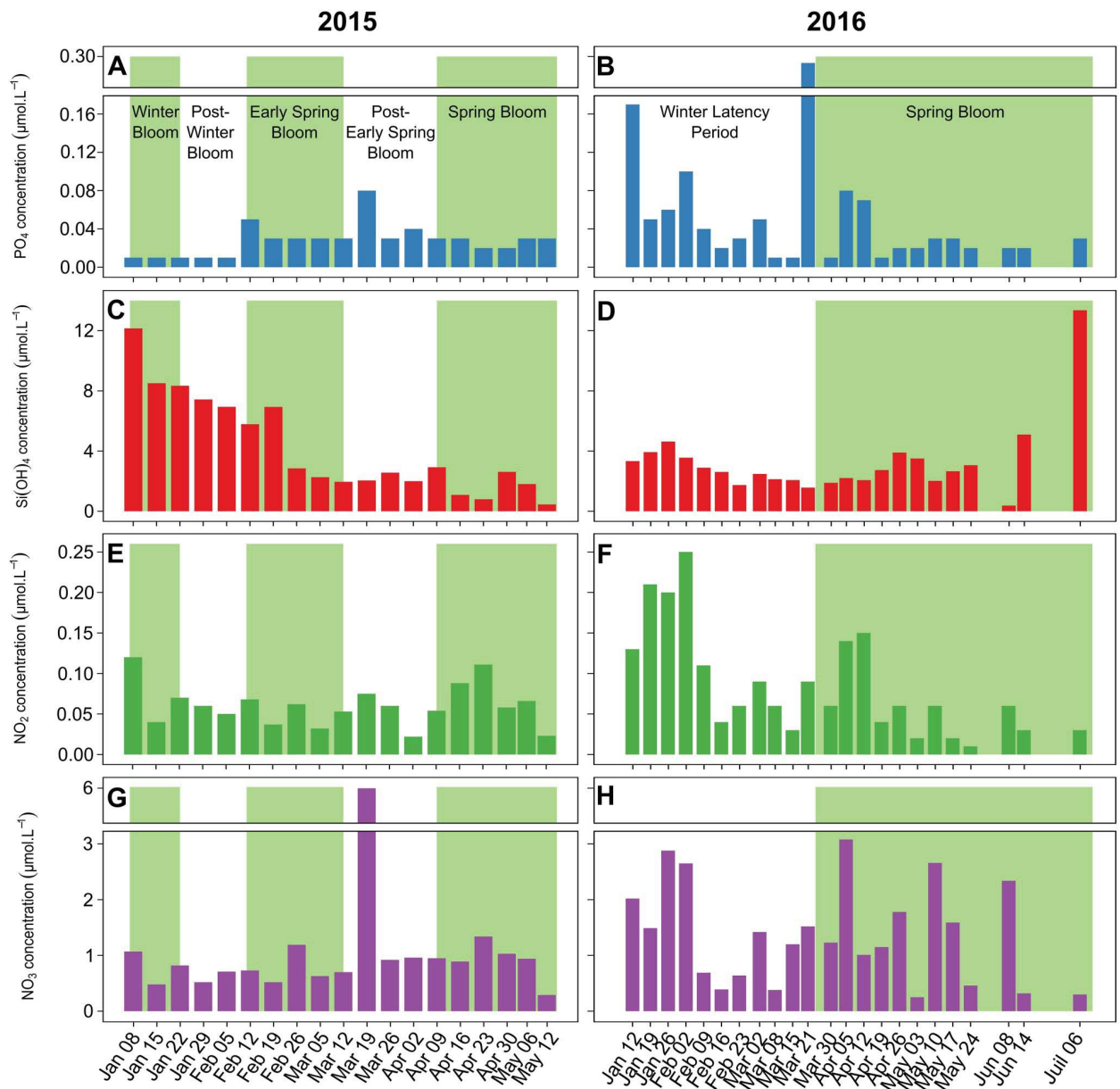


Fig 5. Nutrient concentrations. Nutrient concentrations in 2015 (left) and 2016 (right) for PO₄ (A and B), Si(OH)₄ (C and D), NO₂ (E and F), and NO₃ (G and H). The background colors for the various periods are the same as in Fig 2.

<https://doi.org/10.1371/journal.pone.0214933.g005>

nanoeukaryotes during the spring bloom in 2016 ($6.53 \pm 1.38 \times 10^4$ cells mL⁻¹) was more than twice that in 2015 ($2.84 \pm 1.73 \times 10^4$ cells mL⁻¹). One of the main differences between 2015 and 2016 was that during winter and early spring, the cyanobacteria (< 1 μm) abundance in 2016 ($2.19 \pm 2.19 \times 10^3$ cells mL⁻¹) was almost 10 times higher than that in 2015 ($3.02 \pm 2.55 \times 10^2$ cells mL⁻¹). Then, during the spring bloom, cyanobacteria abundances increased to a maximum on May 06, 2015 (6.01×10^4 cells mL⁻¹), and a lower maximum on May 10, 2016 (2.70×10^4 cells mL⁻¹). The Wilcoxon signed-rank test showed that the mean abundances of cyanobacteria (*p*-value < 0.01), picoeukaryotes (< 1 μm) (*p*-value < 0.01) and nanoeukaryotes

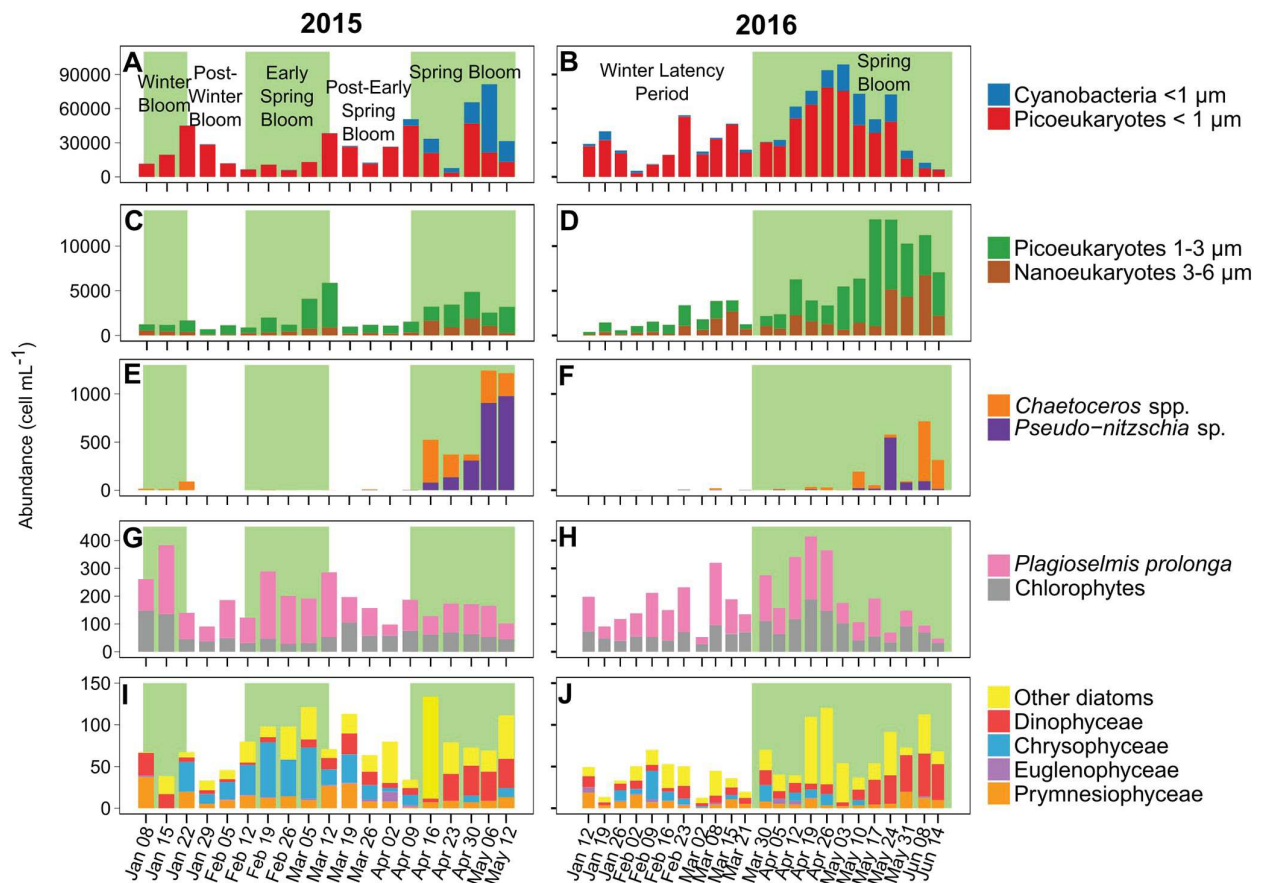


Fig 6. Phytoplankton abundances and diversity. Analyzed by flow cytometry for 2015 (A and C) and 2016 (B and D). Dominant taxa observed by microscopy for 2015 (E, G and I) and 2016 (F, H and J). The background colors for the various periods are the same as in Fig 2.

<https://doi.org/10.1371/journal.pone.0214933.g006>

(p -value < 0.05) were significantly higher in 2016 than in 2015, but there was no significant difference for picoeukaryotes (1–3 μm). Tests for correlations between the biological variables (picophytoplankton and nanophytoplankton abundances and Chl a fluorescence) and the environmental variables (wind conditions, light conditions, salinity, air and water temperature, oxygen, turbidity and nutrients) showed a negative correlation of picoeukaryotes (1–3 μm) with PO_4 concentrations in 2015 ($\rho = -0.54$, p -value < 0.05) and with NO_3 in 2016 ($\rho = -0.50$, p -value < 0.05). Picoeukaryotes (< 1 μm) were negatively correlated with wind conditions in 2015 (wind speed: $\rho = -0.57$, p -value < 0.05; wind direction: $\rho = -0.50$, p -value < 0.05).

The patterns of community composition and total abundances of phytoplankton (6–200 μm) were different between 2015 and 2016 (Fig 6E to 6J). The total abundances of phytoplankton (6–200 μm) were quite similar during winter and early spring in 2015 (266 ± 81 cells mL^{-1}) and 2016 (212 ± 91 cells mL^{-1}). During the spring bloom, however, the total phytoplankton (6–200 μm) abundances in 2015 were almost three times those in 2016 (982 ± 433 cells mL^{-1} and 378 ± 123 cells mL^{-1} , respectively). This result was confirmed by the Wilcoxon signed-rank test showing that total phytoplankton abundances (6–200 μm) were significantly higher in 2015 than in 2016 (p -value < 0.01). The maximum abundances of phytoplankton (6–200 μm) were reached on May 6, 2015, and June 8, 2016 (1470 cells mL^{-1} and 923 cells mL^{-1} , respectively). In 2015, during the winter and early spring blooms and their post-bloom

periods, the phytoplankton community was dominated numerically by *Plagioselmis prolunga*, a cryptophyte with a diameter of 8–12 μm ($41\pm 13\%$), and chlorophytes ($\sim 6\ \mu\text{m}$) ($38.0\pm 8.5\%$). In addition, chrysophyceae ($\sim 6\ \mu\text{m}$) were also abundant during the early spring bloom ($18\pm 2\%$). In 2016, *P. prolunga* dominated the phytoplankton (6–200 μm) community during the winter latency period and the first 11 weeks of the spring bloom ($48\pm 11\%$), and chlorophytes ($\sim 6\ \mu\text{m}$) were also abundant but less abundant than in 2015 ($29\pm 9\%$). *Pseudo-nitzschia* sp. (25–50 μm) and *Chaetoceros* spp. (10–50 μm), which are large, colonial diatoms, successively dominated the phytoplankton (6–200 μm) community during the spring bloom in early April 2015 ($72\pm 13\%$) and the second part of the spring bloom from mid-May 2016 ($65\pm 23\%$) until the end of the study periods. *Chaetoceros* spp. abundances were significantly lower in 2015 than in 2016 (Wilcoxon signed-rank test, p -value < 0.05), but *Pseudo-nitzschia* sp. abundances were not.

The phytoplankton community was dominated numerically by picoeukaryotes ($< 1\ \mu\text{m}$), accounting for 51 to 95%, depending on the period (Table 3). However, in terms of carbon biomass, picoeukaryotes were never dominant. In 2015, the carbon biomass was dominated by *P. prolunga* in the winter and early spring blooms and by *Chaetoceros* spp. in the spring bloom. Nanoeukaryotes contributed most of the carbon biomass throughout 2016.

Correlations between weekly measurements of phytoplankton abundances (6–200 μm), Chl *a* fluorescence and environmental variables were calculated separately for 2015 and 2016. In 2015, *P. prolunga* abundance ($\rho = -0.60$, p -value < 0.05) was negatively correlated with PO_4 concentration, and *Chaetoceros* spp. abundance was positively correlated with Chl *a* fluorescence ($\rho = 0.67$, p -value < 0.01). In 2016, *Pseudo-nitzschia* sp. abundance was positively correlated with Chl *a* fluorescence ($\rho = 0.55$, p -value < 0.05), and *Chaetoceros* sp. abundance was positively correlated with NO_3 concentration ($\rho = 0.58$, p -value < 0.01).

Discussion

Role of water temperature and winter cooling in phytoplankton blooms

Based on the time-lag correlations, water temperature played a significant role in determining Chl *a* dynamics, especially the onset of blooms (Table 2). This is the first time that rising water temperature has been identified as the main factor triggering phytoplankton blooms in an aquatic ecosystem (ocean, coastal zone or lake). This relationship was true for all the main blooms observed in 2015 and 2016, and the strength, number of occurrences and consistent positive sign of the correlations between water temperature and Chl *a* fluorescence suggested that water temperature was the main driver. Other parameters such as wind conditions and salinity were correlated with blooms (see below) but the number of occurrence and non-consistent sign of the correlations suggested that they were not the main drivers. The water temperature was positively correlated with Chl *a* fluorescence with 0 to 5 days of lag suggesting that the biomass accumulation represented by increasing Chl *a* fluorescence was driven by the increase in water temperature over the 5 previous days. Furthermore, every bloom onset corresponded to a period of increase in water temperature, while such correspondence was not detected for other parameters.

The effect of temperature on phytoplankton physiology and metabolic processes is well known. First, under light-saturated conditions, higher temperature increases specific phytoplankton productivity by acting on photosynthetic carbon assimilation [47,48]. In addition, under non-limiting nutrient conditions, an increase in water temperature increases phytoplankton nutrient uptake [49,50]. Moreover, phytoplankton growth rates increases with increasing of temperature, almost doubling with each 10°C increase in temperature (Q_{10} temperature coefficient) [51]. Furthermore, the growth rate of phytoplankton is higher than that

Table 3. Relative contributions of the dominant phytoplankton groups to the carbon biomass and abundance.

	2015										2016			
	Winter Bloom		Post-Winter Bloom		Early Spring Bloom		Post-Early Spring Bloom		Spring Bloom		Winter Latency Period		Spring Bloom	
	C	Ab	C	Ab	C	Ab	C	Ab	C	Ab	C	Ab	C	Ab
Cyanobacteria (< 1 μm)	0.17	0.62	0.54	0.89	0.38	1.54	1.10	1.92	7.81	40.60	3.48	6.83	5.67	19.82
Picoeukaryotes (< 1 μm)	6.86	90.50	16.03	94.74	5.49	79.06	14.43	89.49	2.78	51.43	12.38	86.50	5.45	67.86
Picoeukaryotes (1–3 μm)	4.81	4.07	8.60	3.25	15.05	13.88	16.49	6.54	3.62	4.29	7.96	3.56	9.73	7.75
Nanoeukaryotes (3–6 μm)	28.52	3.01	13.44	0.64	35.26	4.06	28.87	1.43	14.26	2.11	46.23	2.59	39.87	3.97
<i>Plagioselmis prolunga</i>	31.99	0.92	19.02	0.24	37.41	1.17	27.93	0.38	4.50	0.18	22.43	0.34	6.77	0.18
<i>Chlorophytes</i>	14.68	0.81	5.61	0.14	4.63	0.28	9.11	0.23	1.58	0.12	5.91	0.17	2.69	0.14
<i>Chaetoceros</i> spp.	12.97	0.08	36.76	0.10	1.78	0.01	1.92	0.01	52.96	0.45	1.43	0.00	27.31	0.17
<i>Pseudo-nitzschia</i> sp.	0.00	0.00	0.00	0.00	0.00	0.00	0.14	0.00	12.48	0.82	0.17	0.00	2.50	0.11

Mean relative contribution (in percent) to the carbon biomass (CB) and numerical abundance (Ab) of the dominant phytoplankton groups during each period. Species and period abbreviations and background colors are the same as in Table 2. The highest contribution for each period is in bold.

<https://doi.org/10.1371/journal.pone.0214933.t003>

of herbivorous grazers at low temperatures [51,52]. Thus, an increase in water temperature, particularly at relatively low *in situ* temperatures such as those in this study (6–14 °C), can be more favorable for phytoplankton than for their grazers, allowing phytoplankton biomass accumulation, which starts the bloom. Therefore, the initiation of phytoplankton biomass accumulation can result from phytoplankton growth temporarily exceeding grazing-induced losses as a result of increasing temperature.

In previous studies, water temperature was identified as the main driver of blooms of particular species, especially cyanobacteria [53,54]. However, the present study underlined that an increase in water temperature triggered blooms of all phytoplankton community blooms, not just a particular species. Furthermore, the spring blooms started at a temperature of 13.9 °C in 2015 and 11.2 °C in 2016, while the early spring bloom in 2015 began when the water temperature was 6.1 °C. This wide water temperature range for bloom initiations indicates that there is not a threshold water temperature that triggers phytoplankton blooms; instead, blooms are initiated by an increase in water temperature.

Interannual comparison showed that winter 2015/2016 was the warmest winter recorded in France according to MétéoFrance (<http://www.meteofrance.fr/climat-passe-et-futur/bilans-climatiques/bilan-2016/hiver>), which led to exceptionally high winter water temperatures. In contrast in 2015, the winter cooling of the water was typical of this coastal site. As a result, the Chl *a* dynamics in 2016 were completely different from those in 2015 (Fig 1). The absence of an early spring bloom and the slower biomass accumulation during the 2016 spring bloom can be explained by the difference between the meteorological conditions. The abnormally high water temperature during the 2016 winter may have been the cause of biomass stagnation during the winter latency period, slowing phytoplankton biomass accumulation during the spring. The absence of significant winter cooling and the relatively mild water temperatures may have allowed predators (e.g., ciliates and copepods) as well as filter feeders (e.g., oyster and mussels) to remain active during this period and maintain grazing pressure on the phytoplankton [55,56], in turn delaying the ecosystem disturbance required to start a bloom until mid-March, when the water temperature started to rise. Therefore, winter water temperature seems to be a crucial factor influencing the dynamics of the spring bloom in temperate shallow coastal zones. The effect of the winter water temperature on the magnitude of the spring bloom has already been reported [57,58], with larger spring blooms and more phytoplankton biomass after cold winters and smaller spring blooms after mild winters in the Wadden Sea. With

global warming, these mild winters could become more frequent [59] and may reduce phytoplankton biomass accumulation during spring blooms. This modification of the bloom phenology might potentially change the structure of the plankton community assemblages and, therefore, directly affect the food web. Such modification is particularly important in shallow temperate coastal zones of economic interest as changes in bloom phenology and magnitude may affect fish and shellfish production.

There were short (2–3 weeks) winter blooms in both 2015 and 2016. Winter blooms are known to occur in marine ecosystems, but they are less common than spring blooms. Winter blooms can be rare, exceptional events [60], but they may occur regularly every year, as in the Bahia Blanca Estuary in Argentina [61] or in tropical and subtropical seas [62–64]. Winter blooms in the coastal site of the present study were recorded once before, in December 1993 [65,66], whereas the present study documented winter blooms of a magnitude similar to that of the spring bloom in two consecutive years. These winter blooms represent an important part of annual primary production (daily mean net growth rates of $0.055 \mu\text{g L}^{-1} \text{d}^{-1}$ in 2015 and $0.031 \mu\text{g L}^{-1} \text{d}^{-1}$ in 2016), providing food for the whole plankton food web, and can sometimes be the most important biomass accumulation event during the year [61]. Winter blooms in shallow coastal zones are generally triggered by a combination of forcing factors such as high nutrient concentrations due to autumn rains, an increase in light penetration into the water column due to a reduction in suspended matter or sediments and low grazing pressure due to low water temperature or tidal conditions [61]. In this study, water temperature was associated with the increase in Chl *a* fluorescence during the winter bloom of 2016. For 2015, however, the winter bloom had already been triggered when the monitoring started, and the link between water temperature and Chl *a* for this winter bloom could not be established as the time-lag correlations could not be determined. Additional observations will be necessary to establish whether an annual winter bloom has become a rule, which might indicate that an ecological shift has occurred in this system. The winter bloom may also have been the result of particular climatic/environmental conditions that occurred during the study period. In fact, even though the impact of the El Niño-Southern Oscillation (ENSO) on the Mediterranean climate is still a source of discussion [67], 2015 was a strong El Niño year with an ENSO Oceanic Niño Index (ONI) value of approximately 2, making it less important than that in 1997–1998 but more than that in 1991–1992 [68], which could potentially explain the exceptional 2015–2016 winter climatic conditions.

Role of other environmental forcing factors in phytoplankton blooms

Nutrient input from runoff, rain events or sediment resuspension is widely considered a key factor triggering blooms in coastal zones. However, there was no direct link between nutrient concentrations and Chl *a* fluorescence in this study, suggesting that nutrients are not the sole driver of Chl *a* dynamics and that a more complex functioning drives blooms in this mesotrophic system (Fig 5). The absence of a link with nutrient concentrations could be explained by the meteorological conditions of this shallow coastal system, where the wind causes a fairly constant nutrient supply from sediment resuspension, which can maintain the necessary nutrient level for phytoplankton growth but does not produce inputs large enough to reveal show a direct link. The wind conditions (speed and direction) were correlated with Chl *a* fluorescence with 0- to 5-day lags throughout the study periods and during three bloom periods each (Table 2). These correlations may indicate that high-speed winds, generally from the northwest (the tramontane, Figs 3 and 4), reduce biomass accumulation, while low-speed winds, generally from the east and southeast increase biomass accumulation. Millet and Cecchi (1992) [69] already reported this relationship between wind conditions and Chl *a* dynamics in

this shallow coastal lagoon. They suggested that a wind speed of 4 m s^{-1} was optimal for balancing the beneficial effect of vertical turbulent diffusion and the detrimental influence of horizontal advection dispersion. In our study, wind speed was significantly correlated with turbidity, which was probably caused by sediment resuspension (in particular, peaks of wind speed coincided with those of turbidity, Fig 3), as has already been reported for shallow coastal zones [65,70,71]. This sediment resuspension, creating a fairly constant nutrient input to the water column, may have maintained phytoplankton production and biomass. With weekly nutrient sampling, the role of nutrient inputs in bloom dynamics may be masked because phytoplankton communities respond quickly to nutrient inputs [72]. The use of high-sensitivity *in situ* nutrient sensors with high acquisition frequencies is crucial for improving our understanding of the effect of nutrient inputs on blooms in such dynamic systems.

There were some correlations between phytoplankton group abundances and nutrient dynamics, especially for PO_4 . Furthermore, the N:P ratio was almost 3 times the Redfield ratio of 16:1, suggesting that PO_4 could be a limiting factor for some phytoplankton groups during some periods of the year. This result is in agreement with that from a nutrient limitation study of French Mediterranean coastal lagoons [38]. In warmer conditions, as the metabolic demands per unit biomass increase, a higher nutrient supply is needed to support phytoplankton growth. As the nutrient demand increases, stress and competition for nutrients increase and smaller phytoplankton benefit [55,73]. However, the PO_4 and NO_3 concentrations were higher in 2016, especially during the winter latency period. This result supports our hypothesis that the predators remain active because of mild water temperatures, in turn maintaining a high grazing pressure and leading to low levels of phytoplankton biomass and thus lower nutrient consumption.

Chl *a* fluorescence and salinity were correlated two times during blooms. Increases in salinity in the studied system can be due to warm and dry periods inducing high evaporation or the inflow of saltier water from the Mediterranean Sea via winds. Otherwise, a decrease in salinity is generally caused by freshwater inputs from rain, runoff or floods. When the salinity variations result from saltier water inflow or from freshwater inputs, nutrients may also be input [37,74]. In this study, correlations between salinity and Chl *a* fluorescence were positive one time (for the early spring bloom in 2015) and negative one time (for the winter bloom in 2016), suggesting that there was an indirect effect on phytoplankton biomass through nutrient inputs rather than a direct physiological effect of salinity [75]. Rain and consequent runoff events may have enriched the system with nutrients, providing a supply for phytoplankton growth. This may have been the case for the onset of the winter bloom in 2016, where a decrease in salinity was observed and corresponded to a 4-day rain event during the initiation of the bloom (<https://www.historique-meteo.net>). This rain event may have enriched the system with nutrients, facilitating phytoplankton growth. Additionally, saltier water inputs from the sea due to strong winds from the southeast may have led to upwelling of nutrient-rich waters or induced the transport and/or accumulation of phytoplankton in the lagoon by currents. These nutrient enrichments can benefit phytoplankton growth [76,77]; however, nutrients can be rapidly assimilated and thus may have not been detected by our weekly nutrient sampling. Saltier water inputs can also explain the strong positive link detected between salinity and Chl *a* fluorescence during the early spring bloom in 2015. The beginning of this period was characterized by winds coming from the southeast that may have input saltier and more nutrient-rich water from the Mediterranean Sea, in turn contributing to the phytoplankton bloom. The southeasterly wind may also have prevented the dispersion of the accumulated phytoplankton.

One other important result was the lack of correlations between incident light parameters (PAR, UVA and UVB irradiance) and Chl *a* dynamics (Table 2). This lack suggests that in the

study system, light conditions are non-limiting for phytoplankton production, at least during winter and spring. The study site is a shallow lagoon in which light reaches a large part of the water column, with a mean attenuation coefficient of 0.35 m^{-1} [78]. In shallow temperate coastal systems, light is often non-limiting, as the light intensities in the water column are generally higher than the saturating light intensities for phytoplankton growth [79]. The non-limiting light was also supported by the occurrence of winter blooms with similar levels of Chl *a* fluorescence as the spring blooms, even though the light intensities were at their lowest level (Figs 2 and 3). Even though light did not appear to have a direct impact on Chl *a* fluorescence in this study, day length may have played a role in bloom timing [80]. There were also some negative correlations between incident light and Chl *a* fluorescence with zero lag, probably due to the inhibition of phytoplankton under high light intensities, as mentioned in the literature [81,82]. Where there were positive correlations between incident light and Chl *a* fluorescence, they exhibited a time lag of 1 to 3 days. One possible explanation for this result is that the phytoplankton responded, after a delay, to the high light conditions by first recovering from light inhibition and then increasing their biomass once acclimatized.

Small phytoplankton species benefit and diatoms lose out in warmer conditions

The dominant phytoplankton species in terms of carbon biomass in the 2015 winter bloom and the early spring bloom was the cryptophyte *P. prolonga* (6–12 μm). *Plagioselmis* is a widespread genus in Mediterranean coastal waters throughout the year and is sometimes considered the key primary producer in these systems [83,84]. *Plagioselmis* and cryptophytes in general “high-quality food” [85], ensuring efficient energy transfer to higher trophic levels. In 2016, there was a winter latency period but no early spring bloom. Nanoeukaryotes (3–6 μm) dominated in terms of carbon biomass during the winter latency period, with higher abundances than those observed in 2015, while the *P. prolonga* abundance was the same as that in 2015. Nanoeukaryotes (3–6 μm) and *P. prolonga* dominated in terms of biomass and were probably the main sources of available energy for grazers, at least from winter to early spring.

In both 2015 and 2016, the spring bloom was dominated in terms of abundance by chain-forming diatoms. *Chaetoceros* spp. and *Pseudo-nitzschia* sp., dominated the large-phytoplankton community (6–200 μm). Diatoms, including *Chaetoceros* spp. and *Pseudo-nitzschia* sp., are among the most frequent bloom-forming taxa, generally being dominant during spring blooms in coastal zones [17,75]. This is also the case at study sites where spring blooms are usually diatom dominated [86,87]. This dominance is well known and is generally attributed to the fast growth rate of diatoms due to rapid nitrogen uptake (high nitrogen affinity [88]), as confirmed by the correlation found between *Chaetoceros* spp. and NO_3 concentrations in 2015. This rapid response to nitrogen makes these species more competitive than others during the spring, when conditions are favorable (e.g., nutrients, light and temperature). These large cells with a high fatty acid content are known to be a preferential source food for metazooplankton (e.g., copepods) [89,90], which are consumed by planktivorous fish. However, although *Chaetoceros* spp. dominated the biomass during the 2015 spring bloom, nanophytoplankton (3–6 μm) dominated the 2016 spring bloom. In addition, picophytoplankton (< 1 μm) and nanophytoplankton (3–6 μm) abundances were significantly higher in 2016 than in 2015, while *Chaetoceros* spp. abundances were significantly lower. We suggest that the meteorological conditions and in particular the warm winter of 2016 were probably the causes of these differences. Several experimental studies have also suggested that water warming induces a phytoplankton community shift to picoeukaryote and nanoeukaryote dominance in both fresh and marine waters [26,56,91]. The first hypothesis for the shift in phytoplankton composition between 2015 and

2016 is that the relatively high water temperatures throughout winter and spring in 2016 promoted small phytoplankton (e.g., picophytoplankton) rather than larger ones (e.g., diatoms) due to the higher affinity for nutrients, gas uptake (CO_2 and O_2) and maximal growth rate under warmer conditions of the former. This advantage can be explained by the temperature-size relationship, which suggests that smaller organisms are more favored than larger ones in warmer conditions due to faster metabolic processes [56,73]. The second hypothesis is that the warmer winter of 2016 promoted grazers, especially larger ones (e.g., copepods). Heterotrophic protists and metazoans are more sensitive to low temperatures than phytoplankton are, and their grazing activity is higher under warmer conditions. The absence of cooling during the winter may have allowed larger grazers (those that fed on the larger phytoplankton) to remain abundant and active [27,56,92]. Thus, these larger grazers may have reduced larger phytoplankton abundances and thereby made their ecological niche more accessible to smaller phytoplankton. Moreover, large zooplankton feed on small protozooplankton that in turn graze on small phytoplankton, reducing the grazing pressure on small phytoplankton.

According to the first hypothesis, the shift from large phytoplankton to picophytoplankton and nanophytoplankton induced by warming will promote microzooplankton (mostly ciliates), creating an intermediate trophic link between primary producers and copepods. This link will lead to a reduction of the energy transfer from primary production to copepods and in turn to planktivorous fish [26,90]. Warmer water conditions, especially during the winter period, will certainly lead to changes in the plankton community that directly affect the whole food web and ecosystem functioning. In addition, one of the main differences between 2015 and 2016 was cyanobacterial abundance (here, mostly *Synechococcus*). During the winter and the early spring before the bloom, cyanobacterial abundances in 2016 were 10 times higher than those in 2015. Cyanobacteria are known to be strongly controlled by water temperature (and irradiance) and are more abundant during warmer months [75,93,94]. The relatively warm water during the winter and the early spring in 2016, without significant cooling, allowed cyanobacteria to maintain high abundances and compete with other phytoplankton. According to the second hypothesis, the small protozooplankton grazing on cyanobacteria would have been controlled via grazing by larger zooplankton facilitated by warmer conditions, further increasing the population of cyanobacteria. With the general spring water warming in both 2015 and 2016, cyanobacteria became more competitive. Their abundances started to increase when the water temperature was between 12 and 14°C. In some regions, including coastal waters and lakes, cyanobacterial blooms can cause hypoxia and nutrient limitation and can be both environmentally and economically damaging [95,96]. Furthermore, some cyanobacteria can produce toxins that are harmful to most vertebrates, including humans [97], and will cause health concerns if their high abundances become chronic with global warming. Fortunately, this is not the case for the cyanobacteria in our study, which were non-toxic unicellular taxa (e.g., *Synechococcus*).

Picoeukaryotes ($< 1 \mu\text{m}$) dominated the phytoplankton community in terms of abundance throughout the study, followed by picoeukaryotes (1–3 μm), even though they never dominated in terms of biomass (Fig 6 and Table 3). However, picoeukaryotes are known to have high biomass-specific primary production but are also targeted by microzooplankton grazers (e.g., ciliates), which prevents a major part of daily growth [86]. This relationship suggests that despite the low standing stock of carbon, picoeukaryotes play an important role in transferring carbon to higher trophic levels in coastal zones such as the system studied here [98,99]. As picoeukaryotes became more abundant in the water warming period in 2016, including the spring bloom, it is probable that, with global warming, they and small nanoeukaryotes (3–6 μm), will play a greater role in transferring carbon to higher trophic levels including species of commercial interest.

Toward a general explanation of bloom initiation in shallow coastal waters and general considerations

The disturbance recovery hypothesis [9,10] suggests that a disturbance factor disrupts the predator-prey interactions that allow phytoplankton growth to outpace grazing losses and thereby creates a bloom. Later, in response to the high phytoplankton biomass, the predator abundance and grazing pressure increase, re-establishing the new predator-prey equilibrium and hence ending the bloom. In the North Atlantic oceanic system, the disturbance factor disrupting predator-prey interactions is the deepening of the mixing layer. In shallow, coastal, non-oligotrophic systems such as Thau Lagoon, there is no deep mixing, and other forcing factors might be the major disturbance triggering phytoplankton blooms.

In these shallow coastal waters, previous studies reported that nutrient inputs via wind (sediment resuspension or water transport) and river inputs mainly drove phytoplankton production [69,75]. However, even if the role of these forcing factors is confirmed by the results presented here, this study highlights for the first time that water temperature seems to be the key factor triggering phytoplankton blooms. An increase in water temperature can stimulate phytoplankton metabolic rates such as carbon assimilation and nutrient uptake [49,50]. As the growth rates of phytoplankton can respond more rapidly than those of grazers [51], phytoplankton growth outpaces the losses by grazing, leading to a net biomass gain and starting the bloom. The diverse sources of nutrient inputs (resuspension by winds, rain or freshwater inputs or seawater intake) with frequent pulses contribute to favorable phytoplankton growth conditions during periods of increasing water temperature. Rising water temperature enhances primary production and leads to biomass accumulation and phytoplankton blooms.

In contrast, there were no clear contemporaneous correlations between the environmental variables, including water temperature, and Chl *a* fluorescence during the post-bloom periods (except with wind speed for the post-winter bloom period in 2016). This lack of correlations suggested that the end of the blooms in these systems is regulated by biological processes, in particular zooplankton grazing activity [12]. After favorable conditions trigger the bloom, the increased phytoplankton biomass allows the predator abundances to increase until the grazing rate exceeds the phytoplankton growth rate, leading to phytoplankton biomass loss during the post-bloom period. This interaction supports the food web transfer of matter in these systems, which are also known to be productive in terms of secondary production.

Moreover, low winter water temperatures are important for conditioning the phytoplankton bloom phenology and composition. If there is no significant winter water cooling, then the blooms are delayed and reduced in magnitude, and the dominant phytoplankton in communities shift to smaller ones (cyanobacteria (< 1 μm), picoeukaryotes (< 1 μm) and nanoeukaryotes (3–6 μm)). Such a shift can affect primary production and the whole food web by reducing the energy transfer to higher trophic levels, promoting small predators over larger ones (microbial food web rather than the classic herbivorous food web [100]). With global warming, mild winters could become increasingly frequent and might potentially, in the mid-term, totally change the structure of the plankton communities in the most reactive coastal ecosystems. These changes may propagate to upper trophic levels, especially those including fish and shellfish, and have a major impact on commercially exploited coastal systems such as like the studied site as these productive ecosystems are an essential economic resource for local populations. However, the mild winter effect on blooms and more generally the decadal water temperature increases due to global warming can be different according to the system. In some open or deep-coastal zones, phytoplankton blooms are triggered by upwelling, which provides nutrients from deep nutrient-rich water. As global warming heats more land than it heats ocean surface, it may strengthen alongshore winds favorable to upwelling, potentially

increasing nutrient inputs and thus bloom events [101]. In open-ocean systems of low and mid latitudes where blooms are not triggered by upwelling, surface temperature increases due to global warming might intensify ocean stratification, and potentially reduce mixing and thus the nutrient inputs from deep water that promote phytoplankton growth. This reduced nutrient supply could diminish the bloom amplitude, net primary production and phytoplankton biomass [25,28,30] and modify bloom timing [102]. However, at higher latitudes, where incident light is limiting, this stratification increase might improve light conditions favorable to phytoplankton growth in the mixing layer and thus increase net primary production and bloom events [103].

However, in the present study, the monitoring was conducted at only one sampling station in Thau Lagoon. In addition, only the winter and spring of two consecutive years were monitored, and 2015 was a “normal” climatic year while 2016 was an exceptional one with a particularly mild winter. Moreover, it is possible that 2015–2016 was influenced by ENSO or North Atlantic Oscillation (NAO) factors. Finally, the influence of tidal phases (spring/neap) on blooms was not studied as in Thau Lagoon the tidal amplitude is very low and frequently masked by climatic factors such as wind conditions [104]. However, tidal phases can influence Chl *a* fluctuations and blooms in coastal waters with higher tidal amplitude [105].

The crucial challenge concerning coastal waters, one of the most productive marine systems, is how these systems will respond to long-term climatic fluctuations such as those expected with global change. The results and conclusion of the present study are the first evidence of rising water temperature as a main driver of phytoplankton blooms in coastal waters. However, for the reasons mentioned above, to confirm our finding as a general rule, other diverse coastal waters should be investigated with adequate monitoring systems for several consecutive years.

Supporting information

S1 Data. Dataset of the high-frequency biological, meteorological and hydrological parameters and weekly water sampling. Sheets one and two correspond to the high-frequency parameters for 2015 and 2016 respectively; three and four to the nutrients concentrations; five and six to the phytoplankton (< 6 μm) abundances; seven and eight to the phytoplankton (6–200 μm) abundances and diversity; nine and ten to the HPLC Chl *a* concentrations. (XLSX)

Acknowledgments

We would like to thank Cecile Roques, Benjamin Sembeil, Océane Schenkels, Judith Duhammeuw and Ludovic Pancin for their help with the sampling and analyses of samples. Sample handling and preservation were done at the Marine Station of the Observatoire de Recherche Méditerranéen de l'Environnement (OSU OREME) in Sète.

Author Contributions

Conceptualization: Francesca Vidussi, Behzad Mostajir.

Data curation: Francesca Vidussi, Sébastien Mas.

Formal analysis: Thomas Trombetta.

Funding acquisition: Francesca Vidussi, Behzad Mostajir.

Investigation: Thomas Trombetta, Sébastien Mas, Behzad Mostajir.

Methodology: Thomas Trombetta, Francesca Vidussi, Monique Simier, Behzad Mostajir.

Project administration: Francesca Vidussi.

Resources: Francesca Vidussi, Sébastien Mas, David Parin, Behzad Mostajir.

Software: David Parin.

Supervision: Francesca Vidussi, Behzad Mostajir.

Validation: Francesca Vidussi, Behzad Mostajir.

Visualization: Thomas Trombetta.

Writing – original draft: Thomas Trombetta.

Writing – review & editing: Thomas Trombetta, Francesca Vidussi, Sébastien Mas, Monique Simier, Behzad Mostajir.

References

1. Field CB, Behrenfeld MJ, Randerson JT, Falkowski P. Primary Production of the Biosphere: Integrating Terrestrial and Oceanic Components. *Science*. 1998; 281: 237–240. <https://doi.org/10.1126/science.281.5374.237> PMID: 9657713
2. Cloern JE. Tidal stirring and phytoplankton bloom dynamics in an estuary. *J Mar Res*. 1991; 49: 203–221. <https://doi.org/10.1357/002224091784968611>
3. Sverdrup HU. On Conditions for the Vernal Blooming of Phytoplankton. *ICES J Mar Sci*. 1953; 18: 287–295. <https://doi.org/10.1093/icesjms/18.3.287>
4. Townsend DW, Keller MD, Sieracki ME, Ackleson SG. Spring phytoplankton blooms in the absence of vertical water column stratification. *Nature*. 1992; 360: 59–62. <https://doi.org/10.1038/360059a0>
5. Behrenfeld MJ. Abandoning Sverdrup's Critical Depth Hypothesis on phytoplankton blooms. *Ecology*. 2010; 91: 977–989. <https://doi.org/10.1890/09-1207.1> PMID: 20462113
6. Taylor JR, Ferrari R. Shutdown of turbulent convection as a new criterion for the onset of spring phytoplankton blooms. *Limnol Oceanogr*. 2011; 56: 2293–2307. <https://doi.org/10.4319/lo.2011.56.6.2293>
7. Ferrari R, Merrifield ST, Taylor JR. Shutdown of convection triggers increase of surface chlorophyll. *J Mar Syst*. 2015; 147: 116–122. <https://doi.org/10.1016/j.jmarsys.2014.02.009>
8. Huisman J, van Oostveen P, Weissing FJ. Critical depth and critical turbulence: Two different mechanisms for the development of phytoplankton blooms. *Limnol Oceanogr*. 1999; 44: 1781–1787. <https://doi.org/10.4319/lo.1999.44.7.1781>
9. Behrenfeld MJ, Doney SC, Lima I, Boss ES, Siegel DA. Annual cycles of ecological disturbance and recovery underlying the subarctic Atlantic spring plankton bloom. *Glob Biogeochem Cycles*. 2013; 27: 526–540. <https://doi.org/10.1002/gbc.20050>
10. Behrenfeld MJ, Boss ES. Resurrecting the Ecological Underpinnings of Ocean Plankton Blooms. *Annu Rev Mar Sci*. 2014; 6: 167–194. <https://doi.org/10.1146/annurev-marine-052913-021325> PMID: 24079309
11. Cushing DH. The seasonal variation in oceanic production as a problem in population dynamics. *ICES J Mar Sci*. 1959; 24: 455–464. <https://doi.org/10.1093/icesjms/24.3.455>
12. Banse K. Grazing and Zooplankton Production as Key Controls of Phytoplankton Production in the Open Ocean. *Oceanography*. 1994; 7: 13–20.
13. Marra J, Barber RT. Primary productivity in the Arabian Sea: A synthesis of JGOFS data. *Prog Oceanogr*. 2005; 65: 159–175. <https://doi.org/10.1016/j.pocean.2005.03.004>
14. Chiswell SM. Comment on “Annual cycles of ecological disturbance and recovery underlying the subarctic Atlantic spring plankton bloom”. *Glob Biogeochem Cycles*. 2013; 27: 1291–1293. <https://doi.org/10.1002/2013GB004681>
15. Behrenfeld MJ, Doney SC, Lima I, Boss ES, Siegel DA. Reply to a comment by Stephen M. Chiswell on: “Annual cycles of ecological disturbance and recovery underlying the subarctic Atlantic spring plankton bloom” by M. J. Behrenfeld et al. (2013). *Glob Biogeochem Cycles*. 2013; 27: 1294–1296. <https://doi.org/10.1002/2013GB004720>
16. Sommer U. *Plankton Ecology: Succession in Plankton Communities*. Springer Science & Business Media; 2012.

17. Carstensen J, Klais R, Cloern JE. Phytoplankton blooms in estuarine and coastal waters: Seasonal patterns and key species. *Estuar Coast Shelf Sci.* 2015; 162: 98–109. <https://doi.org/10.1016/j.ecss.2015.05.005>
18. Colijn F, Cadée GC. Is phytoplankton growth in the Wadden Sea light or nitrogen limited? *J Sea Res.* 2003; 49: 83–93. [https://doi.org/10.1016/S1385-1101\(03\)00002-9](https://doi.org/10.1016/S1385-1101(03)00002-9)
19. Glé C, Del Amo Y, Bec B, Sautour B, Froidefond J-M, Gohin F, et al. Typology of environmental conditions at the onset of winter phytoplankton blooms in a shallow macrotidal coastal ecosystem, Arcachon Bay (France). *J Plankton Res.* 2007; 29: 999–1014. <https://doi.org/10.1093/plankt/fbm074>
20. Tian T, Su J, Flöser G, Wiltshire K, Wirtz K. Factors controlling the onset of spring blooms in the German Bight 2002–2005: Light, wind and stratification. *Cont Shelf Res.* 2011; 31: 1140–1148. <https://doi.org/10.1016/j.csr.2011.04.008>
21. Costanza R, de Groot R, Sutton P, van der Ploeg S, Anderson SJ, Kubiszewski I, et al. Changes in the global value of ecosystem services. *Glob Environ Change.* 2014; 26: 152–158. <https://doi.org/10.1016/j.gloenvcha.2014.04.002>
22. Costanza R, d'Arge R, de Groot R, Farber S, Grasso M, Hannon B, et al. The value of the world's ecosystem services and natural capital. *Nature.* 1997; 387: 253.
23. Rabalais NN, Turner RE, Díaz RJ, Justić D. Global change and eutrophication of coastal waters. *ICES J Mar Sci.* 2009; 66: 1528–1537. <https://doi.org/10.1093/icesjms/fsp047>
24. Platt T, Fuentes-Yaco C, Frank KT. Marine ecology: Spring algal bloom and larval fish survival. *Nature.* 2003; 423: 398–399. <https://doi.org/10.1038/423398b> PMID: 12761538
25. Koeller P, Fuentes-Yaco C, Platt T, Sathyendranath S, Richards A, Ouellet P, et al. Basin-scale coherence in phenology of shrimps and phytoplankton in the North Atlantic Ocean. *Science.* 2009; 324: 791–793. <https://doi.org/10.1126/science.1170987> PMID: 19423827
26. Sommer U, Lengfellner K. Climate change and the timing, magnitude, and composition of the phytoplankton spring bloom. *Glob Change Biol.* 2008; 14: 1199–1208. <https://doi.org/10.1111/j.1365-2486.2008.01571.x>
27. Vidussi F, Mostajir B, Fouilland E, Le Floch E, Nouguier J, Roques C, et al. Effects of experimental warming and increased ultraviolet B radiation on the Mediterranean plankton food web. *Limnol Oceanogr.* 2011; 56: 206–218. <https://doi.org/10.4319/lo.2011.56.1.0206>
28. Calbet A, Sazhin AF, Nejstgaard JC, Berger SA, Tait ZS, Olmos L, et al. Future Climate Scenarios for a Coastal Productive Planktonic Food Web Resulting in Microplankton Phenology Changes and Decreased Trophic Transfer Efficiency. *PLOS ONE.* 2014; 9: e94388. <https://doi.org/10.1371/journal.pone.0094388> PMID: 24721992
29. Pernet F, Malet N, Pastoureaud A, Vaquer A, Quéré C, Dubroca L. Marine diatoms sustain growth of bivalves in a Mediterranean lagoon. *J Sea Res.* 2012; 68: 20–32. <https://doi.org/10.1016/j.seares.2011.11.004>
30. Fiandrino A, Giraud A, Robin S, Pinatel C. Validation d'une méthode d'estimation des volumes d'eau échangés entre la mer et les lagunes et définition d'indicateurs hydrodynamiques associés. 2012; <https://archimer.ifremer.fr/doc/00274/38544/>
31. Souchu P, Bec B, Smith VH, Laugier T, Fiandrino A, Benau L, et al. Patterns in nutrient limitation and chlorophyll a along an anthropogenic eutrophication gradient in French Mediterranean coastal lagoons. *Can J Fish Aquat Sci.* 2010; 67: 743–753. <https://doi.org/10.1139/F10-018>
32. Mostajir B, Mas S, Parin D, Vidussi F. High-Frequency physical, biogeochemical and meteorological data of Coastal Mediterranean Thau Lagoon Observatory. SEANO. 2018;
33. Carritt DE, Carpenter JH. Comparison and evaluation of currently employed modifications of Winkler method for determining dissolved oxygen in seawater: a NASCO report. *J Mar Res.* 1966; 24: 286–318.
34. Tréguer P, Le Corre P. Manuel d'analyse des sels nutritifs dans l'eau de mer (utilisation de l'autoanalyser II Technicon R). Brest, France: UBO; 1975.
35. Zapata M, Rodríguez F, Garrido JL. Separation of chlorophylls and carotenoids from marine phytoplankton: a new HPLC method using a reversed phase C8 column and pyridine-containing mobile phases. *Mar Ecol Prog Ser.* 2000; 195: 29–45.
36. Marie D, Partensky F, Vaulot D, Brussaard C. Enumeration of Phytoplankton, Bacteria, and Viruses in Marine Samples. *Current Protocols in Cytometry.* John Wiley & Sons, Inc.; 2001.
37. Pecqueur D, Vidussi F, Fouilland E, Floch EL, Mas S, Roques C, et al. Dynamics of microbial planktonic food web components during a river flash flood in a Mediterranean coastal lagoon. *Hydrobiologia.* 2011; 673: 13–27. <https://doi.org/10.1007/s10750-011-0745-x>
38. Sournia A, Ricard M, Chrétiennot-Dinet M-J, editors. Atlas du phytoplancton marin. Paris: Editions du Centre national de la recherche scientifique: Diffusion, Presses du CNRS; 1986.

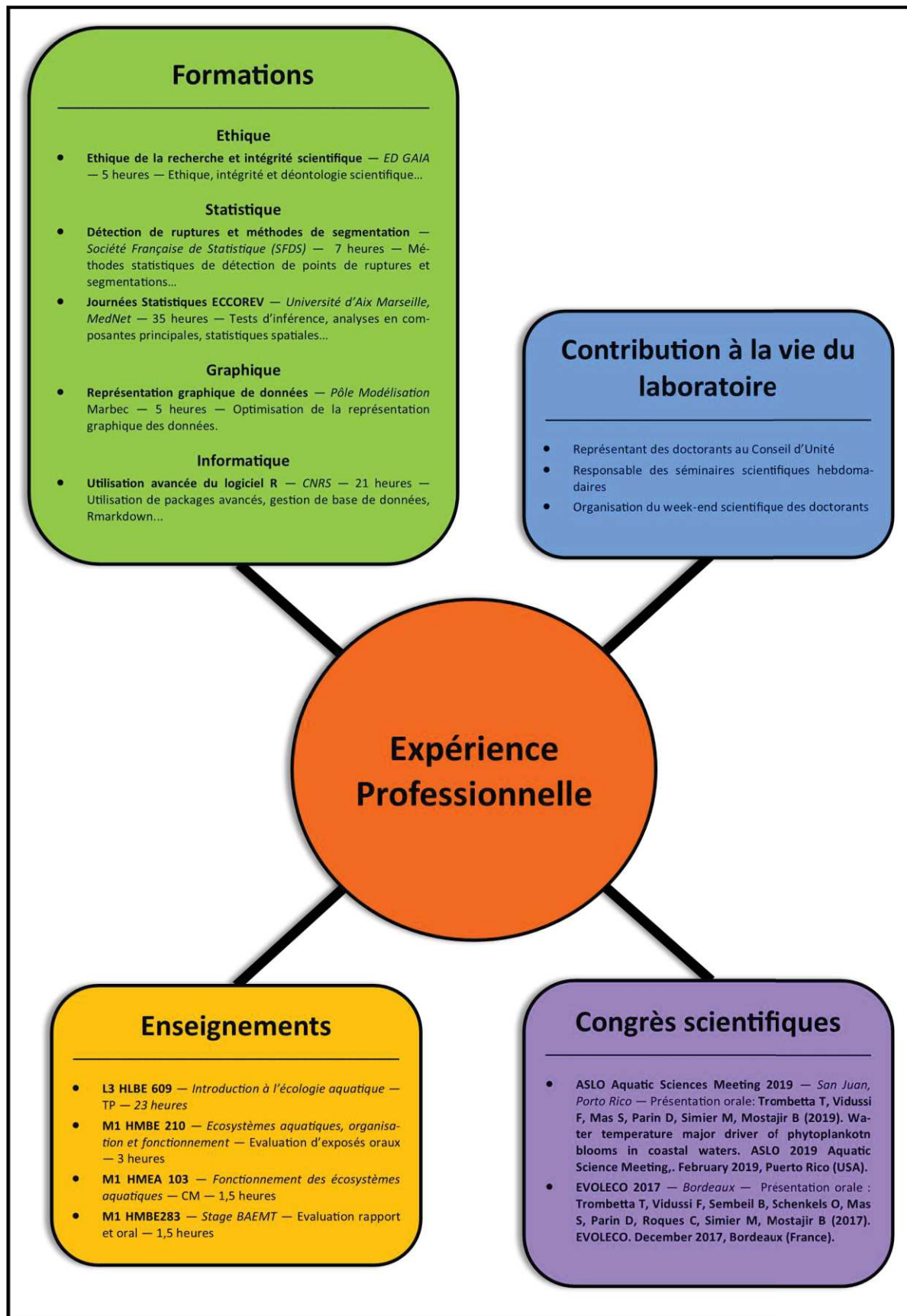
39. Kemp PF, Cole JJ, Sherr BF, Sherr EB. Handbook of Methods in Aquatic Microbial Ecology. CRC Press; 1993.
40. Wetzel RG, Likens GE. Composition and Biomass of Phytoplankton. Limnological Analyses. Springer, New York, NY; 2000. pp. 147–174.
41. Menden-Deuer S, Lessard EJ. Carbon to volume relationships for dinoflagellates, diatoms, and other protist plankton. *Limnol Oceanogr*. 2000; 45: 569–579. <https://doi.org/10.4319/lo.2000.45.3.0569>
42. Moal J, Martin-Jezequel V, Harris R, Samain J-F, Poulet S. Interspecific and intraspecific variability of the chemical-composition of marine-phytoplankton. *Oceanol Acta*. 1987; 10: 339–346.
43. Roesler C, Uitz J, Claustre H, Boss E, Xing X, Organelli E, et al. Recommendations for obtaining unbiased chlorophyll estimates from in situ chlorophyll fluorometers: A global analysis of WET Labs ECO sensors. *Limnol Oceanogr Methods*. 15: 572–585.
44. Rousseuw K. Modélisation de signaux temporels hautes fréquences multicapteurs à valeurs manquantes : Application à la prédiction des efflorescences phytoplanctoniques dans les rivières et les écosystèmes marins côtiers [Internet]. PhD Thesis, Université du Littoral Côte d'Opale. 2014. <https://tel.archives-ouvertes.fr/tel-01320681/document>
45. Aragon Y. Séries temporelles avec R: Méthodes et cas [Internet]. Paris: Springer-Verlag; 2011. www.springer.com/gb/book/9782817802077
46. Pyper BJ, Peterman RM. Comparison of methods to account for autocorrelation in correlation analyses of fish data. *Can J Fish Aquat Sci*. 1998; 55: 2127–2140. <https://doi.org/10.1139/f98-104>
47. Falkowski PG, Raven JA. Aquatic Photosynthesis: Second Edition. Princeton University Press; 2013.
48. Lewandowska AM, Breithaupt P, Hillebrand H, Hoppe H-G, Jürgens K, Sommer U. Responses of primary productivity to increased temperature and phytoplankton diversity. *J Sea Res*. 2012; 72: 87–93. <https://doi.org/10.1016/j.seares.2011.10.003>
49. Gillooly JF, Brown JH, West GB, Savage VM, Charnov EL. Effects of Size and Temperature on Metabolic Rate. *Science*. 2001; 293: 2248–2251. <https://doi.org/10.1126/science.1061967> PMID: [11567137](https://pubmed.ncbi.nlm.nih.gov/11567137/)
50. Cross WF, Hood JM, Benstead JP, Huryn AD, Nelson D. Interactions between temperature and nutrients across levels of ecological organization. *Glob Change Biol*. 2015; 21: 1025–1040. <https://doi.org/10.1111/gcb.12809> PMID: [25400273](https://pubmed.ncbi.nlm.nih.gov/25400273/)
51. Rose JM, Caron DA. Does low temperature constrain the growth rates of heterotrophic protists? Evidence and implications for algal blooms in cold waters. *Limnol Oceanogr*. 2007; 52: 886–895. <https://doi.org/10.4319/lo.2007.52.2.0886>
52. Huntley ME, Lopez MD. Temperature-dependent production of marine copepods: a global synthesis. *Am Nat*. 1992; 140: 201–242. <https://doi.org/10.1086/285410> PMID: [19426057](https://pubmed.ncbi.nlm.nih.gov/19426057/)
53. Liu X, Lu X, Chen Y. The effects of temperature and nutrient ratios on *Microcystis* blooms in Lake Taihu, China: An 11-year investigation. *Harmful Algae*. 2011; 10: 337–343. <https://doi.org/10.1016/j.hal.2010.12.002>
54. Hunter-Cevera KR, Neubert MG, Olson RJ, Solow AR, Shalapyonok A, Sosik HM. Physiological and ecological drivers of early spring blooms of a coastal phytoplankton. *Science*. 2016; 354: 326–329. <https://doi.org/10.1126/science.aaf8536> PMID: [27846565](https://pubmed.ncbi.nlm.nih.gov/27846565/)
55. Peter KH, Sommer U. Phytoplankton Cell Size: Intra- and Interspecific Effects of Warming and Grazing. *PLOS ONE*. 2012; 7: e49632. <https://doi.org/10.1371/journal.pone.0049632> PMID: [23226215](https://pubmed.ncbi.nlm.nih.gov/23226215/)
56. Sommer U, Peter KH, Genitsaris S, Moustaka-Gouni M. Do marine phytoplankton follow Bergmann's rule sensu lato? *Biol Rev*. 2017; 92: 1011–1026. <https://doi.org/10.1111/brv.12266> PMID: [27028628](https://pubmed.ncbi.nlm.nih.gov/27028628/)
57. Martens P. Effects of the severe winter 1995/96 on the biological oceanography of the Sylt-Rømø tidal basin. *Helgol Mar Res*. 2001; 55: 166–169. <https://doi.org/10.1007/s101520100078>
58. van Beusekom JEE, Loebel M, Martens P. Distant riverine nutrient supply and local temperature drive the long-term phytoplankton development in a temperate coastal basin. *J Sea Res*. 2009; 61: 26–33. <https://doi.org/10.1016/j.seares.2008.06.005>
59. Solomon S, Qin D, Manning M, Marquis M, Averyt K, Tignor MMB, et al. Climate Change 2007—The Physical Science Basis: Working Group I Contribution to the Fourth Assessment Report of the IPCC. Cambridge University Press; 2007.
60. Wang J, Hong H, Jiang Y. A coupled physical–biological modeling study of the offshore phytoplankton bloom in the Taiwan Strait in winter. *J Sea Res*. 2016; 107: 12–24. <https://doi.org/10.1016/j.seares.2015.11.004>

61. Guinder VA, López-Abbate MC, Berasategui AA, Negrin VL, Zapperi G, Pralongo PD, et al. Influence of the winter phytoplankton bloom on the settled material in a temperate shallow estuary. *Oceanologia*. 2015; 57: 50–60. <https://doi.org/10.1016/j.oceano.2014.10.002>
62. Madhupratap M, Kumar SP, Bhattathiri PMA, Kumar MD, Raghukumar S, Nair KKC, et al. Mechanism of the biological response to winter cooling in the northeastern Arabian Sea. *Nature*. 1996; 384: 549–552. <https://doi.org/10.1038/384549a0>
63. Banse K, English DC. Geographical differences in seasonality of CZCS-derived phytoplankton pigment in the Arabian Sea for 1978–1986. *Deep Sea Res Part II Top Stud Oceanogr*. 2000; 47: 1623–1677. [https://doi.org/10.1016/S0967-0645\(99\)00157-5](https://doi.org/10.1016/S0967-0645(99)00157-5)
64. Tseng C-M, Wong GTF, Lin I-I, Wu C-R, Liu K-K. A unique seasonal pattern in phytoplankton biomass in low-latitude waters in the South China Sea. *Geophys Res Lett*. 2005; 32. <https://doi.org/10.1029/2004GL022111>
65. Souchu P, Vaquer a A, Collos Y, Landrein S, Deslous-Paoli J-M, Bibet B. Influence of shellfish farming activities on the biogeochemical composition of the water column in Thau lagoon. *Mar Ecol Prog Ser*. 2001; 218: 141–152.
66. Collos Y, Bec B, Jauzein C, Abadie E, Laugier T, Lautier J, et al. Oligotrophication and emergence of picocyanobacteria and a toxic dinoflagellate in Thau lagoon, southern France. *J Sea Res*. 2009; 61: 68–75. <https://doi.org/10.1016/j.seares.2008.05.008>
67. Kalimeris A, Ranieri E, Founda D, Norrant C. Variability modes of precipitation along a Central Mediterranean area and their relations with ENSO, NAO, and other climatic patterns. *Atmospheric Res*. 2017; 198: 56–80. <https://doi.org/10.1016/j.atmosres.2017.07.031>
68. Jacox MG, Hazen EL, Zaba KD, Rudnick DL, Edwards CA, Moore AM, et al. Impacts of the 2015–2016 El Niño on the California Current System: Early assessment and comparison to past events. *Geophys Res Lett*. 2016; 43: 7072–7080. <https://doi.org/10.1002/2016GL069716>
69. Millet B, Cecchi P. Wind-induced hydrodynamic control of the phytoplankton biomass in a lagoon ecosystem. *Limnol Oceanogr*. 1992; 37: 140–146. <https://doi.org/10.4319/lo.1992.37.1.0140>
70. Paphitis D, Collins MB. Sediment resuspension events within the (microtidal) coastal waters of Thermaikos Gulf, northern Greece. *Cont Shelf Res*. 2005; 25: 2350–2365. <https://doi.org/10.1016/j.csr.2005.08.028>
71. Constantin S, Constantinescu Ștefan, Doxaran D. Long-term analysis of turbidity patterns in Danube Delta coastal area based on MODIS satellite data. *J Mar Syst*. 2017; 170: 10–21. <https://doi.org/10.1016/j.jmarsys.2017.01.016>
72. Kang Y, Kudela RM, Gobler CJ. Quantifying nitrogen assimilation rates of individual phytoplankton species and plankton groups during harmful algal blooms via sorting flow cytometry. *Limnol Oceanogr Methods*. 2017; 15: 706–721. <https://doi.org/10.1002/lom3.10193>
73. Daufresne M, Lengfellner K, Sommer U. Global warming benefits the small in aquatic ecosystems. *Proc Natl Acad Sci*. 2009; 106: 12788–12793. <https://doi.org/10.1073/pnas.0902080106> PMID: 19620720
74. Fouilland E, Trottet A, Bancon-Montigny C, Bouvy M, Le Floc'h E, Gonzalez JL, et al. Impact of a river flash flood on microbial carbon and nitrogen production in a Mediterranean Lagoon (Thau Lagoon, France). *Estuar Coast Shelf Sci*. 2012; 113: 192–204. <https://doi.org/10.1016/j.ecss.2012.08.004>
75. Cloern JE. Phytoplankton bloom dynamics in coastal ecosystems: A review with some general lessons from sustained investigation of San Francisco Bay, California. *Rev Geophys*. 1996; 34: 127–168. <https://doi.org/10.1029/96RG00986>
76. Fouilland E, Trottet A, Alves-de-Souza C, Bonnet D, Bouvier T, Bouvy M, et al. Significant Change in Marine Plankton Structure and Carbon Production After the Addition of River Water in a Mesocosm Experiment. *Microb Ecol*. 2017; 74: 289–301. <https://doi.org/10.1007/s00248-017-0962-6> PMID: 28303313
77. Deininger A, Faithfull CL, Lange K, Bayer T, Vidussi F, Liess A. Simulated terrestrial runoff triggered a phytoplankton succession and changed seston stoichiometry in coastal lagoon mesocosms. *Mar Environ Res*. 2016; 119: 40–50. <https://doi.org/10.1016/j.marenvres.2016.05.001> PMID: 27209121
78. Deslous-Paoli J-M. Programme OXYTHAU: le bassin de Thau : relation milieu- ressources dans les secteurs conchylicoles. Importance des mécanismes d'échanges verticaux. IFREMER; 1996.
79. Domingues RB, Guerra CC, Barbosa AB, Galvão HM. Are nutrients and light limiting summer phytoplankton in a temperate coastal lagoon? *Aquat Ecol*. 2015; 49: 127–146. <https://doi.org/10.1007/s10452-015-9512-9>
80. Lambert S, Tragin M, Lozano J-C, Ghigliione J-F, Vaulot D, Bouget F-Y, et al. Rhythmicity of coastal marine picoeukaryotes, bacteria and archaea despite irregular environmental perturbations. *ISME J*. 2018; <https://doi.org/10.1038/s41396-018-0281-z> PMID: 30254323

81. Takahashi M, Shimura S, Yamaguchi Y, Fujita Y. Photo-inhibition of phytoplankton photosynthesis as a function of exposure time. *J Oceanogr Soc Jpn.* 1971; 27: 43–50. <https://doi.org/10.1007/BF02109329>
82. Worrest RC, Caldwell MM. Stratospheric Ozone Reduction, Solar Ultraviolet Radiation and Plant Life. Springer Science & Business Media; 2013.
83. Novarino G. Nanoplankton protists from the western Mediterranean Sea. II. Cryptomonads (Cryptophyceae = Crptomonadea). *Sci Mar.* 2005; 69: 47–74. <https://doi.org/10.3989/scimar.2005.69n147>
84. Šupraha L, Bosak S, Ljubešić Z, Mihanović H, Olujić G, Mikac I, et al. Cryptophyte bloom in a Mediterranean estuary: High abundance of *Plagioselmis cf. prolunga* in the Krka River estuary (eastern Adriatic Sea). *Sci Mar.* 2014; 78: 329–338.
85. Sterner RW, Schulz KL. Zooplankton nutrition: recent progress and a reality check. *Aquat Ecol.* 1998; 32: 261–279. <https://doi.org/10.1023/A:1009949400573>
86. Bec B, Husseini Ratrema J, Collos Y, Souchu P, Vaquer A. Phytoplankton seasonal dynamics in a Mediterranean coastal lagoon: emphasis on the picoeukaryote community. *J Plankton Res.* 2005; 27: 881–894. <https://doi.org/10.1093/plankt/fbi061>
87. Vaquer A, Troussellier M, Courties C, Bibent B. Standing stock and dynamics of picophytoplankton in the Thau Lagoon (northwest Mediterranean coast). *Limnol Oceanogr.* 1996; 41: 1821–1828. <https://doi.org/10.4319/lo.1996.41.8.1821>
88. Lomas MW, Glibert PM. Comparisons of Nitrate Uptake, Storage, and Reduction in Marine Diatoms and Flagellates. *J Phycol.* 2000; 36: 903–913. <https://doi.org/10.1046/j.1529-8817.2000.99029.x>
89. Irigoien X, Harris RP, Verheye HM, Joly P, Runge J, Starr M, et al. Copepod hatching success in marine ecosystems with high diatom concentrations. *Nature.* 2002; 419: 387–389. <https://doi.org/10.1038/nature01055> PMID: 12353032
90. Sommer U, Stibor H, Katchakis A, Sommer F, Hansen T. Pelagic food web configurations at different levels of nutrient richness and their implications for the ratio fish production:primary production. *Sustainable Increase of Marine Harvesting: Fundamental Mechanisms and New Concepts.* Springer, Dordrecht; 2002. pp. 11–20.
91. Rasconi S, Gall A, Winter K, Kainz MJ. Increasing Water Temperature Triggers Dominance of Small Freshwater Plankton. *PLOS ONE.* 2015; 10: e0140449. <https://doi.org/10.1371/journal.pone.0140449> PMID: 26461029
92. Sommer U, Sommer F. Cladocerans versus copepods: the cause of contrasting top-down controls on freshwater and marine phytoplankton. *Oecologia.* 2006; 147: 183–194. <https://doi.org/10.1007/s00442-005-0320-0> PMID: 16341887
93. Iriarte A, Purdie DA. Size distribution of chlorophyll a biomass and primary production in a temperate estuary (Southampton Water): the contribution of photosynthetic picoplankton. *Mar Ecol Prog Ser.* 1994; 115: 283–297.
94. Agawin NSR, Duarte CM, Agustí S. Growth and abundance of *Synechococcus* sp. in a Mediterranean Bay: seasonality and relationship with temperature. *Mar Ecol Prog Ser.* 1998; 170: 45–53.
95. Paerl HW, Fulton RS. Ecology of Harmful Cyanobacteria. *Ecology of Harmful Algae.* Springer, Berlin, Heidelberg; 2006. pp. 95–109.
96. Vahtera E, Conley DJ, Gustafsson BG, Kuosa H, Pitkänen H, Savchuk OP, et al. Internal ecosystem feedbacks enhance nitrogen-fixing cyanobacteria blooms and complicate management in the Baltic Sea. *Ambio.* 2007; 36: 186–194. PMID: 17520933
97. Jakubowska N, Szeląg-Wasielewska E. Toxic Picoplanktonic Cyanobacteria—Review. *Mar Drugs.* 2015; 13: 1497–1518. <https://doi.org/10.3390/md13031497> PMID: 25793428
98. Reckermann M, Veldhuis MJW. Trophic interactions between picophytoplankton and micro- and nanozooplankton in the western Arabian Sea during the NE monsoon 1993. *Aquat Microb Ecol.* 1997; 12: 263–273. <https://doi.org/10.3354/ame012263>
99. Brown SL, Landry MR, Barber RT, Campbell L, Garrison DL, Gowing MM. Picophytoplankton dynamics and production in the Arabian Sea during the 1995 Southwest Monsoon. *Deep Sea Res Part II Top Stud Oceanogr.* 1999; 46: 1745–1768. [https://doi.org/10.1016/S0967-0645\(99\)00042-9](https://doi.org/10.1016/S0967-0645(99)00042-9)
100. Legendre L, Rassoulzadegan F. Plankton and nutrient dynamics in marine waters. *Ophelia.* 1995; 41: 153–172. <https://doi.org/10.1080/00785236.1995.10422042>
101. García-Reyes M, Largier J. Observations of increased wind-driven coastal upwelling off central California. *J Geophys Res Oceans.* 2010; 115. <https://doi.org/10.1029/2009JC005576>
102. Henson SA, Cole HS, Hopkins J, Martin AP, Yool A. Detection of climate change-driven trends in phytoplankton phenology. *Glob Change Biol.* 2018; 24: e101–e111. <https://doi.org/10.1111/gcb.13886> PMID: 28871605

103. Behrenfeld MJ, O'Malley RT, Siegel DA, McClain CR, Sarmiento JL, Feldman GC, et al. Climate-driven trends in contemporary ocean productivity. *Nature*. 2006; 444: 752–755. <https://doi.org/10.1038/nature05317> PMID: [17151666](https://pubmed.ncbi.nlm.nih.gov/17151666/)
104. Audouin J. Hydrologie de l'étang de Thau. *Rev Trav Inst Pêch Marit*. 1962; 26: 5–104.
105. Blauw AN, Benincà E, Laane RWPM, Greenwood N, Huisman J. Dancing with the Tides: Fluctuations of Coastal Phytoplankton Orchestrated by Different Oscillatory Modes of the Tidal Cycle. *PLOS ONE*. 2012; 7: e49319. <https://doi.org/10.1371/journal.pone.0049319> PMID: [23166639](https://pubmed.ncbi.nlm.nih.gov/23166639/)

Annexe 2 : Formations, contribution à la vie du laboratoire, enseignements et congrès scientifiques



Annexe 3 : Description de l'ANR PHOTO-PHYTO

Cette thèse est financée dans son intégralité par l'ANR PHOTO-PHYTO et ce travail de recherche s'inscrit dans ses objectifs.

Le projet ANR « Effet du réchauffement climatique sur le déclenchement du bloom phytoplanctonique : photopériodisme, composition et adaptation » est désigné sous le nom « PHOTO-PHYTO » (<https://anr.fr/Projet-ANR-14-CE02-0018>). Ce projet a pour objectif d'étudier le rôle et la hiérarchisation des facteurs environnementaux comme la température, et intrinsèques comme l'horloge circadienne (contrôlant le photopériodisme) dans l'initiation des efflorescences printanières. Dans le contexte de réchauffement climatique, le projet PHOTO-PHYTO propose d'étudier à plusieurs échelles, de la génomique à l'écologie des communautés microbiennes, les réponses biologiques induites par les différents forçages environnementaux pendant les efflorescences et l'effet d'une hausse des températures à long terme. Pour se faire le projet propose de se baser sur un suivi des variables hydrologiques, météorologiques et biologiques de la lagune de Thau et de la baie de Banyuls, ainsi que des expérimentations en milieux contrôlés (mésocosme), en utilisant une approche pluri-disciplinaire, combinant l'écologie, la physiologie, la génétique et l'évolution, pour répondre aux questions suivantes.

(1) Quels sont les principaux facteurs *in situ* contrôlant les efflorescences phytoplanctoniques printanières ? (2) Comment la température et la photopériode interagissent-elles pour déclencher les efflorescences printanières ? (3) L'adaptation au réchauffement affecte-t-elle le photopériodisme et les interactions trophiques ? (4) Quel est l'effet du réchauffement sur les communautés microbiennes naturelles ?

Le projet, financé par l'ANR à hauteur de 711 635€ pour une durée de 5 ans, a commencé en octobre 2014 et se finira en octobre 2019. Les partenaires du projet sont le Laboratoire d'Océanographie Microbienne CNRS (Univ Paris 06), la SA METABOLIUM et l'unité mixte de recherche MARBEC (CNRS, Université de Montpellier). Le coordinateur du projet est François-Yves Bouget (Laboratoire d'Océanographie Microbienne CNRS, Univ Paris 06) et la coordinatrice du côté du laboratoire MARBEC est Francesca Vidussi.

Résumé

Dans les écosystèmes marins des zones tempérées, la majeure partie de la production primaire annuelle est générée au printemps lors de phénomènes d'accumulation rapide de biomasse phytoplanctonique, appelés « efflorescences », supportant la diversité et le fonctionnement de ces systèmes. Plusieurs mécanismes physico-chimiques et biologiques expliquant l'initiation des efflorescences phytoplanctoniques sont évoqués pour ces écosystèmes. En revanche pour les zones côtières peu profondes sous influence de forçages complexes, les mécanismes à la base de ce phénomène restent encore mal connus. L'objectif de cette thèse était donc d'identifier et hiérarchiser les facteurs contribuant à l'initiation des efflorescences phytoplanctoniques dans ces zones, notamment le rôle des forçages physico-chimiques et des interactions biologiques au sein du réseau microbien, mais également de tenter de comprendre les conséquences de l'élévation de la température sur ce fonctionnement dans le contexte du réchauffement climatique. Dans cette optique, un suivi à deux approches a été réalisé dans la lagune de Thau (lagune côtière du Nord-Ouest de la Méditerranée) : un suivi *in situ* à haute fréquence (15 min) des paramètres hydrologiques (salinité, turbidité, température de l'eau, etc.), météorologiques (vents, lumière incidente, température de l'air, etc.) et biologiques (fluorescence de la chlorophylle *a*) ; et un suivi hebdomadaire de l'abondance de la communauté microbienne (virus, bactéries, phytoplancton, flagellés hétérotrophes et ciliés) et de sa diversité avec une attention particulière pour le phytoplancton. Ces suivis ont été réalisés de l'hiver au printemps sur deux années consécutives, 2015 et 2016. En plus de ces suivis, une expérimentation en mésocosmes *in situ* a été réalisée au printemps 2018, simulant l'élévation de la température selon le scénario du réchauffement climatique attendu dans le futur, et en présence et absence du mésozooplancton. L'objectif de cette expérience était d'identifier les effets directs du réchauffement et ceux indirects dus au zooplancton sur la dynamique, la composition pigmentaire et la succession du phytoplancton, avant, pendant et après une efflorescence phytoplanctonique. Une analyse basée sur les réseaux de corrélations entre 110 différents groupes/taxon/espèces observés (« *correlation network analysis* » en anglais) a permis de mettre en évidence les interactions majeures au sein du réseau planctonique microbien qui caractérisaient les périodes phénologiques et leurs différences entre les deux années étudiées. Pendant les périodes d'efflorescences les interactions de compétition intraguilde au sein du phytoplancton dominaient, tout comme les interactions mutualistes entre le phytoplancton et les bactéries hétérotrophes, suggérant un transfert d'énergie basée à la fois sur la biomasse phytoplanctonique et bactérienne effectué par la prédation du microzooplancton. Pendant les épisodes sans efflorescence, les interactions entre les ciliés et les bactéries (bactériorivorie) dominaient, suggérant un transfert d'énergie basée essentiellement sur la biomasse bactérienne. Dans le même temps, les résultats obtenus par le suivi à haute fréquence ont permis de mettre en évidence le rôle prépondérant de l'augmentation de la température de l'eau, notamment à la sortie de l'hiver, dans l'initiation des efflorescences phytoplanctoniques. La combinaison du métabolisme du phytoplancton stimulé par l'augmentation de la température et la faible pression de broutage permettrait l'accumulation de la biomasse phytoplanctonique à l'origine des efflorescences phytoplanctoniques. De plus, l'année 2016, avec l'hiver le plus chaud jamais enregistré par Météo France, était caractérisée par une plus faible accumulation de la biomasse phytoplanctonique à la sortie de l'hiver, une dominance du phytoplancton de plus petite taille au détriment des diatomées, et une dominance des interactions entre microorganismes de petite taille. Les résultats de l'expérimentation en mésocosmes *in situ* ont confirmé l'effet de l'élévation de la température dans la réduction de l'amplitude des efflorescences phytoplanctoniques (diminution de près de 50% de la concentration en chlorophylle *a*) et de la favorisation du petit phytoplancton comme les petites algues vertes (caractérisées par la chlorophylle *b*) ainsi que des dinoflagellés (caractérisés par la péridinine) au détriment des diatomées (caractérisés par la fucoxanthine). De plus, ils ont permis de mettre en évidence que cette modification de l'amplitude et de la composition des efflorescences était principalement liée à un effet indirect sur le phytoplancton due à l'augmentation de la pression de broutage exercée par le zooplancton. De plus, il est apparu que c'était principalement le microzooplancton qui contrôlait la dynamique et la biomasse phytoplanctonique et que le mésozooplancton jouait essentiellement le rôle de consommateur secondaire. Les résultats obtenus lors de cette thèse suggèrent que dans un avenir plus chaud, les efflorescences phytoplanctoniques seront potentiellement fortement réduites et dominées par des espèces de plus petites tailles. Le transfert de ces petites espèces phytoplanctoniques et du bactérioplancton vers les niveaux trophiques supérieurs s'effectuerait davantage au travers du microzooplancton. Ainsi, le réchauffement climatique futur dans la zone côtière peu profonde avantagerait l'établissement du réseau microbien avec potentiellement une efficacité de production et de transfert moins importante que celle du réseau classique.

Mots clés : Phytoplancton, efflorescences, zone côtière, forçages physico-chimiques, réseau d'interaction microbien, microzooplancton, prédation, compétition, réchauffement climatique, mésocosme.

Abstract

In temperate marine ecosystems, the major part of the annual primary production is generated in spring during rapid phytoplankton biomass accumulation periods, called 'blooms', supporting the diversity and the functioning of these ecosystems. Several physical, chemical and biological mechanisms triggering the bloom initiation were evoked for these ecosystems. However, for shallow coastal zones, under the influence of complex environmental forcing factors, mechanisms triggering blooms are not well known. The objective of the present thesis was to identify and classify the forcing factors contributing to the bloom initiation in these zones, especially the role of physical and chemical forcing factors and biological interactions in the microbial network, but also to understand the consequences of the temperature elevation on this functioning in the global warming context. In this frame, a monitoring with a dual approach was carried out in Thau lagoon (coastal lagoon of the North-Western Mediterranean Sea): a high frequency (15 min) *in situ* monitoring of hydrological (salinity, turbidity, water temperature, etc.), meteorological (wind, incident light, air temperature, etc.) and biological (chlorophyll *a* fluorescence) parameters; and a weekly monitoring of the abundance of the microbial community (virus, bacteria, phytoplankton, heterotrophic flagellates and ciliates), and its diversity, with a particular look at phytoplankton. These monitoring were carried out from winter to spring in two consecutive years, 2015 and 2016. Besides these monitoring, an *in situ* mesocosm experiment was carried out during the 2018 spring to simulate the temperature elevation according to the global warming scenario, in the presence and the absence of mesozooplankton. The objective of this experiment was to identify the direct effect of warming and the indirect effect of the zooplankton on the phytoplankton dynamic, the pigment composition and succession, during the pre-bloom, bloom and post-bloom periods. A correlation network analysis between 110 various groups/taxa/species highlighted the major interactions characterizing the microbial interaction network during the bloom and the non-bloom periods and the differences between these two years. During the bloom periods, intraguild phytoplankton competition and mutualism between phytoplankton and heterotrophic bacteria dominated the microbial food web. This suggested an energy transfer based on both bacterial and phytoplanktonic biomass, through the microzooplankton predation. During the non-bloom periods, interaction between ciliates and heterotrophic bacteria (bacterivory) dominated, suggesting an energy transfer mainly based on bacterial biomass. Besides, the high frequency monitoring highlighted the predominant role of the water temperature increase, especially during the early spring, in the initiation of the phytoplankton blooms. The combination between the phytoplankton metabolism stimulated by the temperature increase and the low grazing pressure triggered the phytoplankton biomass accumulation starting the blooms. Furthermore, 2016 year, with the warmer winter recorded in France (Meteofrance), was characterized by a weaker phytoplankton biomass accumulation during the early spring, a dominance of the small phytoplankton at the expense of diatoms, and a dominance of interactions between small size microorganisms. The mesocosm experiment confirmed the role of the temperature elevation on the bloom amplitude reduction (diminution of 50% of the chlorophyll *a* concentration) and the promotion of small phytoplankton such as small green algae (characterized by chlorophyll *b*) and dinoflagellates (characterized by peridinin), at the expense of diatoms (characterized by fucoxanthin). This amplitude and composition modification of phytoplankton blooms was mainly due to the indirect effect of the zooplankton grazing increase under warming. Furthermore, the results underlined that it was microzooplankton which mainly controlled the phytoplankton dynamic and biomass and the mesozooplankton was mainly accomplished the role of the secondary consumer in this system. The results of the present thesis suggest that in the future warmer conditions context, phytoplankton blooms could strongly be reduced and dominated by small phytoplankton. The energy transfer of these small phytoplankton species and heterotrophic bacteria to the higher trophic levels through the microzooplankton grazing could be strengthened. Therefore, under the future warming of the shallow coastal zones, the microbial food web could be promoted with a potential lower production and transfer efficiency than the classical food web.

Keywords: Phytoplankton, blooms, coastal zones, physical and chemical forcing factors, microbial interaction network, microzooplankton, predation, competition, global warming, mesocosm